January 2012

Determination of Isotherms of Enantiomers on a Chiral Stationary Phase Using Supercritical Fluid Chromatography

Wade Newlin Mack Ii
University of South Florida, wmack2@gmail.com

Determination of Isotherms of Enantiomers on a Chiral Stationary Phase Using Supercritical Fluid Chromatography

by

Wade Newlin Mack II

A dissertation submitted in the partial fulfilment
of the requirements for the degree of
Doctor of Philosophy
Department of Chemical and Biomedical Engineering
College of Engineering
University of South Florida

Major Professor: Aydin K. Sunol, Ph.D.
Scott W. Campbell, Ph.D.
Abdul Malik, Ph.D.
Mark L. McLaughlin, Ph.D.
Sermin G. Sunol, Ph.D.
Daniel H. Yeh, Ph.D.

Date of Approval:
November 18, 2011

Keywords: SFC, Adsorption, Isomers, Ibuprofen, Pharmaceuticals, Sorption

DEDICATION

This dissertation is dedicated to my little sister Mary Newlin Mack. She passed away shortly after I started this project. Mary was the best sister and friend one could have. I miss her every day and hold dearly our time together.

ACKNOWLEDGEMENTS

I wish to acknowledge my major professor, Dr. Aydin K. Sunol and my distinguished committee member, Dr. Sermin G. Sunol. Thank you both for the valuable knowledge you have passed to me. I wish to acknowledge and thank the other members of my committee: Dr. Scott W. Campbell, Dr. Abdul Malik, Dr. Mark L. McLaughlin, and Dr. Daniel Yeh. I would like to thank Dr. Edwin Rivera for serving as chair of my dissertation defense. I would like to acknowledge the University of South Florida, the College of Engineering, the Department of Chemical and Biomedical Engineering, and the Laboratory of Environmentally Friendly Engineered Systems. All of the staff deserves acknowledgements and thanks for their contributions to this work. Thank you fellow graduate students and friends, Brandon Smeltzer and Haitao Li. Thank you Brian Smith from Research Computing. Thank you Dr. John Shelton from the Department of Mechanical Engineering. Thank you Dr. Miles Beamguard for being a good friend. Thank you Dr. Keyur Patel for your help. Thank you Catherine Burton for all of your time and support. Thank you Dr. Paul Robinson for your time and energy proof reading this document.

I wish to acknowledge and thank my parents Dr. Patrice C. Mack and Dr. Wade N. Mack for their love and support. I would like to thank my wife Michelle H. Mack for her never-ending devotion and love.

TABLE OF CONTENTS

LIST OF TABLES

LIST OF FIGURES

LIST OF SYMBOLS

A	Surface Area [cm^2]
A_c	Cross Section of Column [cm^2]
A_s	Surface Area of the Adsorbent [cm^2]
b	Coefficient in the Langmuir Isotherm [mL/g]
c_i	Concentration in the Mobile Phase [mg/mL]
$c_{p,I}$	Concentration of Solute in Pore System [mg/mL]
C	Concentration in the Mobile Phase [mg/mL]
d_c	Column Diameter [cm]
d_p	Average Diameter of the Particle [cm]
d_{pore}	Average Diameter of the Pores [cm]
$D_{app,i}$	Apparent Dispersion Coefficient [cm^2/s]
D_{ax}	Axial Dispersion Coefficient [cm^2/s]
F	Phase Ratio [-]
f_i	Fugacity [-] or [bar]
G_{ads}	Molar Gibbs Free Energy of Compound in Adsorbed Phase [kJ/mol]
h	Reduced Plate Height [-]
H_i	Henry Coefficient [-]
HETP	Height of an Equivalent Theoretical Plate [cm]
$k_{ads,i}$	Adsorption Rate Constant [$cm^3/g*sec$]
$k_{des,i}$	Desorption Rate Constant [$cm^3/g*sec$]
$k_{eff,i}$	Effective Mass Transfer Coefficient [cm^2/sec]

k'_i	Retention Factor [-]
L_c	Length of Column [cm]
m_i	Mass [g]
N	Column Efficiency or Number of Theoretical Plates [-]
N_{col}	Number of Columns [-]
n_a	Number of Moles of Adsorbent [mol]
Δp	Pressure Drop [Bar] or [Pa]
P	Pressure [Bar] or [Pa]
Pe	Peclet Number [-]
q_i	Solid Load [mg/g] or [mM]
q_s	Saturation Capacity of Stationary Phase [mg/g] or [mM]
R_s	Resolution [-]
Re	Reynolds Number [-]
S_{ads}	Molar Entropy in the Adsorbed Phase [J/mol*K]
S_{BET}	Specific Surface Area [m^2/g]
Sc	Schmidt Number [-]
t	Time [min]
t_M	Hold-up Time [min]
t_{MTZ}	Time of Mass Transfer Zone [min]
t_R	Retention Time [min]
T	Temperature [^oC] or [K]
U_{ads}	Molar Internal Energy Compound in Adsorbed Phase [J/mol]
u_0	Velocity in the Empty Column [cm/min]
u_{int}	Interstitial Velocity in the Packed Column [cm/min]
V	Volume [mL]

V_{ads} Stationary Phase Volume [cm^3]

V_c Column Volume [cm^3]

V_i Molar Volume [mL/mol]

V_{int} Mobile Phase Interstitial Volume [cm^3]

V_m Hold-up Volume [mL]

V_{pore} Pore System Volume [cm^3]

V_{solid} Solid Material Volume [cm^3]

W_{ads} Number of Moles of Adsorbate [mol]

x_i Liquid Phase Mole Fraction [-]

y_i Vapor Phase Mole Fraction [-]

z Dimensionless Distance [-]

Subscripts and Superscripts

1, 2 Component 1 and Component 2

ads Adsorbent

des Desorbent

diff Diffusion

disp Dispersion

eff Effective

exp Experimental

ext Extract

feed Feed

i Component i

in Inlet

inj	Injection
l	Liquid
lin	Linear
max	Maximum
min	Minimum
m	Modifier
out	Outlet
p	Particle
pore	Pore
pipe	Pipe with in Chromatograph
R	Enantiomer R
S	Enantiomer S
raff	Raffinate
sat	Saturation
sel	Selective
SMB	Simulated Moving Bed Process
theo	Theoretical
TMB	True Moving Bed Process

Greek Symbols

α	Separation Factor [-]
β	Phase Ratio [-]
γ	Obstruction Factor for Diffusion or External Tortuosity [-]

Γ Solute Loading [mg/g]

ε Void Fraction of Column [-]

ε_p Porosity of Solid Phase [-]

ε_t Total Porosity [-]

ϕ Internal Energy per Unit Mole of Adsorbent [J/mol]

η Dynamic Viscosity [mPa*sec]

λ Irregularity in the Adsorbent [-]

μ_{ads} Chemical Potential [J/mol]

π Spreading Pressure [Pa]

ρ Density [g/L]

Abbreviations

BET Brunnauer-Emmet-Teller

CD Circular Dichroism Detector

CEC Capillary Electrochromatography

CFC Curve Fitting of the Chromatogram

CLC Column Liquid Chromatography

CSP Chiral Stationary Phase

CTA Cellulose Triacetate

DAC Dynamic Axial Compression

DAD Diode Array Detector

DMF Dimethyl Formamide

DMSO Dimethyl Sulfoxide

DTA Differential Thermal Analysis

ECP Elution by Characteristic Points

FA Frontal Analysis

FACP Frontal Analysis by Characteristic Points

FDA Food and Drug Administration

GC Gas Chromatograph

GRM General Rate Model

HETP Height of an Equivalent Theoretical Plate

HPLC High Performance Liquid Chromatography

IAST Ideal Adsorbed Solution Theory

IEX Ion Exchange

IR Infrared

LC Liquid Chromatography

MS Mass Spectroscopy

NP Normal Phase

ODE Ordinary Differential Equation

PDE Partial Differential Equation

RI Refractive Index

SEC Size Exclusion Chromatography

SEM Scanning Electron Microscopy

SFC Supercritical Fluid Chromatography

$scCO_2$ Supercritical Carbon Dioxide

SMB Simulated Moving Bed

TFA Trifluoroacetic Acid

TLC Thin Layer Chromatography

TMB True Moving Bed

UV Ultraviolet

ABSTRACT

Supercritical fluids provide a robust, tunable environment with favorable transport properties and enhanced solubility. Supercritical carbon dioxide is an environmentally friendly substance that has distinct advantages to traditional solvents used in large scale chemical processing. Ibuprofen is an enantiomeric drug that has been shown to fight prostate cancer and has been used as a mild Alzheimer's disease treatment in the S conformation. Purification of high value products with decreased hazardous material consumption is accomplished by employing supercritical fluid chromatography (SFC). Large scale, single enantiomer purification of pharmaceuticals is dependent on scale-up information. Equilibrium isotherms provide the necessary information to scale-up these pharmaceutical processes. Purification of pharmaceuticals and isotherm determination was accomplished. Experimental fact has demonstrated that SFC is a reliable technology for pharmaceutical processing. Equilibrium isotherms for pure component ibuprofen enantiomers were determined using Frontal Analysis (FA), Frontal Analysis by Characteristic Points (FACP), Elution by Characteristic Points (ECP), at pressures ranging from 100-150 Bar and 35^{o}C-55^{o}C. The data was fitted to a two parameter Langmuir model with RMSE's ranging from 0.0972-0.6652. FA, FACP and ECP, provided consistent isotherms, as well as, minimum adsorbent bed requirements for purge and regeneration of the SFC system.

CHAPTER 1

INTRODUCTION

Chromatography is the most widely used analytical technique in the world and is an essential part of separation science. Research and development efforts in the last two decades has increased the acceptance and industrial applicability of chromatographic processes. Equilibrium information contained in adsorption isotherms directly impacts successful design and operation of preparative and production scale chromatographic processes. Adsorption isotherms describe the distribution of a solute, between the mobile and stationary phases respectively, over concentration range of interest at equilibrium (Schmidt-Traub, 2005).

Additionally, adsorption isotherms give information to the processes involved in chromatographic retention (Jacobson, Frenz, & Horvath, 1987). Isotherm determination may also be a starting point for optimization of preparative chromatography a priori (Milbachler, Kaczmarske, Seidel-Morgenstern, & Guiochon, 2002). Comprehensive assessment of the isotherm gives the required parameters for a chromatographic purification scheme. In the last twenty years, semi-preparative and preparative chromatography usage has grown considerably. In particular, the pharmaceutical industry which uses preparative chromatography as an important and common separation technique, has made many contributions to the overall understanding to chromatographic separation. (Guiochon, Felinger, Shirazi, & Katti, 2006).

1.1. Chromatography

According to Leslie S. Ettre, chromatography is the physical separation method in where the analytes of interest (the solutes) are distributed between two phases within the column, the stationary and mobile phases. Importantly, this key distinction sets two essential guidelines for a chromatographic process. There are two distinct phases that are in contact with each other: one phase is stationary (the column packing material) while the other, the mobile phase, is moving in a definite direction (Ettre & Hinshaw, 1993).

The chromatographic separation is a result from the repeated sorption process during the migration of the analytes. Separation occurs based on the differences in the solute distribution between the two phases. The solute distribution is based on the sorption processes taking place and in the case of column chromatography, the entire process is achieved in a column packed with sorbent (stationary phase) through which a fluid (mobile phase) is flowing.

The three most common classifications of chromatography are distinguished by their mobile phase fluid state. There is gas chromatography (GC), where a gas is the mobile phase. Liquid chromatography or high-performance liquid chromatography (HPLC) employs a liquid as the mobile phase. Supercritical fluid chromatography (SFC) involves utilizing a supercritical fluid as its mobile phase. Tables 1.1 and 1.2 delineate the various distinctions between these three modes of chromatography.

Table 1.1. Chromatography Classification Based on State of the Mobile Phase

	Advantages	**Disadvantages**
Gas Chromatography (GC)	High efficiency Universal Detection	Only for Highly Volatile and Thermally Stable Substances
Liquid Chromatography (HPLC)	Low Volatile Substances Thermally Unstable Substances	Lower Efficiency than GC and No Universal Detection
Supercritical Fluid Chromatography (SFC)	Low Volatile Substances Thermally Unstable Substances	Lower Efficiency than GC

Table 1.2. Chromatography Classification According to Mobile Phase

	Gas Chromatography (GC)	**Liquid Chromatography (HPLC)**	**Supercritical Fluid Chromatography (SFC)**
Mobile Phase	Gas	Liquid	Supercritical
Example Components	1	1 – 4	1 – 3
Temperature	50 – 350 ^{o}C	Ambient (0-40 ^{o}C)	0 – 80 ^{o}C
Back Pressure	1 Bar	1 Bar	70 – 400 Bar

The properties of the mobile phases for gas, supercritical fluid, and HPLC chromatography, and may be viewed in Figure 1.1. Figure 1.1 shows that SFC shares some of the properties such as high mass transfer with GC. In addition, SFC also carries high solvent power, similar to that of HPLC. Thus, supercritical fluid chromatography has the combined assets from GC and HPLC making it an attractive process for research and development.

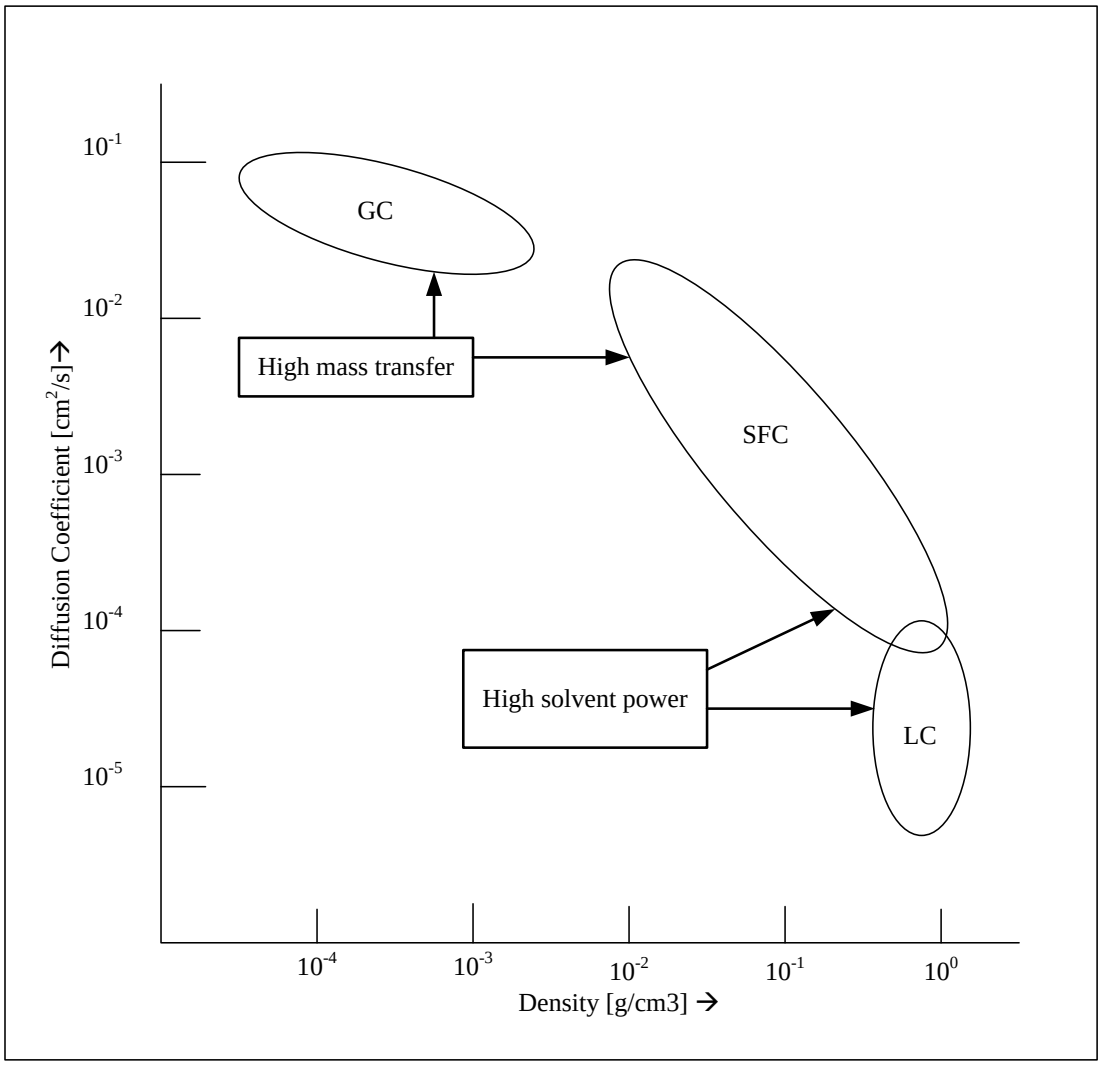

Figure 1.1. Solvent Properties According to Physical Classification of Mobile Phase

1.2. Chirality

In many biological and chemical systems, chirality is commonplace. The spatial configuration of molecules known as chirality may be seen in such examples as D and L amino acids. Since the first studies by Pasteur involving this concept, the understanding of biomolecular interactions, synthesis and purification has grown (Pasteur, 1848). This growth may be best supported by the development of highly specific pharmaceuticals.

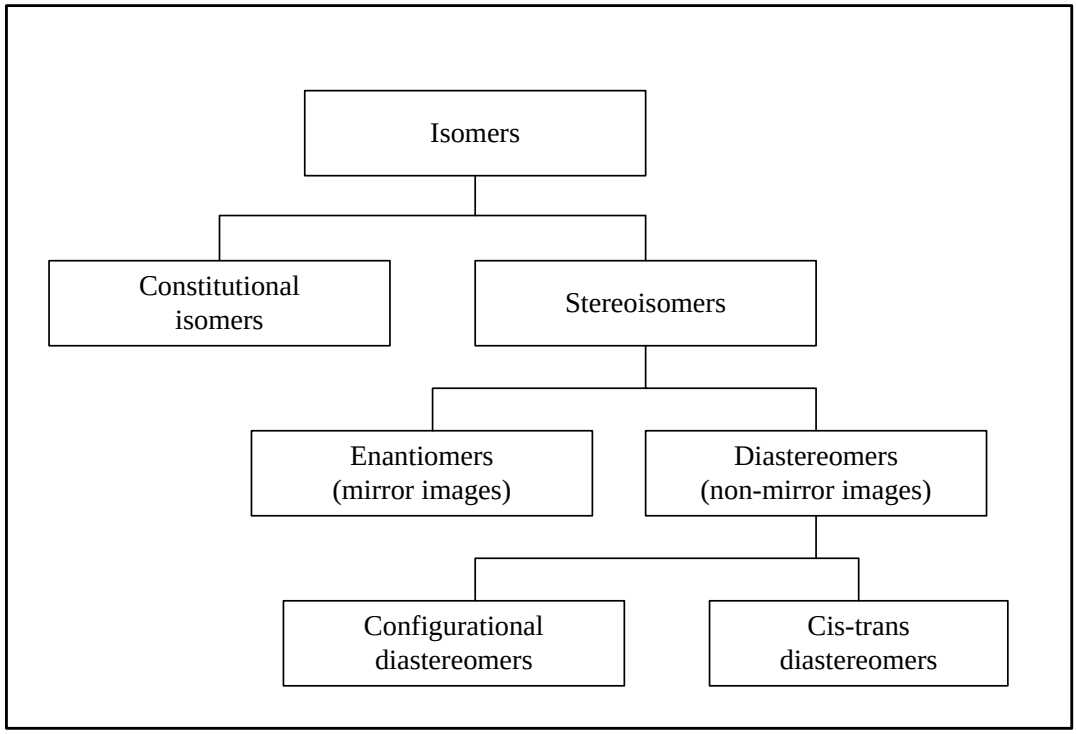

Figure 1.2. Types of Isomers and Nomenclature of Stereochemistry

Stereochemistry is the study of three-dimensional structures of molecules. Isomers are molecules with the same molecular formula, but different structures. Constitutional isomers are isomers that differ in order of bonding atoms. An example of a constitutional isomer is shown by the molecular formula C_2H_6O. This may be either

CH_3-CH_2-OH which is ethanol, or CH_3-O-CH_3 which is dimethylether. Stereoisomers are isomers that are atomically bonded in the same order but with different arrangements in space. There are two types of stereoisomers. These are enantiomers and diastereomers as shown in Figure 1.2. Enantiomers are compounds that are non-superimposable, mirror images of each other. An example of enantiomers is analogous to a pair of human hands. Diastereomers are stereoisomers that are not mirror images of each other. An example, geometric isomers also known as cis-trans isomers are diastereomers. Table 1.3 highlights important milestones in stereochemical analysis.

Table 1.3. Milestones in Stereochemistry

1815	J.B. Biot	Rotation of Plane-Polarized Light by Passing Through Aqueous Solutions of Sugar
1820	J.L. Gay-Lussac	Proof of Difference Between Natural Tartaric Acid (L-Form) to Industrial Tartaric Acid (DL-Tartaric Acid)
1848	L. Pasteur	Separation of Large Mirror Image Crystals From D- & L-Sodium Ammonium Tartrate
1874	J.H. van't Hoff J.A. LeBel	Tetrahedral Shape of the Saturated (Asymmetric) Carbon Atom

Molecules existing in enantiomeric forms to each other are said to be chiral. Enantiomers are chiral. An atom is chiral only if it has four different groups bonded to it. Molecules that are not chiral are described as achiral. A racemate is an equimolar mixture of an enantiomer pair. Enantiomers have the same physical properties but different names, toxicity and effects in the body. Table 1.4 contains some interesting properties of enantiomers.

Table 1.4. Properties of Enantiomers

Enantiomers Have the Same	**Enantiomers Have Different**
Boiling Point	Polarimetry
Melting Point	Interactions with Other Chiral Molecules
Vapor Pressure	Physiological Effects
Density	Toxicity
Refractive Index	Nomenclature

Chiral molecules are stable and observable stereoisomers if their respective conversion energy barrier is greater than 80 kJ / mole (Moss, 1996). Additionally, compounds which exist as enantiomers have nearly identical physical and chemical properties, making the individual component resolution difficult.

When enantiomers are present in equimolar amounts within a mixture, the resultant mixture is termed racemic. Racemic mixtures are optically inactive in part because the net plane polarized light rotation is negated by the equal concentrations of each enantiomer. Louis Pasteur in 1848 successfully resolved enantiomers from their

racemic mixture. Pasteur managed to resolve a racemic mixture of sodium ammonium tartrate (Sheldon, 1993). Table 1.5 shows examples of enantiomers and their qualitative differences.

Table 1.5. Examples of Chiral Substances and Qualitative Differences by Enantiomer

	R-Enantiomer	**S-Enantiomer**
Asparagine	Sweet Taste	Bitter Taste
Histidine	Sweet Taste	Bitter Taste
Leucine	Sweet Taste	Bitter Taste
Limonene	Orange Odor	Lemon Odor
Carvone	Caraway Seed Odor	Spearmint Odor
Menthol	Mint Taste	Mint, Cooling Effect
Citalopram	Inactive	Antidepressant
Ketamine	Hallucinogen	Anesthetic
Contergan	Analgesic	Teratogen

Today, chirality of drugs is an important issue in the discovery, design, development and marketing of new drugs. Additionally, stereochemistry has a key part in pharmacology. Since the new technologies development to handle chiral drugs in the 1980s, a significant decrease in the production of racemates has occurred (Caldwell, 1999). Pure enantiomer preparation has increased as well as the interest in stereochemistry (Agranat, Caner, & Caldwell, 2002). Stereoselective analysis has led to the understanding that each enantiomer play a part in overall drug action is of great

importance. Moreover, if one enantiomer provides the desired effect, its complement enantiomer may be either inert, somewhat active, act as rival to the useful enantiomer, or harbor a different activity.

After examining these possibilities, one may see the advantages in using stereochemically pure drugs. Advantages such as a more precise dose and response relationship as well as a reduction in the total dose administered have increased single enantiomer processing in industry (Shah, 2003).

1.3. Pharmaceutical Trends

Establishing the pharmacological activity of all components in a commercial drug is crucial. There have been substantial increases in single isomer pharmaceuticals commercially available over the past quarter century (Brooks, Guida, & Daniel, 2011). This single drug form trend has been brought about partly by the Food and Drug Administration and interestingly also by the production of a variety of pharmaceuticals that no longer have patent protection.

The FDA requires medicine manufacturers to report specific issues including pharmaceutical properties of the individual isomers as well as the racemic mixture (U.S. Food and Drug Administration, 2003). Enantiomeric medications with out of date patent protection are drawing a throng of overseas manufacturers. These activities may offer valuing rivalry and promote the generic drug obtainability from manufacturers with high throughput capacity. Chiral drugs also represent a large share of the pharmaceutical market. As of 1996 enantiomer medications made up almost eighty billion dollars of the world marketplace. Large quantities of enantiomer medications employed for production

in prescription forms were worth almost twenty five billion dollars (Van Arnum, 2006). Figure 1.3 shows the global distribution of drugs according to chirality and achirality. The majority of drugs in this time frame clearly harbor chiral properties.

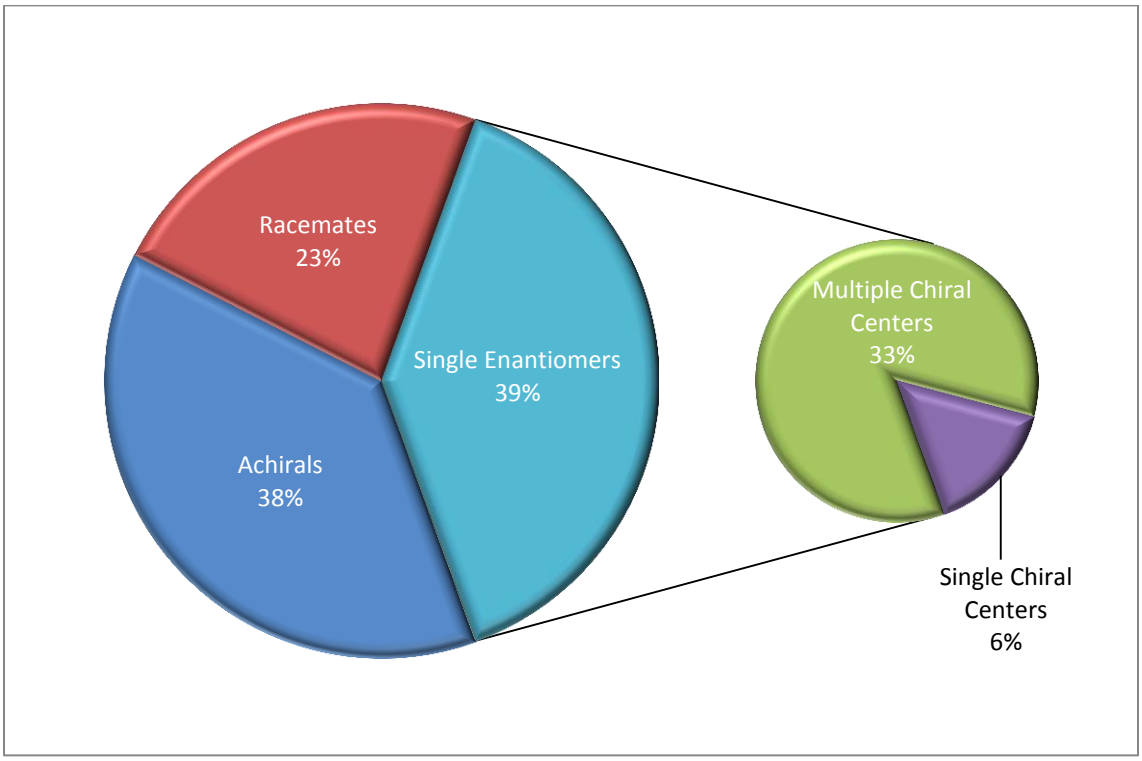

Figure 1.3. Distribution of Drugs According to Chirality from 1983-2002

As seen in Figure 1.3, the twenty year period from 1983 to 2002 shows how single enantiomers passed achirals and racemates making up a remaining 23% of worldwide approved drugs. During the period from early 1983, a pure enantiomer was a major part of permitted medications and sanctioned enantiomeric pharmaceuticals. These trends were probably a function of the changing times in regulatory agencies encouraging the advance of pure chiral medications as opposed to racemic mixtures which would

therefore account for a rather significant change in corporations manufacturing pharmaceuticals intent on a safe production of single-enantiomer and or non-chiral drugs as opposed to racemate mixtures (Brooks, Guida, & Daniel, 2011).

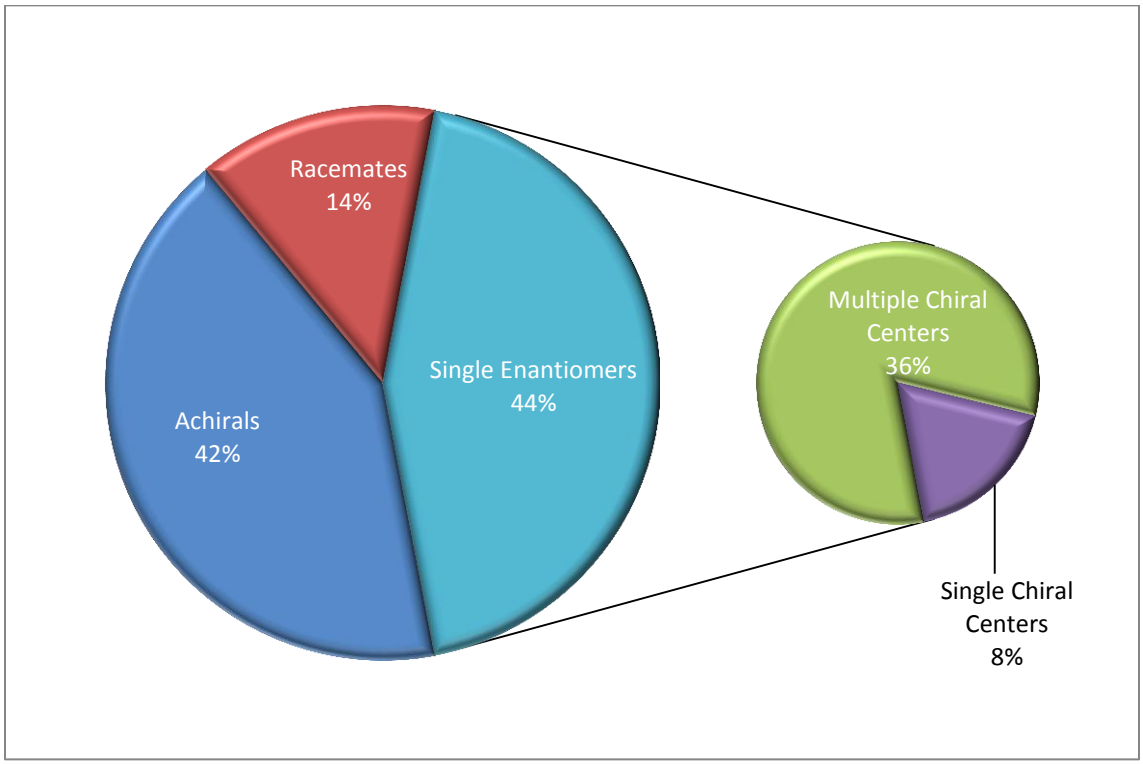

Figure 1.4. Distribution of Drugs According to Chirality from 1991-2002

The worldwide supply of medications during a time range from 1991 to 2002 as seen in Figure 1.4, shows single enantiomer drugs as the leading category followed by achirals and lastly racemates making up 14%. Racemates dropped significantly during this period thus reflecting the trend and interest in stereochemical drugs.

An interesting and germane anecdote about thalidomide is worth noting. The racemic drug thalidomide was the source of tragedy in 1961. Thalidomide used to be

promoted and sold outside of the U.S. market from 1950 to around 1960 as an insomnia drug to treat nausea for pregnant women. Pregnant women who were taking this medication gave birth to children with deformities. During this period thalidomide was still unapproved by the Food and Drug Administration. It has been speculated that this catastrophe involving thalidomide was preventable if the single chiral product was utilized rather than the racemate. This conclusion was misleading however, and in 1998 racemic thalidomide was awarded FDA approval for the treatment of a rare skin condition called erythema nodosum leprosum (ENL) (Agranat, Caner, & Caldwell, 2002).

Table 1.6. Processing Technologies of Single Enantiomers

	Chemical Asymmetric Hydrogenation	**Biochemical Enzymatic**	**Chromatography**
Production	Great	Small	Modest
Selectiveness	Fluctuates	Great	Great
Yield	Fluctuates	Great	Great
Process Handling	Fluctuates	Complex	Fluctuates
Development Time	4-5 Years	2-4 Years	6-8 Months
Development Cost	$3-5 Million	$2-3 Million	$0.5-0.8 Million

Processing single enantiomers is typically achieved by chemical, biological, and physical (chromatographic) processes. Table 1.6 shows the parameters associated with asymmetric hydrogenation, enzymatic, and chromatographic methods for single enantiomer processes. It becomes clear that chromatography is well suited and preferred in some respects for enantiomer processing.

1.4. Chiral Stationary Phases

The advance of chiral stationary phases (CSP) used in preparative chromatography has grown significantly in the past 15 years (Brunellia, Zhao, Brown, & Sandra, 2008). As the first commercially available phases were introduced in the early 1980s, the quality control of their reproducibility has improved as well. CSPs used most frequently in preparative chromatography include the Whelk O1. Offering high loading capacity, these stationary phases are used for a variety of separations of different racemic mixtures. Amylose based and cellulous based stationary phases are most often used for preparative work specifically simulated moving bed (SMB) (Ganetsos & Barker, 1993). Table 1.7 contains examples of stationary phases and their commercial names used for enantiomer processes (Johannsen, 2007).

Table 1.7. Chiral Stationary Phases Used for Enantiomer Processes

Type of Stationary Phase	**Commercial Example**
Cellulose and Amylose Derivatives	Chiracel, Chiralpak
Synthetic Polymers	Chirapher, CHI-DMB
Cyclodextrins	ChiraDex, Cyclobond
Brush Type	Whelk O1, Whelk O2
Crown Ether	Crownpak
Macrocyclic Glycopeptides	Chirobiotic

The research and improvement of novel CSPs for preparative use is to this day an important and germane topic even though hundreds are available commercially. Key design improvements needed include better selectivity, higher capacity, and mechanical as well as chemical stability. Additionally, all of these features need to be applicable to an even wider range of solvents.

However, optimization for selectivity of chromatographic processes is only needed up to a pragmatic value. Selectivities, for the example of operating a SMB unit, are generally between 1.3 and 2.0 (Wankat, 1986). This is because when one uses too high of a selectivity, it results in very high eluent consumption necessary to desorb the solute compound from the stationary phase. Table 1.8 shows the development phases of chiral drugs from their discovery to their final production (Johannsen, 2007).

Table 1.8. Development of Chiral Drugs

	Innovation	**Initial Development**	**Complete Development**	**Engineering**
Amount	mg–50g	100g–10kg	5–100kg	Tons
Enantiomer Needed	Active and Inactive	Active and Inactive	Only Active	Only Active
Time Frame	Days	Weeks	Months	Years
Cost Importance	Negligible	Negligible	Medium	Major
Scale-up Feasibility	Negligible	Negligible	Important	Required

Chiral SMB processes have become more commonly utilized. Some key developments are highlighted in Table 1.9. HPLC-SMB, GC-SMB, and SFC-SFC have all been employed for chiral drug processing. Table 1.9 also shows the different stationary phases used and investigators who carried out the method development (Brunner & Johannsen, 2005).

Table 1.9. Examples of Chiral SMB Processes

Technique	**Solute of Interest**	**Stationary Phase Packing**	**Column N x(ID x L) [mm]**	**Investigator**
HPLC-SMB	EMD 53986 Ca Sensing Agent	Chiralcel OJ	8 x (26 x 50)	Peper et al., 2002
HPLC-SMB	Tramadol Analgesic	Chiralpak AS	12 x (21 x 100)	Peper et al., 2002
HPLC-SMB	Guaifenesin Antitussive	Chiralcel OD	16 x (16 x 60)	Jusforgues et al., 1995
GC-SMB	Enflurane Anesthetic	Cyclodectrin	8 x (15 x 800)	Jusforgues et al., 1995
SFC-SMB	Ibuprofen Analgesic	Kromasil CHI-TBB	8 x (30 x 97)	Peper et al., 2002

Table 1.10 shows the breakdown of some SMB-chiral processes. The dates of manufacturing show the SMB evolution as a viable process for chiral drugs. Also, it should be illustrated that the global utilization of this SMB technology is shown in Table 1.10 (Johannsen, 2007).

Table 1.10. Simulated Moving Bed Processes for the Production of Enantiomers

Year	**System**	**Capacity [ton/year]**	**Location**
1994	LicoSep 8-200	1	Separex, France
1997	LicoSep 6-450	1	UCB-Pharma, Belgium
1998	LicoSep 12-100	1-3	Daicel, Japan
2000	LicoSep 6-800	10	Aerojet Fine Chemicals, USA
2000	UOP SMB	10-20	UPT, USA
2000	LicoSep SMB	10-15	Honeywell Specialty Chemicals, Ireland
2001	LicoSep SMB	10-15	Bayer, Germany
2002	LicoSep SMB	10-15	Lundbeck, Denmark
2003	LicoSep SMB	10-15	Finoga, France

1.5. Supercritical Fluids

A fluid is known as supercritical when it has a temperature and pressure exceeding its critical point. Above the critical point one cannot distinguish or delineate the existence between the liquid and gas phases. A supercritical fluid may transport into and around solid phases like gases do, and solubilize a material similar to liquids. Near this critical area, slight variations in temperature and or pressure or temperature will lead to vast density fluctuations. This permits tuning of the physical properties of a supercritical fluid by manipulating temperature and pressure. A supercritical fluid may be used as an ancillary for otherwise typical solvents employed in both industrial and laboratory settings. Water and CO_2 typically are employed the most for supercritical fluid substitution. Supercritical carbon dioxide (scCO2) is being used for various processes such as decaffeination of beverages and supercritical fluid extraction of nutraceuticals (Felix, Berthod, Piras, & Roussel, 2008).

Charles Cagniard de la Tour is credited for proving the existence of the critical point of a substance. He made this discovery in 1822 by working with a cannon and cannonball detonation. He observed this when he noted the sound gaps from a cannonball in a closed experimental apparatus. The apparatus was a cannon loaded with different pure fluid solutions at numerous temperatures. In doing so, Cagniard witnessed the existence of various critical temperatures. Beyond the critical temperature, the density of the gas and liquid converge to the same value. In this region the discrepancy between a gas and a liquid vanishes, ensuing in a phase known as the supercritical. Cagniard also established that every liquid had a specific temperature beyond which that fluid was reluctant to stay in the liquid phase and transitioned to a gas phase, regardless

of how much pressure was applied. Studying water solutions, Cagniard estimated the critical temperature of water to be 362^{o}C (Berche, Henkel, & Kenna, 2009).

Supercritical fluids have properties between gases and liquids. In Table 1.11, the critical properties are shown for some substances that have been used as supercritical fluids (Reid, Prausnitz, & Poling, 1987).

Table 1.11. Critical Properties of Various Solvents

Substance	**Molecular Mass [g/mol]**	**Critical Temperature [K]**	**Critical Pressure [MPa], [atm]**	**Critical Density [g/cm^3]**
Acetone (C_3H_6O)	58.08	508.1	4.70, 46.4	0.278
Carbon Dioxide (CO_2)	44.01	304.1	7.38, 72.8	0.469
Ethane (C_2H_6)	30.07	305.3	4.87, 48.1	0.203
Ethanol (C_2H_5OH)	46.07	513.9	6.14, 60.6	0.276
Ethylene (C_2H_4)	28.05	282.4	5.04, 49.7	0.215
Methane (CH_4)	16.04	190.4	4.60, 45.4	0.162
Methanol (CH_3OH)	32.04	512.6	8.09, 79.8	0.272
Propane (C_3H_8)	44.09	369.8	4.25, 41.9	0.217
Propylene (C_3H_6)	42.08	364.9	4.60, 45.4	0.232
Water (H_2O)	18.015	647.1	22.064, 217.7	0.322

Additionally, supercritical fluids have no surface tension. This is due to a lack of a gas and liquid state boundary. Making a change in the temperature or pressure of a supercritical fluid, the physical assets may be fine-tuned so as to have more gas or liquid

properties. An important property of a supercritical fluid is the solubilizing power of the SF on a substance. The solubility of a SF will rise corresponding to the density of the SF at temperatures held constant. As an increased density propagates with pressure, the solubilizing power also rises. The affiliation of a supercritical fluid with temperature is not as straightforward. In systems where density the solubilizing power will rise with temperature increase. However, around the critical region the system density may decrease dramatically as the temperature is increased. So, a fluid around the critical region can show a decrease and subsequent increase in solubilizing power as the temperature rises (Martinez, 2008). To gain better understanding, the critical point may be determined by employing an equation of state. These may include the Soave-Redlich-Kwong and Peng-Robinson equations of state (Soave, G., 1972) and (Peng, D. & Robinson, D., 1976).

Table 1.12 shows various parameters of fluids such as density and viscosity. In Table 1.12, the difference between gases used in GC, and liquids used in HPLC support the use of supercritical fluids in SFC as comparison (Brunner, 2005).

Table 1.12. Contrast of Gases, Liquids, and Supercritical Fluids

	Density [kg/m^3]	**Diffusivity [mm^2/s]**	**Viscosity [µPa*s]**
Gases	1	1-10	10
Liquids	1000	0.001	500-1000
Supercritical Fluids	100-1000	0.01-0.1	50-100

1.6. Isotherms for Sorptive Process Design

The ideal solute movement theory is useful to an extent as it accounts for the development and physical understanding of operating methods. It is not however, a design method. Linear theories of chromatography are useful for dilute systems, but for most commercial processes, in which the isotherms are non-linear, the need for pragmatic design methods is apparent (Wankat, 1986).

One procedure that is employed in adsorption column design is described by the LUB/equilibrium concept method (Hines & Maddox, 1985). This method splits the frame of reference of the packed-bed adsorber into two sections, the equilibrium section and the LUB (Length of Unused Bed) section. The size of the equilibrium section is determined by the equilibrium adsorption data at the bed design temperature. These data are also known as isotherms. The length of the equilibrium section may be representative of the shortest length possible and is described as the stoichiometric length. This assumption is justified since the stationary phase or adsorbent in the equilibrium section of the bed is considered to be at steady state with the mobile phase solute. A stoichiometric wave front egresses through the bed as a step function as seen in Figure 1.5.

The equilibrium concept fails to provide an accurate estimate of the packed-bed length since the length of mass transfer zone in not known a priori. Moreover, because of the presence of the mass transfer zone, all of the adsorbent behind the actual solute wave front will not be at its maximum capacity. This leads to an additional quantity of adsorbent which must be accounted for to compensate for the presence of the mass transfer zone. This equivalent quantity of adsorbent is known as the LUB.

The assumptions of the LUB/equilibrium section concept have been summarized as follows (Collins, 1967).

1. The holdup of the adsorbable component in the voids is small comparable to the equilibrium adsorbate loading.
2. The flow rate, temperature, and concentration of the feed are constant.
3. The temperature, composition, and velocity do not vary in the radial direction.
4. The bed temperature and initial adsorbate loading are uniform.
5. The initial bed and feed temperatures are equal.
6. Chemical reactions do not occur.
7. The bed operation is isothermal.
8. The mass transfer zone is stable.

Figure 1.5 shows the plot of a solute breakthrough curve. Also Figure 1.5 shows how the LUB or length of unused bed is determined graphically. Figure 1.5 shows the dimensionless concentration on the y-axis versus time on the x-axis. The t_{MTZ} is the time associated with the mass transfer zone. This time represents the initial step increase in solute concentration and the leveling off of that concentration (Wankat, 1986).

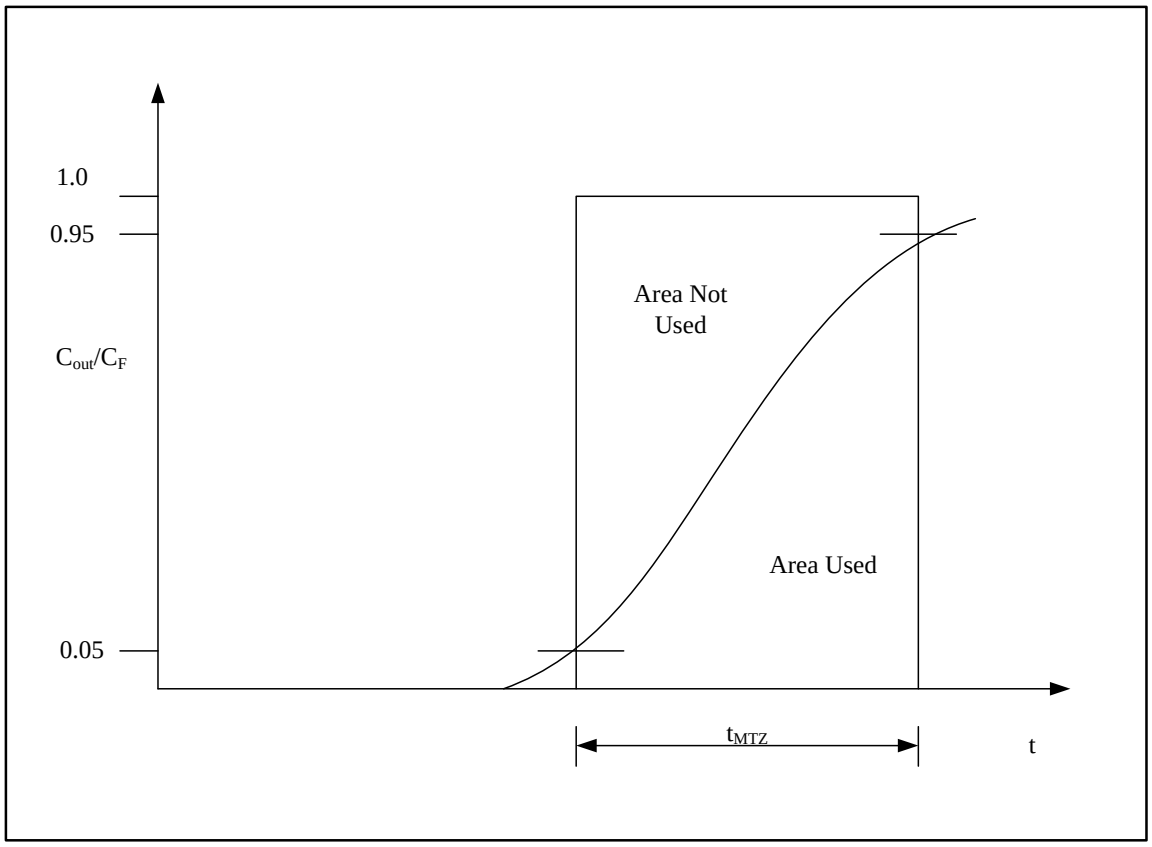

Figure 1.5. Graphical Description of LUB from a Breakthrough Curve

Actual design practices must take into account the shock waves scattering from the effect of dispersion and finite mass transfer rates. The spreading due to dispersion is opposed by the isotherm and sorption effects which tend to form shock waves. The net result of these opposing forces is the formation of what is called a constant pattern wave. The constant pattern wave keeps a constant shape while traveling through the packed-bed column. This constant pattern analysis may be used for process design by employing experimental breakthrough curves (Wankat, 1986).

The LUB approach has its limitations as well. The first is that it is limited to constant pattern systems. Meaning it works for a favorable isotherm, much like the Langmuir Model represents. The LUB approach is also limited to isothermal systems. Therefore adiabatic sorption cannot be modeled. Large temperature changes can destabilize the mass transfer zone and give non-constant patterns. The LUB approach requires experimental data, which is actually not a disadvantage since obtaining data of the chemical systems to be separated is very useful. Gathering data will reveal if any trace components are present that might affect the adsorbent adversely.

The constant pattern will always form when conditions are appropriate and constant. Constant pattern systems are amiable to significant mathematical simplification. Since the shock wave pattern is constant, partial differential equations can be converted to ordinary differential equations based on the distance from the stoichiometric front also known as the shock wave location (Wankat, 1986).

1.7. Preparative Chromatography and Moving Bed Systems

Scales of chromatography are important and contribute in different ways to solving a chromatographic separation. Analytical chromatography uses columns with a maximum of 10 mm inner diameter and a flow rate in the range of 0.1 – 30 mL/min. Analytical chromatography determines the chemical composition of a sample. It also separates that sample and quantifies it. Preparative chromatography uses columns with an inner diameter of 7 – 50 mm and a flow rate range of 20 - 1200 mL/min. Preparative chromatography is used to purify and collect one or more components of a sample in the mass range of microgram to gram. Production scale chromatography employs columns

up to 1600 mm I.D. and a flow rate greater than 1000 mL/min. Table 1.13 contains the various scales of chromatography based on the amounts of throughput and column inner diameter (Brunner & Johannsen, 2005).

Table 1.13. Scales of Chromatography

Scale of Chromatography	**Mass Range of Components**	**Inner Diameter of Column [mm]**
Analytical	µg-mg	4-10
Preparative Laboratory Scale	mg-g	4-25
Preparative Pilot Scale	g–kg	25-80
Preparative Production	kg–ton	80-1500

The foremost methods of action of preparative chromatography are displacement, elution, and frontal. Frontal chromatography is essentially the same as the sorption design procedure introduced in Section 1.6. Elution chromatographic separation is the most widely used preparative method of action since it is not difficult and relatively quick to learn. Chromatography by elution is performed using a flow of mobile phase. Using an elution method the solute and solvent mix is introduced into the chromatograph as a defined impulse. After introduction, the analytes of interest as well as the solvent travel

through the chromatograph at varied velocities. The velocities of these components are associated with the mobile phase flow rate and the solute phase distribution. The solutes distribute between the stationary phase (SP) and the mobile phase (MP) (Guiochon, Felinger, Shirazi, & Katti, 2006).

Chromatographic purification by using a displacer is a procedure often used for large molecule separations. The difference between using a displacer and using elution is the added solvent to displace the solute. A displacement solution is chosen with a greater interaction with the adsorbent bed than any of the initial solute compounds introduced. Therefore, the system is loaded with a high volume of initial solution then the displacer is introduced at a steady rate which aids in desorption.

The procedure of using a displacer works by the analytes competing for sorption spots in the adsorbent SP. This is driven by sorption affinity and MP concentration. The displacement chromatographic mode works because different analytes travel in the column with rates higher than those defined predominantly by each specific component isotherm.

The solutes elute from the adsorption column in wave zones. The more concentrated solutes elute as defined by their respective sorption binding constants (Ahrends & Schluter, 2010).

Chromatographic elution for large systems is usually done by excessive loading of volume and or mass. This is intended to raise production capacity. The overfilling of volume means that the amount of solute is kept constrained to the linear potion of the isotherm while the solution volume increases. Main drawbacks to overloading the solution volume are the lack of column utilization along with decreased egress. The

stacking of solution mass takes the solute concentration outside the linear region of adsorption. This results in a non-Gaussian elution curve. It is also possible to use both volume and mass in an overloaded capacity. This combination may optimize output in large scale chromatographic separation by elution (Guiochon, Felinger, Shirazi, & Katti, 2006).

1.7.1. True Moving Bed Chromatography

An idealized adsorption design concept is known as true moving bed (TMB) chromatography. The simulated moving bed (SMB) chromatographic approach may be used and employed by first describing the true moving bed process. TMB employs different operating principles as opposed to conventional batch chromatography. To illustrate, a toroid is used to demonstrate the TMB process. Assume that the toroid is filled with water and adsorbent as seen in Figure 1.6.

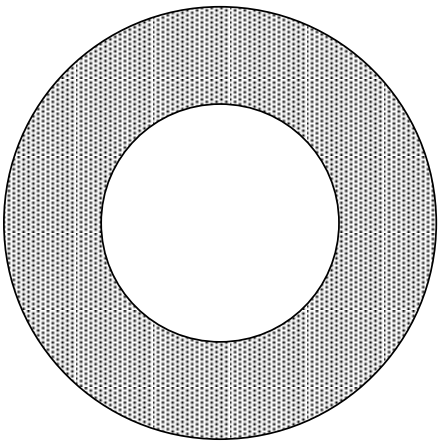

Figure 1.6. Toroid Filled with Adsorbent Resin and Water

Now assume a continuous, clockwise flow of water in inside the toroid, as in Figure 1.7. Figure 1.7 shows the water circulation inside the toroid. Note that for this example, we have clockwise circulation.

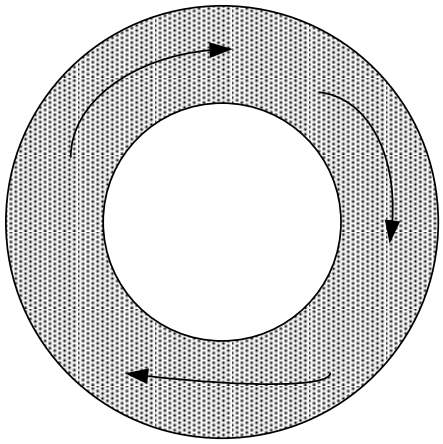

Figure 1.7. Water Circulating Clockwise Inside the Toroid

Now assume that the toroid itself rotates counterclockwise. Figure 1.8 shows the simultaneous motion of water circulation and toroid spinning.

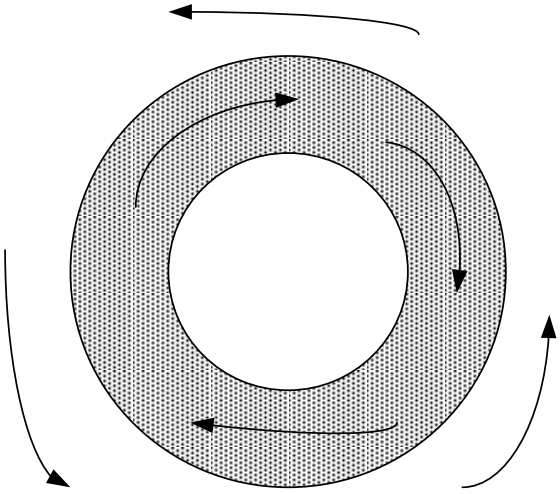

Figure 1.8. Simultaneous Clockwise Flow and Countercurrent Rotation

For the purpose of clarity, assume that the movement the toroid and internal water are real. A significant feature of the TMB is this countercurrent movement. Then by introducing a feed mix that needs to be purified continuously at one part of the toroid as in Figure 1.9, the solute with more interaction travels with the resin and the less retained compound travels with the aqueous flow. Continuous separation can be accomplished by aligning the flow rate of the aqueous stream and the toroid circulation.

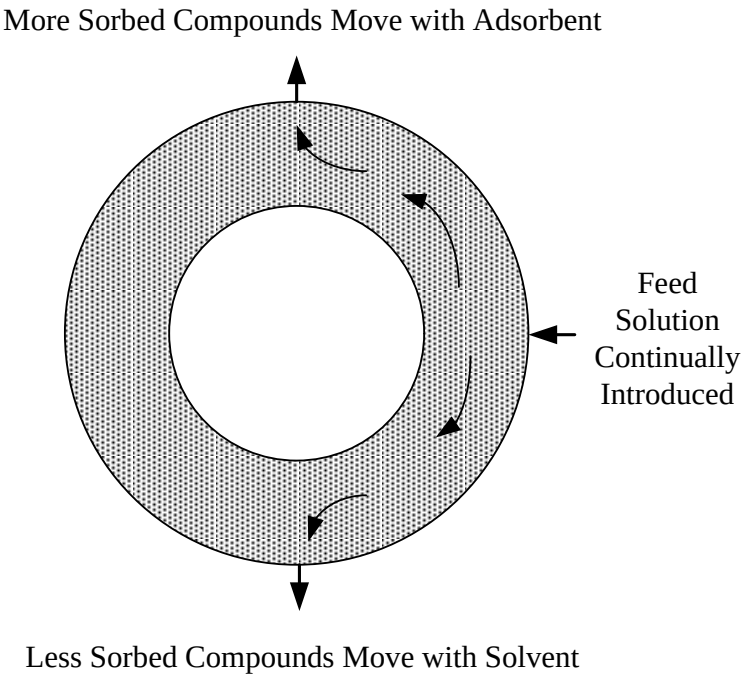

Figure 1.9. Feed Containing Binary Mixture of a True Moving Bed

Figure 1.9 exemplifies one form of continual chromatographic separation. The advantages seen in TMB are lower consumption of solvent as well as lower adsorbent needed for a purification scheme. The solvent or mobile phase can introduced to the

system in a continual fashion making the processing appear as Figure 1.10. Figure 1.10 shows that the more retained compound is defined as the extract while the lesser retained compound is known as the raffinate (Subramanian, 1995).

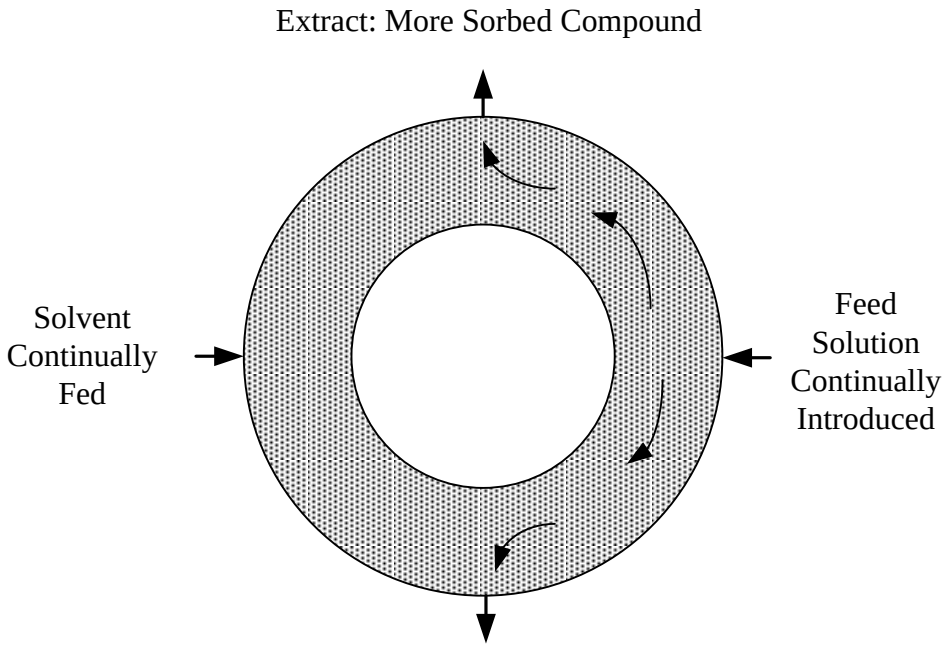

Figure 1.10. True Moving Bed Process

TMB is limited to separation of two components. As opposed to elution chromatography which may resolve several compounds of a mix. The TMB process can be regarded as binary purification process. The compounds that travel with the solvent water and the compounds that travel with the adsorbent are treated differently.

TMB technology has some features that are different than elution chromatography. One feature of TMB is that path length is extended. Elution processes have finite column lengths. The greater the column length the better the separation and resolution will be. Additionally, as path length increases so do the theoretical plates. In TMB, the interacting solute and adsorbent path may be raised beyond the actual length of sorbent by manipulating the flow rates of the two phases.

Changing the flow rate in both the adsorbent and solvent ensures that the incoming feed mix interacts with more stationary phase. The advantage of the TMB technology over batch elution systems lay in this increase of perceived adsorbent length. However, the sorbent path can only be increased up until the pressure drop or adsorption dynamics become unwanted (Charton & Nicoud, 1995).

1.7.2. Simulated Moving Bed Chromatography

A pragmatic use of TMB chromatography is the simulated moving bed (SMB). The simulated moving bed harbors similar attributes of the TMB. A simulated moving bed is an extension of the idealized TMB process. A simulated moving bed system can be represented as a series of columns, shown in Figure 1.11 (Charton & Nicoud, 1995).

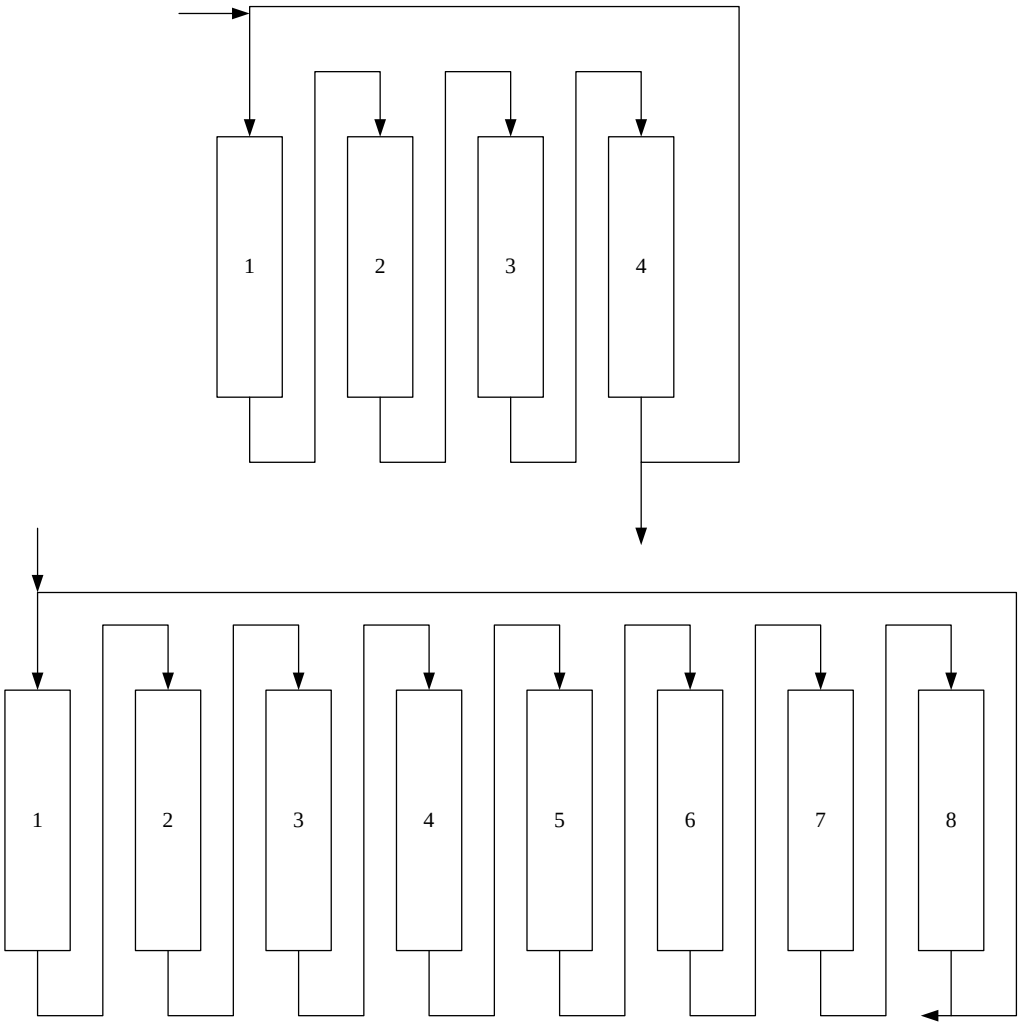

Figure 1.11. Example SMB Four Column and Eight Column Scheme

The outlet from the first SMB stage enters the top of the next stage on so on and as the solute propagates through the SMB. Simulating a moving bed system from a true moving bed is understandable when viewing from a top, circular point of view. In Figure 1.12, an SMB is shown as a loop. Similar to the four column scheme shown in Figure 1.11, Figure 1.12 details the action of a simulated moving bed.

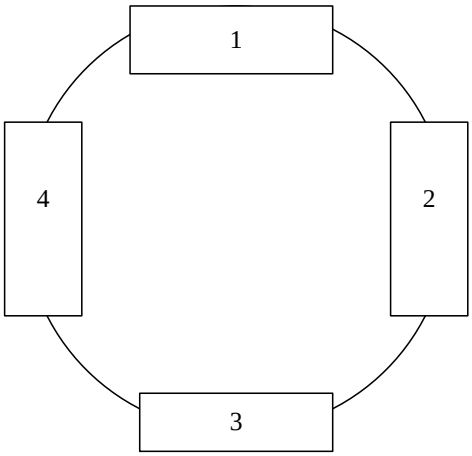

Figure 1.12. SMB Viewed as a True Moving Bed System

The SMB system as in Figure 1.12 illustrates the similarities with a true moving bed process as a continual re-circulation of solution flow from left to right. The transport of solvent is done using pumps in series with the columns.

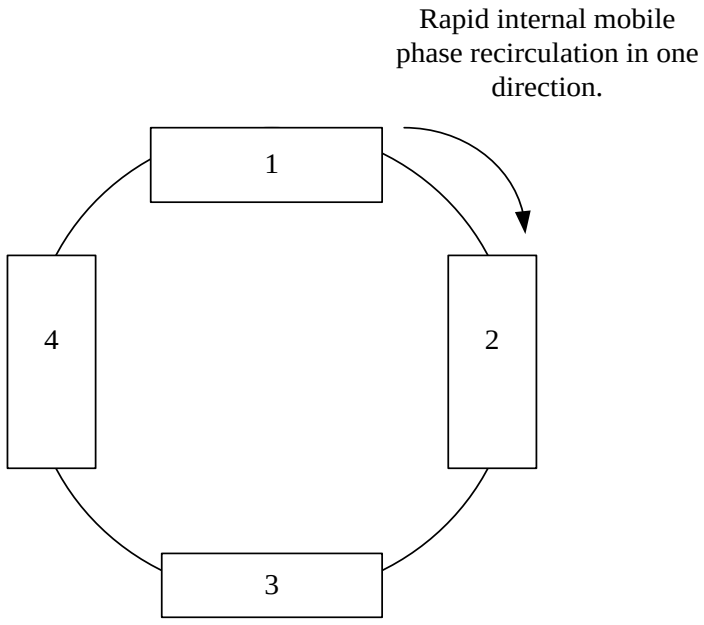

Figure 1.13. SMB Showing Clockwise Internal Mobile Phase Flow

The adsorbent residing in the columns is stationary however. Different from the TMB, the adsorbent does not actually move in the opposing directions compared to the solvent flow. As a solution mix is introduced in a section connecting two columns, the solute moves with the solvent fluid flow. The unwanted TMB effect is correct by the SMB. The key aspect of the simulated moving bed process is the adsorbent egress may be replicated in the opposing solution feed direction by manipulating a switching, feed valve. Manipulations of the other system valves control the extract line, the eluent line, and the raffinate line. Figures 1.14 through 1.17 illustrate the SMB process at work.

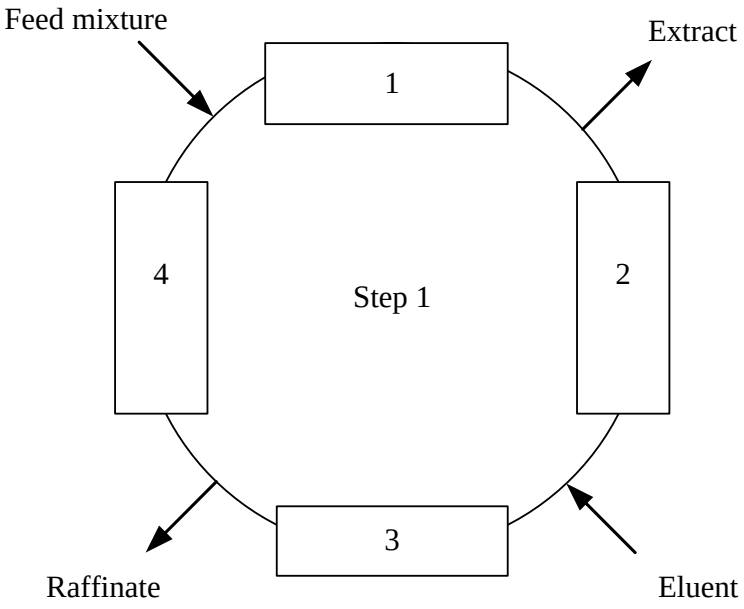

Figure 1.14. Simulated Moving Bed Time Step One

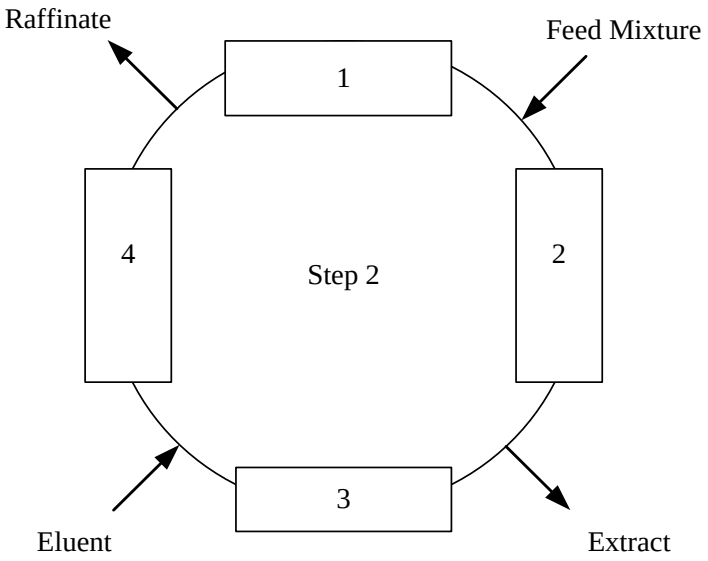

Figure 1.15. Simulated Moving Bed Time Step Two

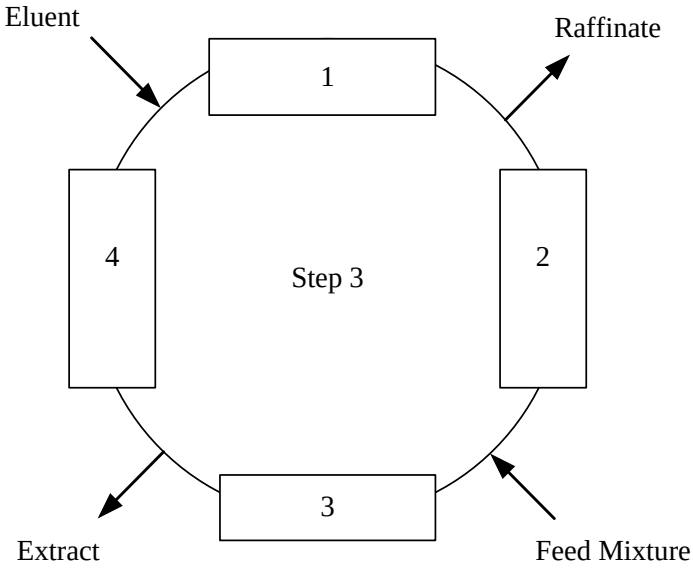

Figure 1.16. Simulated Moving Bed Time Step Three

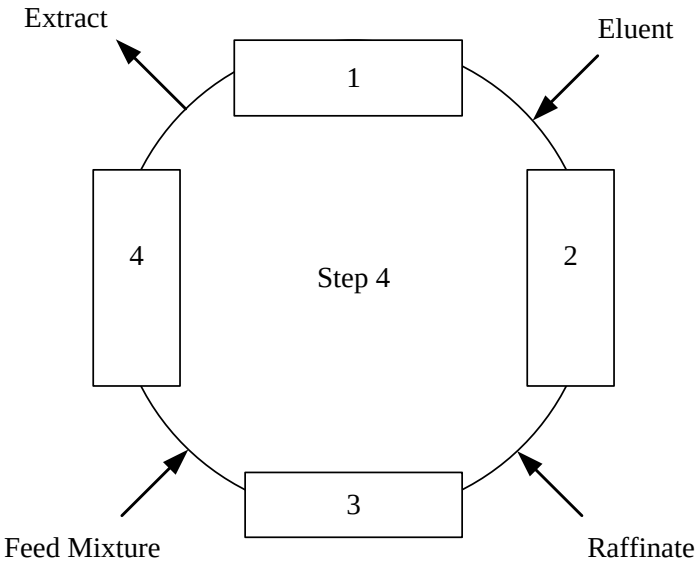

Figure 1.17. Simulated Moving Bed Time Step Four

Therefore, to simulate a moving bed system the valves need to be switched on and off at various points to affect a change in the flow of eluent through the system. The simulated moving bed is still does not approach the idealized true moving system. This is because the adsorbent motion replicated via the switch valve system is a semi-continuous operation rather than continuous like TMB. To a certain extent, the eluting solution moves sporadically through the columns of the SMB. Therefore, as the number of columns increases in an SMB the TMB process concept is approached. A countless amount of columns are needed to reach the idealized TMB process for an exact replication. Luckily a four or twelve column scheme is usually adequate to reproduce the advantages of a TMB process(Charton & Nicoud, 1995).

1.8. Elements of Dissertation

This dissertation is prepared into seven chapters. The introduction presents key concepts and relevant topics encountered in this dissertation. Chapter 2 contains a published works review for chromatography with an emphasis on supercritical fluid chromatography applications. Chapter 3 details the theoretical aspects of adsorption processes as well as the background of isotherm determination methods available. Chapters 4 contain the mathematical modeling of a chromatographic system using the constant pattern analysis and equilibrium-dispersive model. Chapter 5 focuses on the system designed to run these experiments. It includes the hardware and chemicals used. and present the experimental results to support this dissertation. Chapter 6 presents the outcome of the separation and isotherm determinations made and a discussion of these experimental results. Chapter 7 provides conclusions and recommendations for future work.

Chapter 2 will cover select published works in chromatography. Additional reviews of GC, LC, and SFC publications are resented. SFC is shown in this survey rival HPLC is its applications and reliability.

CHAPTER 2

CHROMATOGRAPHY PUBLISHED WORKS REVIEW

Chromatography is the most widely used analytical technique today. It has been called the separation technique of the 20th Century. Invented by a botanist over one hundred years ago, chromatography continues to evolve and grow in methodology from partition chromatography and paper chromatography to thin-layer chromatography, gas chromatography, high-performance liquid chromatography, and supercritical fluid chromatography. Leslie S. Ettre of the Chemical Engineering Department at Yale University wrote that chromatography is more than a simple technique and is quoted in the nesxt sentence (Ettre L. S., 2000). "It is an important part of science encompassing chemistry, physical chemistry, chemical engineering, biochemistry and cutting through different fields."

Chromatography history and applications are covered in this chapter. Table 2.1 highlights some of the key researchers in the area of chromatography (Schmidt-Traub, 2005). The invention of chromatography by a botanist to the development of GC, HPLC, and SFC is reviewed. Supercritical fluid chromatography is reviewed. Applications of SFC including natural products, food processing, and pharmaceuticals are discussed. Chiral SFC applications are reviewed at the end of Chapter 2.

Table 2.1. Milestones of Chromatography

Year	**Investigators**	**Separation**
1850	Runge Schonbein Goppelsroder	Separation of Dyes of Filter Paper
1903	Tswett	Separation of Plant Pigments by Means of Open-column Liquid Chromatography on Calcium Carbonate (Chalk)
1931	Kuhn and Lederer	Preparative Liquid Chromatographic Separation of Alpha and Beta Carotenes From Carrots
1941	Martin and Synge	Development of Partition Chromatography (Nobel Prize of Chemistry in (1952)
1949	Spedding and Tompkins	Ion-Exchange Chromatography (IEX)
1959	Porath and Flodin	Size Exclusion Chromatography (SEC)
1966	Piel Horvath	High-Performance Liquid Chromatography (HPLC)
1966	Broughton	Simulated Moving Bed Technology (SMB)

2.1. The Invention of Chromatography and Tswett

A Russian botanist named Mikhail Semenovich Tswett (1872-1919) is accredited with the invention of chromatographic separation. Tswett was fascinated by the pigment of chlorophyll present in plant systems. He worked to purify chlorophyll from plants and noted that polar-organic solutions may extract the chlorophyll. Conversely, when the chlorophylls were separated, they were solvable in non-polar, organic solutions. He accurately determined that the dyes of chlorophyll existed in the plant as a sorption phase and that the non-polar solutions were incapable of breaking the forces of sorption. This effort eventually developed into the method of chromatographic separation, which involved the discriminating sorption in a fluid system (Tswett, 1906). A detailed discussion of the discovery process of chromatography by Tswett may be read by (Ettre & Sakodynskii, 1993).

Chromatography had far to go as it was still a slow process due to the use of gravity as a driving force for the mobile phase flow. Additional enhancements such as adding pressure to the head of the column helped chromatography as a technique. However, it was not until the monumental contributions of Martin and Synge that essentially changed chromatography forever with their introduction of the notion of partitioning as the basis of separation. Kuhn and Lederer have been recognized for their contributions in the development of preparative liquid chromatographic separations of alpha and beta-carotenes from carrots (Ettre, 2000).

2.2. Liquid Partition Chromatography

The practice and development of liquid partition chromatography was first developed 1941 by A. J. P. Martin and R.L.M. Synge (Martin & Synge, 1941). Liquid partition chromatography as first applied to the separation of monoamino monocarboxylic acids found in wool. Although Martin and Synge had difficulty accomplishing the separation, it was in this difficulty that led Archer Martin to try something different in fixing one of the phases while keeping the other mobile. Martin and Synge's major contribution was the introduction of the partition as the basis of separation. This meant that chromatography was viewed as a linear process in which its system features depended on the sample size introduced. It was by introducing this linear relationship that allowed Martin and Synge to develop a good mathematical model of chromatography. In doing so, the improvement of separations was detailed as well as the use of the theoretical plate concept. The work of Martin and Synge forever changed chromatography as well as chemical and biochemical techniques of investigation. During 1952 Martin and Synge both were awarded the Nobel Prize in Chemistry for their great achievements (Ettre, 2000).

2.3. Gas Chromatography

The results of Martin and James represent the first published work in the area of Gas Chromatography or GC for short (James & Martin, 1952). Additional work by James and Martin was published later that year and lay the groundwork for what developed into gas chromatography (James, Martin, & Smith, 1952) and (James, 1952). As gas-liquid partition chromatography grew so did its adoption by the analytical

chemistry world. By 1952, GLPC was one of the main topics of discussion during the Inaugural International Congress on Analytical Chemistry located at Oxford, England (Ettre, 2000). Gas chromatography lent itself greatly to the petrochemical industry at that time. New petroleum processes were being introduced which required the need for good analytical techniques to quality control production. Gas chromatography offered a simple and effective method of characterization without sacrificing speed of analysis. Much of this practice in the Shell laboratories was documented and quickly adopted by many petrochemical companies (Keulemans, 1957).

Gas chromatography impacted the development of analytical chemistry in another, maybe more important way. Since gas chromatography could not be done using glass tubes as in classical liquid chromatography, the need for technical instrumentation became a fast growing industry. This paved the way for physicists, engineers and chemists to help create what is now a multimillion dollar scientific instrument industry (Ettre, 1990).

Gas chromatography started with simple operations and equipment. Typically packed columns being temperature controlled for isothermal operation and detection by thermal-conductivity. Not long after, gas chromatography started to see the use of temperature gradient programming (Griffith, James, & Phillips, 1952) and (Dal Nogare & Harden, 1959).

The use of ionization detectors was incorporated with the growth of gas chromatography (Lovelock, 1958) and (Dewar, 1960). Additional contributions from van Deemter and Golay described the authority of fluid velocities, diffusion, column dimension, and the resistances to diffusion between the stationary and mobile phases (van Deemter, Zuiderweg, & Klinkenberg, 1956).

2.4. High-performance Liquid Chromatography

Gas liquid chromatography was considered to be more evolved than classical liquid chromatography for some time. This was due to the slow nature of the liquid method, many times manual methods, and to the lack of scientific instrumentation available. For example, a typical analysis time for liquid chromatography took five to eight hours to complete. This measured up to gas chromatography as essentially three orders of magnitude slower. It was hoped that the methods and theory developed for gas chromatography could be applied to liquid chromatography in effort to make it more useful. It was determined that the rate of diffusion needed to be improved in order to make better use of liquid chromatography. To accomplish this limiting factor, the size of the packing particles needed to be drastically reduced and uniform in shape. Also the pressure of the system had to be increased dramatically (Giddings, 1963). It should be noted that Martin and Synge theorized that the theories of gas chromatography could be extended to liquid chromatography in their 1941 paper (Ettre & Zlatkis, 1979).

Csaba Horvath at Yale University was one of the first to develop a reliable liquid chromatograph in the mid-1960s (Ettre, L. S., 2000). His publication in Nature in 1966 is one of the first instances of the HPLC (Horvath & Lipsky, 1966). Horvath used new and innovative techniques to obtain smaller particle size of the adsorbent. He used particles of glass approximately 40 micrometers in diameter packed into a column 1 millimeter in diameter to achieve separations. Additionally, Lloyd Snyder worked towards developing liquid adsorption chromatography at the same time (Snyder, L., 1967).

Horvath pioneered this new technique of high-performance liquid chromatography or HPLC for short. Additionally, Dr. Kirkland of DuPont pioneered the adsorbent phases used during this time and soon after became commercially available (Kirkland, J., 1971). HPLC was primarily used at that time in reversed-phase chromatography mode. That meant using a non-polar stationary phase with a polar mobile phase. Kirkland and Horvath paved the way for reversed phase high-pressure liquid chromatography and further supported chromatography as a discipline. The development of HPLC continued rapidly. HPLC is still evolving today and has overcome GC as the most extensively employed analytical technique. As long as there is a need for speedy and reproducible quantification of analytes, liquid chromatography will remain universal.

2.5. Supercritical Fluid Chromatography

Supercritical fluid chromatography or SFC has elements of both liquid and gas chromatography. In a supercritical fluid (SF), the mass transfer of analytes is quicker than in a liquid but not quite as fast as in gases. Unlike gas chromatography, separations using supercritical fluid mobile phases may be accomplished at much lower temperatures. This is a huge benefit of SFC in that one may work with non-volatile, temperature sensitive compounds that cannot be handled by gas chromatography. James E. Lovelock first recommended the exploit of a supercritical fluid mobile phase in 1958 at a chemistry conference (Lee & Markides, 1990).

During the 1960s, SFC developed quickly and was pioneered by three main groups. M. N. Myers conducted high-pressure GC studies and J. Calvin Giddings at the University of Utah worked with SFC (Myers & Giddings, 1966). Ernst Klesper at Johns Hopkins University separated isomers using what he called high-pressure gas chromatography (Klesper & Corwin, 1962). A few years later, in 1966 began comprehensive experiments using supercritical fluid chromatography by a group at the Shell Laboratory in the Netherlands (Sie & Rijnders, 1967) and (Sie, Van Beersum, & Rijnders, 1966). This work although isolated from the other work by Klesper and Giddings, provided more evidence of possible advantages of using supercritical fluids over liquid mobile phases. SFC grew slowly over the next twenty years until a lab at HP Inc. customized an HPLC unit to run supercritical CO_2 as a mobile phase using a 100 mm long column loaded with three micrometer particles. (Gere, Board, & McManigill, 1982). They used supercritical carbon dioxide modified with polar organics to enhance solubility (Ettre, 2000).

In the later part of the 1980s, SFC saw major developments with the manufacturing of specialty instruments as well as startup of smaller SFC companies (Ettre & Zlatkis, 1979). It was predicted that SFC would overtake GC and HPLC during this time as well. This did not happen however. One benefit at this time of decline was when supercritical fluid extraction was employed in conjunction with supercritical fluid chromatography. Using supercritical carbon dioxide to both extract and separate an analyte of interest proved both difficult but reliable for sensitive, thermally labile work (Ettre, 2000).

A number of applications using supercritical fluid chromatography have been employed more recently. SFC is a well-defined method for both analysis and purification of analytes. Having many of the benefits of gas chromatography and liquid chromatography, SFC has been useful to a multiplicity of varied applications. Some interesting applications are summarized in the following sections.

2.5.1. Natural Products

The application of supercritical fluid chromatography to the study of natural occurring isoprenoid alcohols and fat mixes has been acknowledged as an instance for the purification of hydrophobic metabolic compounds (Bamba, 2008). Non-developed supercritical fluid conditions of singular homologues with 10−100 mer units were purified. The employment of a cyanopropyl adsorption stationary phase achieved the purification of 14 fatty acids. The run time was less than fifteen minutes with successful detection of the fatty acids.

Isolation, fractionation, and identification of sucrose esters from aged oriental tobacco employing supercritical fluids have been completed (Ashraf-Khorassani, Nazem, Taylor, & Coleman, 2008). In addition to supercritical fluid extraction, semi-preparative SFC provided for an additional purification of the sucrose ester enriched fraction after column optimization. Structural assignments of the SFC fractions were facilitated using GC/MS accompanied by N,O-bis(trimethylsilyl)trifluoroacetamide-dimethylformamide derivatization of the free hydroxyl groups and HPLC-MS (Ettre, 2000).

Furocoumarins are a type of biomolecules produced by different plants. Purification of a furocoumarin system has applications to beauty products and holistic healing remedies. Due to the variety of components and their slight structural difference, the purification needs HPLC or SFC processing. Isocratic conditions were established to obtain a satisfactory separation in 10 min (Desmortreuxa, Rothaupt, West, & Lesellier, 2009).

A 2D study was achieved by studying the fractioning of components on a 2-ethyl pyridine sorbent. Purification was then achieved using a penta-fluoro-phenyl sorbent. These approaches allowed the structure of the compound to be related to interaction behavior, which was abnormal due to the utilized penta-fluoro-phenyl SP (Ettre, 2000).

2.5.2. Food Processing

Separation of γ-lactones was achieved using a chiral stationary phase column on a supercritical fluid chromatograph by Gary Yanik of PDR Chiral (Xie & Yanik, 2011). Several mixtures γ-lactones that are used for flavorings and fragrances were effectively separated in under 15 min. The most favorable purifications of these compounds were accomplished predominantly below the supercritical region. The purification parameters were determined by methodically studying the result of changing the composition of isopropyl alcohol in the MP. Additionally, system pressure, temperature, and flow rate was optimized. The chiral stationary phase used and co-solvent proved most optimal for the separation of the lactone compounds with supercritical fluid chromatography. Enantiomer separation was optimized by using the tuned parameters of flow rate, temperature and pressure. This optimization was verified with resolution and selectivity calculation.

The purification of fats and their ester derivatives was accomplished using supercritical fluid chromatography(Senorans & Ibanez, 2002). Various scientific methods were reviewed to purify the fatty acids and their ester moieties. The tuned parameters of the MP and SP were studied for open-tube and packed-tube supercritical fluid chromatography. The move toward the polar tuning of the SP as a method of raising the span of components studied via supercritical fluid chromatography utilizing neat carbon dioxide is detailed for fatty acid compounds. Consequently, using pure carbon dioxide negates the need for using co-solvents in supercritical fluid chromatography.

Table 2.2 shows some additional applications of supercritical fluids being used in food biotechnology. The removal of fats, alcohols and enrichment of key vitamins are shown in Table 2.2 (Johannsen, 2007). These processes include supercritical fluid chromatography and supercritical fluid extraction.

Table 2.2. Additional Applications of SCF in Food Biotechnology

Application	**From**	**Investigators**
Removal of Fatty Acids	Food Products	(King, Johnson, & Friedrich, 1989)
Enhancement of Tocochromanol (Vitamin E)	Natural Sources	(Brunner, 2005)
Enhancement of Beta-carotene (Vitamin A)	Natural Sources	(Sanal, Bayraktar, Mehmetoglu, & Ucalimli, 2005)
Reduction of Alcohol	Beer and Wine	(L'Italien, Thibault, & LeDuy, 1989) & (Guvenc, Mehmetoglu, & Calimli, 1998)
Encapsulation of Fluids	Engineering Solid Applications	(Heremans & Smeller, 1998)

2.5.3. Pharmaceuticals

The retention characteristics of pharmaceuticals in supercritical fluids with polar stationary phases were studied by means of linear solvation energy relationships or LSER for short (Bui, Masquelina, Peruna, Castlea, Dagea, & Kuoa, 2008). More than 200 drug-like compounds were examined. The main contributor to useful interaction was found in the hydrogen donor acid bonding of the analytes. Specifically, for columns using sorbent made of amines and pyridines. An additional provider to enhanced retaining was the hydrogen acceptor alkalinity of the analytes fabricated for column sorbents containing diols and amine functional groups. This study proved that supercritical fluid chromatography using CO_2 modified with methyl alcohol and a polar SP closely mimicked the published HPLC experiments which used an alkane MP. A better understanding of the character of analyte-SP and analyte-MP interactions will provide a quicker and capable alternative for large volume selection of compound databases.

The prospect of successful high-throughput purifications alongside HPLC comparable run times using a series of six columns with 100,000 theoretical plates was presented (Brunellia, Zhao, Brown, & Sandra, 2008). An effective test of a group of twenty different drugs was accomplished in under 20 minutes. Optimal outcomes were obtained on by attaching the cyano-propyl columns with acetonitrile and methanol co-solvent to di-isopropyl-amine and tri-fluoro-acetic acid at 100 Bar system pressure. The thermal effect on selectivity and efficiency was noteworthy and additionally enlarged after the employment of longer packed columns.

Work aimed to develop a generic gradient method and validate it, for a pharmaceutically relevant application was the goal of this publication (Brunelli, Dunkle,

Morris, & Sandra, 2009). A secondary goal was the determination of thiourea in a pharmaceutical intermediate at low level (0.01% w/w). The applied method validation acceptance criteria were consistent with those used for Active Pharmaceutical Ingredient late stage development and regulatory submission. This suggested that with some further research and instrumental developments, SFC could potentially reach the same maturity as GC and LC. Generic conditions were CO_2/MeOH containing 20 mM ammonium acetate. The modifier was programmed from 5%, held for one minute, to 40% at 2% per minute. The pressure was 150 Bar; the temperature was 40°C, and the flow rate was 2.0 mL/min. The advantage of using ammonium acetate as an additive was that this is the preferred volatile salt for SFC/MS. System suitability and precision based on six injections of a 7.5 µg/mL thiourea (0.05% w/w) solution showed an RSD of 3.13% for peak area and of 0.09% for retention time.

2.5.4. Chiral Applications

The enantioseparation of over one hundred chiral drugs by supercritical fluid chromatography was reviewed (Felix, Berthod, Piras, & Roussel, 2008). The mobile phase compositions with organic modifiers were detailed. These data were gathered and assembled from the ChirexBase library located in Marseille, France. The chiral pharmaceuticals integrated are classified consistent with their therapeutic properties and functionality.

The function of the MP impeded the exploit of numerous classifications of chiral stationary phases (CSPs) such as crown ether SPs, ligand exchange SPs, and protein CSPs. The poly-saccharide CSPs accounted for 60% of the chiral purifications reviewed.

Another review outlined the purification of enantiomer drugs using HPLC, capillary electrochromatography, SFC, sub-critical fluid chromatography, and thin layer chromatography employing poly-saccharide chiral stationary phases (Ali, Saleem, Hussain, Gaitonde, & Aboul-Enein, 2009). Coated versus immobilized CSPs were evaluated. A comparison of different chiral stationary phase producing companies was presented as well.

Enantioselective chromatography and its uses in SFC were reviewed (Huhnerfussa & Shah, 2009). Supercritical fluid chromatography was shown to be a robust method for the discernment of biotic and non-biotic conversion methods of enantiomeric ecological pollutants. Another review of chiral supercritical fluid chromatography spanning the published works from the year 2000 on also appeared (Mangelings & Vander Hayden, 2008). (2, 2, 2)-tri-fluoro-ethanol or TFE for short was studied as a substitute co-solvent for the identification and separation of polar organic susceptible compounds by supercritical fluid chromatography (Byrne, Hayes-Larson, Liao, & Kraml, 2008). Five enantiomers were chosen for their susceptibility to alcohol. They were studied with TFE and poly-saccharide and Pirkle type CSPs to generate selectivity and resolution up to 1.5 and 7.3 respectively.

Simulated moving bed, preparative HPLC, and SFC have been illustrated by three case studies in a published paper (Freund, Abel, Huthmann, & Lill, 2009). Various methods were compared, and their pros and cons were evaluated. The most powerful separation technology was suggested to be simulated moving bed or SMB. These results are reflected by some commercial drugs where the manufacturing processes involve SMB. Capital costs are high, and SMB is restricted to binary separations however.

"SFC is superior to HPLC, but HPLC systems are omnipresent," as Leslie Ettre has written. The most progress in chiral chromatography will be made in the field of stationary phases, but it is important to note once again that some patents of the most successful chiral stationary phases have expired (Ettre, 2000).

In Chapter 3, a brief theoretical background of isotherms will be presented. This includes some thermodynamic formulations and isotherm determination methods. Additional isotherm model equations are presented as well.

CHAPTER 3

THEORETICAL BACKGROUND OF ISOTHERMS AND ISOTHERM DETERMINATION

The greatest distinction may be made regarding analytical versus preparative chromatography by extending the range of interest of the isotherm from the linear to non linear region. A complete picture of solute loading behavior must be examined carefully. Published works that develop the foundations of these thermodynamic fundamentals are well outlined by (Ruthven, 1984) and later by (Guiochon et al., 2006). To design a preparative chromatograph, the information found in fundamental thermodynamic relationships is needed. These relationships are defined by the adsorption equilibrium isotherm. Josiah Willard Gibbs described this thermodynamic equilibrium as the chemical potential equality of all interacting phases. The well-developed thermodynamic methods that exist for predicting gas-liquid equilibria do not yet exist for the theoretical purpose of determining isotherm data. Therefore, these equilibrium relationships need to be determined by experimental means.

Different methods have been developed and used to establish isotherms by experiment. Chapter 3 reports various ways to measure quantify sorption data. These methods are be discussed and evaluated. Professor Georges Guiochon has spent forty years of work on this subject and is this author's primary source and inspiration.

3.1. Experimental Determination of Adsorption Isotherms

The design and optimization of a preparative supercritical fluid chromatograph requires that the isotherms of the system under study be identified. These functions cannot be determined without experiment. Different methods are employed to calculate isotherms by experiment. Many of the main techniques used to gather sorption isotherms are presented in this chapter. The primary focal point is the technique where a transient change is made to the sorption system. Then the analyses of the sorption bands are gathered by detection at the end of the chromatographic system. In some published works, techniques of isotherm measurement are reviewed and contrasted (Huber & Gerritse, 1971), (Jacobson, Frenz, & Horvath, 1987), and (Seidel-Morgenstern, 2004).

3.2. Isotherm Development

The adsorption of molecules on to a solid phase may be quantified as a load. The subsequent surface load is the amount of sorbed material per unit area such as the dimensional units mg/cm^2. On the other hand, the inside surface area of a sorbent is tough to quantity and is usually proprietary knowledge of stationary phase manufactures. That is why it is more common to see dimensional units of mass per unit volume or mass per unit gram of adsorbent.

Thus, the loading expressed as mg/g although strange at first glance, actually signifies milligrams of solute per gram of adsorbent material. This is a useful approach for downstream, scale up purposes.

Additionally, the adsorbent volume may be used to express the frame of reference for loading. The adsorbent volume V_{ads} represents the total adsorbent volume while the solid phase volume is denoted by subtracting the pore volume from the total volume (V_{ads}-V_{pore}). The following equation represents the total loading of adsorbent.

$$q_i^* = \varepsilon_p C_i + \left(1-\varepsilon_p\right) q_i \tag{3.1}$$

This relation is both useful and equivocal as it contains a loading term q_i on both the right and left side of the equation. The q_i^* represents the total load of the adsorbent and the q_i represents the pure solid load. The porosity of the particle system is ε_p and the initial solute concentration is given as C_i. A clear frame of reference must be kept in mind when reviewing published works in this field as contributions are made by those from the chemistry world as well as chemical engineering world and so on. A graphical presentation of the pure solid loading may be seen in Figure 3.1 (Schmidt-Traub, 2005).

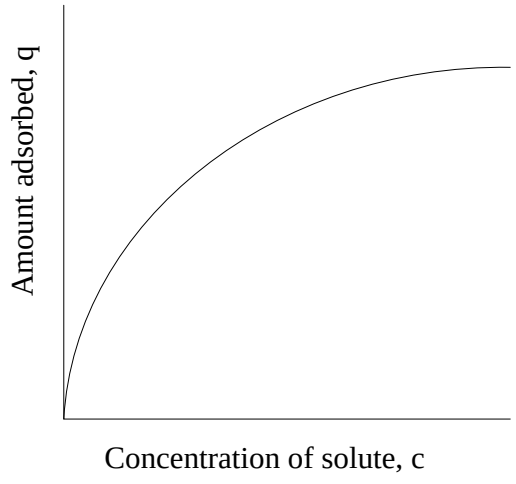

Figure 3.1. Concave Isotherm with Favorable Loading

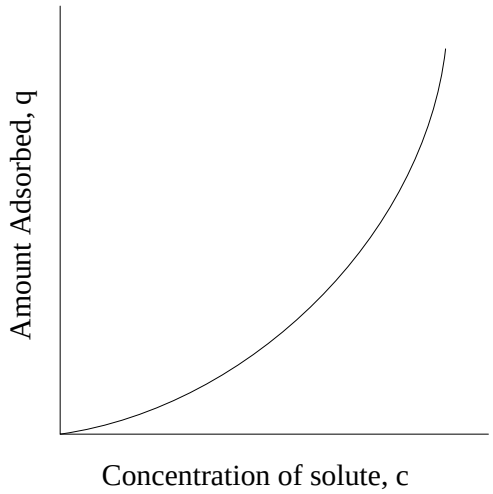

Figure 3.2. Convex Isotherm Shows Unfavorable Loading

Figures 3.1 and 3.2 depict typical isotherm shapes showing their concave and or convex nature. The adsorption equilibrium isotherm is therefore a graphical illustration of the loading or total sorbent loading versus solute concentration in the MP at isothermal conditions. Interestingly, predictive methods for VLE systems exist but do not for the theoretical calculation of sorption isotherms. Moreover, the only way to construct a multi component isotherm is by first using a pure component isotherm.

Therefore, the importance of repeated experimental technique over excessive statistical methods and computer simulation will always be preferred by this author to accurately model real physical systems.

A tremendous amount of work has gone into the modeling and simulation of preparative chromatography. As a result many models of isotherms have been suggested to represent experimentally determined data. Interestingly, there are more isotherm models available than isotherm determination methods. Nonetheless, many of these mathematical equations are useful and have their roots primarily in gas adsorption. Extensive published work may be found in the textbooks of (Guiochon et al., 2006), (Ruthven, 1984), and (Do, 1998).

The adsorption isotherm is the influencing factor of the chromatogram. This is why it is necessary to determine single and multi-component isotherms of a system with good accuracy. Another important aspect is to determine the unidentified parameters for a chosen isotherm model. Some special parameters like the Henry coefficient and saturation capacity are shared with all of the isotherm model equations. Most often, the choice of a particular isotherm model needs to be made on its capability to forecast the experimentally determined solute bands as opposed to the curve matching routine using equilibrium data. More detailed information on isotherm determination methods may be found in well-written monographs (Guiochon et al., 2006). Table 3.1 provides a summary of static isotherm determination methods (Schmidt-Traub, 2005).

The methods are differentiated by their experiment difficulty and precision. Also, they are restricted to chromatographic systems and availability of materials. Moreover, most techniques are inappropriate for columns with few theoretical plates. The experimental set-up should be a close replication to scaled-up operating conditions for preparative work.

Table 3.1. Static Isotherm Determination Methods

Name	**Methods**	**Isotherm**	**Comments**
Batch Method (Closed system)	-Immersion of Adsorbent in Solution -Mass Balance	Single and Multi-Component	-No packed column -No Detector Calibration -Tedious
Adsorption/ Desorption Method	-Loading and Unloading of Column -Mass Balance	Single and Multi-Component	-Detector Calibration Needed -Arduous but Accurate
Circulation Method	-Closed System -Stepwise Injection & Circulation of Components Until Equilibrium -Mass Balance	Single and Multi-Component	-Lower Amount of Sample Material Error Accumulation From Injection Possibility for Automation

Table 3.2. Dynamic Isotherm Determination Methods

Name	**Methods**	**Isotherm Type**	**Comments**
Frontal Analysis	Integration of Step Response (Breakthrough Curves)	Single and Multi-Component	-High Accuracy -Vast Sample Use -Suitable for Low Efficiency Columns -No Kinetic Errors
Analysis of Disperse Fronts: ECP and FACP	Numerical Integration and Mass Balance Pulse or Step Injection of High Concentration Slope of Dispersive Rear	Single and Multi-Component	-Efficient Columns -Detector Calibration
Peak Maxima	Peak Injection with Systematic Overload Peak Maximum Equal to Retention Time	Single and Multi-Component	-Small Sample Amounts -Less Sensitive to Low Efficiency Columns

3.3. Equilibrium Isotherms

Equilibrium isotherms are thermodynamic functions relating two phases in equilibrium. Isotherms represent the interaction between the amount solutes distributed between the stationary and mobile phase of the chromatograph at constant pressure and temperature. Isotherm attributes are a function of the interaction of the compounds with the MP and SP.

It is vital to know sorption isotherm in order to measure the elution band profile at high concentration. Departure from steady state in a chromatographic system is seldom important when using chromatographic systems. This is avoided in choosing the proper systems so as to minimize phase deviation. Diffusion is also a result when equilibrium is departed from in a phase system. High flow rates avoid diffusion influences almost completely (Guiochon et al., 2006).

In analytical applications, the solute concentrations in the MP are usually low. For cases like these, linear models can be assumed for the isotherm. Therefore at steady state, the solute concentration in the MP is a linear function to its concentration in the SP.

Linear isotherms are often assumed in many analytical chromatographic experiments. However, this breaks down as the concentration of the solute increases and loading enters the non-linear portion of the isotherm. This is the case in most large scale chromatographic systems. In the non-linear portion of the isotherm, the solute concentration is no longer proportional to its stationary phase or loading concentration.

Chromatographic purification is a physical separation method. Predominantly, a solute mixture is separated. Additionally, the MP sometimes is used modified rather in its pure form. These modifiers or co-solvents interact more with the SP and aid in the achievement of a particular separation goal.

At large solute amounts, the compounds dissolved in the feed mixture vie for interaction with the stationary phase. However, the stationary phase has a maximum amount of interaction energy and available sites for sorption. This is seen in some systems where competition is a result of the sorbent saturation capacity.

It becomes too complicated to track the influence of each solute, co-solvent, displacer, and modifier in a chromatographic system. Thus making the relation between the key players in a feed stream rather than all of the compounds is sufficient when modeling these complicated systems

Often it is sufficient to track only the concentrations of a couple moieties in order to determine the equilibrium concentration in both the stationary and mobile phases (Guiochon & Lin, 2003). The solute curves of many compounds in a feed may be resolved from their competitors. Upon sample introduction the localized solute concentration is desorbed near to a known elution profile and has an influence on the isotherm. This is due to the steric effect that the solute has on other surrounding compounds eluting at the same time.

To better comprehend the essentials of the interaction mechanics at a definite concentration, it is important to start by close examination of the pure component isotherm. Using a chromatograph consisting of 100% MP or an MP an co-solvent mixture with a minimum of entrainer composition so as not to be in competition with the solute under study.

Sorption of gases on a solid phase as well as liquid vapor equilibrium has had more detailed examination than LC or SFC (Ganetsos & Barker, 1993). LC or a liquid and solid system of sorption has grown in importance primarily due to the amount of energy and research put into gas-solid systems. Multi-component sorption competitive sorption are research areas for future exploration (Do, 1998).

The development of preparative chromatography and its applications are improving. In the following section, the fundamentals of adsorption are presented. Problems arising from the surface heterogeneity of adsorbents may have considerable importance in practical applications.

The retention mechanism involved in multi-component sorption is still not well understood. Moreover, the thermodynamic functions that drive multi-component systems are still not easily simulated or modeled. However, those in engineering and chemistry disciplines of study continue to develop methodologies and techniques that advance the study of these complex systems. The development of more consistent stationary phases is one key direction of research. Also, stationary phases with more binding sites and less silanol groups will be the future for those companies manufacturing chromatography columns.

3.3.1. Basics of Sorption Equilibria

Phase equilibrium is integral to thermodynamic study. Phase equilibrium deals with the sensitivity states of matter have with intensive variable changes. Intensive variables like temperature and pressure effect the mobile composition.

The phase systems in liquid-solid chromatography are sensitive to intensive variable changes. HPLC is an extension of LC employing a sorbent phase and a fluid phase. The sorbent phase is a solid. This solid phase has functional moieties that interact with certain compounds dissolved in the fluid solution.

Stationary phases may additionally be relatively inactive like silica gel. Just a solid phase that is porous will enact phase equilibrium with certain feed mixtures. To better understand the extent of this phase equilibrium a graph is made showing the isotherm. Isotherms are graphs of the amount of sorbed compound in equilibrium with its corresponding fluid concentration.

Willard Gibbs first provided the theoretical background for the thermodynamics of sorption. His relation shows the concentration of sorbed species per surface area including surface tensions and forces. Gibbs primarily focused on solid and vapor phase equilibrium. Solid and liquid phase thermodynamics become much more complicated.

In solid and liquid phase equilibrium, the liquid phase rivals the dissovel solute for interaction sites on the solid or stationary phase sorbent. This is not so in the gas of GC where the gaseous phase does not interfere with the sorbing solute. Therefore, the majority of solid and liquid phase equilibrium is still empirically derived. Solid and gas phase equilibria are classified into six main types. The classification is based on the shape of the isotherm, as shown in Figure 3.3.

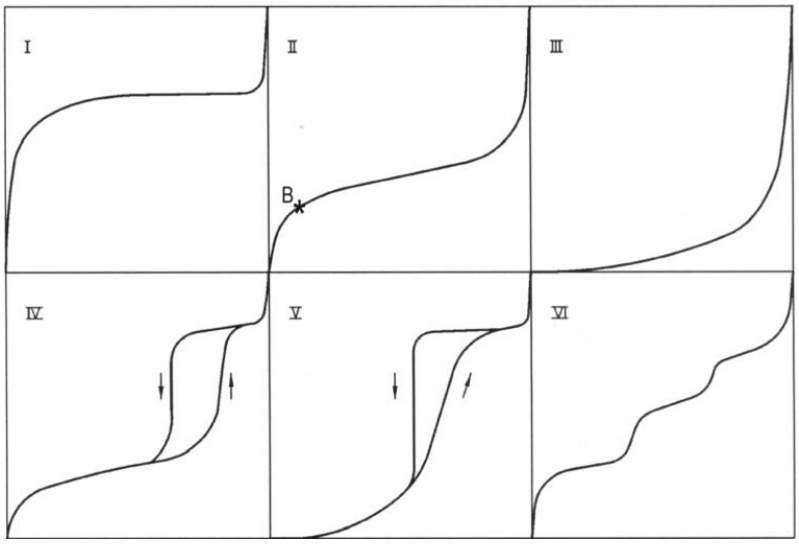

Figure 3.3. Isotherm Classifications According to Shape

Langmuir isotherm model is represented in Figure 3.3 as class I. Class I isotherms dominate adsorption classification. Class II isotherms have a concave up shape which is representative to the pressure exerted by the solute while in phase equilibrium. Class III isotherms are similar to class II as shown in Figure 3.3. The intermediate slope has been thought to be a result of condensing MP in the pore structure of the solid substrate.

According to Guiochon, there is little equivalence in solid and liquid phase equilibrium. This may be due to solvent's solubilizing power of the solute of interest and its finite capacity on the column. Moreover, isotherms are determined up to the stationary phase column saturation capacity. The isotherm provides information up to the saturation capacity of the column at which there is little change in the isotherm slope (Guiochon et al., 2006).

Isotherms exhibiting shapes consistent with class IV and class V show a hysteresis. This could be a result capillary condensation and or more than one layer of solute sorption being formed. It is abnormal in solid and liquid sorption for solutes bound to the SP to create more than one level of coating. This single layer is often called the mono-layer in sorption studies. The reasons why liquid and solid systems and supercritical fluid and solid systems do not promote solute multi-layer formation is an area for further investigation. Guiochon suggested that the formation of mono-layers could be a result of solute-solute interaction.

3.3.2. Thermodynamics of Sorption

Sorption systems may be accounted for by starting with the laws of thermodynamics. Writing Equation 3.2 which includes the thermodynamics' first and second laws account for the sorbed compound in a sorption system at equilibrium.

$$dG_{ads} = - S_{ads}dT + V_{ads}dP - \phi dn_a + \mu_{ads}dn_{ads} \qquad (3.2)$$

In Equation 3.2, G_{ads}, S_{ads}, V_{ads}, ϕ, and μ_{ads} are parameters of the solute in the sorbed equilibrium phase. The n_a term stands for the number of moles of sorbent and is assumed to be negligible in the sorption process for modeling purposes.. The molar Gibbs free energy of the solute in the sorbed phase is given by G_{ads}. The molar entropy, of the sorbed phase is given as S_{ads}. Also, T is the temperature of the system, μ_{ads} is the chemical potential, P the pressure, V_{ads} is the molar volume, n_a is molar amount of solute,

W_{ads} is the molar amount of sorbent, and ϕ is the internal energy change per unit mol of sorbent (Guiochon et al., 2006).

Phi or ϕ is a function of the spreading pressure Pi or π, and is given by Equation 3.3. Equation 3.3 relates the internal energy to the spreading pressure and is written as:

$$\phi dn_a = \pi dA \tag{3.3}$$

where A is the area of the sorbent surface. Spreading pressure may be related using Equation 3.4 and is shown as such:

$$\pi = -\left(\frac{\partial U_{ads}}{\partial A}\right)_{S_{ads} V_{ads} n_{ads}} \tag{3.4}$$

The molar internal energy or U_{ads} of the solute in the adsorbed phase is in the numerator of Equation 3.4. Since the spreading pressure is used it should be noted that this relationship represents the physical distinction between a solute free sorbent bed and solute loaded sorbent bed. Also, the assumption of perfect isothermal and isobaric system parameters is used to continue model development. Moreover, the isoteric heat of adsorption is assumed to be negligible as well. Using these assumptions, Equation 3.2 may be integrated while keeping constant the temperature and pressure terms to give Equation 3.5:

$$G_{ads} = -\phi n_a + \mu_{ads} n_{ads} \tag{3.5}$$

Taking the first derivative of Equation 3.5 and then subtracting the result from Equation 3.2 provides Equation 3.6. Equation 3.6 is shown below and may be further manipulated.

$$n_a d\phi = A d\pi = n_{ads} d\mu_{ads} \tag{3.6}$$

The Gibbs Duhem relation is modeled in the same fashion as the result shown in Equation 3.6 (Prausnitz, Lichtenthaler, & Azevedo, 1999). The Gibbs model is shown in Equation 3.7 and is a result of substitution of the chemical potential by the ideal gas equation. Equation 3.7 shows this resultant substitution.

$$A\left(\frac{\partial \pi}{\partial p}\right)_T = \frac{RT}{P} n_{ads} \tag{3.7}$$

By assuming an EOS for the sorbed phase and starting with the Gibbs model, several fundamental isotherm models may be written. They are the Linear, Langmuir, Volmer, van der Waals, and Virial isotherms.

3.3.3. Linear Equilibrium Isotherm

If it is assumed that the equation of state for the adsorbed phase is similar to the equation of state of an ideal gas, Equation 3.8 results

$$\pi A = n_{ads} RT \tag{3.8}$$

which combines with the Gibbs isotherm in Equation 3.7 to give the relation for the spreading pressure. Equation 3.9 shows how the spreading pressure, Henry coefficient, H and system pressure, P are related.

$$\pi = HP \tag{3.9}$$

The equation can be extended to relate the SP solute amount, q with the MP solute amount, C. Equation 3.10 shows the relation the loading has with other properties of the chromatographic column. The linear isotherm is shown in Equation 3.10.

$$q = \frac{n_{ads}}{A} = \frac{Kp}{RT} = HC = k' \frac{\varepsilon}{1-\varepsilon} C = \frac{k'}{F} C \tag{3.10}$$

In Equation 3.10, H represents the initial slope of the isotherm and is known as the Henry constant of adsorption. The retention factor is given as k'. Note $k'=(t_R - t_M)/t_M$, where the retention time is t_R, and the hold-up time is t_M. The phase ration is given as F. Note that $F=(1-\varepsilon)/\varepsilon$, where the column void is ε. The column void is the amount of the column the fluid phase can contact.

In the linear isotherm relationship, the concentration of the analyte sorbed onto the SP is a linear function to the concentration of the same analyte in the MP. The linear model is often used in chromatographic separations on analytical scales since the amount of analyte is small. The linear model breaks down when higher analyte amounts are charged onto the column. This is when the interactivity and competition become important to track (Guiochon & Lin, 2003).

3.3.4. Langmuir Isotherm Model

It was postulated that an equation of state more detailed than the linear isotherm should be formulated. This EOS accounts for the limited area taken by a sorbed speicie on the stationary phase. Equation 3.11 closely resembles an EOS for a gas system where the volume is accounted for.

$$\pi(A - \beta) = n_{ads}RT \tag{3.11}$$

Differentiation of Equation 3.11 gives Equation 3.12:

$$\left(\frac{\partial\pi}{\partial A}\right)_T = -\frac{n_{ads}RT}{(A - \beta)^2} \tag{3.12}$$

Combining Equations 3.11 and 3.7 results in Equation 3.13. Note that the Gibbs model is Equation 3.7. Equation 3.13 is shown below.

$$\frac{dp}{p} = -\frac{AdA}{(A - \beta)^2} \tag{3.13}$$

Equation 3.13 may be integrated assuming that low interaction. Then the following relation is shown in Figure 3.14. Theta represents the surface solute coverage.

$$bP = \frac{\theta}{1 - \theta} \tag{3.14}$$

In Equation 3.14, $\theta=2\beta/A$ which is also$=q/q_s$. The last term represents the ratio of loading to the saturation capacity of the column. Equation 3.14 may be shown in the more useful form as in Equation 3.15. The Langmuir model is represented by both Equation 3.14 and Equation 3.15 shown below.

$$q = \frac{bq_s P}{1 + bP} \tag{3.15}$$

The primary benefit that the Langmuir model has is that upon mathematical manipulation the pure component loading, q may be determined. The Langmuir model can be solved for explicitly as opposed to the other isotherm models detailed in this chapter.

The Langmuir model is also valid for an ideal gas in addition to a liquid and a supercritical fluid. This is due to the assumption of low solute-solute interaction and the composite isotherm character. Statistical thermodynamics has supported the Langmuir model as thermodynamically consistent as well. This is achieved by assuming an ideal gas phase in steady state with an ideal solid phase. Next, one assumes a binding site density of unity. Next, it is assumed that the binding sites are uniform and contain an equal amount of latent energy. Lastly, it is assumed that the solutes themselves do not interact with each other.

A kinetic explanation of the Langmuir model may be written. The sorbent is occupied by a definite amount of sorption sites with the capability of binding with only one solute species. Next, the MP is assumed to be ideal. Also, no solute-solute interactions are occurring.

Then the extent of sorption of solutes from the MP is a function of the binding site density and the system pressure. Then Equation 3.16 may be written as:

$$\left(\frac{dQ}{dt}\right)_a = k_a P(1 - \theta) \tag{3.16}$$

where θ is the SP coating. The speed of sorption is then a function of the extent of stationary phase coating of solute. This may be written as Equation 3.17.

$$\left(\frac{dQ}{dt}\right)_d = k_d \theta \tag{3.17}$$

Equation 3.17 is similar to Equation 3.14 At steady state the two rates of sorption cancel out when $b = k_a/k_d$.

3.3.5. Volmer Isotherm Model

Keeping the same assumptions with regards to β with respect to A, the integration of Equation 3.13 or the Gibbs model yields the Volmer isotherm.

$$bP = \frac{\theta}{1 - \theta} e^{\frac{\theta}{1 - \theta}} \tag{3.18}$$

In Equation 3.18, θ is given as β/A. In solid and liquid or solid and SF chromatography, $\theta=q/q_s$ and the concentration, C is substituted instead of P, the pressure. Equation 3.18 is not as useful as the Langmuir equation however. This is because Equation 3.18 may not provide a solution of theta, thus obviating this model for preparative chromatography and modeling (Guiochon & Lin, 2003).

3.3.6. Van der Waals Isotherm Model

If one assumes that the MP is modeled using the van der Waals isotherm, then the ideal gas assumption is replaced and subsequently Equation 3.19 is written as follows:

$$\left(\pi + \frac{\alpha}{A^2}\right)(A - \beta) = n_{ads}RT \tag{3.19}$$

Following the modeling operations as detailed with the Langmuir isotherm, the van der Waals isotherm is written in Equation 3.20.

$$bP = \frac{\theta}{1-\theta} e^{\frac{\theta}{1-\theta}} e^{-\frac{2\alpha q_s \theta}{RT}} \tag{3.20}$$

3.3.7. Virial Isotherm Model

A lot of progress has been made in semi-empirical studies of the properties of fluids by using a virial EOS. A virial EOS may be used to represent the sorbed layer:

$$\frac{\pi}{n_{ads}RT} = 1 + A_1 n_{ads} + A_2 n_{ads}^2 + \ldots + A_p n_{ads}^p + \ldots \tag{3.21}$$

Equation 3.21 may be utilized with the Gibbs model from Equation 3.7. The virial isotherm equation results in Equation 3.22. The Virial equation represented in Equation 3.22, allows for equilibrium data modeling at conditions where the MP is non-ideal.

$$\frac{bP}{n_{ads}} = e^{\left(2A_1 n_{ads} + 1.5A_2 n_{ads}^2 + \ldots\right)} \tag{3.22}$$

Equation 3.22 is used often in solid and gaseous sorption studies. Many times Henry constants are determined from equilibrium isotherms. That is the benefit of using equations that model higher concentrations where non-idealities exist. If one graphed Equation 3.22 using the logarithm of bP/n_{ads} vs. n_{ads} where the isotherm is linear at low values of n_{ads}, then the Henry coefficient may be determined by the intersect of the y-axis (Guiochon et al., 2006).

Section 3.3.8 briefly details some commonly used isotherm equations. These are mainly empirical and practical models. Table 3.3 shows several major isotherm model equations along with their various limitations. A more detailed description of these isotherm equations may be found in a few key monographs (Do, 1998), (Guiochon et al., 2006), and (Tien, 1994).

Table 3.3 shows some empirical isotherm equations, which are commonly used in adsorption studies (Do, 1998). The Langmuir equation (3.15) is a two-parameter expression that represents adsorption equilibrium data of type I behavior as seen in Figure 3.3.

3.3.8. Pure Component Adsorption Equilibria

Table 3.3. Empirical Isotherm Equations

Author	Equation	Comments
Freundlich	$q = KC^{\frac{1}{n}}$	No Henry Law Limit and No Saturation Limit
Sips (Langmuir-Freundlich)	$q = q_s \frac{(bC)^{\frac{1}{n}}}{1 + (bC)^{\frac{1}{n}}}$	No Henry Law Limit and Finite Saturation Limit
Toth	$q = q_s \frac{bC}{\left[1 + (bC)^t\right]^{\frac{1}{t}}}$	Has Henry Law Limit and Finite Saturation Limit
Unilan	$q = \frac{q_s}{2s} \ln\left(\frac{1 + \bar{b}e^{s}C}{1 + \bar{b}e^{-s}C}\right)$	Has Henry Law Limit and Finite Saturation Limit
Keller et al	$q = q_s \alpha_m \frac{bC}{[1 + (bC)^{\alpha}]^{\frac{1}{\alpha}}}$	Has Henry Law Limit and Finite Saturation Limit
Dubinin-Radushkevich	$V = V_0 \exp\left[-\frac{1}{(\beta E_0)^2}\left(R_g T \ln\frac{C}{C_0}\right)^2\right]$	No Henry Law Limit, but will Reach a Finite Limit when C Goes to C_0
Jovanovich	$q = q_s\left(1 - e^{-bC}\right)$	Has Henry Law Limit and Finite Saturation Limit
Temkin	$v(P) = C\ln(cP)$	No Henry Law Limit and No Saturation Limit

Table 3.3 shows several empirical isotherm equations, which are commonly used in practice. The Langmuir equation (3.15) is a two-parameter expression that represents adsorption equilibrium data of type I behavior as seen in Figure 3.3. The Freundlich isotherm is the simplest equation to represent equilibrium data. It does have a serious defect though in that it fails to observe Henry's law behavior in the limiting situation when the pressure or concentration goes to zero. The Sips is actually the Langmuir and Freundlich equations combined. The Sips or Langmuir-Freundlich isotherm equation contains three parameters q_s, b, and n. Here q_s is the saturation capacity, b is the adsorption coefficient, and n is the reciprocal of the exponent of the Freundlich isotherm equation. There are other three parameter models such as the Toth isotherm. The Toth equation may be viewed as a modification of the Langmuir equation. The additional isotherm equations listed in Table 3.3 are not generally used for supercritical conditions. Additionally, the BET equation for multilayer adsorption is not applicable for supercritical fluid sorption.

3.4. Isotherm Determination Methods

An isotherm accounts for the knowledge necessary in understanding interactions an analyte has with a sorbent. Isotherm information will allow the better understanding of the purification problem at hand and how much SP is needed to carry it out. Moreover, isotherm determination is needed for designing chromatography purification (Guiochon et al., 2006). Regrettably, isotherm prediction is still impossible. Therefore, isotherms need to be experimentally determined.

However, the accurate determination of sorption isotherms is important. Even the slightest variation in the isotherm can propagate changes in the solute band profile eluting (Jacobson, Frenz, & Horvath, 1987). Therefore, the accurate measurement of equilibrium data is essential in sorption process modeling.

In the next section, isotherm determination methods will be discussed. The frontal analysis, frontal analysis by characteristic points and pulse methods will be presented.

3.4.1. Frontal Analysis

Determining sorption isotherms using frontal analysis or FA is the inverse method as compared to the prediction of elution bands from known isotherm equations. The theory provided in the previous sections of this chapter allows a predictive method to elucidate characteristics of elution band profiles. Additionally, the concentration on a plateau and retention time of solute wave may be used as well. Using these experimental data one may solve the inverse method of chromatography.

The FA method is often used to determine pure component isotherms from the corresponding mass at the plateau concentration of the solute shock wave. Isotherms are determined by making solute step changes in the positive or negative direction at the inlet of the chromatograph (Guiochon et al, 2006)

To model and optimize large scale purifications, identifying the fundamental thermodynamic functions, in this case the isotherm, is the key relation desired. FA is often used to measure pure component isotherm relationships.

The conjectural conditions of this method are supported by the theory of sorption. Frontal analysis measures the solute elution profile for isotherm determination. Using the SFC system, one line was delivering carbon dioxide, while the second line was submerged in a graduated cylinder containing a measured concentration of the enantiomer dissolved in the organic modifier. The amount pumped through the system from the solute reservoir was kept constant until the step response was reflected in the detector. The retention time of the breakthrough curve and the detector signal were recorded.

Figure 3.4 shows a typical flow chart for the determination of equilibrium data from experiment (Schmidt-Traub, 2005). The sorption data are gathered from experimental breakthrough of solutes through a packed column. Then the resulting chromatogram is compared to the theoretical results determined from modeling the system.

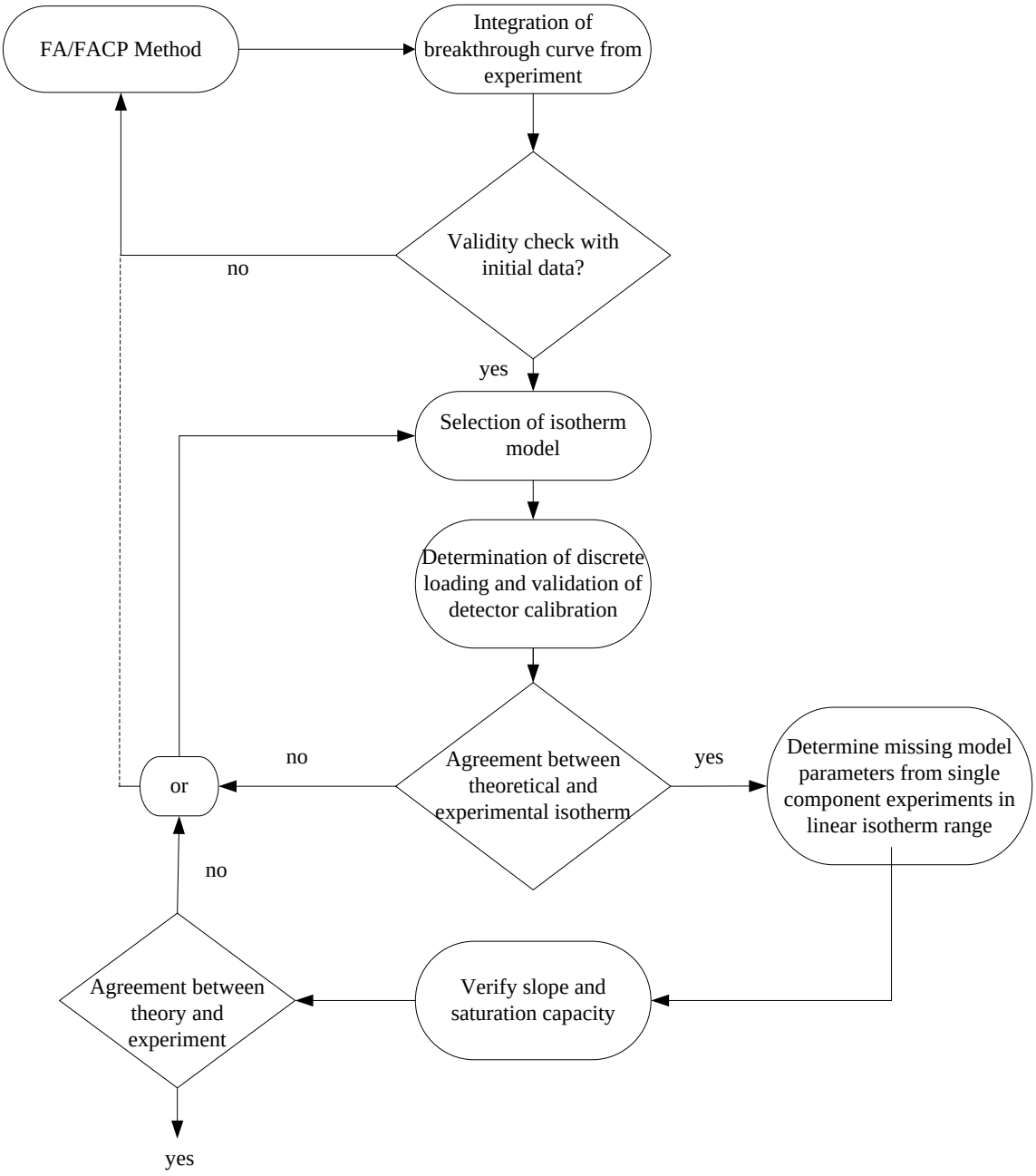

Figure 3.4. Flow Chart for Bulk Sorption Isotherm Determination

3.4.2. Theoretical Background of Frontal Analysis

The majority of dynamic isotherm determination methods rely on the analysis of experimental data within the framework of classical equilibrium theory of chromatography. This well-established theory is detailed in several great monographs (Guiochon et al., 2006), and (Laub & Pecsok, 1978). Essentially, equilibrium theory is based on the concept that only solute distribution occurs between the mobile phase and stationary phase. Kinetic effects that lead to elution profile broadening are assumed negligible.

This notion is known as the ideal model of chromatography. The shape of elution profiles and breakthrough curves predicted by the equilibrium theory is a direct function of the isotherm.

Starting with time equal to zero a step with concentration C_i is injected onto the sorbent until it hits the plateau C_f. Then once again the feed concentration is lowered to its initial state. The outflowing solute amount is detected and measured. The injection amount needs to be sufficiently great to enact a plateau concentration. Figure 3.5 is an example of this concentration step up and down in chromatographic system.

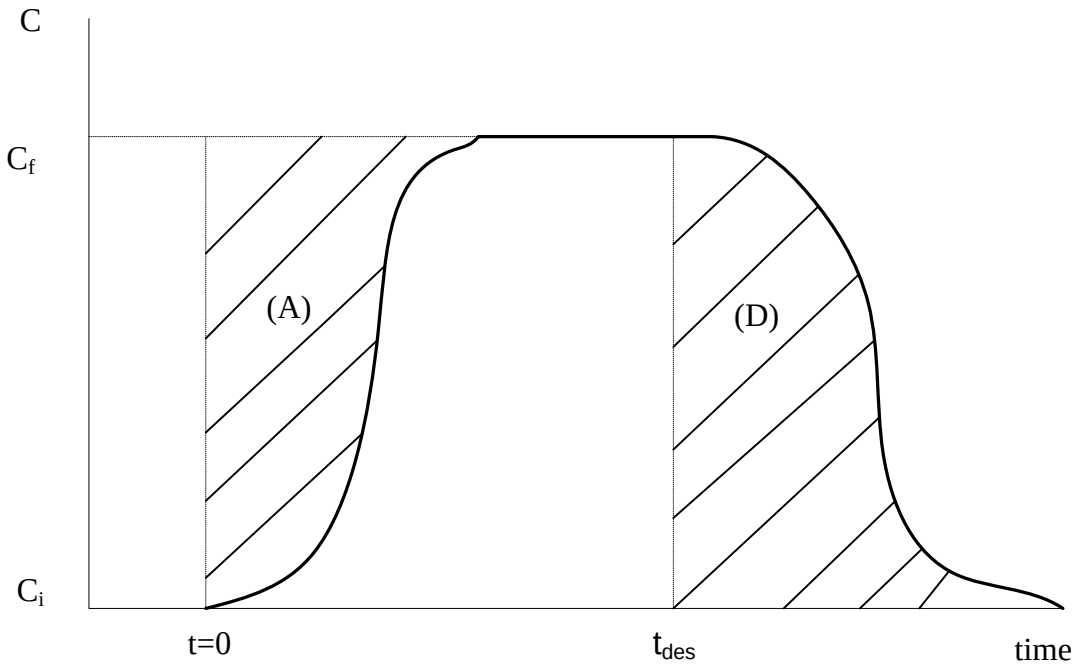

Figure 3.5. Adsorption and Desorption of Solute

After the time the solute needs to travel through the piping, it reaches the plateau and during this adsorption step a new equilibrium is established. Similarly, while the sorption step down, the starting steady state is restored with the delay of time. This is due to the expanding front in which the solute velocity is inversely proportional to the local isotherm slope. To estimate the equilibrium state established, one must calculate the overall mass balance by numerical integration. As seen in Figure 3.5, area (A) is equivalent to the solute accumulation inside the column and the piping.

$$V_{tot}(C_f - C_i) + V_c\{\varepsilon_t(C_f - C_i) + (1 - \varepsilon_t)[q(C_f - C_i)]\} = \dot{V}\int_0^{t_{des}} [C_f - C(t)]dt \qquad (3.23)$$

In Equation 3.23, V_{tot} is the total volume, V_c is the column volume, and $\dot{V}$ is the volumetric flow rate. C_f and C_i are the final and initial concentrations. Epsilon is the column porosity and q is the solute loading.

FA is simple when beginning with a clean, solute free column. Step desorption results are gathered when the concentration plateau has completely eluted. The area (D) in Figure 3.5 has to be equal to area (A). Contrast of both values may serve as a reliability check and is an independent method in its own right. Although the equilibrium theory also predicts the shape of multi-component elution profiles, frontal analysis is rarely used for the determination of competitive isotherms (Seidel-Morgenstern, 2001).

Frontal analysis measures solute loading and unloading (adsorption and desorption) on a substrate. Kinetic effects are eliminated because only the adsorption and desorption profiles are of interest in the frontal analysis approach. The quantity of solute needed for frontal analysis is high. The experimental time needed is another negative aspect of frontal analysis. Detector calibration is extracted from the detector response at the plateau of a known concentration. This is possible because we know the amount of solute entering the system. This is directly related to the signal response of the detector at column saturation. The case of adsorption in which FA is based on is the condition of a constant isotherm chord. The constant isotherm chord means that the solute concentration in the mobile phase and the initial clean-bed solute concentration breakthrough simultaneously. The inverse of the isotherm chord is also known as the minimum sorption bed requirement (Guiochon et al., 2006).

Isotherm calculation procedure of frontal analysis is shown in Figure 3.6. The detector records the chromatogram and intermediate steps are reflected in the flow chart. The flow chart for sorption data and was employed for analysis in this work.

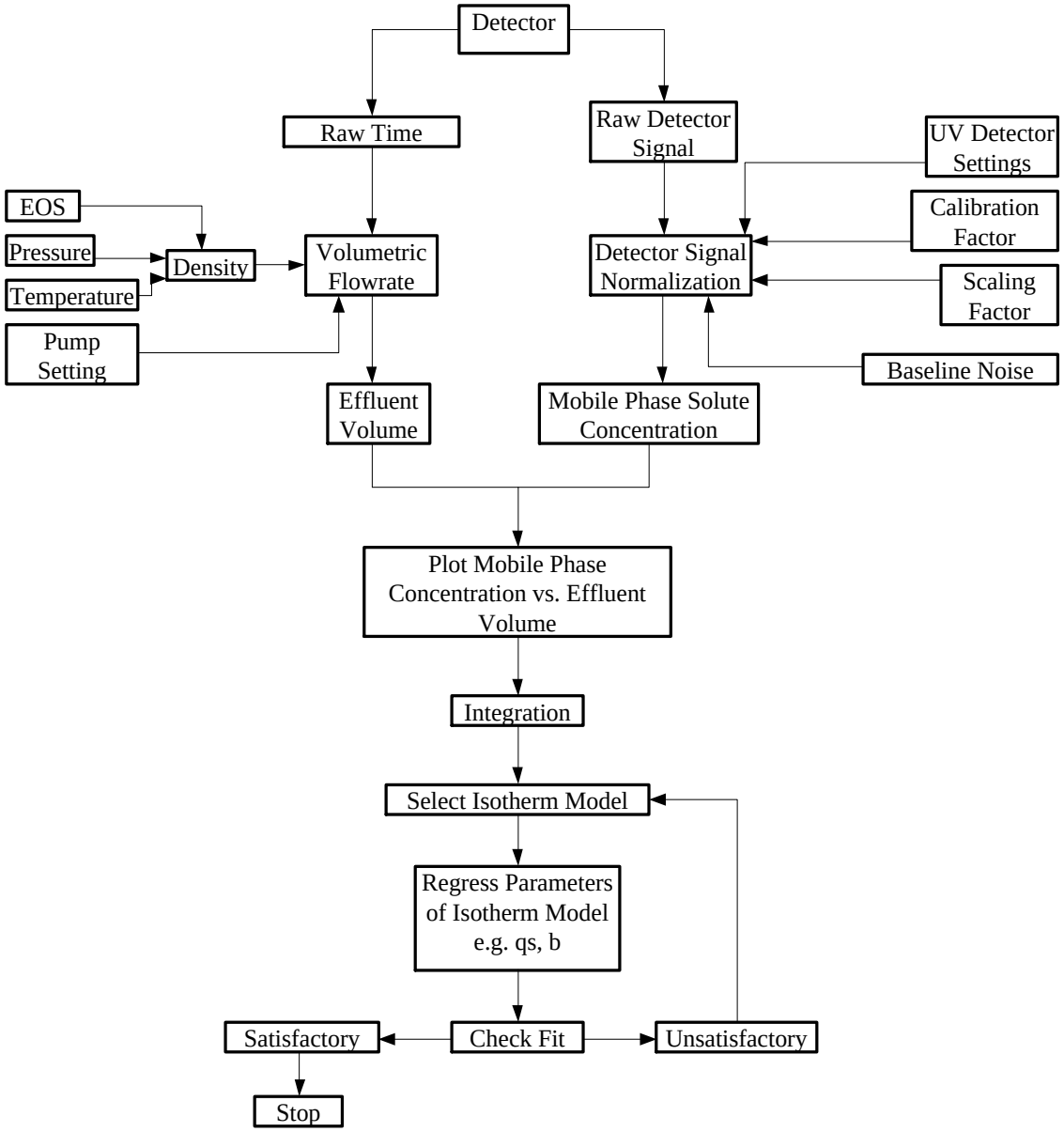

Figure 3.6. Flow Chart of Frontal Analysis Method

3.4.3. Theoretical Background of FACP Method

As the feed solution is loaded on the column forming a band, further development of the band occurs as the solutes move through the column. The regions in the front and rear of the adsorption band are called boundaries. These boundaries may be sharp or diffuse according to the type of adsorption isotherm obtained for the particular case of stationary phase, solute and mobile phase. In the case of multiple solutes the term boundary is applied to all parts where concentration gradients exist. The adsorption isotherm is the influencing factor on the chromatogram. This is why it is necessary to determine isotherms of a system with good accuracy.

Another aspect is to determine the unknown parameters for a chosen isotherm model. Some special parameters like the Langmuir adsorption coefficient and saturation capacity are shared with all of the isotherm model equations. Most often, the decision on a certain isotherm equation needs to be made on the ability to predict the experimental overloaded concentration elution profiles rather than fitting the experimental isotherm data. More detailed information on isotherm determination methods may be found in the excellent work by (Seidel-Morgenstern, 2004) and (Guiochon, 2006).

3.4.4. Mathematical Justification of FACP Method

The movement of any type of boundary is governed by the mass-conservation principle, which means that if we consider the solute content of a very thin slice of the chromatographic band, its increase or decrease is given by the difference of the inflowing and outflowing solute (Glueckauf, 1942). The movement of the elution band may be considered in two ways. The first is if one mentally fixes their eyes on a given particle of

the solute. Then this point of fixed mass within the band of single solute, the concentration moves with a given amount of mobile phase ν according to Equation 3.24 (Wilson, 1940).

$$\left[\frac{\Delta x}{\Delta v}\right]_m = \frac{c^0}{f_{(c^0)}} \tag{3.24}$$

Likewise if one tracks a point of constant concentration in a diffuse boundary which is described well by Equation 3.25 (De Vault, 1943), (Weiss, 1943).

$$\left[\frac{\Delta x}{\Delta v}\right]_c = \frac{dc}{df_{(c)}} = \frac{1}{f'(c)} \tag{3.25}$$

Upon integration the resulting equations relate the amount of solute in the elution curve between the concentrations c and c=0. In the case of the rear boundary we have Equation 3.26.

$$\mu = \bar{x} f_{(\bar{c})} - \nu \bar{c} \tag{3.26}$$

In addition, for a diffuse front boundary, as seen in Figure 3.5, we get Equation 3.27.

$$\mu' = (v - v^0)\bar{c} - \bar{x} f_{(\bar{c})} \tag{3.27}$$

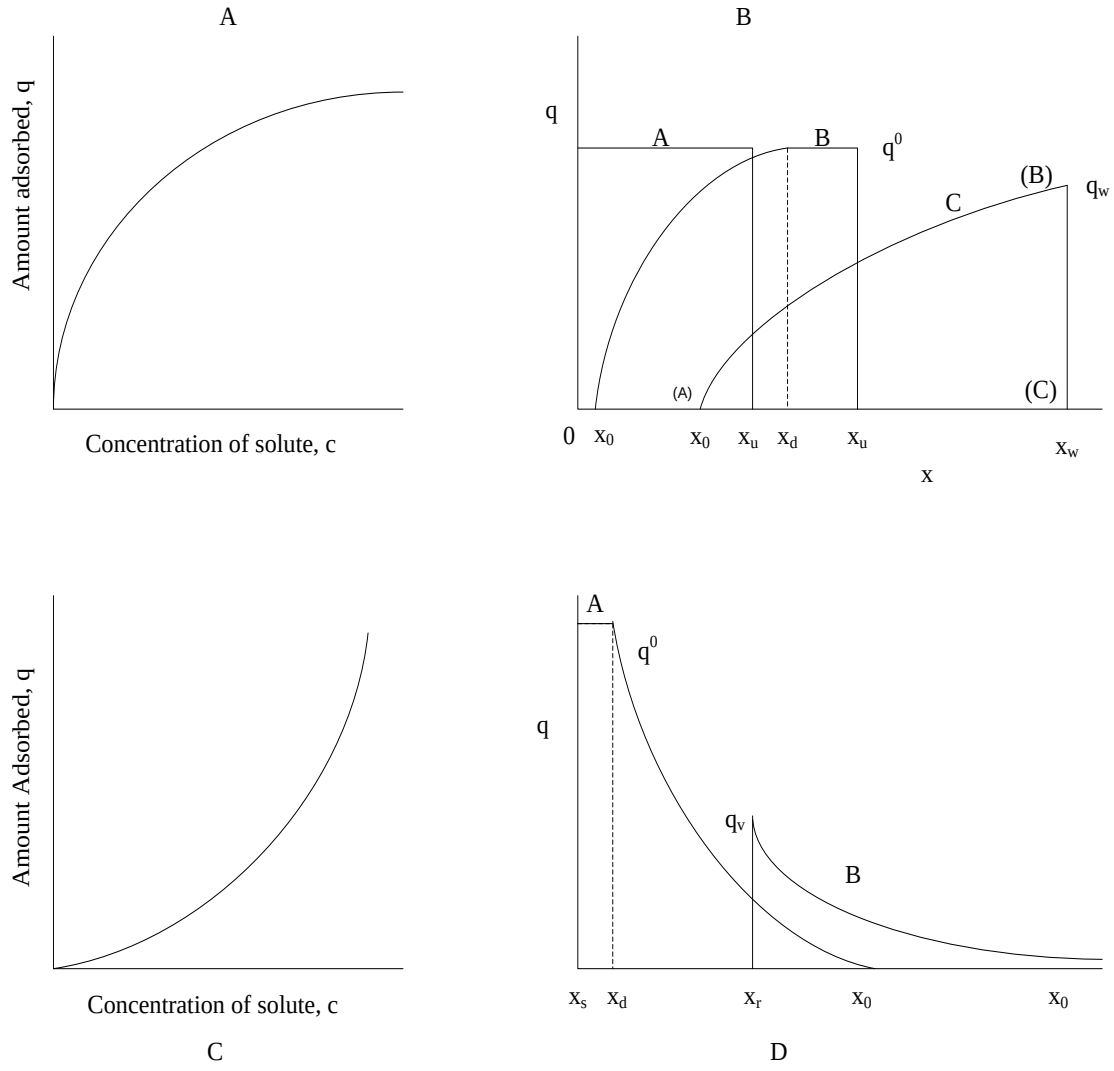

Figure 3.7. Concave and Convex Isotherm Scheme

Figure 3.7 A exhibits isotherm concave behavior. The following relations are based on the scheme shown in Figure 3.7.

$$x_0 = \frac{v}{f'_{(0)}} \tag{3.28}$$

$$x_d = \frac{v}{f'_{(c^0)}} \tag{3.29}$$

$$x_u = \frac{(v + v^0)c^0}{f_{(c^0)}} \tag{3.30}$$

$$x_w = \frac{m}{\left(f_{(c_w)} - c_w f'_{(c_w)}\right)} \tag{3.31}$$

$$v = \frac{mf'_{(c_w)}}{\left(f_{(c_w)} - c_w f'_{(c_w)}\right)} \tag{3.32}$$

The frontal concentration c_f is shown and is defined by two conditions of movement for the front boundary:

$$[x_f]_{c_f \text{const.}} = \frac{(v + v^0)}{f'_{(c_f)}} \tag{3.33}$$

From Equation 3.25 for the diffuse part is represented by Equation 3.34.

$$[x_f]_{\mu=0} = \frac{c_f(v - v^0)}{f_{(cf)}} \tag{3.34}$$

Equations 3.35 and 3.36 may be combined for the condition of c_f :

$$f'_{(c_f)} = \frac{f_{(c_f)}}{c_f} \tag{3.35}$$

The rear concentration c_e is defined by the conditions of mass conservation.

$$\frac{v}{x} = \frac{\Delta f_{(c)}}{\Delta c} = \frac{\left(f_{(c^0)} - f_{(c_e)}\right)}{(c^0 - c_e)} \tag{3.36}$$

By tracking the movement of a point of the diffuse rear boundary of constant concentration c_e.

$$\frac{v}{x} = f'_{(c_e)} \tag{3.37}$$

which leads to the result of

$$f'_{(c_e)} = \frac{\left(f_{(c^0)} - f_{(c_e)}\right)}{(c^0 - c_e)} \tag{3.38}$$

Using Equations 3.35 and 3.37 the concentrations c_e and c_f may be obtained.

3.4.5. Theoretical Background of Pulse Technique

Sorption isotherms of S and R enantiomers can be determined using pulse elution chromatography. The retention volume in an elution peak is proportional to the derivative of adsorption. The isotherms were calculated from single peaks, the height of the peak being proportional to the concentration of the enantiomer in the fluid phase. Equation 3.39 shows the volume of the gas phase V_g is equal to the tangent of the isotherm slope at its maximum loading.

$$V_g = \frac{dq}{dC} \tag{3.39}$$

The formulas used for the determination of adsorption isotherms have been modified from ECP formulas used in Gas Chromatography (Mack & Sunol, 2005). The detection method used in this experiment is a UV detector. A UV detector provides time versus absorbance data. These data are used to obtain V_g, which is shown in Equation 3.40.

$$V_g = \frac{F(t_R)}{w} \tag{3.40}$$

In gas chromatography V_g represents the volume of gas per weight of adsorbent that has passed through the chromatographic column and t_R. F is the flow rate of the mobile phase through the column and w is the total mass of packing in the column. This formula can be modified for supercritical fluids as follows:

$$V_{sf} = \frac{F(t_R)}{w} \tag{3.41}$$

V_{sf} is the volume of supercritical fluid per mass of packing material. Determination of F requires the density of the supercritical fluid in the column. The density is found with PRSV and Wong Sandler mixing rules (Patel, 2007). Next C (concentration of solute in the mobile phase) is determined.

$$C = \frac{Abs*N}{A*F} \tag{3.42}$$

Abs is the absorbance reading from the UV detector in units of volts, N is the total number of moles of solute injected and A is the total area under the curve. Figure 3.8 shows an example of the pulse method chromatogram. From the desorption part of the curve shown in Figure 3.8, the intermediate volume of the gas phase is determined. This is shown in Figure 3.9 after integration of the desorption part of the curve is performed.

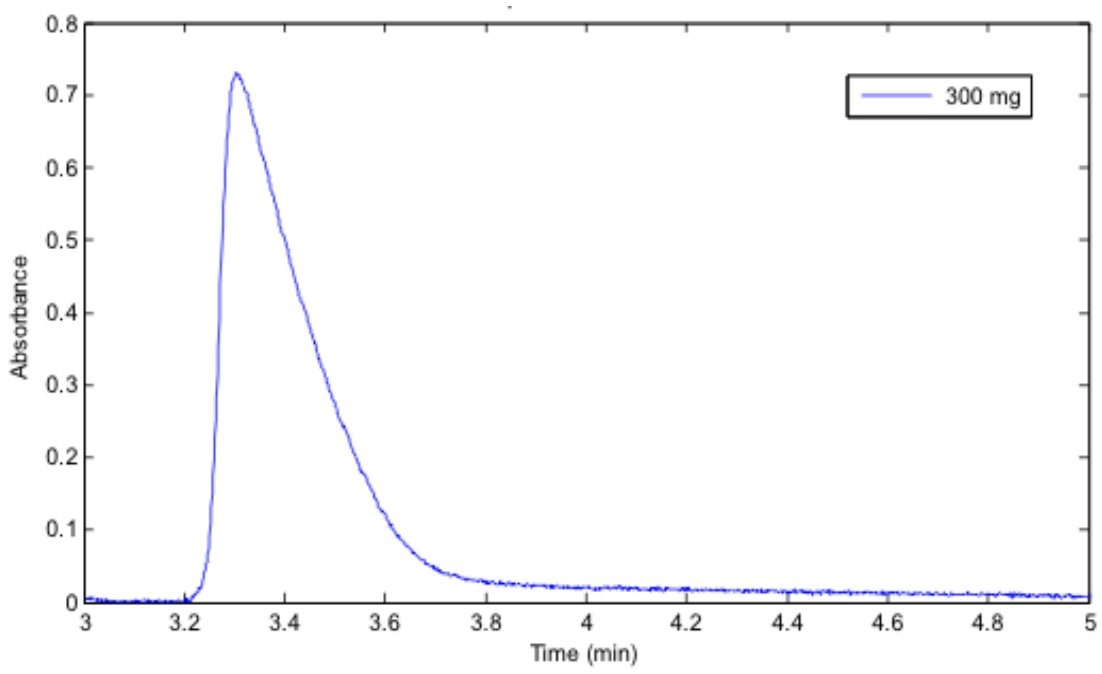

Figure 3.8. Example Chromatogram using ECP Pulse Method

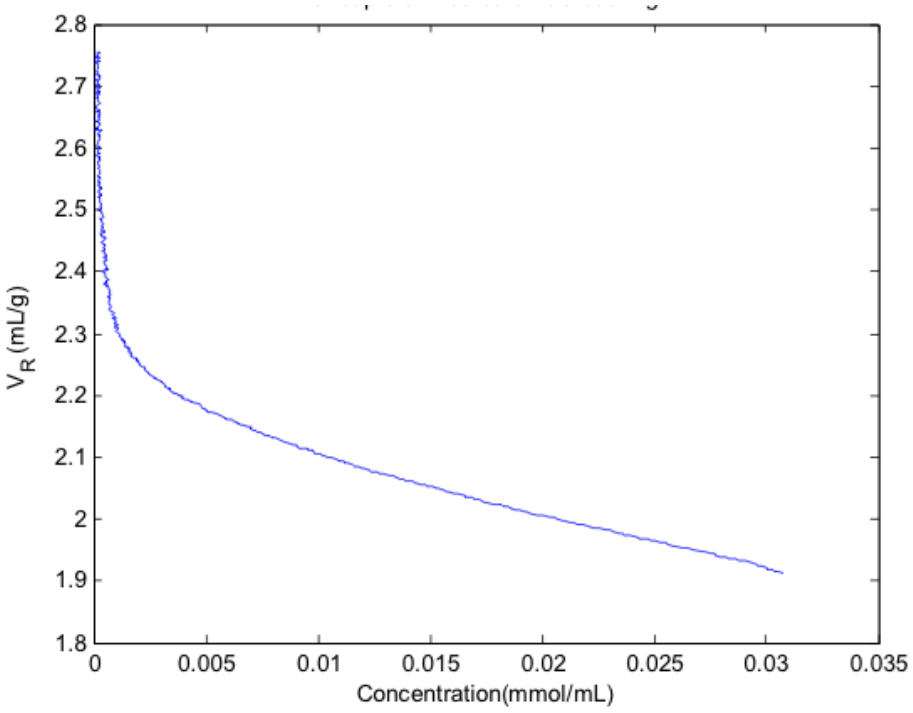

Figure 3.9. Example of Intermediate Calculation by ECP Pulse Method

Figure 3.9 is an example of the intermediate graph obtained before the isotherm is determined. To determine the isotherm, Figure 3.9 is integrated and the loading of the solute versus the mobile phase concentration is plotted.

3.5. Isotherm Calculation Mapping for Each Method

Figure 3.10 below shows the calculation mapping when using the ECP Pulse method of isotherm determination. The key distinction is that the solute is introduced as a small pulse onto a flowing feed stream of mobile phase.

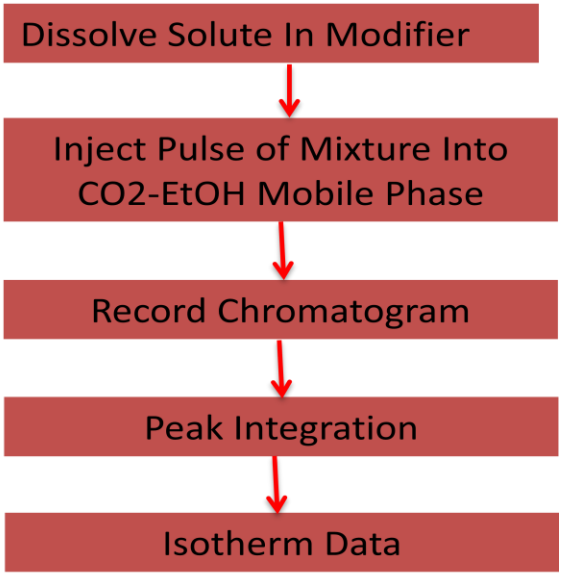

Figure 3.10. Calculation Map of ECP Pulse Method

In Figure 3.11 the calculation mapping is shown for the frontal analysis method. Here examining the front or positive step increase in the chromatogram makes the key distinction.

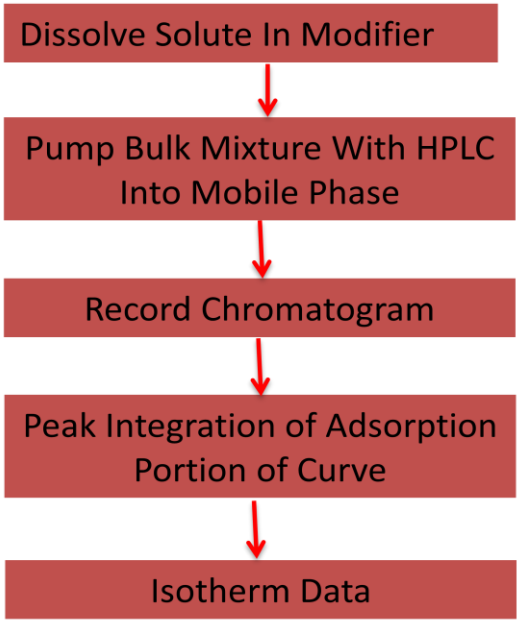

Figure 3.11. Calculation Map of FA Method

Figure 3.12 shows the FACP method mapping. The FACP method is essentially the same as the FA method. However, the negative step of the elution curve is accounted for isotherm determination.

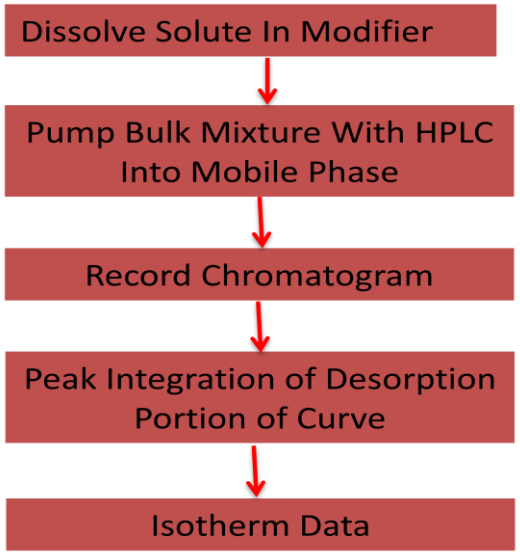

Figure 3.12. Calculation Map of FACP Method

A typical isotherm determined from the bulk and pulse method is shown in Figure 3.13. The comparison of the pulse determined isotherms versus the bulk-determined isotherms are evident. The pulse determined isotherm produces a straight line with a slope consistent with the Henry coefficient. The bulk isotherms that are determined by FA and FACP have a finite saturation capacity as opposed to a straight-line relationship. The non-linear portion of the isotherm is well accounted for using the bulk methods of FA and FACP. The initial slope is adequately accounted for using the pulse method. It is advantageous to try both experimentally in order to gain a full understanding of the system being studied. The loading information is provided on the y-axis of Figure 3.13, with the corresponding mobile phase concentration on the x-axis.

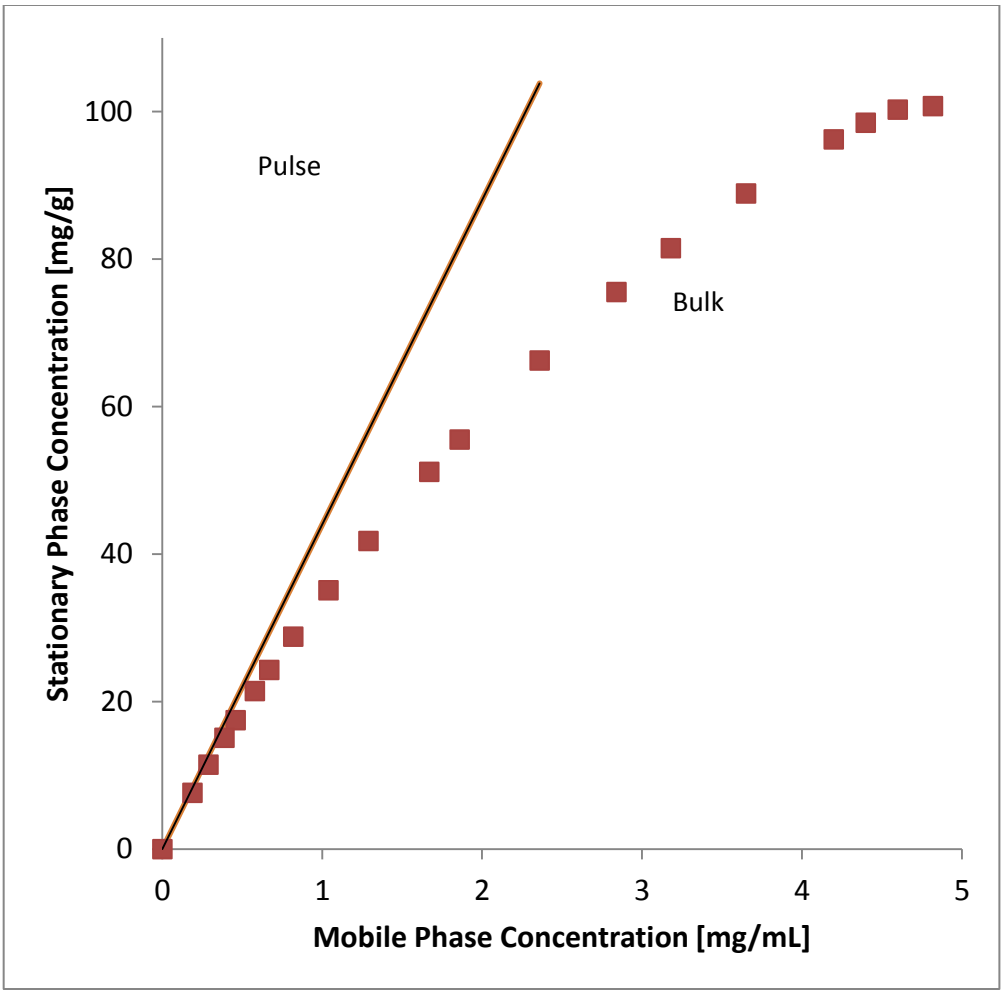

Figure 3.13. Example of Isotherms Determined by Bulk and Pulse Methods

In Chapter 4 the mathematical modeling of the chromatographic system is considered. The chromatographic column is modeled using a mass balance. The separation of two solutes is treated mathematically. Additional refinements for supercritical fluid chromatography are included at the end of Chapter 4.

CHAPTER 4

CHROMATOGRAPHIC MODELING

Tswett has been credited with the invention of chromatography. He had a substantial understanding of the physic-chemical phenomena involved in chromatography. He was a botanist and had an insouciant regard from chromatographic modeling. Moreover, his famous observations that led to the invention of chromatography were not even formulated in to algebraic relations. Modeling of chromatographic separations went largely ignored until one serious development forced the issue. During World War I, the development and use of the gas mask facilitated the analysis of chromatographic modeling. The cartridge of the gas mask essentially operated under the breakthrough principle curve, meaning the mask wearer remains well protected until the wave of toxic gas breaks through the cartridge. In 1920, Bohart and Adams developed a transport model of the breakthrough curve of the cartridge in the gas mask. This marked this first attempt at modeling nonlinear chromatography (Bohart & Adams, 1920). This work was the basis for the program written to automate the data gathering of raw elution data and perform the curve fitting isotherm method.

4.1. Types of Chromatographic Models

The complexity of the model required to simulate a particular system depends on the nature of that system, and the accuracy required. An important issue to keep in mind is the level of experimental work required to accurately determine the model parameters, and the error propagation inherent in using these parameters.

Linear chromatography assumes that the equilibrium concentration of each component in the mobile phase is always proportional to the concentration in the stationary phase. The individual components do not interact, and the band shapes and retention times are independent of sample composition or concentration. The peak heights are proportional to the feed concentrations, and the component isotherms are straight lines passing through the origin. Linear models perform well when the concentrations of solutes in the feed are sufficiently low, and generally do an adequate job in analytical chromatography. They are attractive because they are less computationally rigorous than other models, and often allow for closed form solutions.

In non-linear chromatography the concentration of components in the stationary phase is not linearly proportional to their concentration in the mobile phase. Interaction between individual components for sorption sites causes the equilibrium phase isotherms to be dependent on the system composition. Elution profiles, retention times, and peak heights are also dependent on the composition of the system. Non-linear systems are more difficult to solve in closed-form, and solution methods involve certain assumptions.

Ideal chromatography assumes that the efficiency of the column is infinite. Axial dispersion is negligible, and the mass transfer kinetics is instantaneous. In such systems, the band profiles are controlled only by the phase equilibrium, which allows for analysis

of the thermodynamic influences on separation independent of the effects of mass transfer kinetics and axial dispersion. Ideal, non-linear models are important from a theoretical standpoint, and may approximate actual behavior.

In non-ideal chromatography, the efficiency of the column isn't assumed to be infinite. Axial dispersion and mass transfer kinetics influence the band profiles to varying degrees, depending on what assumptions are made in choosing a particular model. Some important non-ideal models are described in the following sections.

The equilibrium-dispersive model assumes that all contributions resulting from a lack of equilibrium can be lumped into a constant apparent axial dispersion term. The model is a very close approximation if mass transfer in the column is controlled only by molecular diffusion across the mobile phase flowing around the packing particles and if the exchange of adsorbed solutes between the mobile and stationary phase is very rapid. This is generally the case for high efficiency chromatographic adsorbents with non-viscous solutions at low concentration (Guiochon et al., 2006).

4.2. Modeling Separation

Separation of solutes occurs in the chromatographic column because different solutes move at different velocities due to their interactions with the stationary phase. The specific solvent velocity is dictated by the equilibrium. This means that the solute motion may be predicted with an understanding of the physical geometry and mathematical modeling. Solute diffuses between the moving mobile fluid and the stagnant fluid trapped in the pores of the stationary phase. In these pores solute may adsorb on the solid or into to stationary fluid coating. The solute moving in the mobile

phase has an interstitial velocity v, of the mobile phase, while the solute either sorbed onto the solid or in the stagnant fluid has an interstitial velocity of zero. An individual solute spends time in the mobile fluid and then spends time in the stagnant fluid and back again randomly. This movement is a process of random actions and is different for each solute. Therefore, the overall average velocity of all solute molecules of a specific system is attainable. However, the prediction of the random motion is not as straightforward and is the cause of band broadening or zone spreading. The majority of solute molecules have an average velocity equal to the time they are in the mobile phase multiplied by the interstitial fluid velocity (Wankat, 1986).

$$u_{solute} = (v)(\text{fraction of solute in the mobile phase}) \tag{4.1}$$

Now if one considers the incremental change in solute concentration Δc, which causes an incremental change in the amount sorbed Δq, we get Equation 4.2.

$$\Delta c \text{ in mobile phase} = \frac{\text{Amount in mobile phase}}{\text{Amount in (mobile + stagnant fluid + solid)}} \tag{4.2}$$

The incremental amount of solute in the mobile phase corresponds to Equation 4.3.

$$\text{Amount in mobile phase} = (\Delta z A_c)\alpha \Delta c \tag{4.3}$$

In Equation 4.3, the term $(\Delta z A_c)$ represents the volume of the column segment and alpha is the fraction of that volume which is in the mobile phase. The incremental amount of solute in the stagnant fluid is represented by Equation 4.4.

$$\text{Amount in stagnant fluid} = (\Delta z A_c)(1 - \alpha)\varepsilon K_d \Delta c \tag{4.4}$$

The term $(1-\alpha)$ is the fluid fraction volume of $(\Delta z A_c)$, which is not mobile phase, and ε is the fraction of this amount that is stagnant fluid. K_d describes what fraction of the pores is available to the solute. The amount on the solid is represented by Equation 4.5.

$$\text{Amount on solid} = (\Delta z A_c)(1 - \alpha)(1 - \varepsilon)\rho_s \Delta q \tag{4.5}$$

The first three braced terms provide the volume of the solid. The delta q is typically measured in kilogram moles per kilogram solid thus the solid density ρ_s is needed to convert the volume to weight units. The solid density is the density of the packing material crushed up without any pores. So by substitution we get Equation 4.6.

$$\text{Fraction} = \frac{(\Delta z A_c)\alpha \Delta c}{\Delta z A_c\left[\alpha \Delta c + (1 - \alpha)\varepsilon K_d \Delta c + (1 - \alpha)(1 - \varepsilon)\rho_s \Delta q\right]} \tag{4.6}$$

Substituting and rearranging the previous results leads to Equation 4.7 shown below.

$$u_s = \frac{v}{1 + \left(\frac{1 - \alpha}{\alpha}\right) \varepsilon K_d + \left(\frac{1 - \alpha}{\alpha}\right) (1 - \varepsilon) \rho_s \frac{\Delta q}{\Delta c}} \tag{4.7}$$

This is the solute wave velocity u_s and represents the average velocity of the incremental amount of solute. Upon using this equation one must assume a solid fluid equilibrium in which case the linear or Langmuir isotherm models may be substituted. The linear isotherm model is the easiest to employ and is as follows in Equation 4.8.

$$q_i = k_i(T) c_i \tag{4.8}$$

Upon substitution into the result for solute wave velocity, $\Delta q/\Delta c = k_i(T)$, so the wave velocity is shown in Equation 4.9.

$$u_s = \frac{v}{1 + \left(\frac{1 - \alpha}{\alpha}\right) \varepsilon K_d + \left(\frac{1 - \alpha}{\alpha}\right) (1 - \varepsilon) \rho_s k_i} \tag{4.9}$$

Equation 4.9 states that at low concentration in the linear range of the isotherm the solute velocity does not depend on the concentration. This solute velocity is however a function of temperature and other thermodynamic quantities. This solute wave equation does predict accurately that a separation is possible but not how good it will be

because it does not account for zone spreading. It may also be extended to nonlinear systems.

In cases where the concentrations are much higher, nonlinear isotherms may be employed in the same fashion. The Langmuir isotherm model, shown in Equation 4.10 and its derivative may be used.

$$\frac{\Delta q}{\Delta c} \cong \left(\frac{\partial q}{\partial c}\right)_T = \frac{H}{(1 + bc)^2} \tag{4.10}$$

$$u_s = \frac{v}{1 + \left(\frac{1 - \alpha}{\alpha}\right)\varepsilon K_d + \left(\frac{1 - \alpha}{\alpha}\right)(1 - \varepsilon)\rho_s \frac{H}{(1 + bc)^2}} \tag{4.11}$$

Therefore, in the case of the nonlinear isotherm the solute wave velocity is a function of concentration. In the groundbreaking work on liquid-liquid chromatography, a theory to describe solute zone spreading was developed (Martin & Synge, 1941). This classic model reexamined the chromatographic bed as a several equilibrium stages in series. Each stage consisted of a stationary phase and a mobile phase. The mobile phase then moved in a discrete transition step followed by equilibrium of each stage. It is important to understand that mobile phase from different stages do not mix. Interestingly, this theory was more closely related to modeling of a countercurrent exchange system. The resulting model was a polynomial expression, which reduced to a Gaussian form. The number of plates or stages had to be experimentally determined for each system. However, Martin and Synge had an effective work around to the complex,

coupled partial differential equations of the general rate model of chromatography (Martin & Synge, 1941).

Theoretical plate models are not physical realities however. Although the continuous flow plate model as shown in Figure 4.1 is a more accurate representation to chromatography than countercurrent separation system. In this model the chromatographic column is divided into N equilibrium stages of H height (Martin, 1941). Model assumptions are that each solute is independent and their isotherms are linear. A mass balance around stage j for the solute i is represented in the following Equation 4.12.

$$c_{i,j-1}dV - c_{i,j}dV = V_M dc_{i,j} + M_s dq_{i,j} \tag{4.12}$$

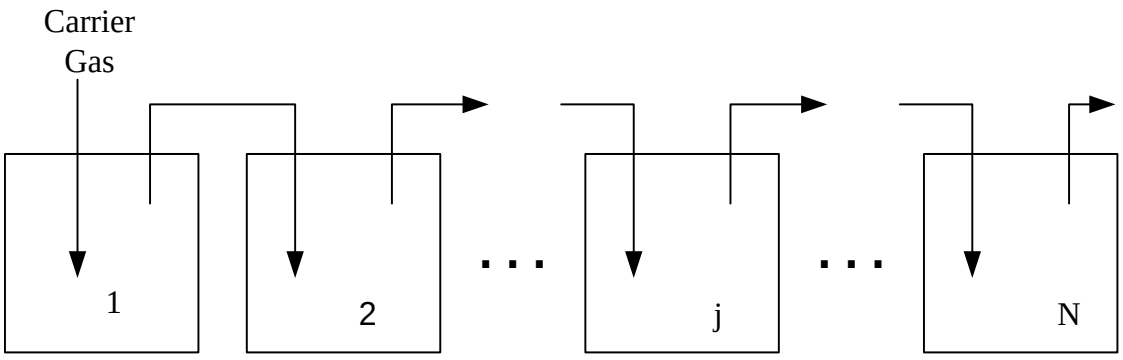

Figure 4.1. Continuous Flow Staged Model of Chromatography

In Equation 4.12, V_M is the mobile phase volume and M_s is the stationary phase mass for each stage. V is the volume of the carrier gas. An expression for the linear isotherm is reflected in Equation 4.13.

$$q_i = k_i(T)c_i \tag{4.13}$$

Substituting and rearranging Equation 4.13 into equation 4.12 yields an ordinary differential equation as shown in Equation 4.14.

$$\frac{dc_{i,j}}{dV} = \frac{c_{i,j-1} - c_{i,j}}{V_M + k_i M_s} \tag{4.14}$$

Now if one were to inject a pulse of F_i moles into stage 1 shown in Figure 4.1, the result is the Poisson distribution:

$$c_{i,j} = \frac{F_i}{V_M + k_i M_s} \frac{e^{-v_i} v_i^j}{j!} \tag{4.15}$$

In Equation 4.15 a dimensionless cumulative flow of mobile phase is given as v_i, and is defined as Equation 4.16.

$$v_i = \frac{V}{V_M + M_s k_i} = \frac{u_{s,i} t}{H} \tag{4.16}$$

The outlet concentration is determined by setting j = N. For step inputs the shell balance below may solved as well. This result is shown in Equation 4.17.

$$c_{i,j-1} dV - c_{i,j} dV = V_M dc_{i,j} + M_s dq_{i,j} \tag{4.17}$$

Equation 4.18 may approximate a large number of stages.

$$c_{i,j} = \frac{F_i}{V_M + k_i M_s} \frac{1}{\sqrt{2\pi j}} e^{-\frac{(v_i - j)^2}{2j}} \tag{4.18}$$

At the column outlet the concentration results in Equation 4.19.

$$c_{i,out} = \frac{F_i}{V_M + k_i M_s} \frac{1}{\sqrt{2\pi N}} e^{-\frac{(v_i - N)^2}{2N}} \tag{4.19}$$

Upon differentiation the equation may relate the location of the peak maxima in dimensionless terms when $v_i = N$.

$$c_{i,max} = \frac{F_i}{V_M + k_i M_s} \frac{1}{\sqrt{2\pi N}} \tag{4.20}$$

Also, the dimensionless peak width is shown in Equation 4.21.

$$w_i = 4\sqrt{N} \tag{4.21}$$

Gaussian peaks have a width of 4σ where σ is the standard deviation, thereby the width is shown in Equation 4.22.

$$\sigma = \sqrt{N} \tag{4.22}$$

The definition of plate height is shown in Equation 4.23. Equation 4.23 shows the relation between the number of theoretical plates N, theoretical plate height H, and column length L.

$$N = \frac{L}{H} \tag{4.23}$$

$$c_i = c_{i,max} e^{\frac{-\left(\frac{u_{s,i}t}{H} - \frac{L}{H}\right)^2}{2\left(\frac{L}{H}\right)}} \tag{4.24}$$

Remembering the definition of retention time as shown in Equation 4.25.

$$t_{R,i} = \frac{L}{u_{s,i}} \tag{4.25}$$

Equation 4.24 becomes after substitution of the retention time Equation 4.26.

$$c_i = c_{i,max} e^{\frac{-(t-t_{R,i})^2}{2\left(\frac{H}{L}t_{R,i}\right)}} \tag{4.26}$$

In terms of length units the equation of solute concentration is shown in Equation 4.27.

$$c_i = c_{i,max} e^{-\frac{(z_i - L)^2}{2LH}} \tag{4.27}$$

In Equation 4.27, z_i is the location of the peak center at the maximum concentration. In standard form, the equation can be written as Equation 4.28.

$$c_i = c_{i,max} \exp\left(\frac{-X^2}{2\sigma^2}\right) \tag{4.28}$$

Comparison of the previous equations 4.29 and 4.30 are shown below.

$$c_i = c_{i,max} e^{-\frac{(t-t_{R,i})^2}{2\left(\frac{H}{L}t_{R,i}^2\right)}} \tag{4.29}$$

$$c_{i,out} = \frac{F_i}{V_M + k_i M_s} \frac{1}{\sqrt{2\pi N}} e^{-\frac{(v_i-N)^2}{2N}} \tag{4.30}$$

The continuous flow staged theory correctly predicts the zone spreading is proportional to the square root of the distance traveled. Also, since the equation for retention time clearly shows that the exit time for each solute peak is proportional to N peaks may always be separated by increasing L as long as the solute wave velocities or distribution coefficients differ. According to Equation 4.30, the zone spreading within the column is the same for all components except for very small differences in their H values. The zone spreading with respect to time is inversely proportional to the solute wave velocity. Therefore, slower moving solutes spread more. Physically when the front of a solute wave reaches the end of the column, the width of the zone inside the column is equal to $4\sigma_1$. That means it takes longer to elute a slowly moving solute this distance and

therefore more spreading is observed on the chromatogram. The value of N is determined from the chromatogram by Equation 4.31.

$$N = 5.545 \left(\frac{t_R}{w_h} \right)^2 \tag{4.31}$$

The width at half-height is the most commonly used measurement for efficiency calculations. Figure 4.2 shows the different parts of the peak that may be used for developing chromatographic parameters.

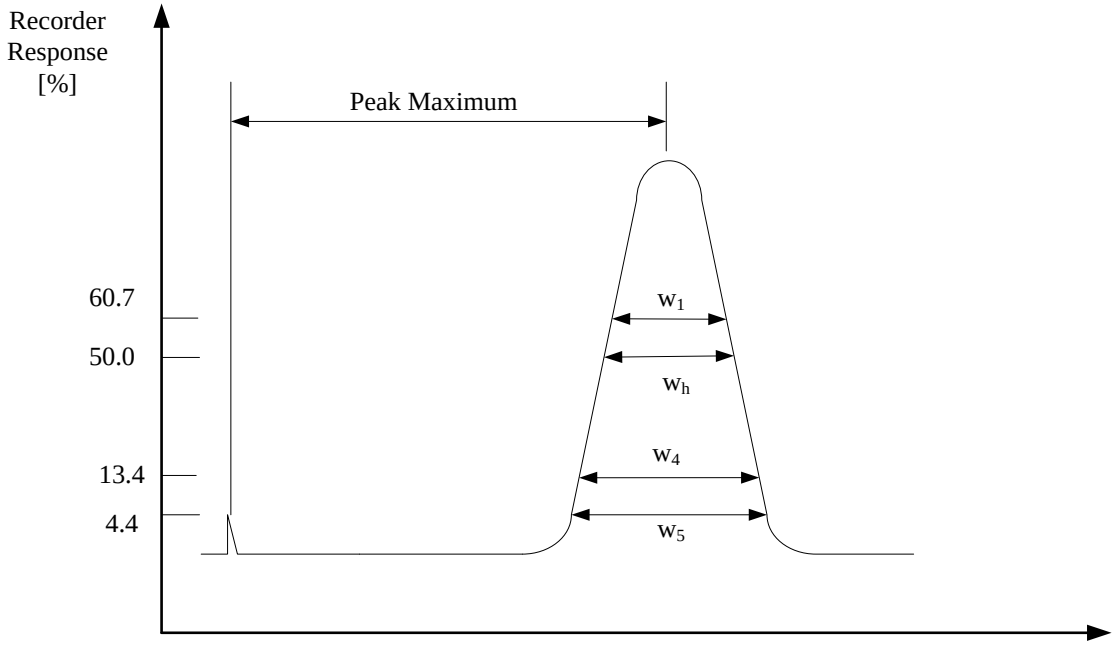

Figure 4.2. Analysis of Chromatographic Peak

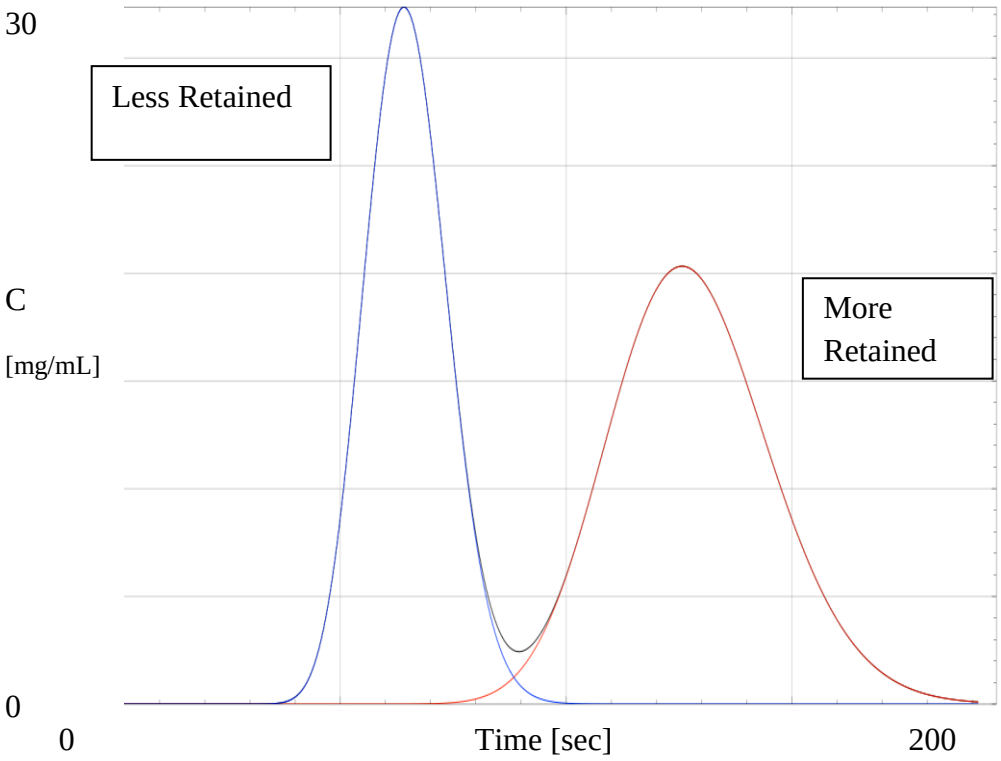

Figure 4.3. Elution Curves from Simulation

Figure 4.3 shows the separation of two solutes using the theory developed by Martin and Synge. The first eluted solute shown in blue is less retained followed by the more retained solute in red. The more retained solute shows a greater degree of interaction with the stationary phase but less efficiency compared to the less retained solute.

In Section 4.3 the mass balance of a chromatographic column is developed. Defining some dimensionless quantities and solving the partial differential equation using the central difference numerical method achieves the solution of this mass balance. The Peclet number, which describes axial dispersion, is assumed to go to infinity. This simplifies the problem to an equation similar to the kinematic wave equation.

4.3. Mass Balance of Chromatographic Column

Assuming that the packing is homogeneous, that radial gradients in temperature, velocity, and concentration are negligible, that the thermal diffusion and pressure diffusion can be neglected, that there are no phase changes other than the adsorption, and that chemical reactions are occurring (Varma & Morbidelli, 1997). Then the mass balance of a chromatographic column is represented in Equation 4.32.

$$-\varepsilon E_a \frac{\partial^2 C}{\partial x^2} + v\frac{\partial C}{\partial x} + \varepsilon\frac{\delta C}{\delta t} + (1 - \varepsilon)\frac{\delta \Gamma}{\delta t} = 0 \tag{4.32}$$

where the stationary phase is at equilibrium with the mobile phase everywhere along the bed. So the loading is linear and given as,

$$\Gamma = F(C) \tag{4.33}$$

Introducing the dimensionless quantities as shown below:

$$u = \frac{C}{C_r} \qquad f(u) = \frac{F(C)}{C_r} \qquad z = \frac{x}{L}$$

$$\tau = \frac{tv}{\varepsilon L} \qquad Pe = \frac{uL}{\varepsilon E_a} \qquad v = \frac{1 - \varepsilon}{\varepsilon}$$

where C_r is a reference concentration, L is a characteristic length, and Pe is the Peclet number describing the effect of axial dispersion in the bed.

Substituting these expressions into the fixed bed mass balance we get Equation 4.34.

$$-\frac{1}{Pe}\frac{\delta^2 u}{\delta z^2} + \frac{\delta u}{\delta z} + \frac{\delta u}{\delta \tau} + v\frac{\delta f}{\delta \tau} = 0 \tag{4.34}$$

In the case of axial dispersion is negligible (Pe goes to infinity), then the above model reduces to the kinematic wave equation as shown in Equation 4.35.

$$\frac{\delta u}{\delta z} + \psi(u)\frac{\partial u}{\partial \tau} = 0 \tag{4.35}$$

where

$$\frac{1}{\psi(u)} = c(u) = \frac{1}{1 - vf'(u)} \tag{4.36}$$

In Equation 4.36, psi (u) is the wave propagation velocity. The equation without axial dispersion is shown in Equation 4.37.

$$\frac{\partial u}{\partial z} + \psi\frac{\partial u}{\partial \tau} = 0 \tag{4.37}$$

Converting first order derivatives to central differences:

$$\frac{u_{i+1,j} - u_{i-1,j}}{2\Delta z} + \psi \frac{u_{i,j+1} - u_{i,j-1}}{2\Delta \tau} = 0 \tag{4.38}$$

Defining coefficients:

$$\alpha = \frac{1}{2\Delta z} \tag{4.39}$$

$$\gamma = \frac{\psi}{2\Delta \tau} \tag{4.40}$$

So that:

$$u_{i,j+1} = \frac{\gamma u_{i,j-1} - \alpha\left(u_{i+1,j} - u_{i-1,j}\right)}{\gamma} + O(\Delta z^2 + \Delta \tau^2) \tag{4.41}$$

Initial and boundary conditions are:

$u_{0,j} = 1$ for all j

$u_{i,0} = 0$ for all $i \neq 0$

The resulting profile is shown in Figure 4.4. Figure 4.4 is a three dimensional plot representing the dimensionless concentration versus column position versus the hold-up volume.

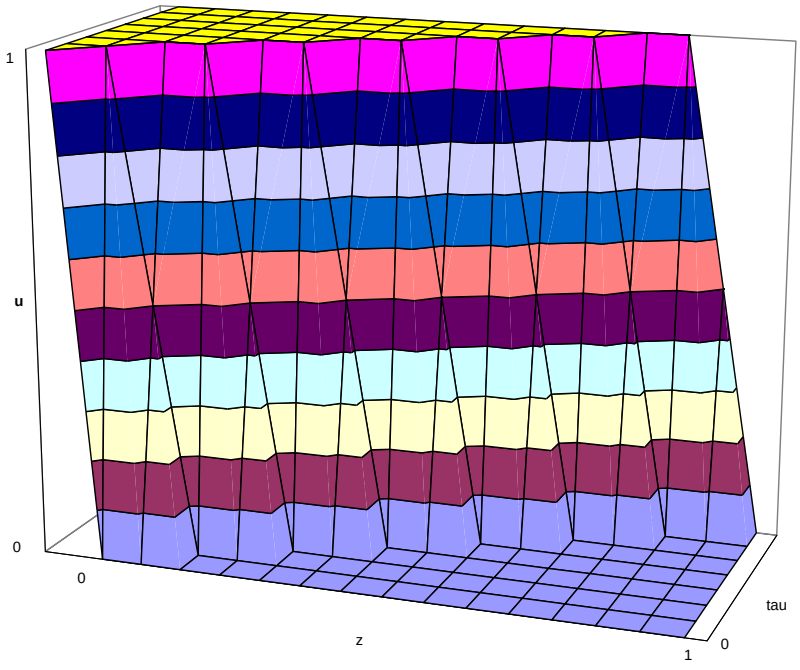

Figure 4.4. Solution of the Chromatographic Column

Now considering the effect of axial dispersion we may write Equation 4.42:

$$-\frac{1}{Pe}\frac{\partial^2 u}{\partial z^2} + \frac{\partial u}{\partial z} + \psi\frac{\partial u}{\partial \tau} = 0 \qquad (4.42)$$

Central difference for second derivative of u with z:

$$\frac{\partial^2 u}{\partial z^2} = \frac{u_{i+1,j} - 2u_{i,j} + u_{i-1,j}}{(\Delta z)^2} \qquad (4.43)$$

For stability reasons, we use the forward difference of u with tau instead of the central difference. This is shown in Equation 4.44.

$$\frac{\partial u}{\partial \tau} = \frac{u_{i,j+1} - u_{i,j}}{\Delta \tau} \tag{4.44}$$

So the finite difference equation is:

$$u_{i,j+1} = \left(\frac{\Delta\tau}{Pe\psi(\Delta z)^2} - \frac{\Delta\tau}{2\psi\Delta z}\right) u_{i+1,j} + \left(1 - \frac{2\Delta\tau}{Pe\psi(\Delta z)^2}\right) u_{i,j} + \left(\frac{\Delta\tau}{Pe\psi(\Delta z)^2} + \frac{\Delta\tau}{2\psi\Delta z}\right) u_{i-1,j} + O(\Delta z^2 + \Delta\tau) \tag{4.45}$$

Simplified Equation 4.45 may be shown as Equation 4.46

$$u_{i,j+1} = \alpha u_{i+1} + \beta u_{i,j} + \gamma u_{i-1,j} \tag{4.46}$$

where:

$$\alpha = \left(\frac{\Delta\tau}{Pe\psi(\Delta z)^2} - \frac{\Delta\tau}{2\psi\Delta z}\right) \tag{4.47}$$

$$\beta = \left(1 - \frac{2\Delta\tau}{Pe\psi(\Delta z)^2}\right) \tag{4.48}$$

$$\gamma = \left(\frac{\Delta\tau}{Pe\psi(\Delta z)^2} + \frac{\Delta\tau}{2\psi\Delta z}\right) \tag{4.49}$$

For a stable solution, the positivity rule requires the definition of Equation 4.50 as shown below.

$$1 - \frac{2\Delta\tau}{Pe\psi(\Delta z)^2} \geq 0 \tag{4.50}$$

which may be rewritten as Equation 4.51:

$$\frac{2\Delta\tau}{Pe\psi(\Delta z)^2} \leq \frac{1}{2} \tag{4.51}$$

Set an additional boundary condition that at z = 1 (the end of the column), du/dz = 0. That is, assuming that the column behaves as if it is infinitely long. The difference equation can determine a profile using the Thomas algorithm and Matlab. The code for this model is located in Appendix E of this work. Constant pattern solutions arise from partial differential equations of order larger than one and are continuous. A typical example is the kinematic wave modified so as to include a dissipation mechanism. To demonstrate this, the chromatography model will be examined. Specifically, the movement of solute waves in the column. Analytes diffuse between the moving mobile phase and the stagnant pores fluid. Analytes in the mobile phase travel at the inter-stitial velocity, v, of the MP. Analytes in the dormant fluid and or adsorbed on to the SP has a velocity near zero. Every analyte species spends time in the MP and then transports back into the dormant fluid and so forth. Therefore, the progress of solute is a series of random steps. The cumulative speed of all the analytes can be determined but the unpredictability of their position accounts for band broadening.

A plot of the dimensionless concentration versus column length profile is shown in Figure 4.5. The curves in Figure 4.5 represent the different dimensionless concentrations versus column position. Figure 4.5 shows the concentration history as it travels along the column.

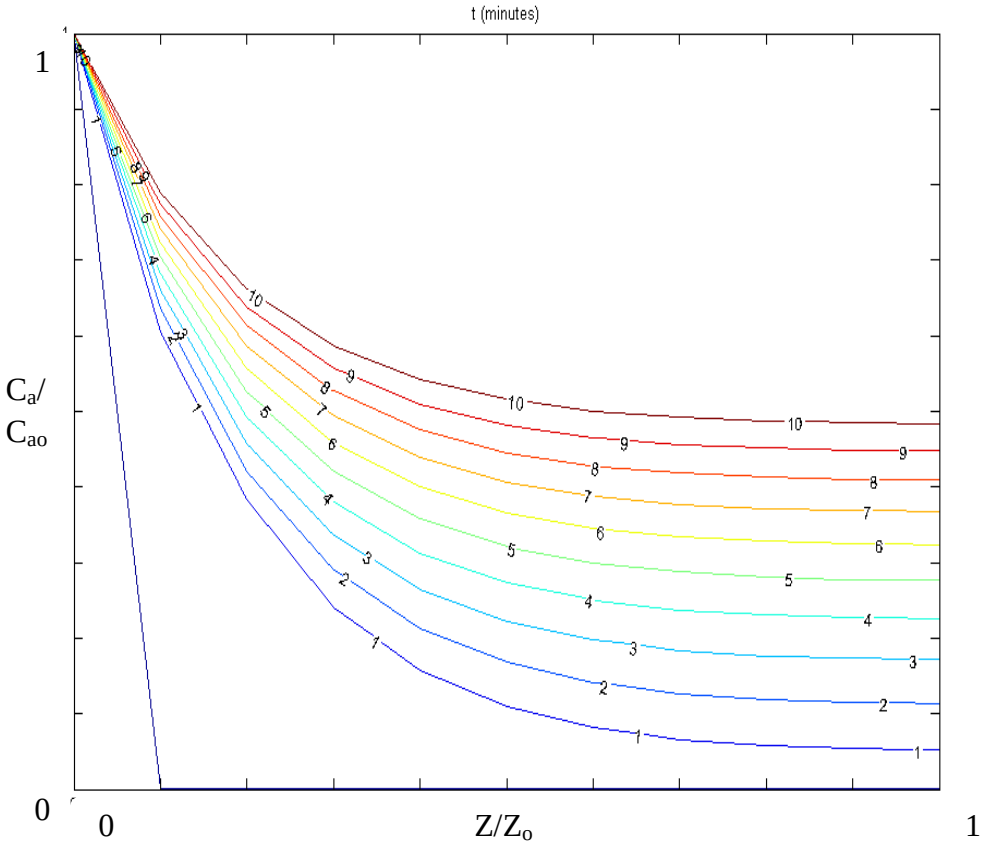

Figure 4.5. Dimensionless Concentration Profile versus Column Position

However, as a surface plot, Figure 4.6 shows the plot of concentration, time, and column position. Figure 4.6 shows the concentration versus time versus column position. This surface plot details how the solute concentration exhibits a waveform as it travels through the column.

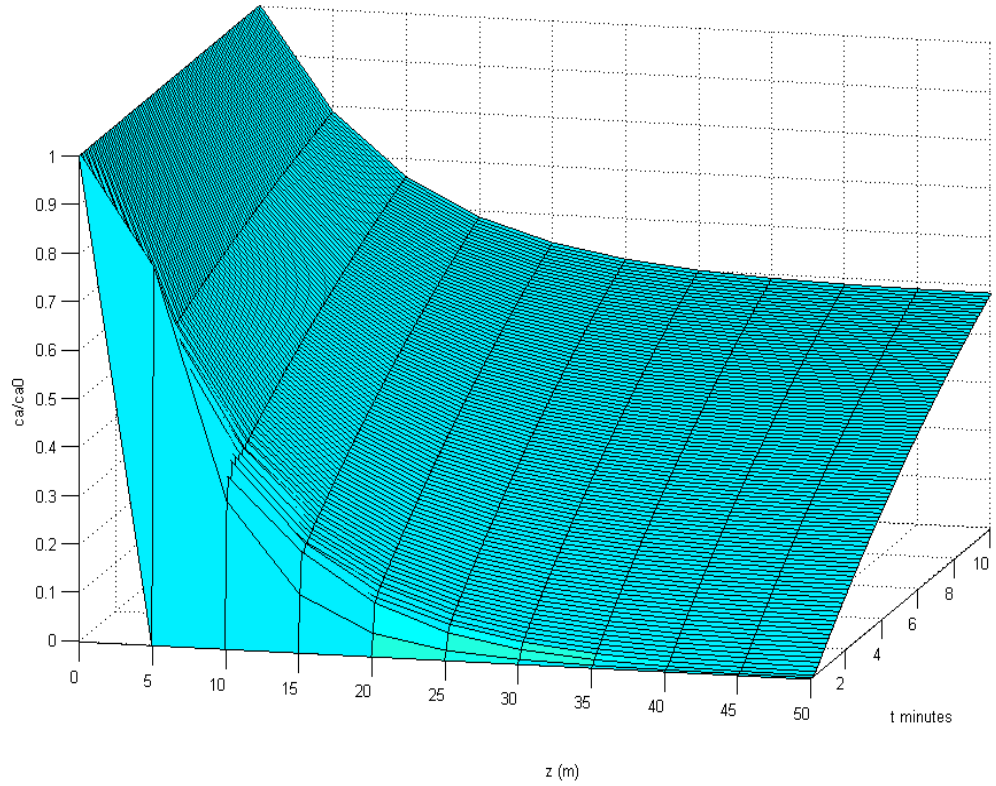

Figure 4.6. Surface Plot of Chromatographic Column Solution

The chromatographic system has a solution that a take the form of a wave propagating in space with constant velocity without changing its shape. This is also known as a constant pattern. In order to obtain the constant pattern solution, the system under examination must first be considered with the removal of its original boundary conditions as to avoid end effects which disturb the shape of the propagating wave. This was achieved by assuming that the wave propagates in an infinite space domain.

4.4. Chromatographic Model Variations

The model complexity needed for a system under study depends on the nature of the separation problem and the level of precision desired. Modeling chromatographic interactions may offer insight in determining system parameters, which may in turn help, reduce experimental time. Additional consideration may be taken regarding the propagation of error inherent in utilizing some of these model parameters.

4.4.1. Linear Chromatography

At low concentrations, the amount of material interacting with the stationary phase is in proportion to the amount of that same material in the mobile phase. This condition is known as linear chromatography. In linear chromatography, solutes do not interact with each other. The height of the peak on the chromatogram is directly related to the feed concentration of the mobile phase. However, elution band profiles and their subsequent retention times are not a function of the initial feed composition or concentration. Therefore, the adsorption equilibrium isotherm is a straight line connecting the origin to the projected saturation capacity with a specific slope. Most analytical chromatography is performed in the linear region of the isotherm. Linear chromatographic modeling is often utilized for its simplicity and reduced computational time.

4.4.2. Non-linear Chromatography

In non-linear chromatography, the amount of the components in the stationary phase is not proportional to their amount in the mobile phase. Interaction between individual components for sorption sites causes the equilibrium isotherms to be dependent on the system composition. Elution band profiles, retention times, and peak heights are also a function of the system composition. Non-linear systems are less amenable to solution in closed-form. Solution methods of non-linear systems generally require simplification. The majority of preparative and non-dilute systems are non-linear.

4.4.3. Ideal Chromatography

Ideal chromatography assumes the efficiency of the column is infinite. Axial dispersion is regarded as negligible. Mass transfer kinetics is assumed to be instantaneous. In these systems, elution band profiles are controlled by the phase equilibrium, which allows for thermodynamic influences to be considered. Ideal and non-linear models are important from a theoretical standpoint, and may approximate real system behavior.

4.4.4. Non-ideal Chromatography

As opposed to ideal chromatography, non-ideal chromatography assumes the column efficiency is finite. Axial dispersion and mass transfer kinetics influence the elution band profiles. To what degree these effects have depends on the choice of model. An important non-ideal, the equilibrium-dispersive model, is described in more depth in the next section.

4.5. Equilibrium-dispersive Model

The mass balance is written as the following relation when mass transfer kinetics is fast but not infinitely so as in Equation 4.52.

$$\frac{\partial C_i}{\partial t} + F\frac{\partial q_i}{\partial t} + u\frac{\partial C_i}{\partial z} = D_{a,i}\frac{\partial^2 C_i}{\partial z^2} \tag{4.52}$$

where the apparent dispersion coefficient, $D_{a,i}$ is given by Equation 4.53.

$$D_{a,i} = \frac{HL}{2t_M} = \frac{Hu}{2} \tag{4.53}$$

The height equivalent to a theoretical plate is H for the component under study t_M is the hold-up time. The expression for the apparent dispersion shown in Equation 4.53 is the result from the relationship between the variance σ_l^2 a Gaussian peak obtained under linear chromatography conditions for a Dirac pulse injection.

$$\sigma_l^2 = HL = 2D_a t_M \tag{4.54}$$

The equilibrium-dispersive model assumes that all contributions from the lack of equilibrium may be lumped together into an apparent dispersion term. This model is a close approximation if the mass transfer in the column is determined by the molecular diffusion across the mobile phase flowing around the stationary phase particles.

Also, this model is appropriate when the exchange of solutes between the mobile and stationary phase is fast. This is an acceptable assumption when considering the fluid phase is supercritical as is the case in this work.

4.6. Modeling Supercritical Fluid Chromatography

The equilibrium-dispersive model is appropriate for modeling a supercritical fluid chromatographic system. Since supercritical fluids offer fast kinetics and diffusion, the equilibrium-dispersive model was employed for this work. Figure 4.7 is graphical representation of the equilibrium-dispersive model solution. The concentration versus time versus column position shows the elution band profile shapes. Figure 4.7 demonstrates that the higher concentrations show a dramatic shape as dictated by the non-linear portion of the isotherm.

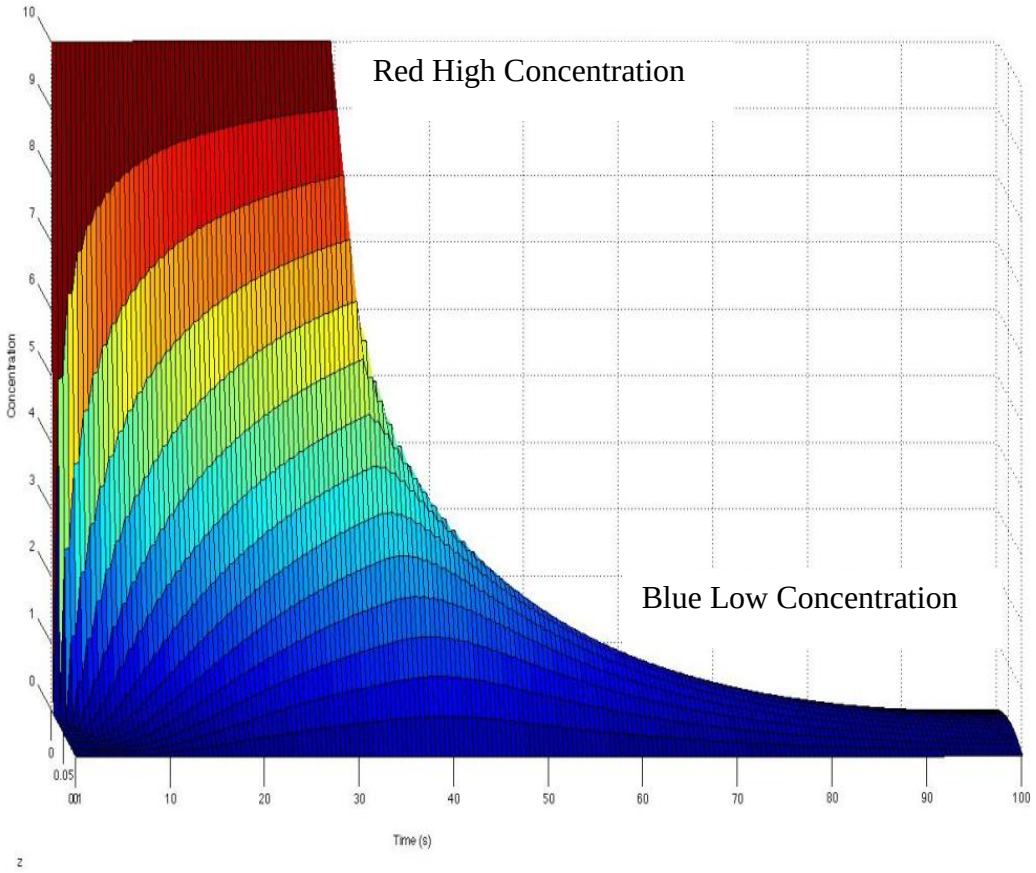

Figure 4.7. Surface Plot of Equilibrium-dispersive Model of Chromatography

The Matlab m-file, written solves the chromatographic bed mass balance. It is provided in Appendix D. The function f = Equilibrium_Dispersive() automatically solves the set of partial differential equations by the forward difference method. The program is robust in that one can input any bed parameters such as column length, porosity and so forth. The model is applicable to SFC by setting the appropriate values for the parameters of the supercritical mobile phase: pressure, temperature, and density.

The distribution of a solute between two phases represents the phase partitioning or distribution coefficient K_i. This ratio of the solute in each phase is shown in Equation 4.55.

$$K_i = \frac{C_i(\text{Phase I})}{C_i(\text{Phase II})} \tag{4.55}$$

Using a symmetrical approach, which uses an Equation of State (EOS) to calculate the phase equilibrium, can be used in determining the distribution coefficient. An asymmetrical approach using the activity coefficient model may be used. Equation 4.56 shows the equation used for the symmetric approach.

$$K_i = \frac{\phi_i^{II}(T,P,x_i)}{\phi_i^{I}(T,P,y_i)} \tag{4.56}$$

Equation 4.57 is used for the asymmetric approach and is as follows.

$$K_i = \frac{\gamma_i^{II}(T,P,x_i)f_i(T,P)}{\phi_i^{I}(T,P,y_i)} \tag{4.57}$$

In Equation 4.57, K_i is the partition or distribution coefficient of coefficient i in phases I and II. Phi is the fugacity coefficient of component i in mixture for phase I or II. Gamma is the activity coefficient of component i in the mixture for phase I or II.

The fugacity of pure component i is given as f_i. For supercritical fluids the symmetrical approach of phase partitioning is commonly used. The solvent may be assumed to be insoluble in the stationary phase. In such cases, Equation 4.58 may represent the solubility of a solid in the supercritical fluid mobile phase.

$$y_i = \left(\frac{P_i^{sub}(T)}{P}\right)\left(\frac{1}{\phi_i^V}\right)\exp\left[\frac{\bar{v}_i^S\left(P - P_i^{sub}(T)\right)}{RT}\right] \qquad (4.58)$$

A B C

The first braced term A represents the ideal gas solubility. In this term, P_i^{sub} is the sublimation pressure and is a function of temperature T. P denotes the equilibrium pressure. The seconded braced term B represents the non-ideality of the system. In this term, the ϕ_i^V term represents the fugacity coefficient of compound i in the vapor phase. The third bracketed term in Equation 4.58 shown as C represents the so-called enhancement factor over ideal gas solubility. Additional information about dense gas solubility may be found in the excellent monograph of molecular thermodynamics (Prausnitz, Lichtenthaler, & Azevedo, 1999). Accounting for these dense gas terms and incorporating them into the equilibrium-dispersive model may amend modeling of the supercritical chromatographic system.

Chapter 5 of this work presents the system studied experimentally. The equipment used to achieve supercritical conditions are detailed along with the experimental procedures carried out. Observations of these experimental results are located in Chapter 6.

CHAPTER 5

EXPERIMENTAL SYSTEM, OPERATION AND THEORY

SFC has historically been used for analytical scale chromatography. SFC may be considered the rebirth of normal phase chromatography. In the 1970s, reversed phase HPLC almost completely replaced normal phased HPLC, because it was faster, more robust and decreased the use of large volumes of toxic, flammable solvent. SFC solves many of the problems of normal phased HPLC and shares some valuable characteristics compared to reversed phased HPLC (Kiran & Brennecke, 1993).

Supercritical fluid chromatography uses most of the same or slightly modified hardware as HPLC. The instruments used were modified to handle high pressures and high temperatures. The design and execution of a supercritical fluid chromatograph for isotherm determination of enantiomers is presented. A reliable and robust SFC unit was assembled. The resulting chromatograms were reproducible and led to accurate isotherm measurement.

5.1. Experimental System Description

The heart of the experimental system is the chromatographic column. The chromatographic column is where the retention and separation of ibuprofen occurs. The ibuprofen is introduced to the system through the auto sampling injector. There, it is carried into the system towards the chromatographic column by the flowing supercritical carbon dioxide. In some additional experiments, the ibuprofen was introduced using the solvent reservoir of the HPLC pump. The other parts of the system involved supercritical carbon dioxide delivery, temperature and pressure control, and detection.

5.1.1. Analytical Supercritical Fluid Chromatograph

A schematic of an analytical SFC is shown in Figure 4.1. There are two high-pressure pumps; one to deliver carbon dioxide and the other to deliver liquids as modifier. The modifier pump delivers liquids and is, for all practical purposes, an HPLC pump. The carbon dioxide pump is a syringe pump with a built in heat exchanger (chiller) to cool the pump head. This ensures that the carbon dioxide remains a liquid. There are two key reasons for chilling the pump head. The first is to prevent the carbon dioxide from undergoing a partial of full phase change to gas. The second is to ensure that the flow rate control units built in to the syringe pump works accurately and does not cavitate when delivering the carbon dioxide. The syringe pump is shown connected to a high-pressure cylinder. The approach is to use high-purity carbon dioxide and a dip tube cylinder to draw the liquid off of the bottom of the cylinder. This type of cylinder ensures that the carbon dioxide is a liquid and will flow without pressure fluctuations.

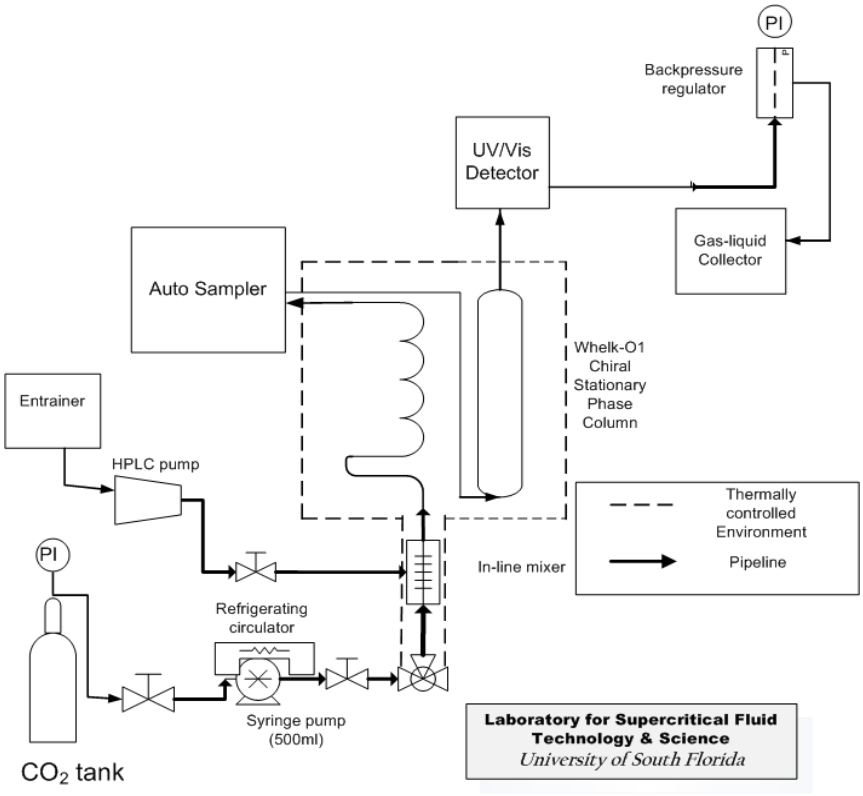

Figure 5.1. Supercritical Fluid Chromatograph Experimental Setup

5.1.2. Whelk O1 Chiral Stationary Phase

The Regis Technologies (R, R)-Whelk-O1 chiral stationary phase packed column was used for this investigation (Morton Grove, IL, USA). The column is 250 mm × 4.6 mm, packed with end-capped (3S, 4R)-Whelk-O1 material, 10μ m particle size with 100 Å sized pores. The Whelk O1 chiral Stationary phase enables analytical and preparative separation of enantiomers with various chemical structures. 4-(3, 5-Dinitrobenzamido) tetra-hydro-phenanthrene, covalently bonded through mono-functional linkage (Regis Tech 2008).

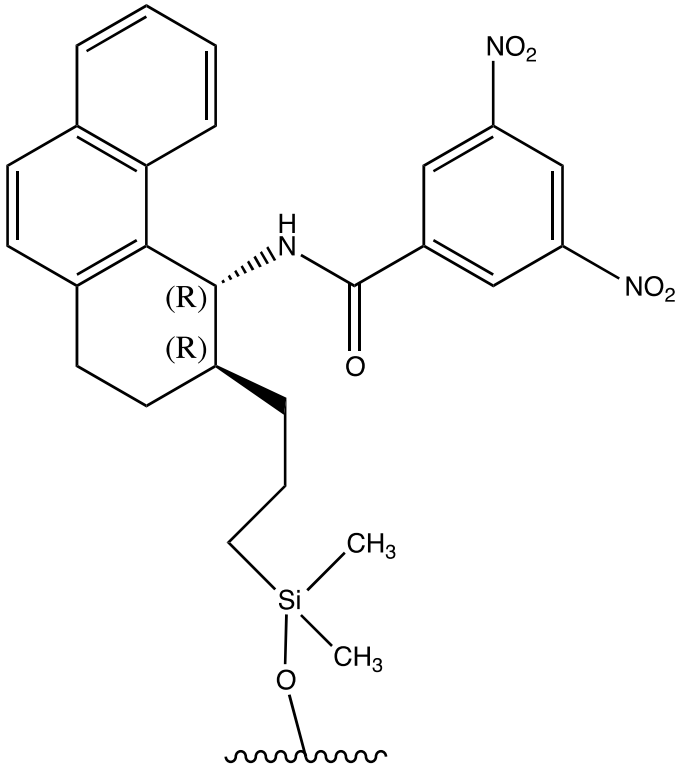

Figure 5.2 Whelk O1 Chiral Stationary Phase

A fundamental characteristic of the Whelk O1 CSP is that it has a simple and rigid structure. From the silica gel surface toward the elution medium 3, 5-dinitrobenzoyl group is directed, which is extremely poor with pi-electrons and thus easily generates pi-pi interactions. A second aromatic group, rich with electrons, is placed behind the previous one, creating a shield in front of the silica gel surface, which lowers the non-productive achiral interactions with the polar silica gel groups.

5.1.3. Syringe Pump

Teledyne ISCO 500D high pressure syringe pump was used. The pump that delivers the supercritical carbon dioxide to the system is a high pressure syringe pump (Model 500D, ISCO, Lincoln, NE) equipped with a cooling jacket to ensure that the carbon dioxide withdrawn from the reservoir tank is cooled is cooled down to a liquid state.

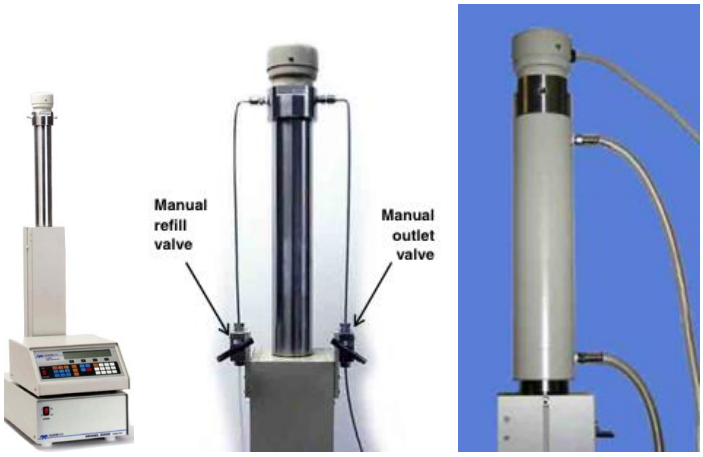

Figure 5.3. The Teledyne ISCO 500D High Pressure Syringe Pump

The 500D syringe pump delivers accurate and reproducible flow rates. Pressure control at flow rates from a micro-liter to above 200 mL/min ranges is possible. Low flow steadiness to 3,750 psia makes the 500D an ideal pump for high-pressure techniques.

Table 5.1. ISCO 500D Syringe Pump Specifications

Capacity	507.38 mL
Flow Range	0.001-204 mL/min
Flow Accuracy	+/-0.5% of Set point
Pressure Range	0.7-258.6 Bar (10-3,750 psig)
Standard Pressure Accuracy	0.5%FS
Plumbing Ports	1/8” NPT
Operating Temperature	5-40^{o}C
High-precision Pressure Transducers	0.1% Linear Accuracy

5.1.4. Temperature Control Jacket

The optional temperature control jacket encircles the cylinder of a Teledyne ISCO Syringe Pump, allowing liquid such as water or a water/ethylene glycol solution to circulate through the 1/4" upper and lower hose connectors, maintaining the temperature of the pumped fluid within the cylinder.

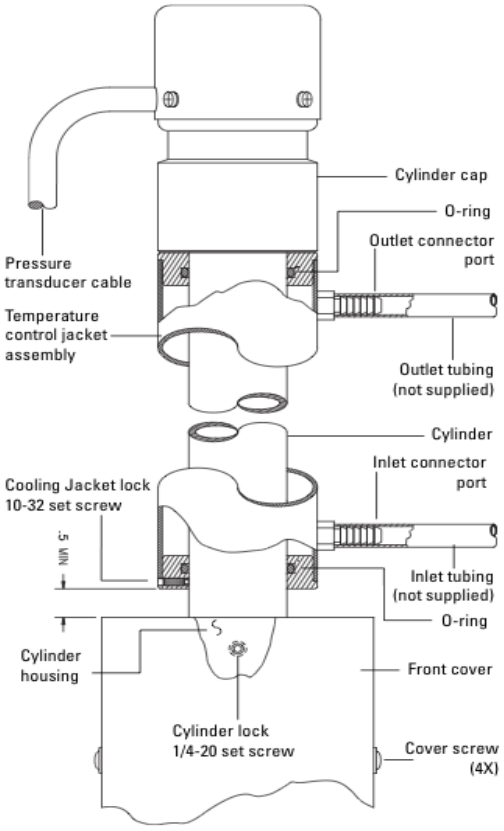

Figure 5.4. Temperature Control Jacket for ISCO 500D Syringe Pump

The jacket is recommended for applications such as: liquid gases and steady flows. The jacket is necessary in SFC applications where cylinder cooling facilitates pump filling with supercritical fluids such as liquid CO_2. The jacket is connected to a circulating temperature-controlled bath to keep the fluid inside the pump at a constant temperature. This is important when operating at very low flows, where temperature fluctuation can cause flow variations. However, the slow rates used were high enough to avoid this. The fluid circulation and cooling reservoir connected to the temperature control jacket was supplied by the Lauda chiller. The cooling jacket is rated from –30 to 100°C.

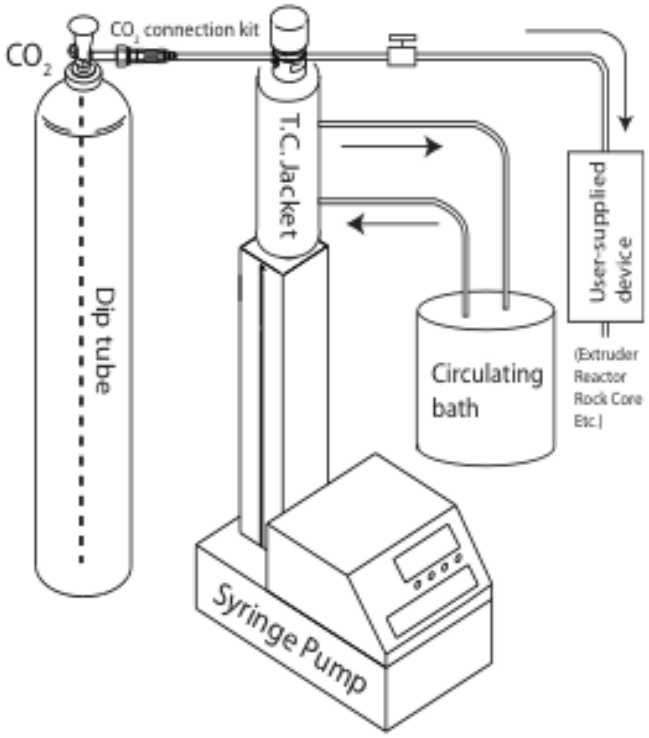

Figure 5.5. Syringe Pump with CO_2 Dip tube Tank and Circulating Bath

5.1.5. Circulation Chiller

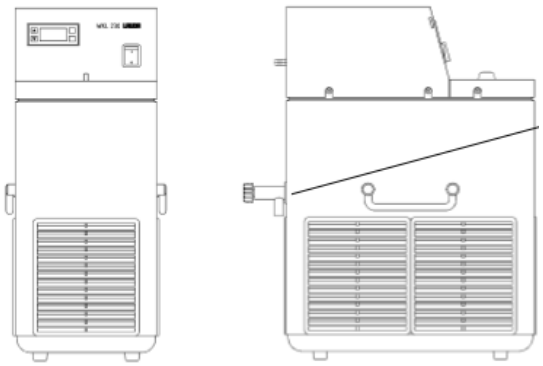

Figure 5.6. LAUDA Circulation Chiller used to Cool Syringe Pump

The purpose of the chiller is to ensure that the carbon dioxide stays in the liquid phase when it is charged into the syringe pump. The chiller works attached to the cooling jacket of the syringe pump and is needed if working when working with solvents whose critical temperatures are near ambient.

All circulation baths made by LAUDA have a refrigeration system in the lower part of the unit, employing a sealed compressor, air-cooled or water-cooled condenser with refrigerant 134a to cool the liquid in the tank through an evaporator.

Table 5.2 LAUDA Temperature Ranges for Different Bath Liquids

Bath Liquid	**Operational Temperature Range [^{o}C]**	**Temperature Accuracy [^{o}C]**
Water (Decalcified Water)	5 to 90	+/-0.5
Monoethylene Glycol/Water	-30 to 90	+/-0.5
Monoethylene Glycol	-40 to 90	+/-0.5

The chiller should be set to a temperature from 1-3^{o}C. Allow at least one hour of circulation time before filling syringe pump with carbon dioxide. At least once per year, the bath liquid needs to be replaced. While the liquid is drained the inside coils should be cleaned with a moderate acid to remove any scaling built up over time. It is recommended to use one molar hydrochloric acid and isopropanol to clean the inside of the bath. The set temperature was selected to be -2^{o}C as to ensure the carbon dioxide in the pump head remained a liquid during charging.

5.1.6. HPLC Pump

The Waters 600E system is a high-performance liquid chromatography (HPLC) multi-solvent delivery system. This is the front end of standard HPLC system without the column and the detector. However, the ability to use four solvent reservoirs and program their delivery is quite useful. The primary function of this pump was to deliver the modifier used to mix with the carbon dioxide. Ethanol was the main modifier used throughout these investigations. The pulse experiments consisted of this pump only delivering modifier that was ethanol.

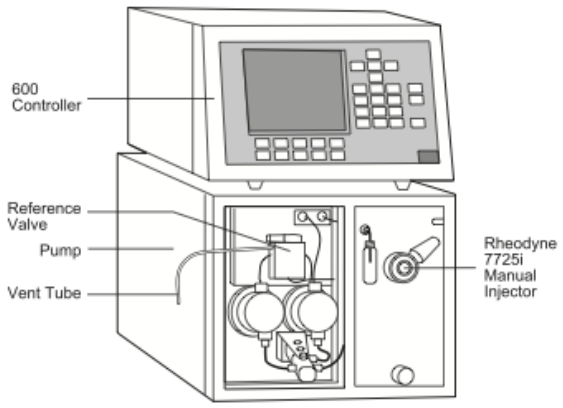

Figure 5.7. Waters 600E HPLC Controller and Dual Piston Pump

5.1.7. Column Oven

The Dionex STH 585 column oven was essential in providing constant temperature of the chromatographic column as well as the coil delivering the carbon dioxide. Figure 5.8 shows the column oven and control pad.

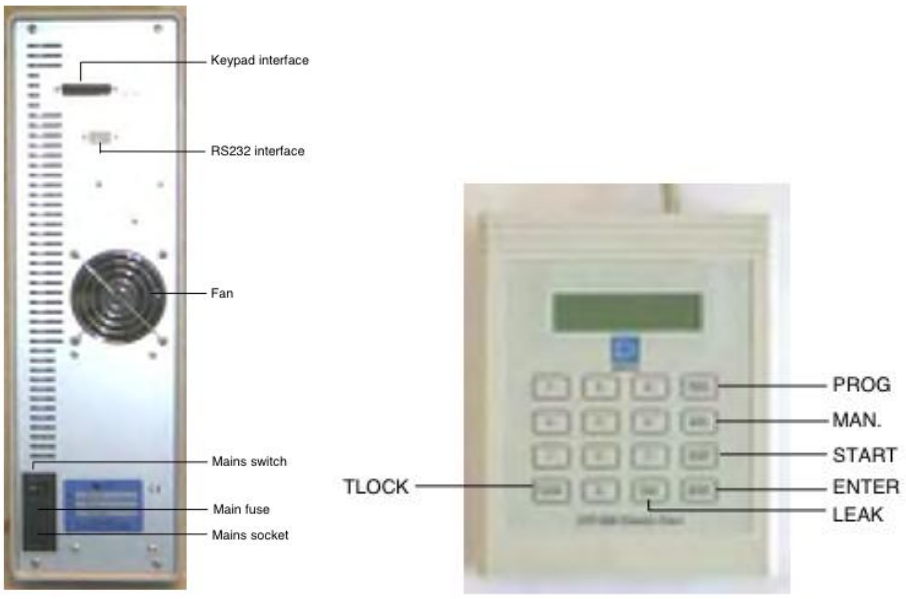

Figure 5.8. Dionex Column Oven STH 585

Table 5.3 shows the tolerances of the column oven. These tolerances are used in Chapter 6 for the error analysis.

Table 5.3. Dionex Column Oven Technical Specifications

Temperature Range	5 to 85^{o}C
Temperature Accuracy	+/- 0.5^{o}C
Temperature Stability	+/- 0.15^{o}C
Temperature Change	2 to 3^{o}C/min

5.1.8. UV/Vis Detector

The Hewlett-Packard 1050 variable wavelength detector was used for these experiments. This is a liquid chromatograph detector from the 1050 series. The HP 1050 is a standalone unit offering grating, photodiode and multi- purpose detection. The performance and features match the requirements of the routine analysis and quality control analysis. The HP 1050 is a standard size detector of 1050 modular type LC series and can be built up with other LC modules. This is done with another pump and an autosampler. Since it is standalone type, it can be also used as an ordinary LC detector. Figure 5.9 shows the front of the HP 1050.

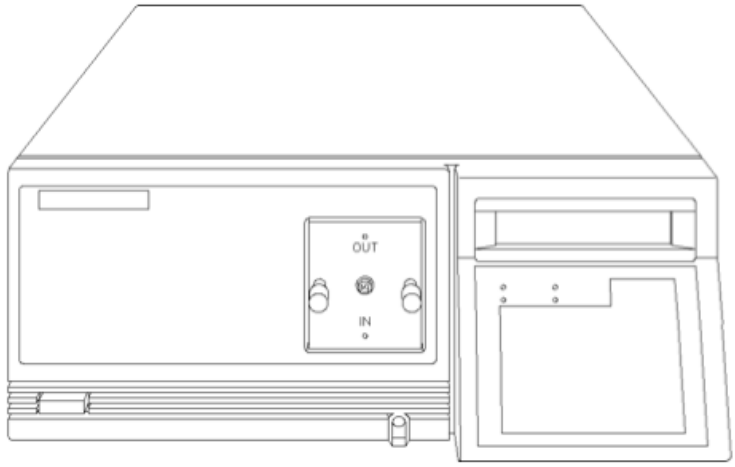

Figure 5.9. UV/Vis Detector-HP 1050 Variable Wavelength Detector

5.1.9. Automated Back Pressure Regulator

The overall pressure of the system was maintained and monitored by an automated backpressure regulator (Thar Technologies, Inc., Pittsburgh, PA). The basic component of a backpressure regulator is a precision valve attached to a motor controller

with a position indicator. The custom needle and seat are designed so they provide precise flow and fast response.

The position indicator of the needle is reported to range from 0 to 6000 points for the minimum flow and maximum flow respectively. The basic theory of operation is that a PID controller sends the needle valve a signal as to how much to open or close according to the offset from the value of pressure.

5.2. Experimental Chemicals

Ibuprofen: (RS)-2-(4-(2-methyl-propyl)-phenyl)-propanoic acid. Racemic ibuprofen (purity > 99%), S enantiomer with a purity of 98% and R enantiomer with a purity of 97%, were also purchased from Sigma-Aldrich (St. Louis, MO, USA). Ibuprofen is an extensively used analgesic and anti-inflammatory drug. It was chosen for these experiments because it is a widely used non-steroidal anti-inflammatory with a chiral center and is relatively inexpensive.

HPLC grade ethanol was purchased from Sigma Aldrich (St. Louis, MO, USA). Ethanol was chosen as the organic modifier for the system for a few reasons. As ethanol has been deemed environmentally friendly, it was chosen as an adequate chemical to be used in this investigation. Ethanol in its role as mobile phase modifier changes the solubility of the mobile phase and allows greater mass loading of solute while also interacting with any unresolved silanol groups in the stationary phase.

Carbon dioxide (99.8% purity) was purchased from Air Gas (Tampa, FL, USA). Carbon dioxide was chosen as the mobile phase for its advantages over liquid solvents. The density and solvent power of carbon dioxide are adjustable by pressure and

temperature. No solute residues are left over after depressurization. Carbon dioxide is inflammable and relatively inexpensive.

5.3. Experimental Procedure

The SFC system used is shown in Figure 5.1. The ISCO 500D syringe pump was used for the CO_2 delivery (Teledyne Tech. Co., Lincoln, NE, USA). The pump head of the 500D was cooled using a Lauda E100 Econoline RE120 recirculating chiller (Delran, New Jersey, USA). A Waters 600E (Milford, MA, USA) HPLC pump was used for the modifier delivery. The CO_2 and modifier streams entered the Dionex STH 585 column oven (Sunnyvale, CA, USA). The CO_2 stream entered a coil of 30 feet to allow ample time to reach supercritical conditions. Then the modifier and CO_2 were mixed at a tee, followed by a static mixer to ensure uniform phase flow. The mobile phase then exited the column oven and entered a Perkin-Elmer ISS-900 auto sampler (Waltham, MA, USA) equipped with a high pressure Rheodyne valve (now IDEX Health and Science Oak Harbor, WA, USA). The auto sampler allowed constant flow throughput of the mobile phase. In the case of the pulse experiments, the sample of interest was loaded onto the 10μl sample loop and the valve switched when signaled, thus putting the solute plug into the mobile phase. In the bulk experiments, the solute was introduced via the HPLC. The outlet of the auto sampler entered into the column oven and directly in to the bottom of a vertically oriented Regis (R, R) Whelk-O1 CSP.

Next, the mobile phase and separated enantiomers leave the column oven and entered the Hewlett Packard 1050 UV/Vis detector fitted with a high pressure 13μl flow cell (Hewlett Packard formerly, currently Agilent Technologies, Palo Alto, CA). As a

note, all of the piping outside the column oven was wrapped with heating tape and controlled by a Variac variable heat transformer to prevent convective cooling of the lines. The system pressure was controlled using an automated backpressure regulator by Thar Designs, BPR-A-200B (now part of Waters Corp. Milford, MA, USA). A BNC-1120 connector was used along with a 6240E data acquisition card, purchased from National Instruments (Austin, TX, USA). Labview logged the UV signal response. MATLAB R2009a and Microsoft Excel 2007 were used to analyze the resulting chromatograms.

The re-circulating chiller was adjusted to supply a temperature of –4.0°C to the cooling jacket of the syringe pump to prevent the vaporization of carbon dioxide. The low temperature allowed for fast reloading of the syringe pump with carbon dioxide. The column heater was adjusted to the desired temperature. The experiments were run with the syringe pump set to flow mode and the backpressure regulator set for the desired system pressure. The flow rate of the CO_2 was set to 2.85 ml/min and the modifier flow rate was set to 0.15 ml/min. The mobile phase flow was started and allowed to equilibrate for an hour before pulse injections were made. The automated backpressure regulator was set to the desired pressure. The UV/visible detector was set for detection at 260nm. The auto sampler was programmed to inject a 10μL sample.

5.4. Experimental Design

In order to determine adsorption isotherms for a given system it is important to optimize the experimental conditions first in order to maximize throughput and resolution. As a priori, much work was dedicated to optimizing the separation of the

analyte of interest. In the case of this project, ibuprofen was used as the solutes of interest. Pulse experiments were carried out at different temperatures and pressures. Early on it was determined that a higher flow rate was desirable to achieve faster separations. The majority of these runs were carried out at a flow rate of three milliliters per minute as opposed to one milliliter per minute. Initially, the modifier selected was isopropyl alcohol. Several sets of experiments were carried out with this modifier. Then, ethyl alcohol was employed as modifier for the majority of the experiments. It was chosen then because it was a desirable, environmentally friendly organic solvent that was being produced from various biological sources. Upon fixing the flow rate, mobile phase composition, and solute, the effects of temperature and pressure had to be determined. To accomplish this, aliquots of known concentrations of solute were made ranging from 5 to 300 mg/mL. These included ibuprofen racemate, S-ibuprofen, and R-ibuprofen.

The temperatures and pressures were varied to fine tune the enantioseparation. Since supercritical fluids are very sensitive to these parameters much effort went into determining the optimal separation conditions. Additionally, there is low surface tension in $scCO_2$. This is due to a lack of a liquid/gas phase boundary. By changing the pressure and temperature of the supercritical fluid, the properties can be tuned to be more liquid-like or more gas-like. An important property of supercritical fluids is the solubility of a material in the fluid. Solubility in a supercritical fluid tends to increase with the density of that fluid at constant temperature. Since density increases with pressure, solubility tends to increase with pressure. The relationship of a supercritical fluid with temperature is not as straightforward. At constant density, solubility will increase with temperature. However, close to the critical point, the density can drop sharply with a slight increase in

temperature. Temperature was set and controlled using the Dionex column oven. Pressure was set and controlled using the Thar automated backpressure regulator. The flow rate of carbon dioxide was set and controlled by the ISCO syringe pump.

The modifier flow rate was set and controlled by the Waters HPLC. Once these flow rates were initiated, thirty to sixty minutes were allotted to allow the system to reach steady state. Once steady state was reached, hold-up time measurements were taken. The hold-up time is the amount of time any solute spends in the mobile phase in its journey through the column. After the hold-up time is determined, then the retention times of the solutes are recorded. The retention time is the time of a solute elapsed from introduction up to the maximum of the elution peak. Then the hold-up time is subtracted from the retention time to get the adjusted retention time. In gas chromatography, methane can represent an un-retained solute. Therefore the methane passes through the chromatographic column and when it is in the mobile phase it moves with the velocity of the mobile phase. The adjusted retention time is the time the solute spent in the stationary phase. The retention factor is determined subsequently. The retention factor is the quotient of the amount of time the solute spends in the stationary phase by the amount of time solute spends in the mobile phase. In other words the retention factor is the adjusted retention time of the solute divided by the hold-up time. Having defined these essential quantities, analysis of the separation of enantiomers may be accomplished.

The enantioseparation of ibuprofen was achieved and allowed the calculation of separation factor and peak resolution at each temperature and pressure. The separation factor is the quotient of the retention factor of the more retained solute divided by the retention factor of the less retained solute. The more retained solute will have a higher

adjusted retention time due to its increased interactions with the stationary phase. It should also be noted that the separation factor may be determined from the quotient of the adjusted retention time of the more retained solute divided by the adjusted retention time of the lesser retained solute. The resolution is perhaps a better way to measure not only the separation value but incorporate the efficiency as well. Resolution is a function of separation factor, retention factor, and theoretical plate number. In chromatography the efficiency is represented qualitatively by the narrowness of the peaks. Therefore, the resolution measures the difference of the retention times divided by the average peak width of the two peaks measured at the base in minutes. The theoretical plate number is the measure of the narrowness of the peaks. A large theoretical plate number means high efficiency in chromatography. Plate number is determined from the peak and is rounded to the nearest one hundredth and must be reported with the solute name.

Determination of these stated parameters while trying to maintain a speed of throughput and efficiency is important. Typically in gas chromatography, a retention factor of five is very good along with a resolution of one and a half. It is possible to exceed these rules of thumb but not without sacrificing run time. In pharmaceuticals, time is money. Therefore, this author set out to find suitable conditions (temperature, pressure) by which to achieve fast, baseline separations. Then those conditions were reproduced when performing the breakthrough experiments for isotherm determination.

A typical pulse experiment would consist of choosing a temperature and pressure, bringing the system to steady state, and performing repeated non-retained solute injections followed by the solute of interest. Even though most solutes eluted in less than ten minutes, at least double that amount of time was allowed in between to ensure that the

system was free of solute and operating at steady state. Keeping the system at steady state is a key aspect in acquiring accurate data. An important aspect of these experiments was keeping the system leak free. Running nitrogen through the system and ensuring all connections were sound accomplished leak detection. If any leaks were present, no matter how insignificant, the system was slowly depressurized allowing for leak repair.

Qualitatively, the system was leak free when the automated backpressure made the least amount of noise per unit time. Alternatively, when the automated backpressure regulator was working constantly to keep the system pressure it was obvious to the carful observer that there was a leak somewhere in the system. It should be noted that one of the benefits of working with carbon dioxide for method development in a laboratory setting is clearly delineated by these investigations.

A table of the pulse experiments analyzed is shown below in Table 5.4. These experiments were repeated three times to ensure reproducibility. Temperatures ranging from 30 to 55 ^{o}C were run at each different pressure of 100, 130 and 150 Bar respectively. Concentration injections ranging from 1, 5, 15, 30, 50, 75, 100, 150, 300 mg/mL were performed.

Table 5.4. Supercritical Fluid Chromatograph Pulse Experiments Analyzed

	Ibuprofen Racemate	**(R)-Ibuprofen**	**(S)-Ibuprofen**
Temperature [^{o}C]	30, 35, 40, 45, 50, 55	30, 35, 40, 45, 50, 55	30, 35, 40, 45, 50, 55
Pressure [Bar]	100, 130, 150	100, 130, 150	100, 130, 150
Pump Set Flow Rate [mL/min]	3	3	3
Mobile Phase Composition [w/w]%	95:5 CO_2:EtOH	95:5 CO_2:EtOH	95:5 CO_2:EtOH
Injection Volume [µL]	10	10	10
UV Detector Wavelength [nm]	260	260	260
Concentration [mg/mL]	5, 10, 15, 30, 50, 75, 100, 150, 300	5, 10, 15, 30, 50, 75, 100, 150, 300	5, 10,15, 30, 50, 75, 100, 150, 300

Table 5.5 below shows the breakthrough experiments analyzed in Chapter 6. The solute was delivered using the HPLC pump for the breakthrough experiments. The step input of a known concentration allows insight towards the equilibrium isotherm, the concentration gradient driving force, and the detector response. The breakthrough experiments were used to verify select pulse experimental results. They provide a situation where saturation of the column occurs and allows for straightforward calculations of isotherms. However, they use up vast amounts of solute and are challenging to accomplish.

Table 5.5. Breakthrough Experiments Analyzed

	(R)-Ibuprofen	**(S)-Ibuprofen**
Temperature [^{o}C]	40	40
Pressure [Bar]	150	150
Pump Set Flow Rate [mL/min]	3	3
Mobile Phase Composition [w/w]%	95:5 CO_2:EtOH	95:5 CO_2:EtOH
UV Detector Wavelength [nm]	260	260
Concentration [mg/mL]	10	10, 30, 40, 50, 100

5.5. Detector Calibration

Detector calibration is of importance when introducing solute via small pulses, as it directly influences the accuracy of the measured data. The system behaved well within the linear range of detectability. This was verified prior by John Whelan who worked previously for this lab. When adsorption isotherms are determined by breakthrough experiments these data may also be used for the detector calibration. In cases when this is not possible, such as lack of solute or time, pulse data may be used for calibration as long as they are varied over a large concentration range. This was accomplished regardless of the bulk experiments carried out. A calibration curve was developed by relating the concentration of the analyte of the detector to the peak volume. The mass of the solute present at the column temperature was related to the volume of the mobile

phase. In this case, the detector output, volts, which were correlated so as one unit volt equaled one unit mass per volume.

In the case when the concentration injected is a known, the plot of c_{feed} versus the detector signal u is the desired relationship and a calibration function is fitted to these values (Schmidt-Traub, 2005). If the form of the calibration function

$$c = f_{cal}(u) \tag{5.1}$$

is known a priori, a pulse experiment may also be used to obtain the calibration curve. For a known amount of sample injected:

$$m_{inj} = V_{inj} * c_{feed} = \dot{V} * t_{inj} * c_{feed} \tag{5.2}$$

The mass balance for the detected peak is:

$$m_{inj} = \dot{V} \int_0^{\infty} c(L_c,t)\, dt = \dot{V} \int_0^{\infty} f[u(t)]dt \tag{5.3}$$

In the specific case of a linear relationship, such as low concentration, Equation 5.4 is used.

$$c = F_{cal} u \tag{5.4}$$

Equations 5.2 and 5.3 combined with the numerical integration of the detector signal allow for the determination of the calibration factor F_{cal}:

$$F_{cal} = \frac{V_{inj} c_{feed}}{\dot{V} \int_0^\infty u(t)\,dt} = \frac{t_{inj} c_{feed}}{\int_0^\infty u(t)\,dt} \tag{5.5}$$

Detectors calibration may be determined by mathematical curve fitting as well. For complex calibration functions with more than one unknown parameter, additional information or pulse experiments with different concentrations are necessary. In the case of this work, both breakthrough and pulse experiments were used to determine the detector calibration curve. The detector showed good response in the linear range.

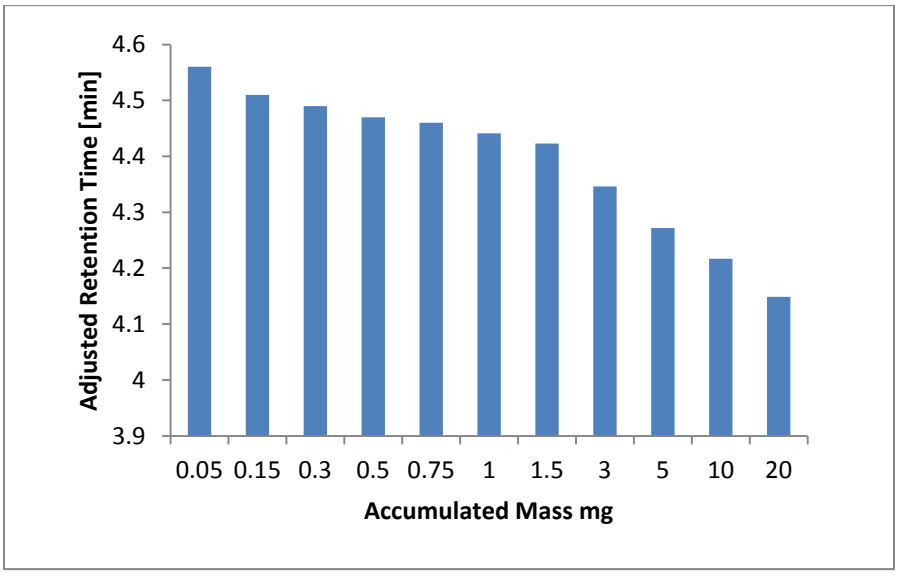

Figure 5.10. Adjusted Retention Time versus Mass

Figure 5.10 shows that increasing the concentration of the S-ibuprofen, decreases the retention time and provides a broad range to determine the detector calibration curve. Increasing the concentration of each pulse allows one to determine the detector response as a function of mass.

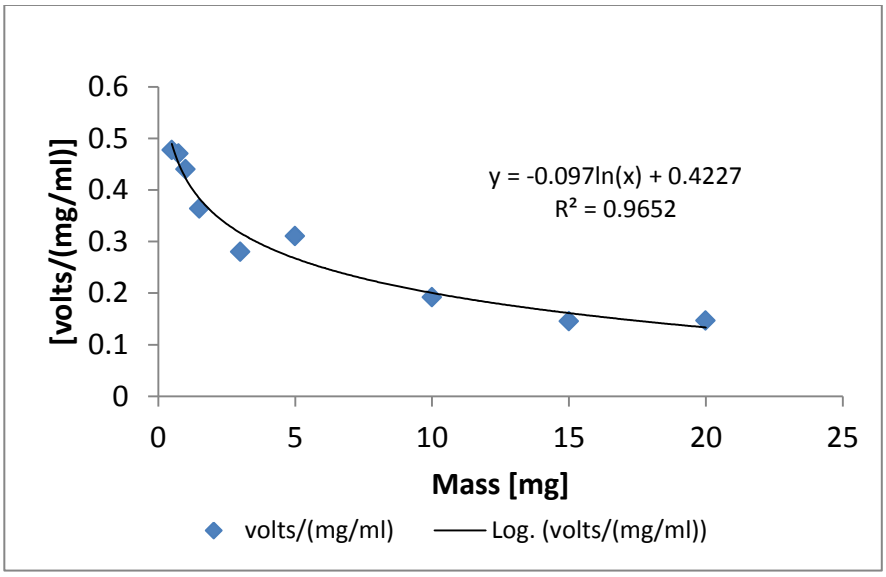

Figure 5.11. Pulsed Mass Calibration Curve S-ibuprofen

Figure 5.11 shows a linear relationship between the volts/mg/mL and the mass. Taking the natural log of the y-axis and x-axis shows this result in Figure 5.12.

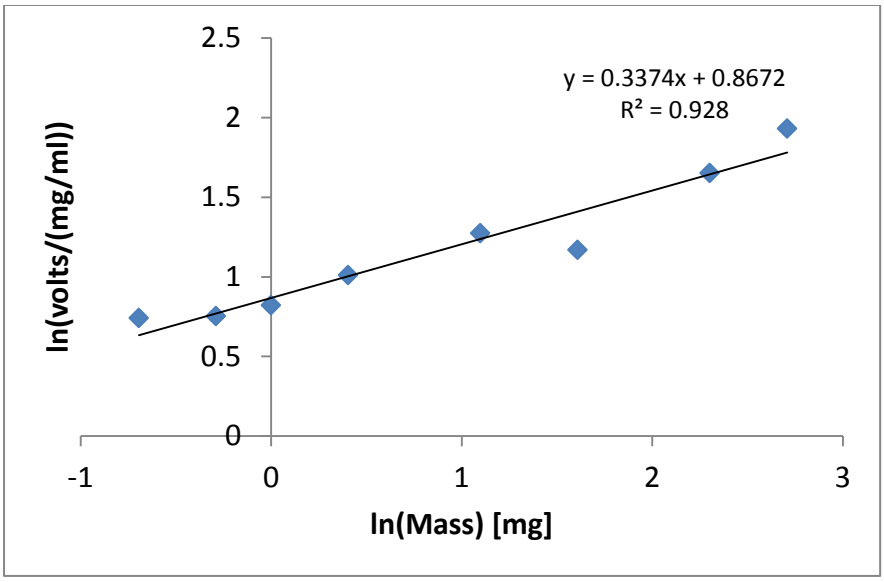

Figure 5.12. Pulsed Mass Calibration Curve for S-ibuprofen

Figure 5.12 shows the relationship between the volts/(mg/mL) and the injected mass. As the pulsed mass injected raises, the voltage needed to read one mg/ml unit goes down. This is a useful result and can serve as a calibration curve for future pulse experiments.

Compared to bulk methods used for the determination of isotherms detector calibration is not as important. This is because the calibration can be made concurrently from the plateaus of the step changes in concentration for other uses as needed. In the pulse feed input, the detector response signal must be converted to concentration units by calibrating the detector. This was accomplished as shown in Figure 5.12. Since the pulse input of solute is different than complete saturation, it was preferred to calculate both detector responses to better understand its behavior at low and high concentrations.

5.6. Column Void and Porosity Determination

Additional parameters that need to be derived from the standard chromatogram are the column porosities and the void fraction. These parameters must be determined and are the basis for detailed modeling, simulation and isotherm determination.

The total volume of the packed column V_c is divided into two sub-volumes. They are the interstitial volume of the fluid phase V_{int} and the volume of the stationary phase V_{ads}.

$$V_c = \pi \frac{d_c^2}{4} L_c = V_{ads} + V_{int} \tag{5.6}$$

Again, V_{ads} consist of the volume of the solid material V_{solid} and the volume of the pore system V_{pore} as seen in the following equation:

$$V_{ads} = V_{solid} + V_{pore} \tag{5.7}$$

Using these relationships for volumes, the different porosities can be calculated. The void fraction, epsilon is:

$$\varepsilon = \frac{V_{int}}{V_c} \tag{5.8}$$

The porosity of the solid phase is:

$$\varepsilon_p = \frac{V_{pore}}{V_{ads}} \tag{5.9}$$

The total porosity is therefore:

$$\varepsilon_t = \frac{V_{int} + V_{pore}}{V_c} = \varepsilon + (1 - \varepsilon)\varepsilon_p \tag{5.10}$$

Practical determination of porosities is accomplished by injection of a non-retained, pore-penetrating tracer substance. In normal phase chromatography, as the case in SFC, toluene and 1, 3, 5-tri-tert-butlybenzene is often used. The interstitial velocity of the mobile phase is given as Equation 5.11.

$$u_{int} = \frac{\dot{V}}{\varepsilon\pi\frac{d_c^2}{4}} \tag{5.11}$$

In addition, it is useful to determine the volume delivered by the pump during the determination of the hold-up time. Then the total porosity can be calculated as:

$$\varepsilon_t = \frac{t_M\dot{V}}{V_c} \tag{5.12}$$

Table 5.6 shows the calculated values described by the previous Equations 5.6 to 5.12. These values allow for proper characterization of the chromatographic column. Now it is possible to evaluate the stationary phase volume, the column voids and the available interstitial space left for separation and sorption processes. Additionally, these parameters are necessary for isotherm determination since the loading is a function of the stationary phase mass and density. The column diameter is 0.46 cm and has a length of 25 cm.

Table 5.6. Calculated Volumes and Porosities of Whelk O1 CSP

Parameter	**Description**	**Calculated Value**	**Units**
V_c	Column Volume	4.15	cm^3
ε	Void Fraction	0.58	cm^3 / cm^3
ε_p	Solid Phase Porosity	0.84	cm^3 / cm^3
ε_t	Total Porosity	0.93	cm^3 / cm^3
u_{int}	Mobile Phase Interstitial Velocity	31.43	cm / min
V_{ads}	Stationary Phase Volume	1.77	cm^3
V_{int}	Mobile Phase Interstitial Volume	2.39	cm^3
V_{solid}	Solid Material Volume	0.28	cm^3
V_{pore}	Pore System Volume	1.48	cm^3

CHAPTER 6

RESULTS AND DISCUSSION

This chapter presents results and observations from the experimental work accomplished in the Laboratory of Environmentally Friendly Engineered Systems at the University of South Florida. Pure component isotherms for ibuprofen were determined on the Whelk O1 chiral stationary phase. Different isotherm determination method results are reflected in this chapter and correspond to Frontal Analysis, Frontal Analysis by Characteristic Point, and Elution by Characteristic Point Pulse Method. Subsequent modeling using the Langmuir isotherm equation provides a frame of reference for these observations. Overall, FA, FACP, and ECP Pulse provide good isotherms from chromatographic separation. The subtle differences being the FA and FACP provide accurate column saturation capacity at equilibrium, while the ECP Pulse provides accurate initial slope estimation with rapid analysis time.

Sources of error and modeling are presented at the end of Chapter 6. The error analysis provides delineation between inherent and systemic error associated with chromatographic isotherm determination. At low concentrations, the effect of temperature fluctuation is significant on the isotherm determination. Overall, the possible pressure fluctuation causes the largest variance in the isotherm determination.

6.1. Frontal Analysis Results

Frontal analysis method was used to determine isotherms from the chromatographic system described in Chapter 5. These results from the FA method are presented in this section. Table 6.1 provides the conditions used for the FA experiments performed.

Table 6.1. Experimental Conditions used in Frontal Analysis for S-ibuprofen

Temperature [^{o}C]	**Pressure [Bar]**	**Mobile Phase Composition [w/w%]**	**UV Detector Wavelength [nm]**	**Concentration [mg/mL]**
40	150	95:5 CO_2:EtOH	260	10
40	150	95:5 CO_2:EtOH	260	30
40	150	95:5 CO_2:EtOH	260	50

Frontal analysis experimental results are shown in Figure 6.1. I started off with CO_2 ethanol plus S-ibuprofen solute. Then after about 30 minutes, the solute feed was switched off and pure CO_2 ethanol was allowed to continue to flow. The sorption of the S-ibuprofen solute is shown in Figure 6.1.

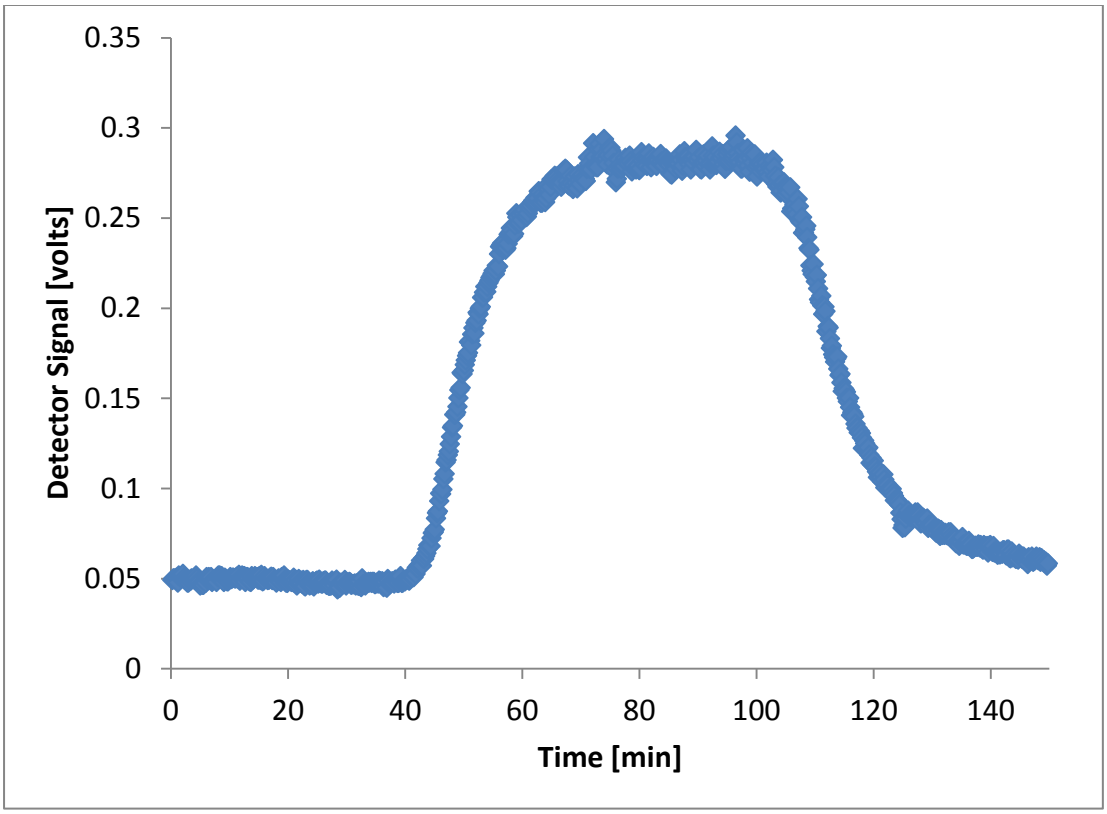

Figure 6.1. 40 mg S-ibuprofen in CO_2:EtOH at 40^{o}C and 150 Bar

CO_2, ethanol and ibuprofen are already flowing at time zero. At about thirty minutes for all FA experiments, the composition was changed to CO_2 and ethanol at (95:5) so that desorption could be observed on the chromatogram. This is shown graphically in Figure 6.1. Once the chromatogram was recorded, a transformation was done to plot the chromatogram as a function of mobile phase flow rate. Figure 6.2 shows the chromatogram transformation of Figure 6.1 to a function of mobile phase flow rate.

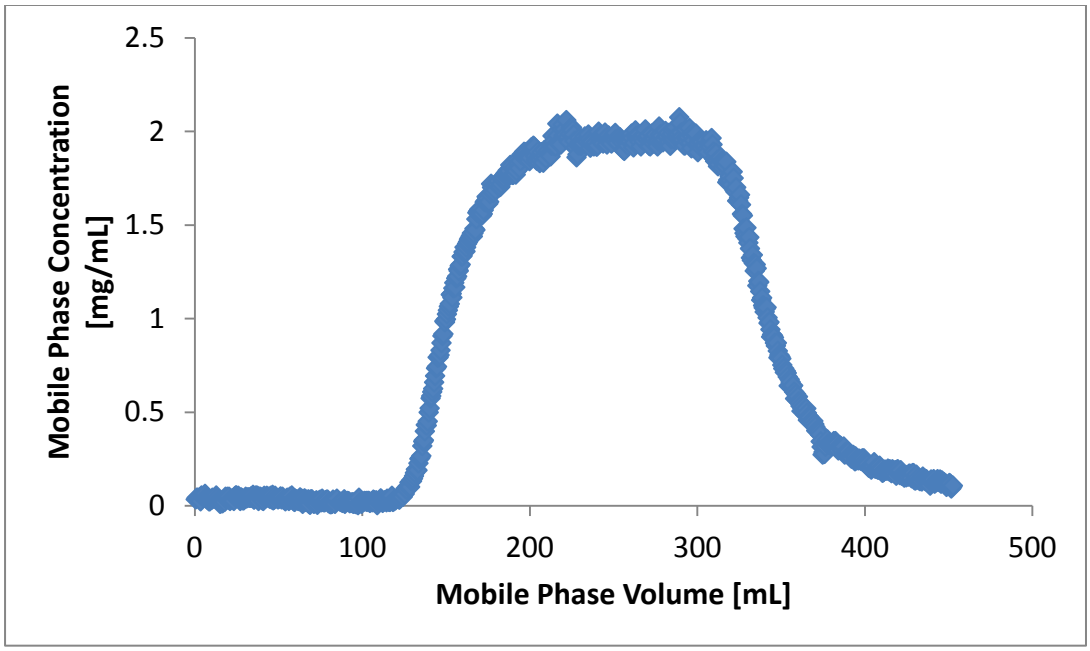

Figure 6.2. Adsorption of 40 mg/mL S-ibuprofen at 40^{o}C and 150 Bar

In its current form Figure 6.2 can be integrated to give the adsorption isotherm. This is done by accounting for the data in the initial step up such that integration is done only up 200 mL for this specific run. Integration of Figure 6.2 yields the isotherm which is shown as Figure 6.3. The translation of the x and y-axis was intended so as the integration of any part of the curve would yield the mass. The area of interest in Figure 6.2 is the first moment of inflection just after 100 mL to the second inflection around 200 mL, where adsorption and desorption begin respectively. Integration of this dynamic response yields the isotherm. Since all isotherms are specific to the stationary phase mass the loading q is divided by the mass of the adsorbent. In this case the Whelk O1 has a mass of 3 mg. Therefore, the q located on the y-axis in Figure 6.3 represents the stationary phase concentration of S-ibuprofen on the Whelk O1in equilibrium with the S-ibuprofen mobile phase concentration in the supercritical CO_2.

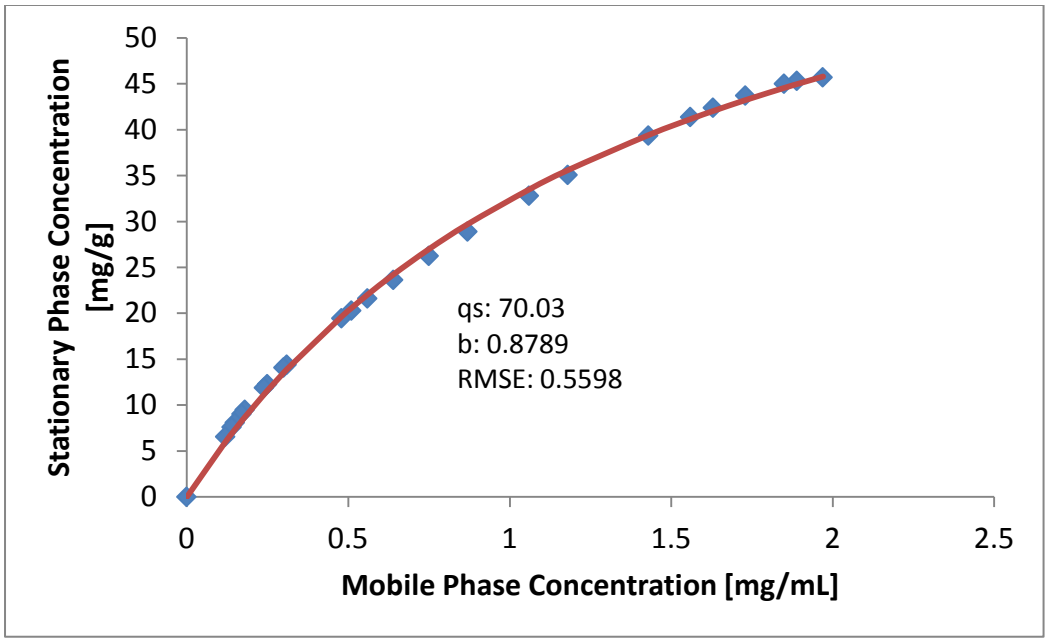

Figure 6.3. Isotherm of 40 mg/mL S-ibuprofen at 40°C, 150 Bar

Figure 6.3 shows the Langmuir isotherm of S-ibuprofen in CO_2 ethanol at 40°C and 150 Bar. The Langmuir isotherm was chosen over other isotherm models due to it thermodynamic consistency and simplicity. Additionally, the Langmuir equation adequately models the linear and non-linear portion of the isotherm. These adsorption data were determined experimentally and then imported into Logger Pro software for the non-linear regression. The q_s and b which are reported in Figure 6.3 reflect the fitted parameters determined by Logger Pro. The RMSE or root mean square of error is determined upon non-linear regression. The RMSE is the square root of the variance between the fitted model and experimental data.

Scatchard plots are useful for graphical clarification. Essentially if the Scatchard plot yields a straight line plot then the isotherm determined is acceptable. This is done graphically as shown in Figure 6.4 by plotting q/c on the y-axis versus q on the x-axis.

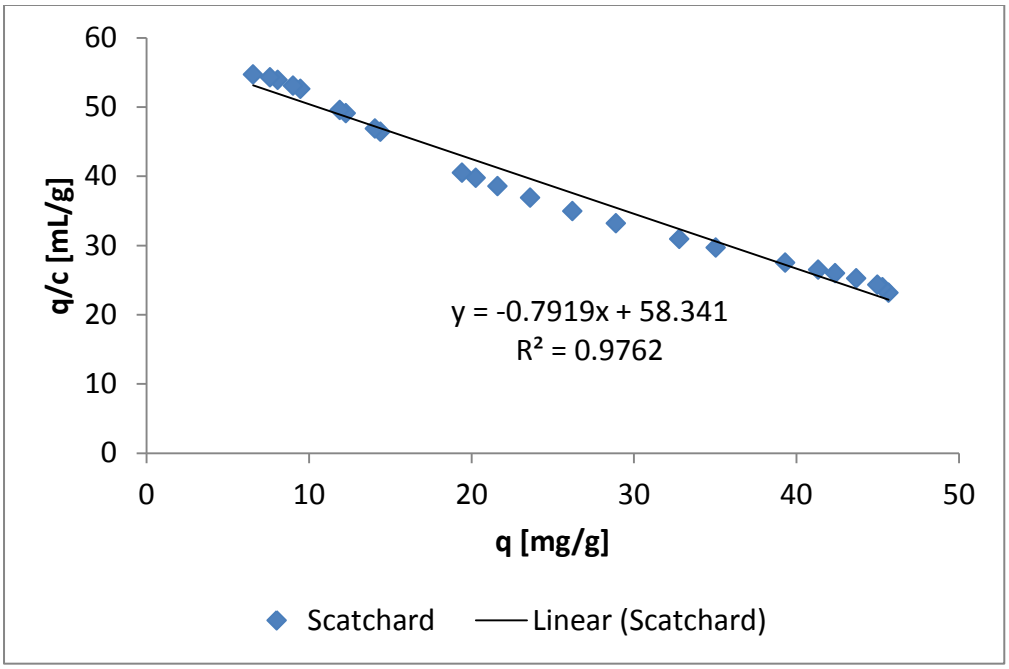

Figure 6.4. Scatchard Plot of S-ibuprofen Equilibrium Data 40°C and 150 Bar

Figure 6.4 shows the Scatchard plot of S-ibuprofen equilibrium data at 40°C and 150 Bar. The straight line fitted using Microsoft Excel 2007 shows about a 98% linear fit. This means two things. The isotherm determination method is valid and the use of the Langmuir equation is acceptable. This is because the Langmuir equation may be linearized to fit adsorption data. This was often done before non-linear regression analysis software like Logger Pro was available.

Following the same methodology with Figures 6.1, 6.2, and 6.3, additional isotherms were determined for other concentration at 40°C and 150 Bar. These are shown in Figure 6.4. The equilibrium data were fit to the Langmuir isotherm using non-linear regression analysis. These results are shown in Table 6.2. The concentrations include 10, 30, and 50 mg/mL.

Figure 6.5 shows three different isotherm concentrations at the same conditions. The 10 mg/mL isotherm shows a decreased slope as compared to the 30 and 50 mg runs. This is due to the decreased concentration gradient driving force as well as the sorption effect. The sorption effect is a result due to the effects in the partial molar volumes of the component in solution in the mobile phase and adsorbed on the stationary phase.

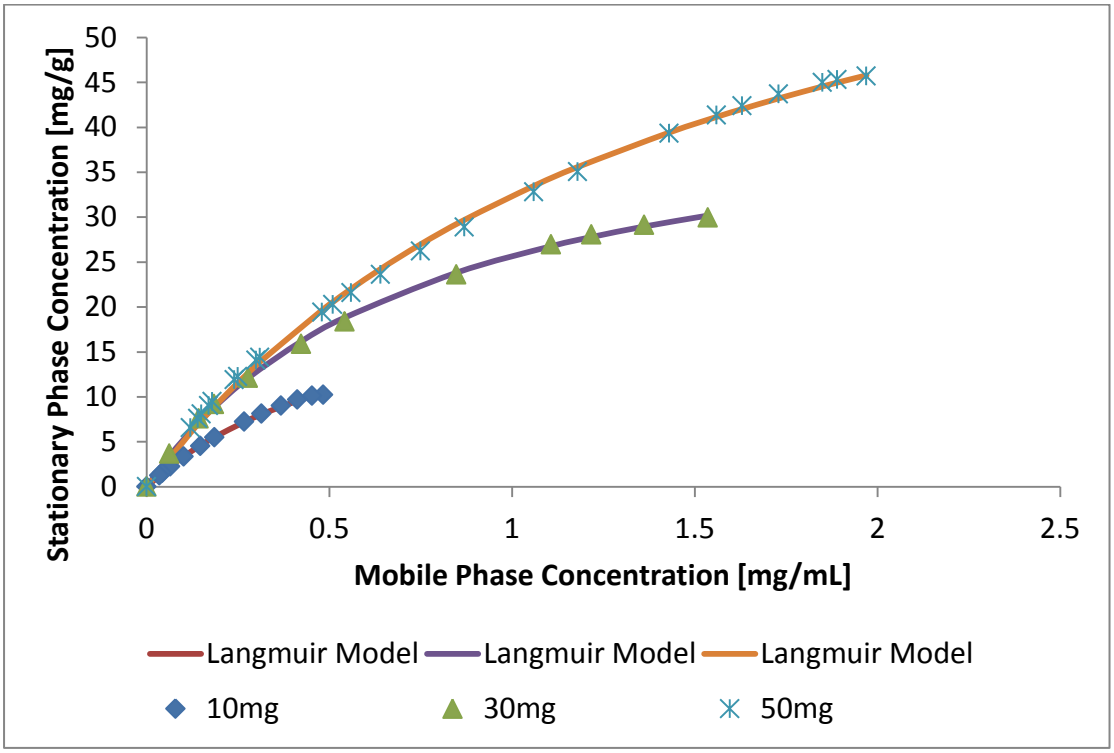

Figure 6.5. Additional Equilibrium Data of S-ibuprofen 40^{o}C and 150 Bar

Table 6.2 shows the fitting parameters of these equilibrium data using the Langmuir isotherm equation. The RMSE for all runs was below one which means that these data show good agreement with the Langmuir model. As the concentration increases, the adsorption coefficient b decreases as shown in Table 6.2. The adsorption coefficient or sometimes called the Langmuir coefficient represents the degree of sticking

interaction the solute has with the stationary phase. Table 6.2 also shows the saturation capacities, q_s. The saturation capacity is a value inherent of the stationary phase. It represents the amount of a component needed to saturate the stationary phase on the column. More specifically, the saturation capacity represents the amount of compound needed to make a monolayer on the adsorbent surface.

Table 6.2. S-ibuprofen FA Experiments at 40^{o}C and 150 Bar

Concentration [mg/mL]	**q_s [mg/mL]**	**b [mL/mg]**	**RMSE**
10	23.67	1.643	0.0972
30	44.96	1.33	0.2956
50	80.03	0.6789	0.5598

6.2. Frontal Analysis by Characteristic Points Results

The FACP method was used in determination of the adsorption equilibrium isotherms for S-ibuprofen. Similar to the FA method, the FACP uses the same chromatogram but the tail end for equilibrium data. Table 6.3 shows the experiments performed using the FACP method for isotherm integration.

FACP was performed by washing the loaded solute, S-ibuprofen from the Whelk O1 CSP by purging with pure mobile phase. The mobile phase being the original (95:5) CO_2:EtOH composition.

Table 6.3. Experimental Conditions used in FACP for S-ibuprofen

Temperature [^{o}C]	**Pressure [Bar]**	**Mobile Phase Composition [w/w%]**	**UV Detector Wavelength [nm]**	**Concentration [mg/mL]**
40	150	95:5 CO_2:EtOH	260	10
40	150	95:5 CO_2:EtOH	260	50
40	150	95:5 CO_2:EtOH	260	100

Figure 6.6 represents the chromatogram of 50 mg/mL S-ibuprofen interacting with the Whelk O1 at the experimental conditions of 40^{o}C and 150 Bar. The wavelength set on the UV detector was set for 260 nm. It should be noted that the mobile phase consisting of CO_2 and ethanol gives a steady signal of 0.05 volts. This baseline voltage is steady and has little noise associated with it. Figure 6.6 shows the total sorption and saturation of S-ibuprofen on the Whelk O1 CSP using SFC.

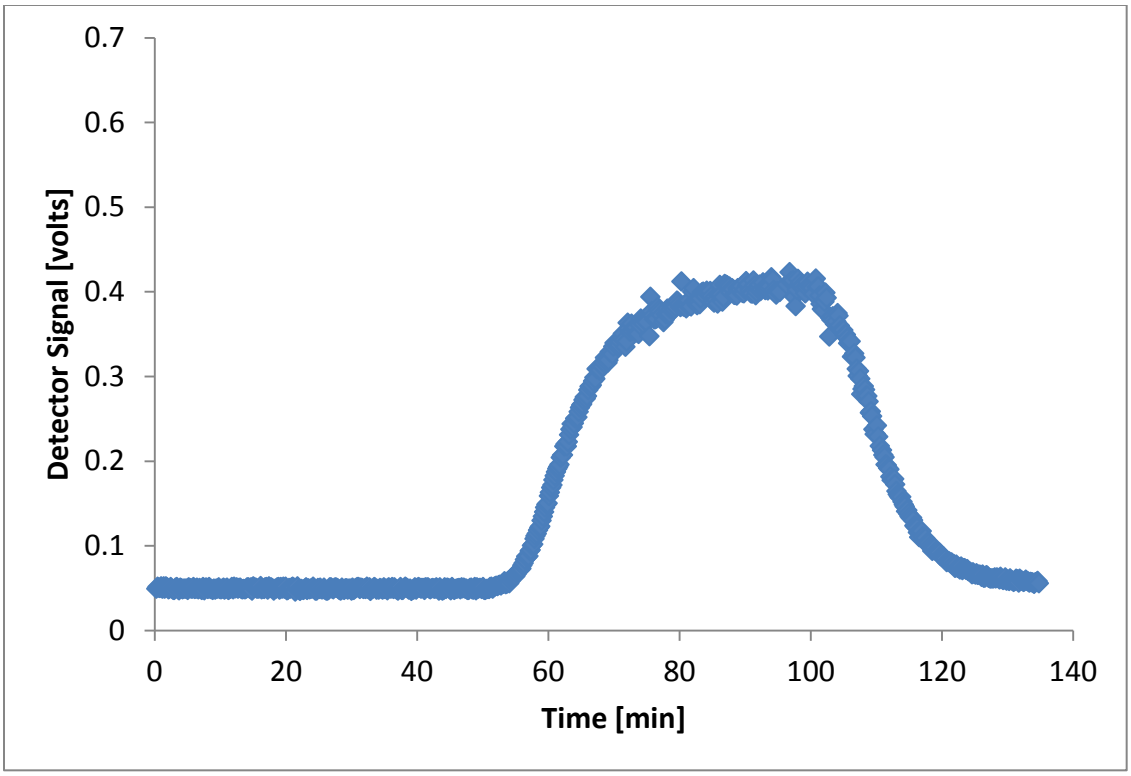

Figure 6.6. Chromatogram of 50 mg/mL S-ibuprofen 40^{o}C and 150 Bar FACP

The chromatogram shown in Figure 6.6 is then transformed into Figure 6.7 by mathematical manipulation. The y-axis which is in units of volts is converted to concentration units of mg/mL. Specifically, the concentration shown in Figure 6.6 on the y-axis is representative of mass of S-ibuprofen per volume of total mobile phase solution. It is important to make a distinction between this value and the initial concentration of the sample. This means that 2.5 mg/mL shown on the y-axis of Figure 6.6 represents the maximum of the original solution concentration of 50 mg/mL. This is due to the extra dilution that happens when the plug of original solution enters the supercritical fluid chromatograph. The x-axis of Figure 6.6 is achieved by multiplying the time data from

Figure 6.6 by the volumetric flow rate. This allows for integration of Figure 6.7 to give the mass of solute loading onto the stationary phase.

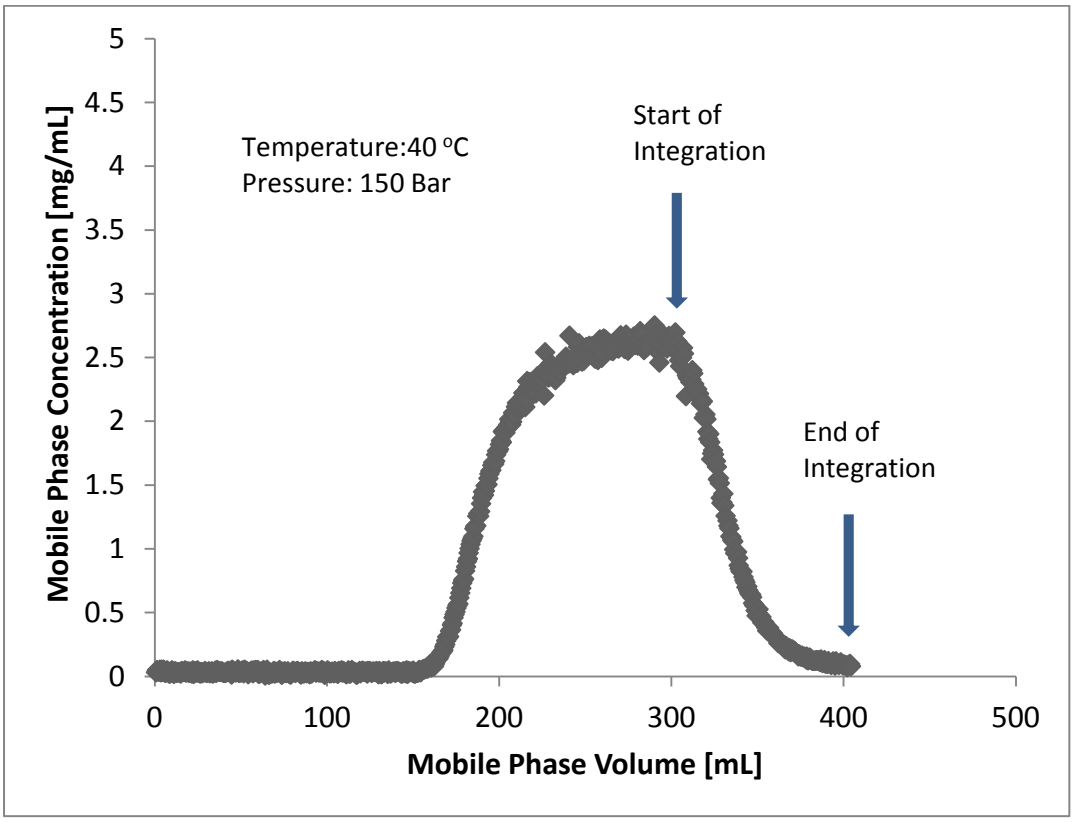

Figure 6.7. Adsorption of 50 mg/mL S-ibuprofen at 40°C, 150 Bar

The volumetric flow rate used for this calculation was the set flow rate of 3 mL total mobile phase solution per minute. It should be noted that the actual flow rate will be higher when the mobile phase transitions to the supercritical fluid regime. This will result in an error associated with these calculations which is discussed in this chapter.

Figure 6.8 is the adsorption equilibrium isotherm for 50 mg/mL of S-ibuprofen at 40°C and 150 Bar. The equilibrium relationship was derived from the rear part of the chromatogram in Figure 6.7. The range analyzed from about 300 mL to 400 mL was

used for the integration and subsequent plot of these equilibrium data. It should be noted that the origin of the isotherm shown in Figure 6.8 corresponds to the points at the start of the integration range marked in a text box located in Figure 6.7.

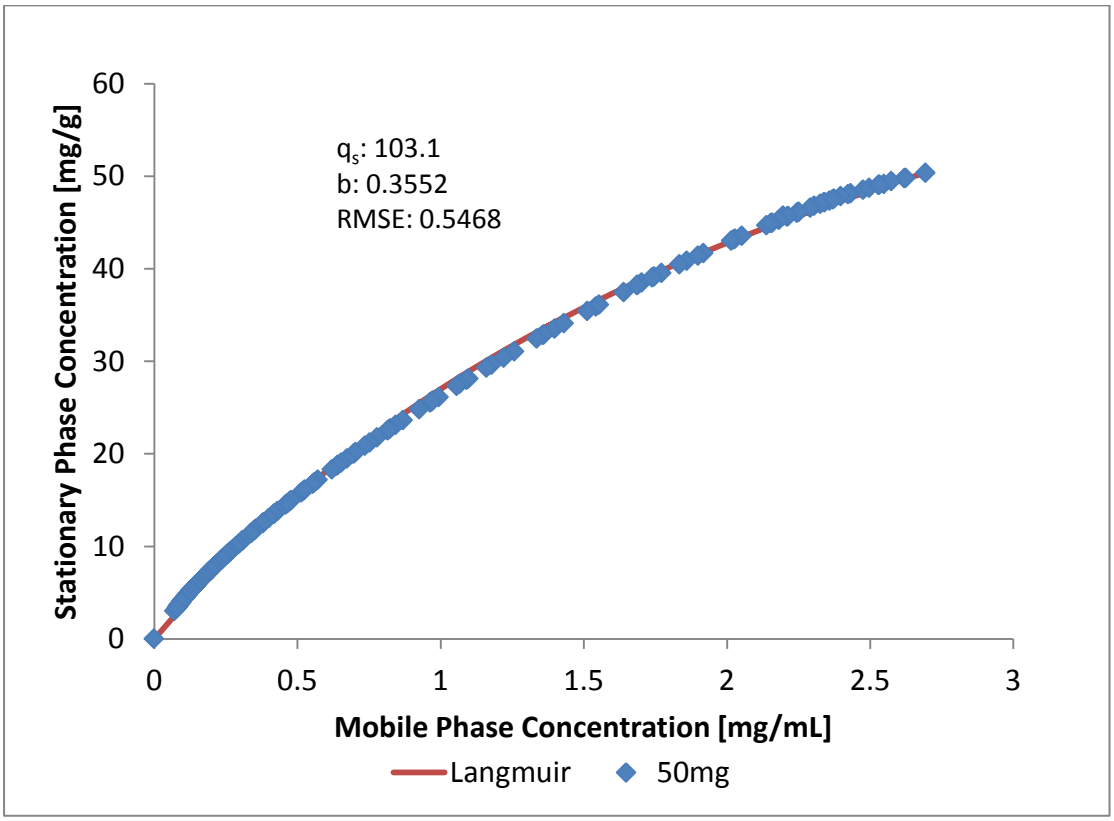

Figure 6.8. Equilibrium Data for 50 mg/mL S-ibuprofen 40°C and 150 Bar FACP

The FACP method provides isotherms similarly to the FA method. A Scatchard plot shown in Figure 6.9 shows how well these equilibrium data are modeled by the Langmuir isotherm. It can be seen in Figure 6.8 that the linear fit is about 94% of these data. The FA method of isotherm determination of a similar system showed a slightly better agreement. This show the inherent susceptibility FACP has to dispersion and kinetic effects. More specifically, FACP itself is just a tool to determine equilibrium

data. However, since the FACP method is derived by integrating the rear, desorption part of a chromatogram, there are certain drawbacks as seen in the Scatchard plot in Figure 6.9. These are that the tail end of chromatograms are influenced by dispersion effects and mass transfer processes that are negligible but apparent.

Nonetheless, these data show a good fit to the model equation. Moreover, the FACP method is in many ways more desirable than FA as it provides insight into these additional diffusion processes.

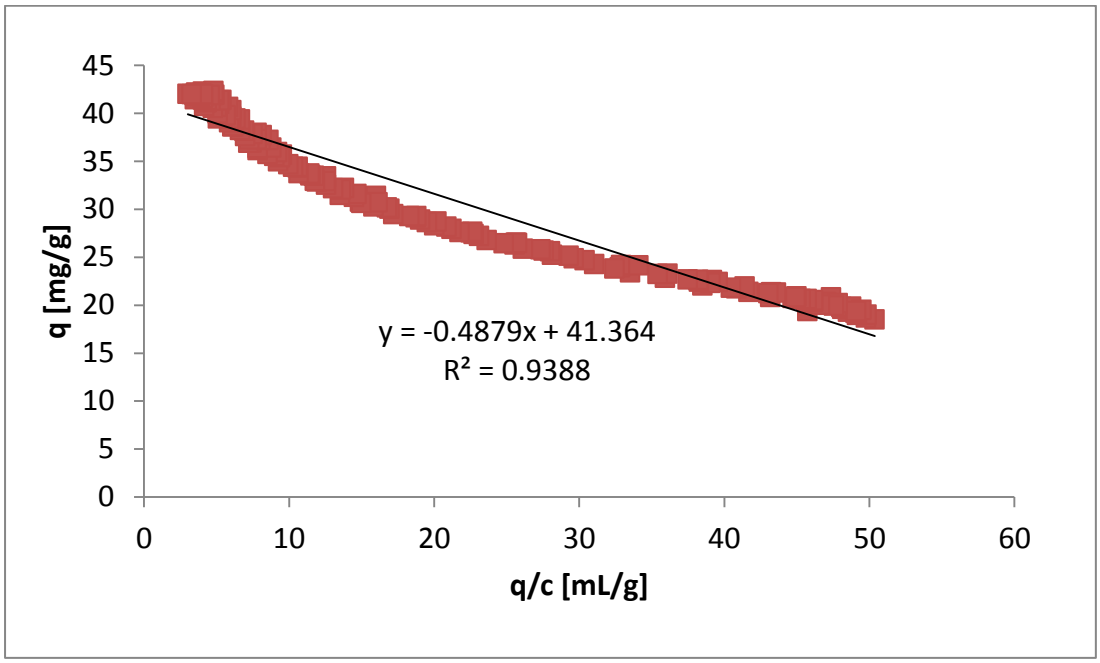

Figure 6.9. Scatchard Plot of 50 mg/mL S-ibuprofen 40^{o}C and 150 Bar FACP

The desorption chromatogram of 100 mg/mL of S-ibuprofen at 40^{o}C, 150 Bar is shown in Figure 6.10. This was the highest concentration successfully loaded onto the supercritical fluid chromatograph. This run provides additional loading information and capabilities of the Whelk O1 CSP.

The mobile phase flow rate was 3 mL/min at a constant ratio of (95:5) CO_2 to ethanol modifier ratio. The isotherm for this run is shown in Figure 6.11.

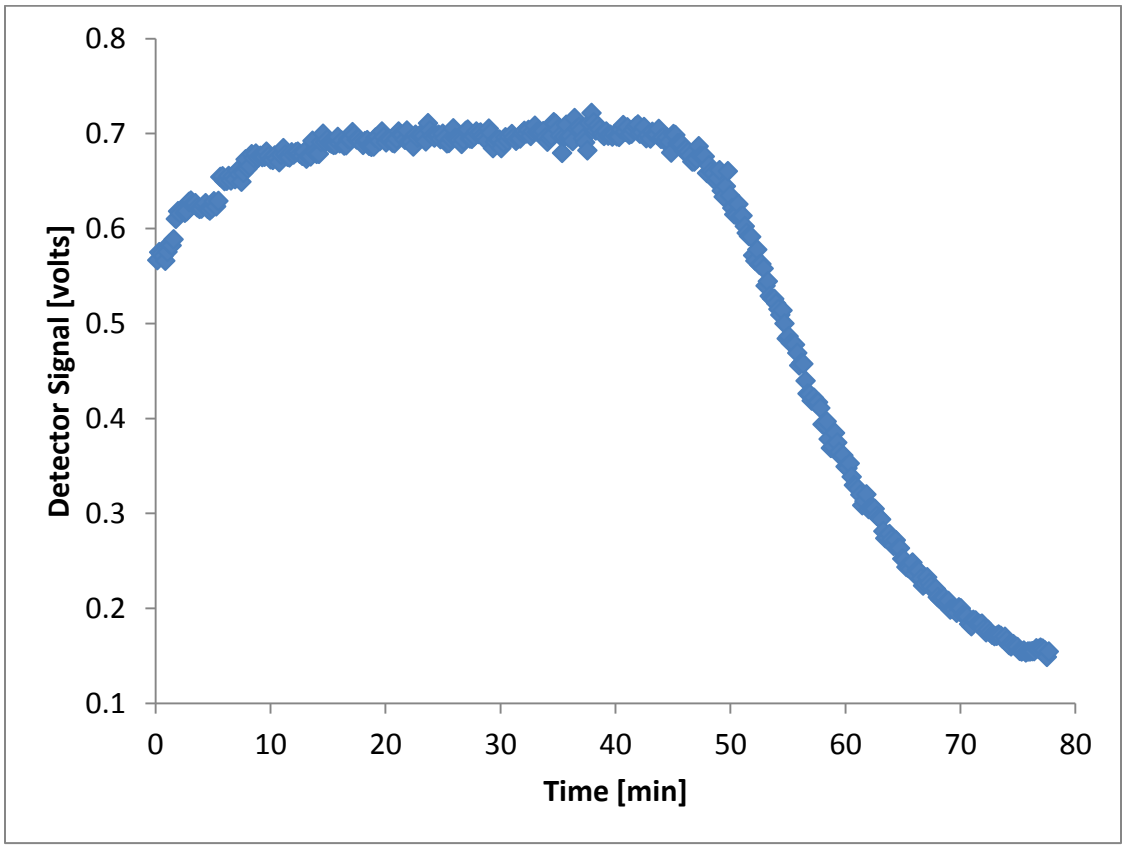

Figure 6.10. Chromatogram of 100 mg/mL S-ibuprofen at 40°C, 150 Bar

Figure 6.11 shows the equilibrium data for 100 mg/mL S-ibuprofen at 40°C, 150 Bar. These data were determined using the FACP method from the desorption of 100 mg/mL of S-ibuprofen at 40°C, 150 Bar as shown in Figure 6.9. This high concentration run took several attempts to complete in that the systems limits were being pushed. This run provides additional loading information and capabilities of the Whelk O1 CSP. The mobile phase flow rate was 3 mL/min at a constant ratio of (95:5) CO_2 to ethanol

modifier ratio. The loading information shows that approximately 5 mg of S-ibuprofen in solution corresponds to 100 mg on the chiral stationary phase at equilibrium. That means that this CSP is capable of twenty times the adsorption of a solute at equilibrium.

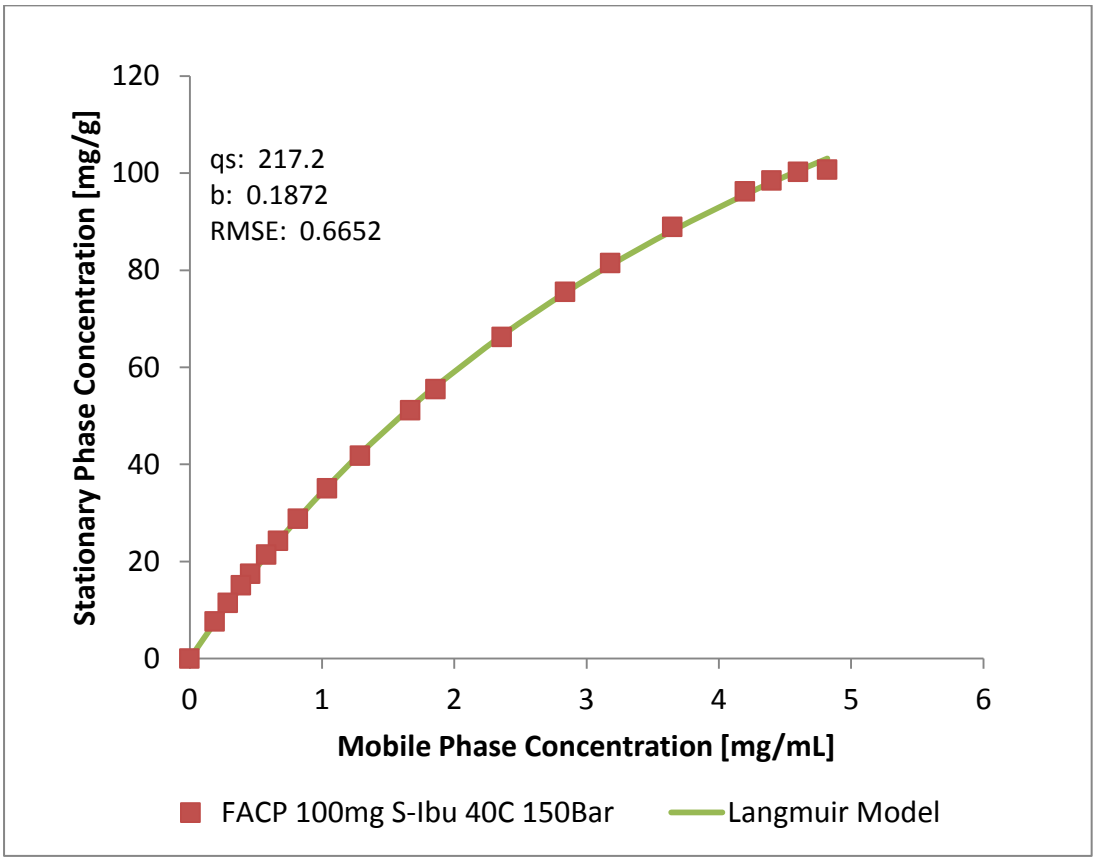

Figure 6.11. Isotherm of 100 mg/mL S-ibuprofen at 40°C, 150 Bar FACP

Figure 6.12 shows the Scatchard plot for 100mg/mL S-ibuprofen 40°C and 150 Bar. FACP was used in the isotherm determination. The Langmuir isotherm model was used to determine the fitting parameters. The Scatchard plot shows the validity of the Langmuir isotherm as well as these equilibrium data. The y-axis of the Scatchard plot represents the quotient of the stationary and mobile phase concentration. When plotted

against the x-axis which represents the solute loading, it may be determined how good the equilibrium data follow a thermodynamically favorable isotherm.

Although these plots are convenient for checking the validity of the model in a particular case, non-linear regression should be the method used in determining the values of b and q_s. These represent the degree of interaction and the amount of interaction with the surface of the stationary phase respectively.

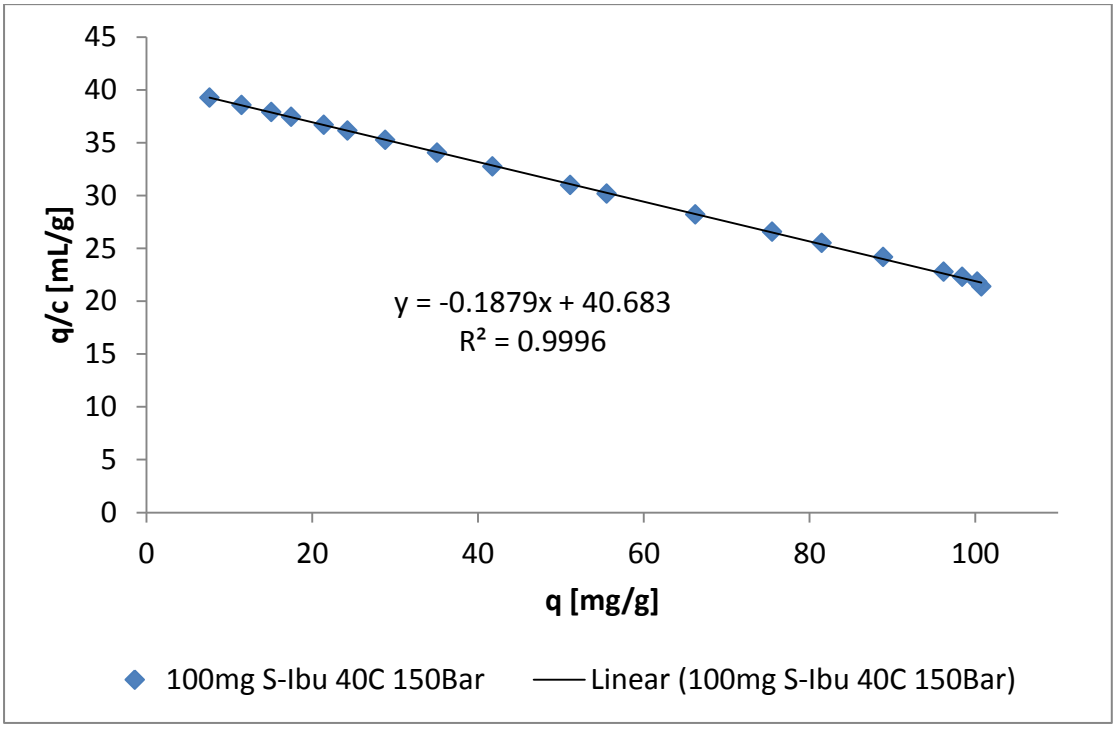

Figure 6.12. Scatchard Plot of 100mg/mL S-ibuprofen 40°C and 150 Bar FACP

Figure 6.13 shows additional isotherms determined using the FACP method. Figure 6.12 shows three different isotherm concentrations at the same conditions. The 10, 50 and 100mg runs are reflected. The increasing concentration shows a different saturation capacity. This is due to the decreased concentration gradient driving force as

well as the sorption effect. The slopes of each isotherm are the same at very low concentrations. This should be expected in that they are well within the linear portion of the isotherm.

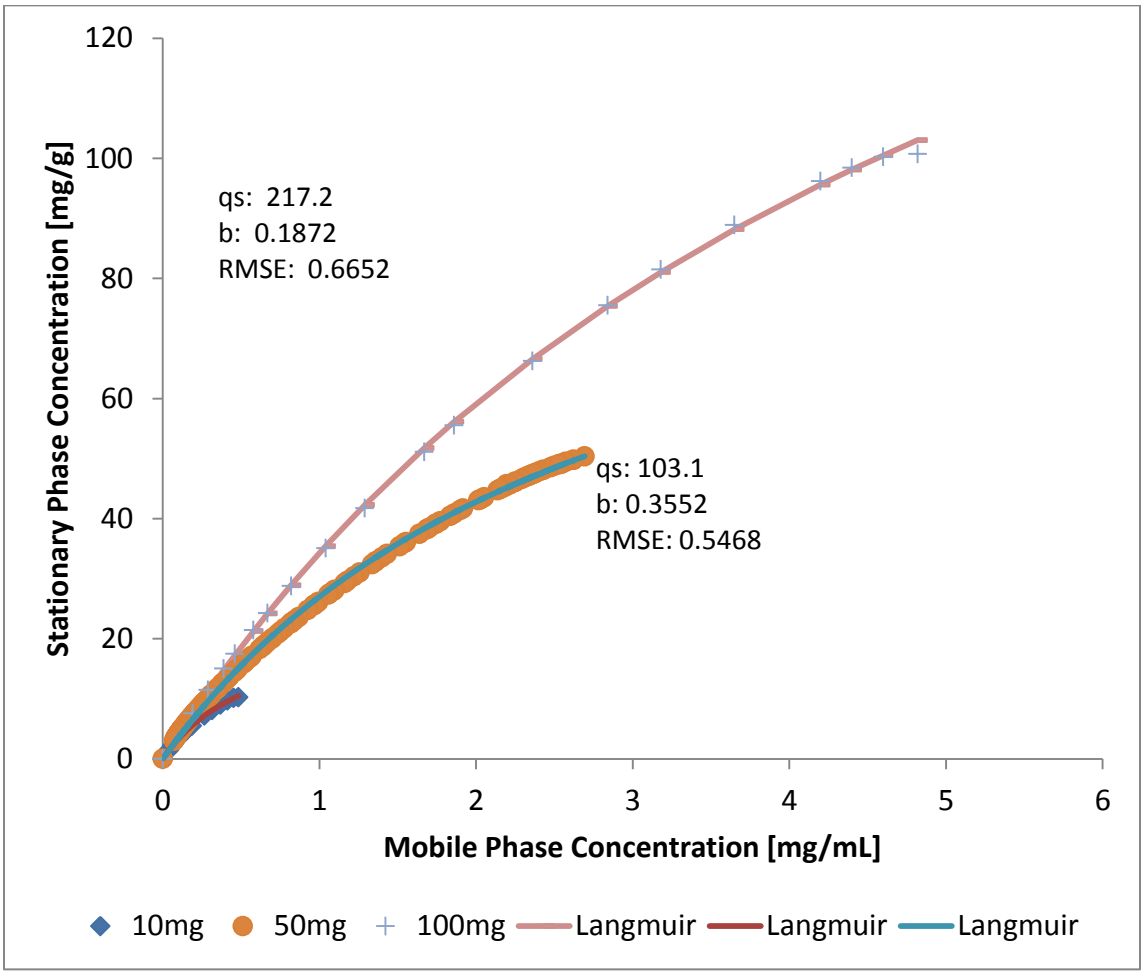

Figure 6.13. Additional Equilibrium Data of S-ibuprofen 40°C and 150 Bar

Table 6.4 shows the saturation capacity, adsorption coefficient and root mean square of the error for the isotherms shown in Figure 6.13. These isotherms for S-ibuprofen were determined at 40^{o}C and 150 Bar using a mobile phase flow rate composition of (95:5) CO_2:EtOH. The sorption effect is probably the reason for the high adsorption coefficient for the 10mg run in Table 6.4.

Table 6.4. S-ibuprofen FACP Experiments at 40^{o}C and 150 Bar

Concentration [mg/mL]	**q_s [mg/mL]**	**b [mL/mg]**	**RMSE**
10	17.23	2.734	0.03372
50	103.1	0.3552	0.5468
100	217.2	0.1872	0.6652

6.3. ECP Pulse Method Analysis Results

ECP Pulse method was used to determine isotherms from the chromatographic system described in Chapter 5. These results from the ECP method are presented in this section. Table 6.5 provides the conditions used for the ECP experiments performed.

Table 6.5. Supercritical Fluid Chromatograph Pulse Experiments Analyzed

	Ibuprofen Racemate	**(R)-Ibuprofen**	**(S)-Ibuprofen**
Temperature [^{o}C]	30, 35, 40, 45, 50, 55	30, 35, 40, 45, 50, 55	30, 35, 40, 45, 50, 55
Pressure [Bar]	100, 130, 150	100, 130, 150	100, 130, 150
Pump Set Flow Rate [mL/min]	3	3	3
Mobile Phase Composition [w/w]%	95:5 CO_2:EtOH	95:5 CO_2:EtOH	95:5 CO_2:EtOH
UV Detector Wavelength [nm]	260	260	260
Concentration [mg/mL]	5, 10, 15, 30, 50, 75, 100, 150, 300	5, 10, 15, 30, 50, 75, 100, 150, 300	5, 10,15, 30, 50, 75, 100, 150, 300

6.3.1. Single Solute S-ibuprofen Results

Pure enantiomers of S-ibuprofen were used to obtain isotherms using the ECP Pulse Method. Additional chromatograms and isotherms are presented in Appendix G. Figure 6.13 shows the single solute elution by pulse of S-ibuprofen using the ECP pulse method. First the time and detector response are recorded. This chromatogram as shown in Figure 6.14 is then converted to the intermediate graph in Figure 6.15. This is done by manipulating the y-axis so as it has units of concentration.

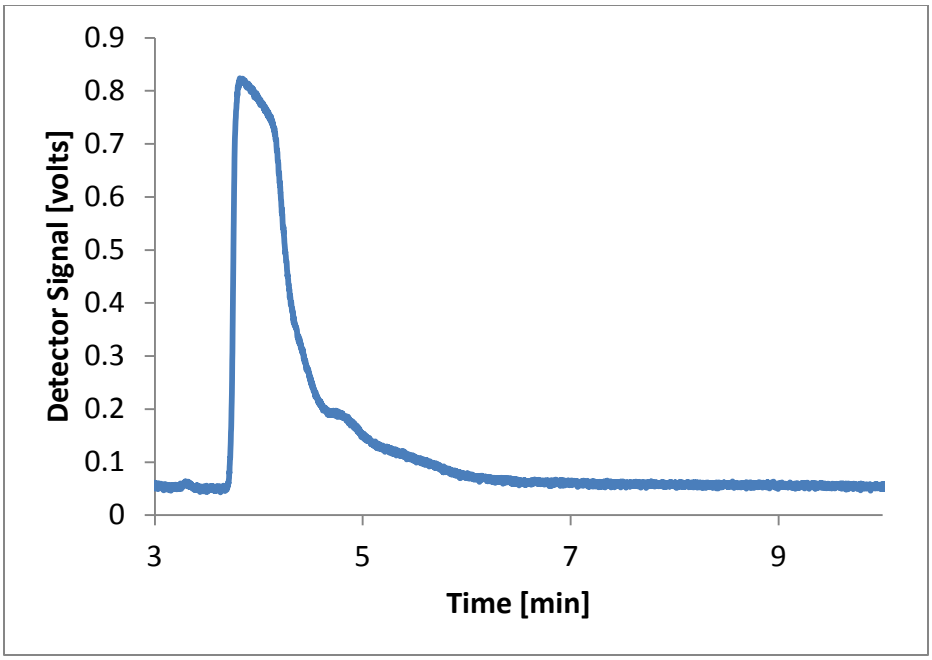

Figure 6.14. Chromatogram of 30mg S-ibuprofen 40^{o}C 130 Bar ECP

Figure 6.15 is the intermediate plot for use in the ECP pulse calculation. Essentially, like the FA and FACP methods, the graph is set up so as an integration be done. However, the integration is done by fitting a polynomial to these data and integrating that polynomial expression.

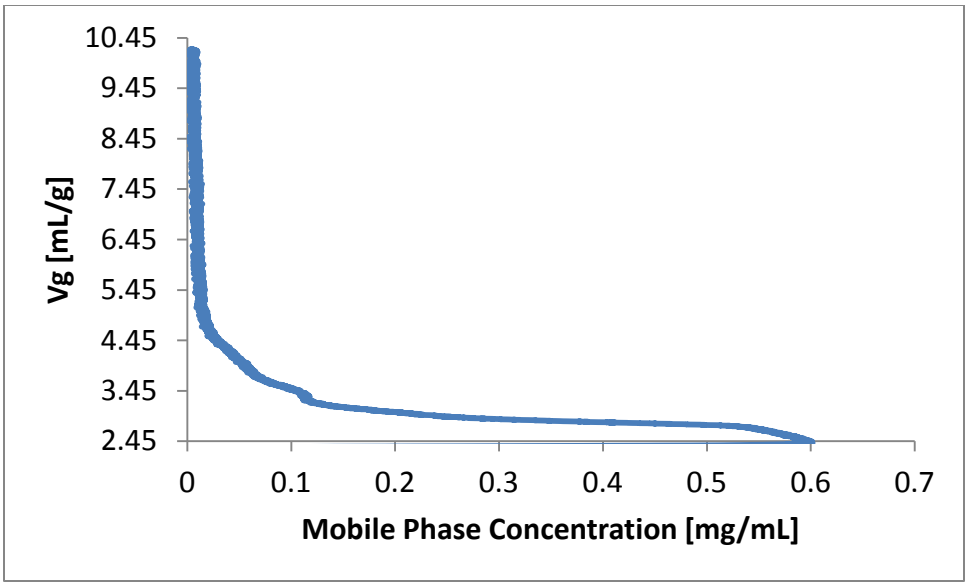

Figure 6.15. Intermediate Plot for Integration using ECP Pulse Method

Figure 6.16 is the isotherm of 30 mg/mL of S-ibuprofen at 40°C 130 Bar using the ECP method. The pulse method does not provide the concave shape.

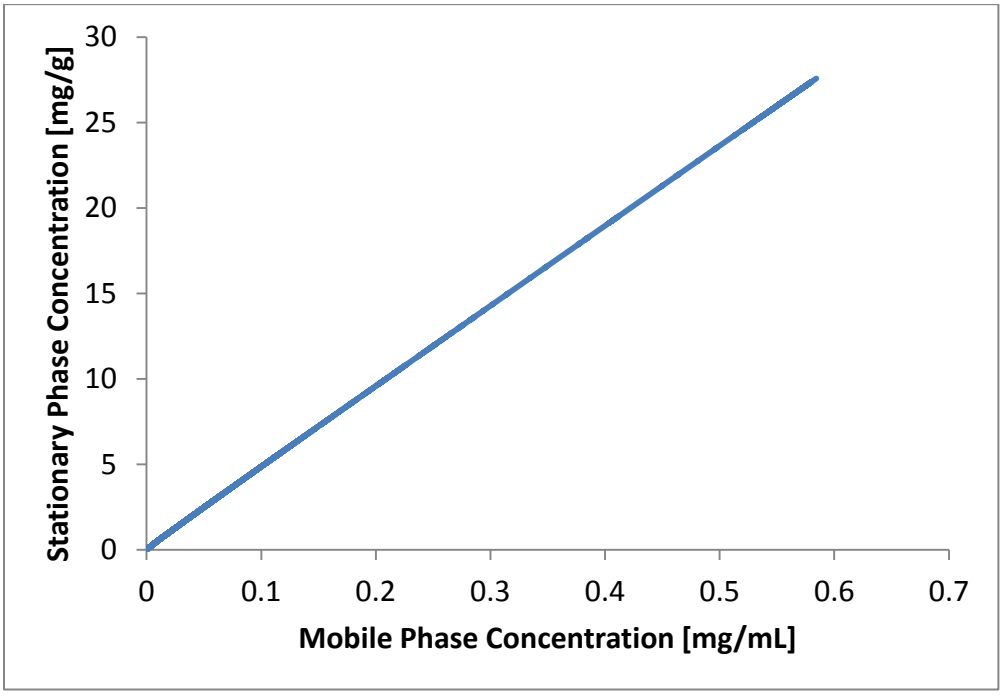

Figure 6.16. Isotherm S-ibuprofen at 40°C 130 Bar ECP Pulse

Figure 6.17 represents the single solute injections made using the ECP pulse method. Essentially, the mass injected was varied while keeping the conditions of the SFC the same. Figure 6.17 shows injections ranging from 0.05mg to 20mg of S-ibuprofen at 40^{o}C 130 Bar.

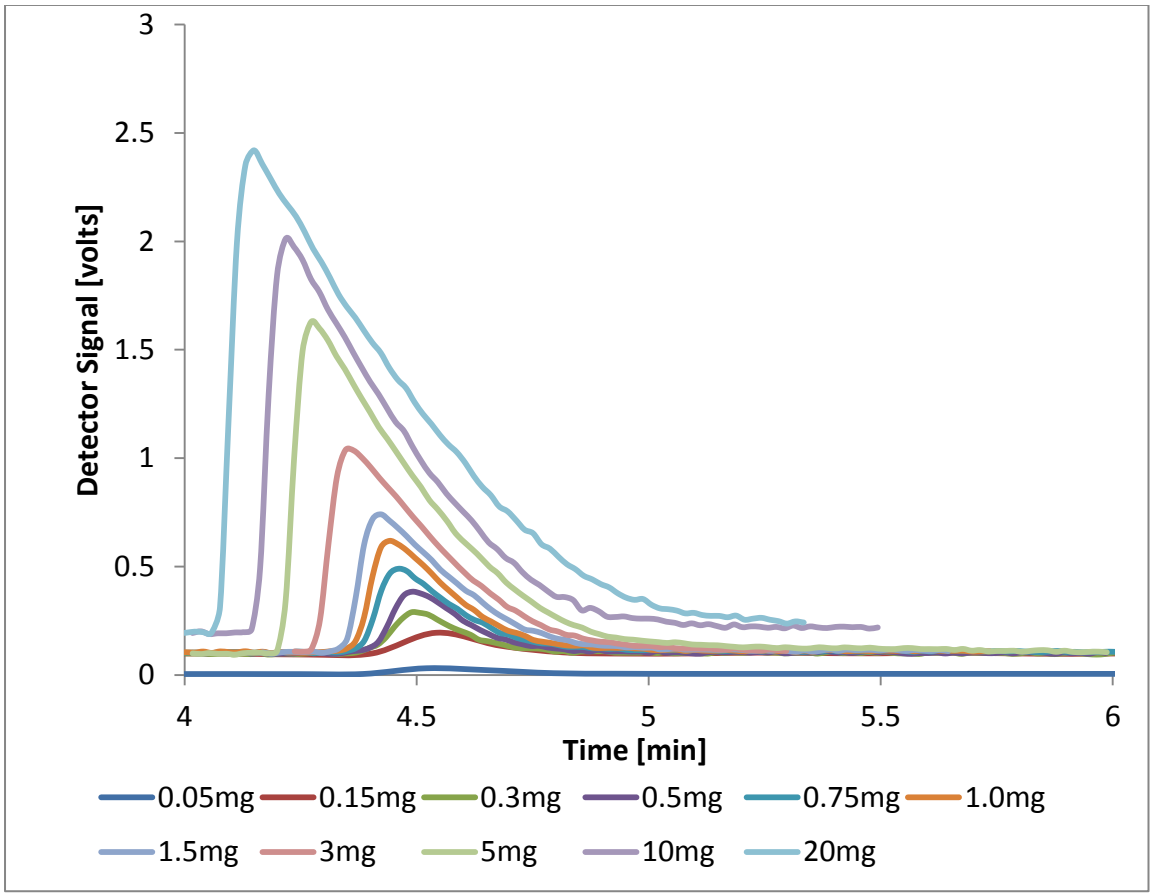

Figure 6.17. Multiple Elution of S-ibuprofen with Increasing Mass 0.05-20mg

Figure 6.17 shows the increasing concentration or mass with the same solute. As a consistency check, the isotherms from each individual run were compared to ensure repeatability. Figure 6.18 shows the results from this exercise and shows the loading in units of mg/mL.

Figure 6.18 shows the result of the isotherms being determined using the ECP pulse method. It should be noted that each experimental run produced an isotherm with the same slope as the others. This is significant in that is shows the reproducibility of the ECP pulse method. Additionally, the ECP pulse method requires only 10 micro-liter samples, which makes this method of isotherm determination robust and economical.

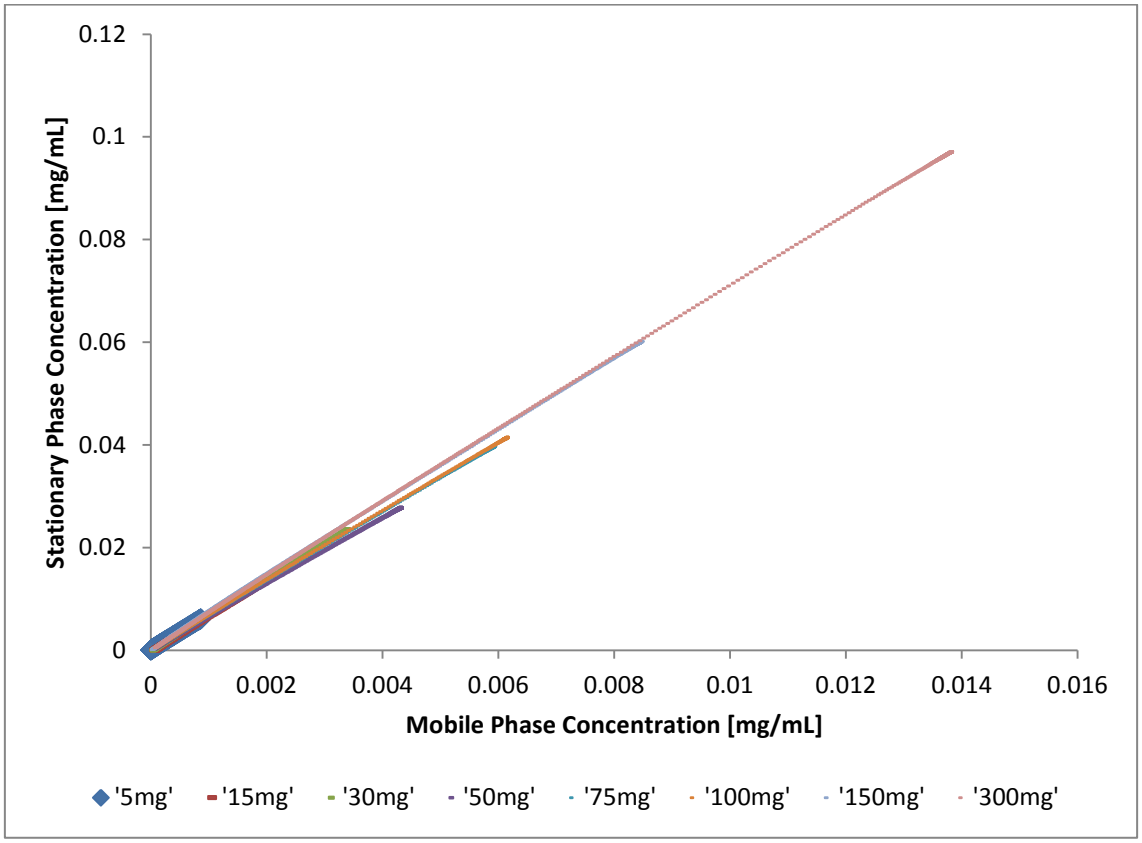

Figure 6.18. Multiple S-ibuprofen Isotherms 5-300 mg

Figure 6.19 shows the variation of system pressure on the determined isotherm. Figure 6.19 shows that as the pressure is increased, the loading of S-ibuprofen decreases. This is known as the retrograde effect. This is the opposite result seen in isotherms

derived from liquid chromatography. In supercritical fluid chromatography, the retrograde adsorption effect is evident up until the crossover pressure is reached. The crossover region refers to range of pressures for a solute system, where the solubility of one component increases with temperature, while the solubility of the other decreases with temperature at a given pressure. Figure 6.20 supports these observations as well.

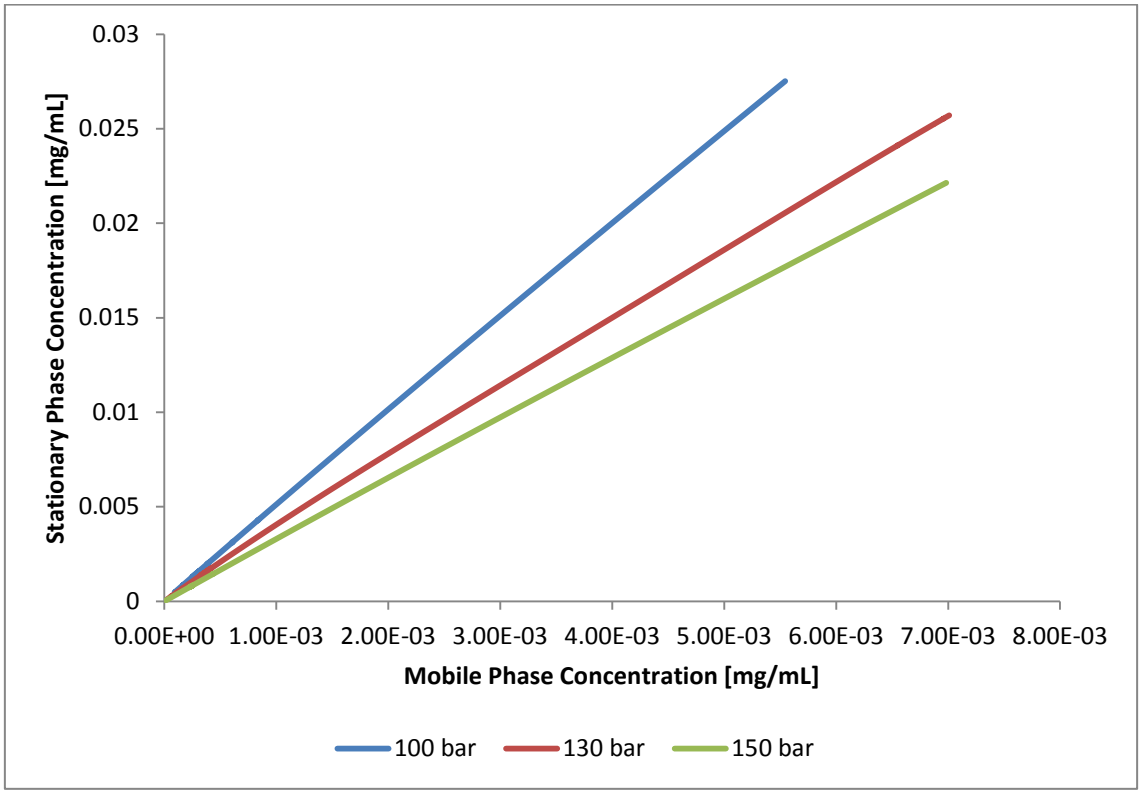

Figure 6.19. Pressure Effect on ECP Pulse Method Isotherm Determination

Figure 6.20 shows the variation of temperature on the loading of S-ibuprofen on the Whelk O1 CSP. Here the pressure was held constant at 130 Bar, while the temperature was varied from 30^{o}C to 55^{o}C. The results seen in Figure 6.20 indicate retrograde sorption behavior. That is the stationary phase loading, represented on the y-

axis shows an increasing trend as temperature increases. This is counter-intuitive to HPLC results. Moreover, since these experiments were run below the crossover region, it may be seen that the trend of solute loading follows that typical of supercritical fluid chromatography.

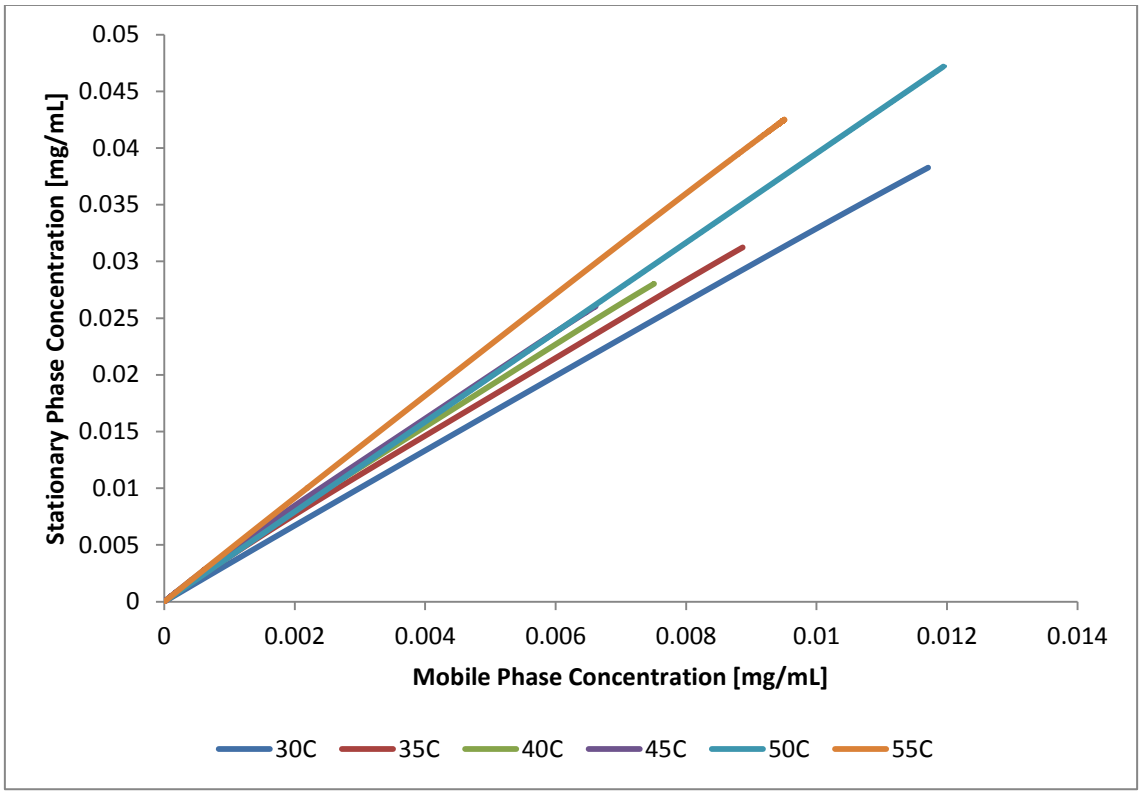

Figure 6.20. Temperature Effect on ECP Pulse Method Isotherm Determination

Section 6.3.2. covers the separation of the racemic ibuprofen using SFC. Although it was not the main focus of this work to cover the analytical separation of enantiomers, it provided valuable information in choosing the optimum conditions for the bulk experiments.

6.3.2. Separation of Ibuprofen Enantiomers with Pulse Method

Figure 6.21 shows the racemic ibuprofen separation of 5mg at 30°C and 130 Bar. This separation chromatogram was plotted using Microsoft Excel. Then the peaks were analyzed by fitting them to straight lines and determining the width of the peak at half-height, inflection height, and base. The three widths are recorded not in length units but rather time units. This allows for direct evaluation of the chromatographic parameters such as peak reolution, separation factor, and theoretical plate height. Table 6.6 contains the calculated chromatographic parameters obtained from Figure 6.21.

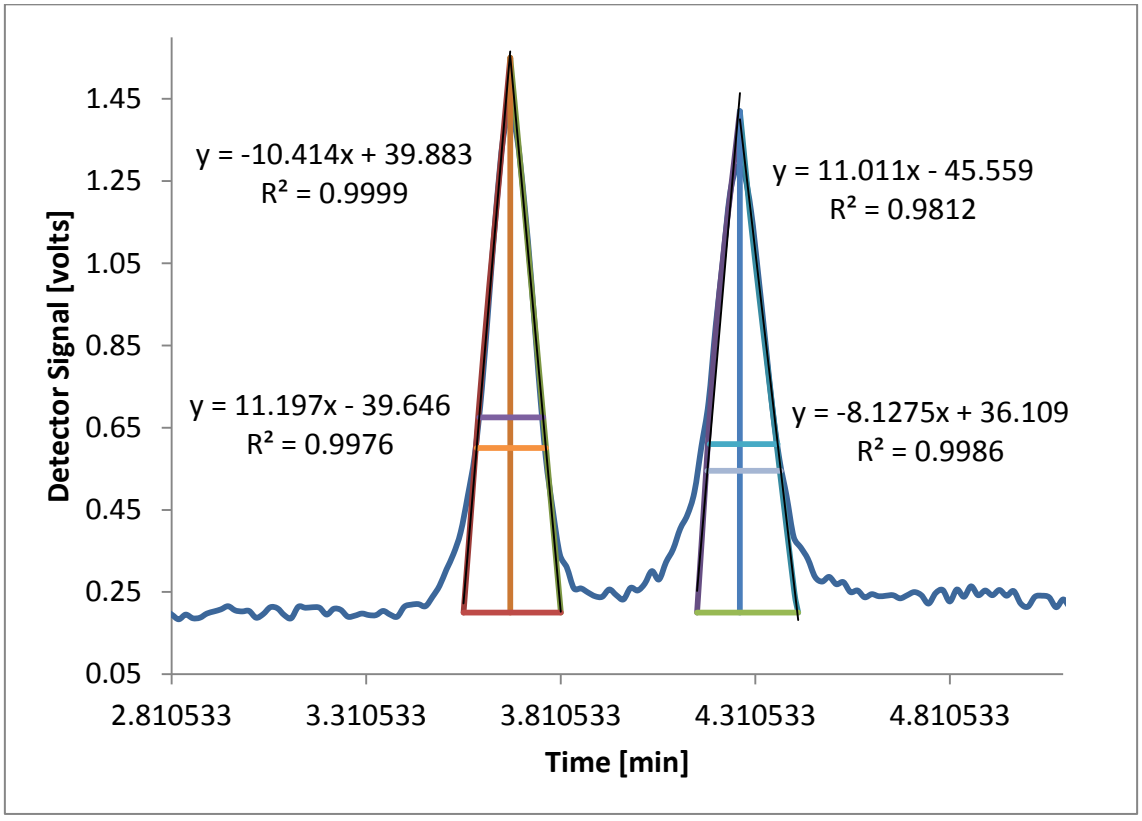

Figure 6.21. Racmemic Ibuprofen Separation 5mg 30°C and 130 Bar

Table 6.6 shows the calculated chromatographic parameters obtained from Figure 6.21. The efficiency is calculated from the three different widths previously detailed. Here it is apparent that the width at half-height gives a different efficiency than the width at base. This an expected result and it is common to have a spread of efficiencies. However, in practice most chromatographers use the width at half height efficiency. Therefore, the calculated values of 2400 and 3200 theoretical plates represents the plate efficiency of the S and R-ibuprofen.

Table 6.6. Racemic Ibuprofen Separation Calculation Results

	Calculation S-Ibuprofen	**Calculation R-Ibuprofen**
Adjusted Retention Time	2.47 min	3.06 min
Efficiency from Width at Half Height	2400 Plates	3200 Plates
Efficiency from Width at Inflection Point	2000 Plates	2700 Plates
Efficiency from Width at Base	3500 Plates	4300 Plates
HETP	0.105 mm/Plate	0.078 mm/Plate
Effective Plate Number	1100 Plates	1500 Plates
Height Equivalent to One Effective Plate	0.23 mm/Plate	0.17 mm/Plate
Reduced Plate Height	10.51 $Plates^{-1}$	7.81 $Plates^{-1}$

Table 6.7 shows the separation factor and peak resolution of the racemic ibuprofen separation shown in Figure 6.20. Table 6.7 shows a value of 1.24 for the

separation. This is a great result considering that the ibuprofen enantiomers were resolved using only 5% modified carbon dioxide. Moreover, the peak resolution value of 2.31 shows that when the width of the overall peak is factored into quantifying the separation, the result is excellent.

Table 6.7. Separation Factor and Peak Resolution of Ibuprofen at 40^{o}C 150 Bar

Separation Factor	1.24
Peak Resolution	2.31

6.4. Comparison of Three Techniques

When you integrate the chromatograms to determine the isotherm, the resulting isotherms are different. This is because each method has its own inherent errors built in. The question then becomes which one to use. If one is dealing with low concentrations the ECP pulse method is sufficient. However, if it is desired to work in the non-linear portion of the isotherm using FA and FACP are good in that they exhibit breakthrough behavior which leads to the saturation capacity of the solute at equilibrium. Figure 6.22 shows the comparison of the three isotherm determination methods used. 30mg of S-ibuprofen at 40^{o}C 130 Bar is used for comparison.

The ECP pulse isotherm does not have the curvature of the FA and FACP determined isotherms. However, the ECP pulse isotherm correctly corresponds to the

initial slope of the FACP. This is expected since both methods derive isotherms from the rear portion of the chromatogram peak. The FA and FACP give roughly the same saturation capacity and more accurately represent the isotherm shape as compared to the ECP pulse method. The slope of the FA differs slightly since the isotherm is determined from the adsorption front.

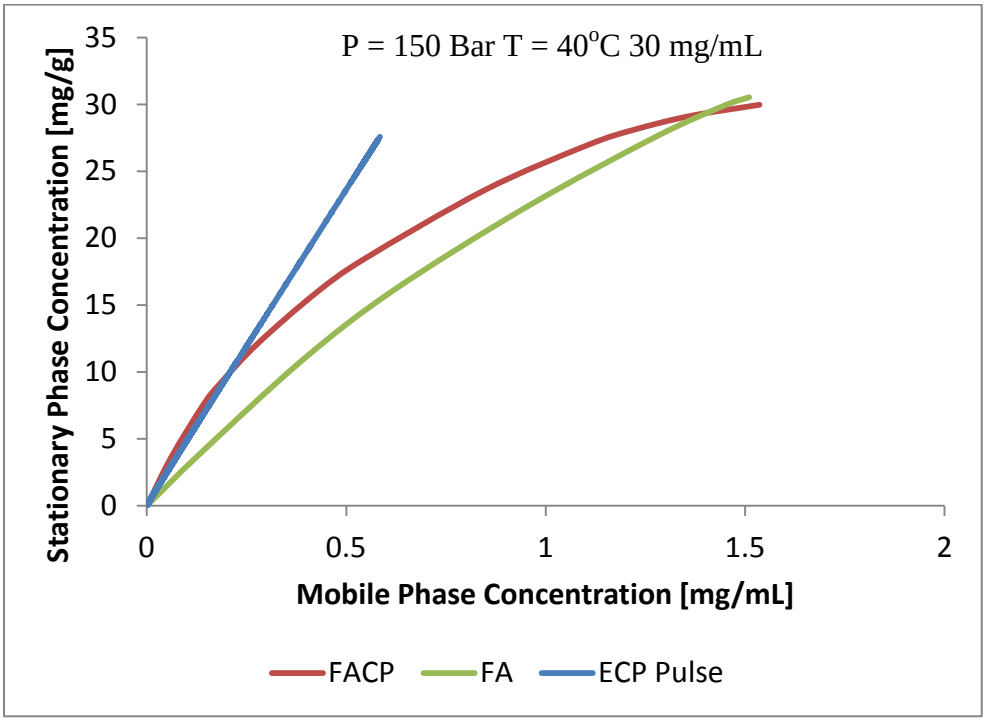

Figure 6.22. Comparison of S-Ibuprofen Isotherms from FA, FACP, and ECP Pulse Methods

The main advantage of FA is that the self-sharpening nature of the front permits accurate determination of the isotherm points even in cases where mass transfer kinetics are relatively slow. The position of the equilibrium point of the breakthrough curve is independent of the kinetics of mass transfer and axial dispersion. If the rate of the kinetics is very low, than a slow mobile phase flow rate may need to be employed

however the method will still be valid provided that the breakthrough curve volume is determined by integration. In cases where the fronts are diffuse and rear parts are self-sharpening which follows the concave upward isotherm, negative concentration steps should be used.

The FA, FACP and pulse methods give very good isotherm results. Especially with modern data acquisition software like Labview and Matlab, multiple points of the isotherm can be determined from the rear part of the elution curve.

The main disadvantages of the pulse methods are the need for detector calibration, the influence of axial dispersion if the flow rate is low, and the possible cumulative error of measurement errors that occur in their calculation. However, many of the drawbacks with these methods are overcome by using a column with high efficiency as seen with the Whelk O1.

The main advantage of ECP over FA and FACP is that much smaller amount of material is needed to determine an isotherm. This point cannot be stressed enough by this author. FACP is the compliment to FA and has an interesting advantage that the comparison of FA and FACP data permits the determination of the possible extent of adsorption hysteresis. As with this work, the best estimates of the two Langmuir isotherm coefficients were with RMSE of 0.1% of the initial slope and 0.3% of the saturation capacity for the small pulse and about 0.7% and 1.5% and bulk. Excellent agreement between theory and experiment was demonstrated throughout these experiments performed in this dissertation.

6.5. Error Analysis

There are two main sources of error, experimental error and modeling error. The experimental error was accounted for by factoring the equipment tolerances into how they affect the calculated isotherm. Table 6.8 shows the tolerances of the equipment used in these experiments.

Table 6.8. Experimental Equipment Tolerances

Equipment Type	**Affected Variable**	**Tolerance**
Column Oven	Temperature	+/- 0.5^{o}C
Syringe Pump	Pressure	+/-0.5% of Set Point
HPLC Pump	Volume	+/-1% of Set Point

The isotherm determination for the various errors is presented below. The sources of error may include volume, temperature, and pressure fluctuation. Figure 6.23 shows the volume fluctuation isotherms of pure CO_2 density at 40^{o}C and 130 Bar. The results from Figure 6.23 show that if the tolerances are varied by 1% in both directions, that the calculated isotherm has a slight difference in the non-linear range. Thus the linear portion of the isotherm is not affected by the volume fluctuation shown in Figure 6.23. Additionally, Figure 6.24 shows the error plot of Figure 6.23. Figure 6.24 shows that when the volume fluctuation is accounted for the error is quite small and increases as the isotherm becomes non-linear to a value of plus or minus 5%.

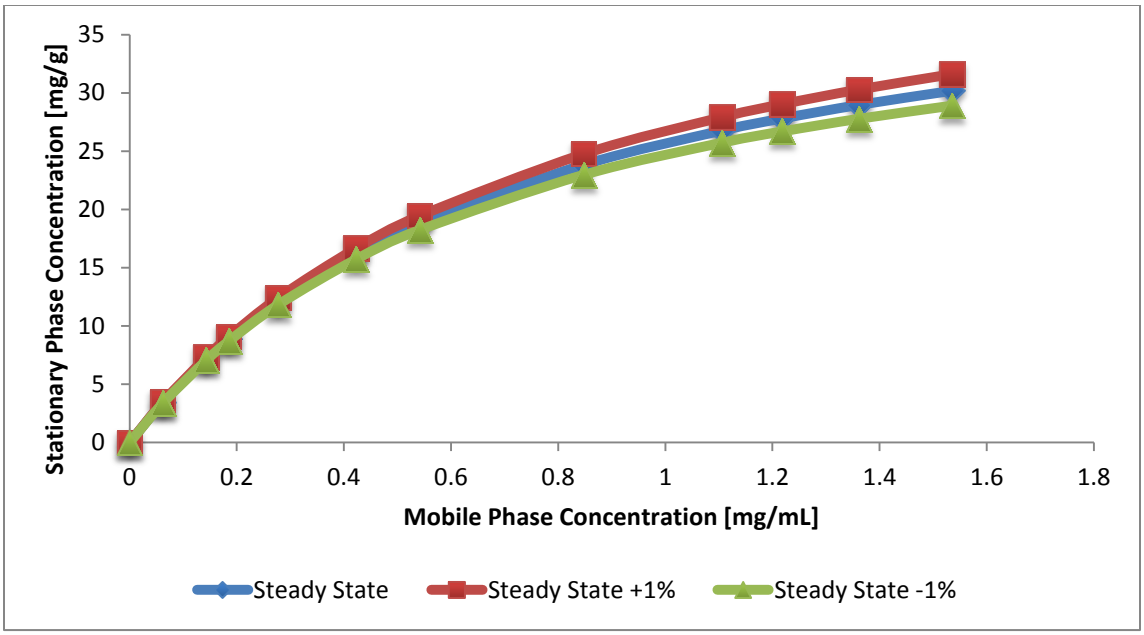

Figure 6.23. Volume Fluctuation Isotherms of Pure CO_2 Density at 40°C 130 Bar

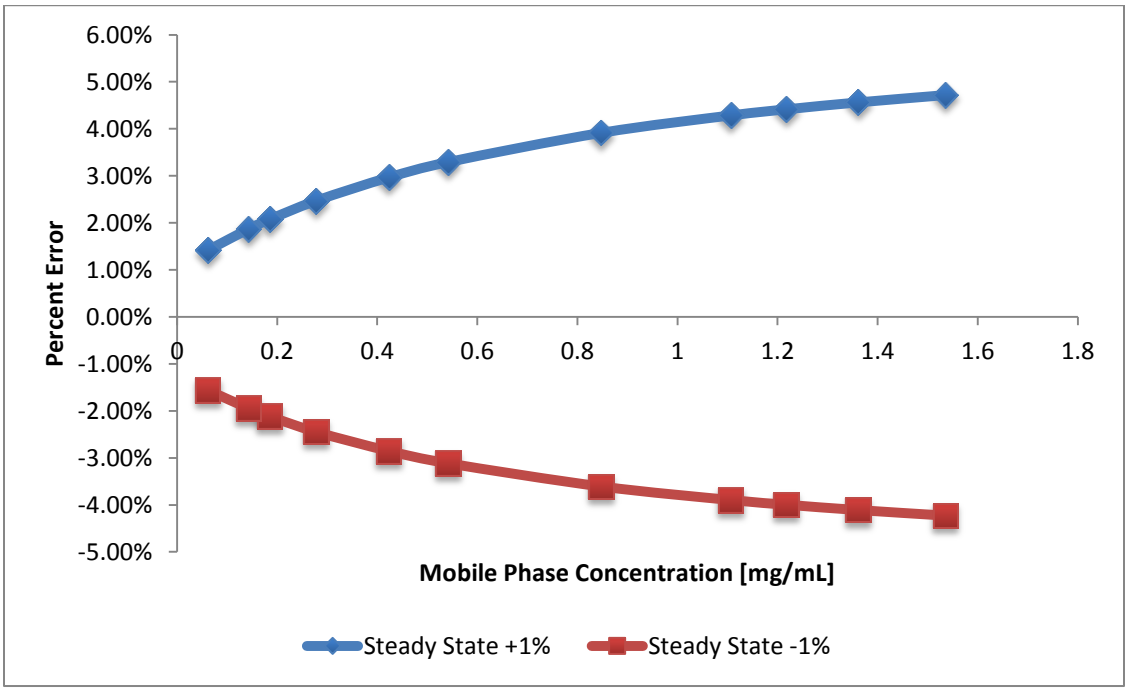

Figure 6.24. Error Plot of Volume Fluctuation of Pure CO_2 Density at 40°C 130 Bar

Table 6.9 shows the volume fluctuation as it affects the saturation capacity and the adsorption. Table 6.9 shows the saturation capacity, adsorption coefficient and RMSE.

Table 6.9. Comparison of Isotherm Parameters for Error Analysis 40°C 130 Bar 30 mg Ibuprofen

	q_s [mg/mL]	**b [mL/mg]**	**RMSE**
Steady State	44.96	1.33	0.2956
Steady State +1%	47.94	1.26	0.3139
Steady State -1%	42.42	1.39	0.2846

Many of SFC work only accounts for the density of pure CO_2 and neglect the additional effects of the entrainer. In this work a mixture of CO_2 and ethanol was used as the mobile phase.

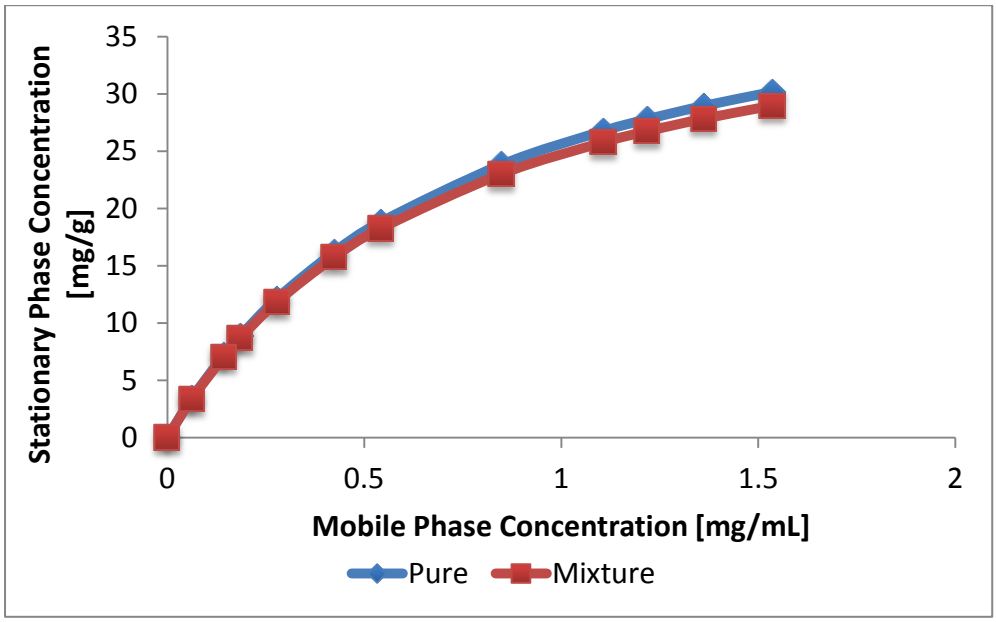

Figure 6.25. Comparison of Pure CO_2 Density and Mixture CO_2:EtOH Density Isotherm at 40°C 130 Bar

This mixture density isotherm shows lower loading because the density of the mobile phase is higher. Figure 6.26 shows this relationship and how the error is affected.

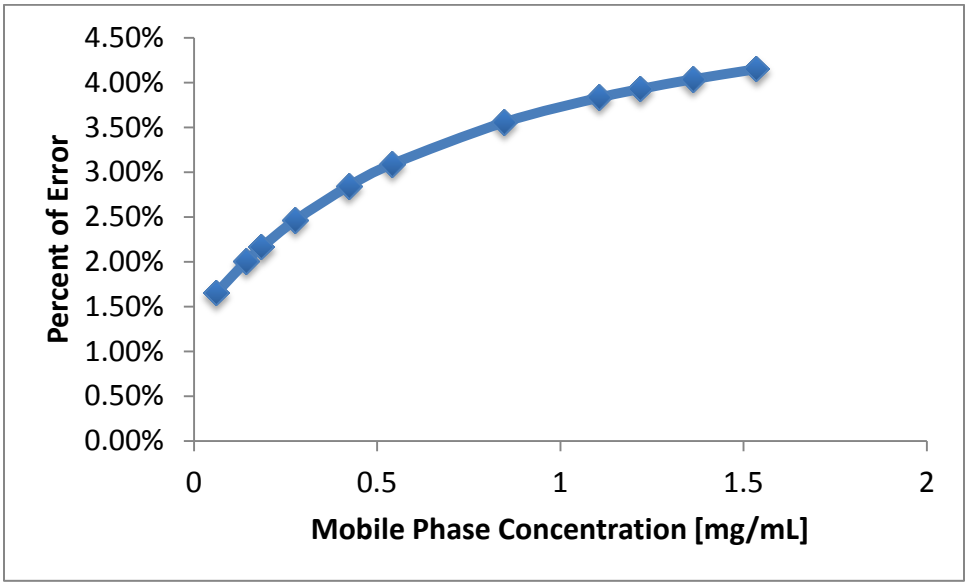

Figure 6.26. Error of Pure CO_2 Density and Mixture Density Relative to Mobile Phase Concentration

Table 6.10. Pure CO_2 and Mixture Comparison of Isotherm Parameters at 40°C 130 Bar

	Density [kg/m^3]	**q_s [mg/mL]**	**b [mL/mg]**	**RMSE**
Pure	743	44.96	1.33	0.2956
Mixture	750	42.6045	1.3875	0.2854

At 1.5 mg/mL we are already at a 4% error. This amount of error is relatively low for small scale. However, when dealing with large quantities the separation will be more prone to error. The mixture at very low concentrations is almost the same as pure CO_2. At higher concentrations there is a deviation between the two.

An error analysis the temperature fluctuation is shown in Figure 6.27. Once again the isotherms were calculated with the influence of the fluctuated variable. In this case temperature was varied. More specifically, the tolerance of the column oven was varied +1°C and -1°C. The isotherms shown in Figure 6.27 show only slight variation with the temperature tolerance factored in. The residuals were plotted in Figure 6.28 and reflect the error associated with the adsorption equilibrium of the S-ibuprofen Whelk O1 system.

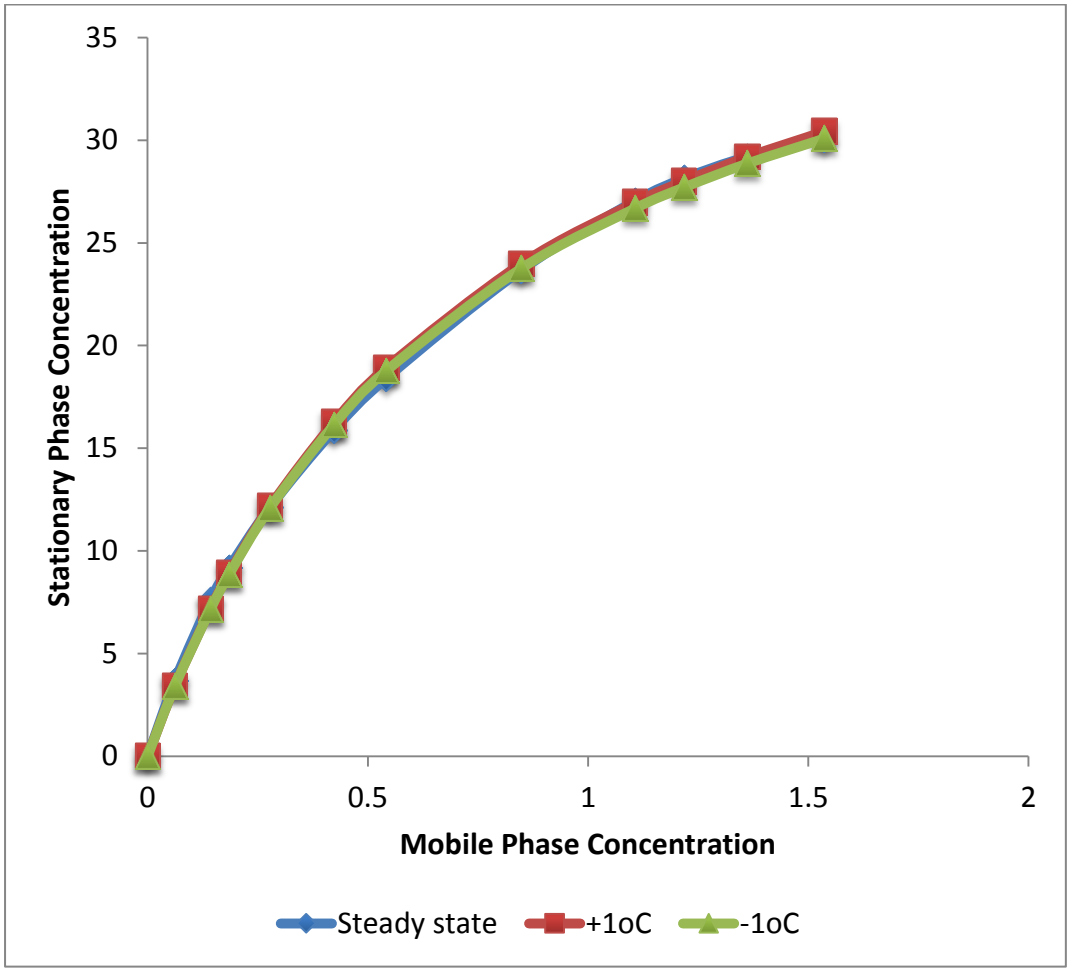

Figure 6.27. Temperature Fluctuation Isotherms at 40°C and 130 Bar

As Figure 6.27 shows, even with the tolerances taken into account the isotherms are superimposed. Therefore a point by point comparison was done to see if any appreciable variance occurred. This is shown in Figure 6.28. The temperature variation shows a different error profile as compared to the volume fluctuation error shown in Figure 6.24.

Figure 6.28 shows that the error transitions from roughly +2% to -2% as the isotherm becomes non-linear. Possible reasons for this observed trend may be due to sorption effect and diffusion processes.

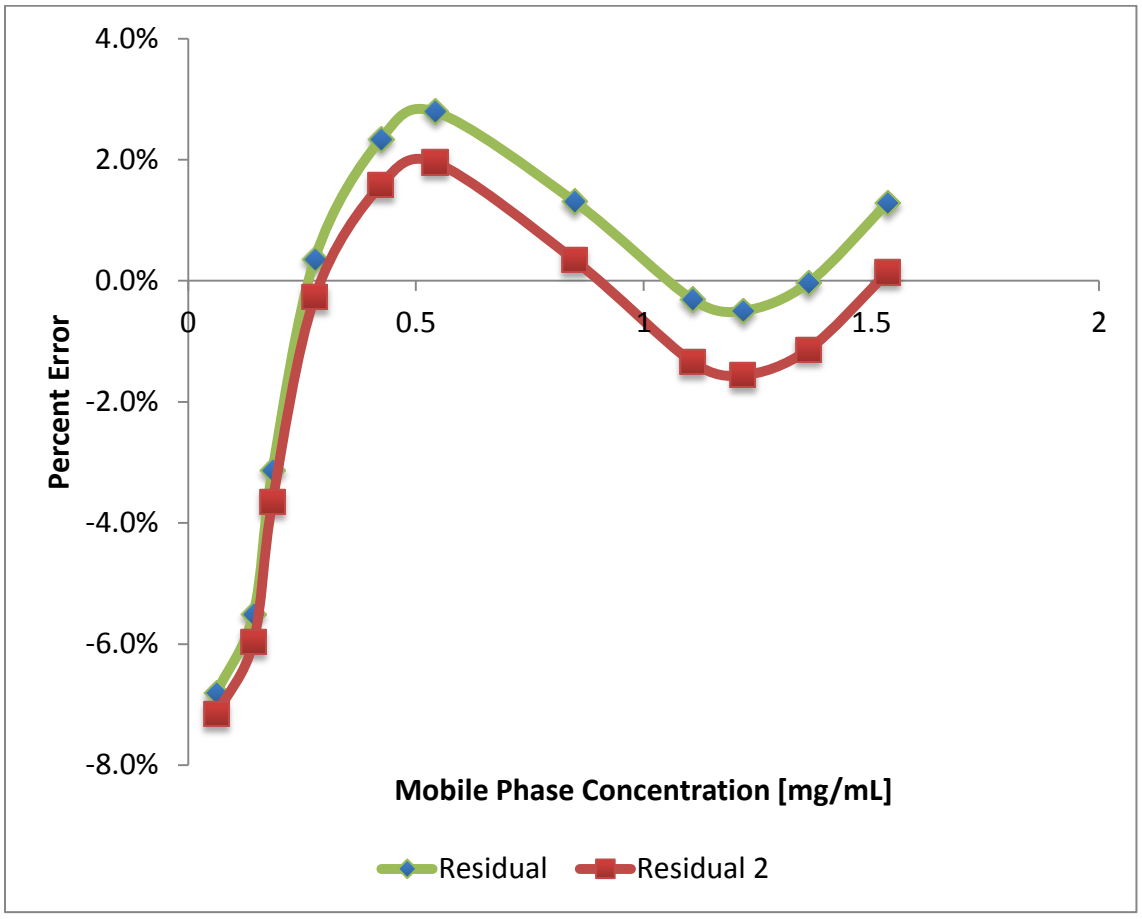

Figure 6.28. Temperature Fluctuation Error

As Table 6.8 showed that the tolerance of the pressure from the pump was 0.5% of the set value. This tolerance was applied to the calculations for the isotherm. Figure 6.29 shows the isotherms with the pressure tolerance. Similar to the temperature fluctuation isotherms in Figure 6.27, the equilibrium data are superimposed.

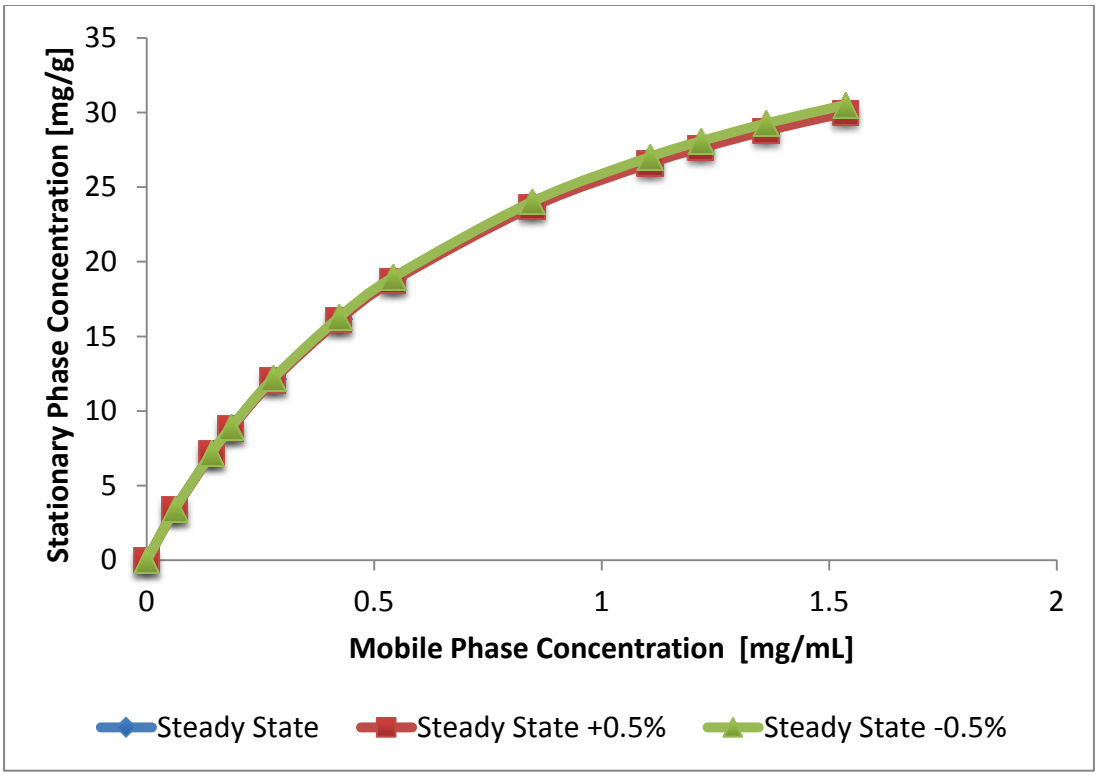

Figure 6.29. Pressure Fluctuation Isotherms of Pure CO_2 Density at 40^{o}C and 130 Bar

Figure 6.29 shows the equilibrium data from S-ibuprofen sorption on a Whelk O1 CSP at 40^{o}C and 130 Bar. The error was calculated of the steady state isotherm varied +0.5% and -0.5% of the set point of pressure.

Figure 6.30 shows the error associated with the pressure variation. The fluctuation of the pressure shows a positive 1.08% and negative 0.66% indicating that the error is not significant.

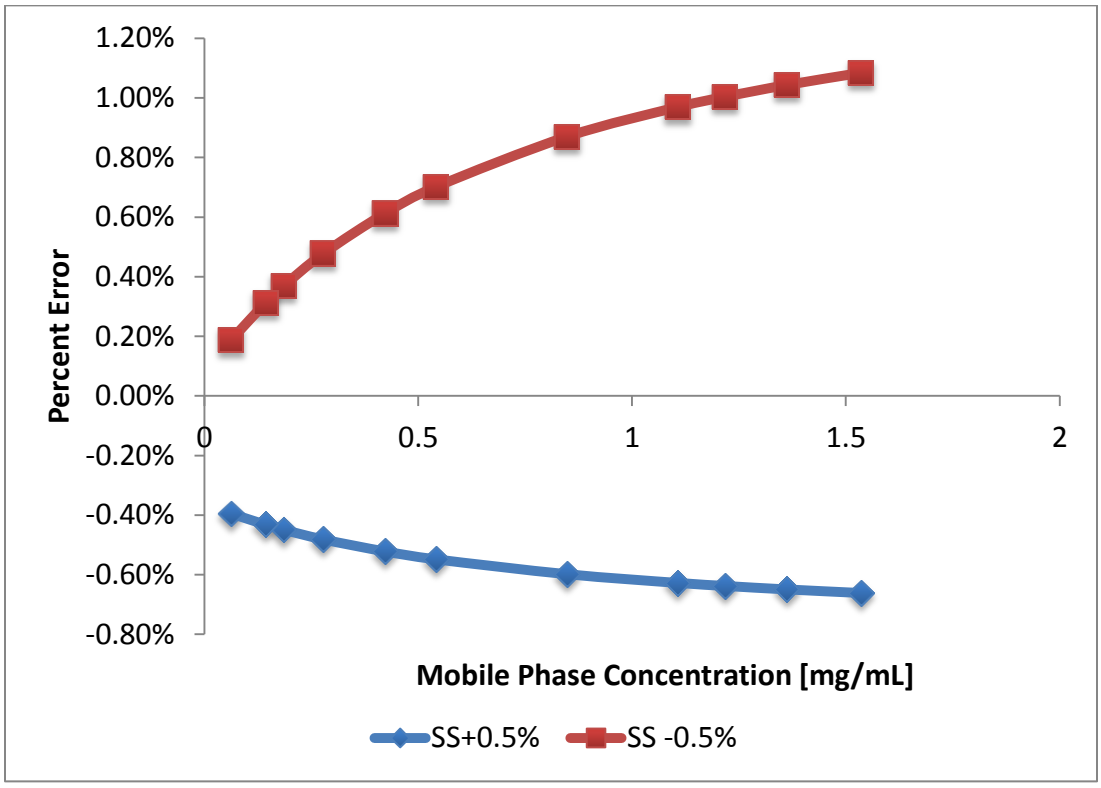

Figure 6.30. Error Plot of Pressure Fluctuation at 40°C 130 Bar

Table 6.11 shows the error and the impact on the isotherm magnitude. At low concentrations, the effect of temperature is significant, graph at -7%. Overall, the density and volume causes the largest variance in the isotherm.

Table 6.11. Summary of Systemic Error

Variable	Error Percent	
	+	-
Density	4.2	5.5
Volume	4.7	4.3
Temperature	2.8	7.0
Pressure	1.08	0.66

CHAPTER 7

CONCLUSIONS AND FUTURE DIRECTIONS

It is possible to achieve separation of the Ibuprofen enantiomers using supercritical fluid chromatography with ethanol entrained CO_2 at 95:5 % volume. CO_2 is a safe and environmentally benign solvent with low critical properties and is relatively inexpensive. The ethanol enhances the solubility of Ibuprofen in CO_2 thus allowing for relatively short experiment run times. The ethanol provides some polarity to the non-polar CO_2 and also creates an interaction with unresolved silanol groups of the stationary phase.

Isotherms for supercritical fluid chromatographic separation of racemic chiral pharmaceuticals like Ibuprofen, can be determined using the pulse method and Frontal Analysis and FACP method. The FA and FACP methods are better suited for isotherm determination of higher concentrations of the drug because they reveal the non-linear relationship between column loading and mobile phase solute concentration at column saturation as compared to the pulse method which does not achieve full saturation. However, the pulse method can provide the initial isotherm slope in the linear portion of the column loading-mobile phase solute concentration relationship. The pulse method can determine isotherms with a much smaller amount of solute compared to the FA and FACP methods.

The two-parameter Langmuir model is satisfactory in modeling the low and high concentrations of Ibuprofen in CO_2:EtOH. The conditions tested include pressures of 100, 130, and 150 Bar and temperatures of 30, 35, 40, 45, 50, 55^{o}C. The Ibuprofen concentrations in ethanol include 5, 10, 15, 30, 50, 75, 100, 150, 300 mg/mL for the pulse

method. For the FA and FACP methods the same concentrations except 150 and 300 mg were tested. The RMSE for the Langmuir isotherm models range from 0.0972-0.6652 for the concentration range listed above with the FACP method.

Four systemic error sources were investigated to determine their individual impact on the slope of the isotherm: density, pressure, temperature and volumetric flow rate. The volumetric flow rate fluctuation was found to provide the greatest positive deviation in the isotherm determination as 4.7% higher than steady state as shown in Table 6.11. Temperature fluctuation was found to provide the greatest negative deviation in the isotherm determination at 7% lower than steady state as shown in Table 6.11.

There are several future directions possible as a result of this research. These isotherms can be applied to the design of a larger-scale, preparative chromatographic experimental set-up. Possible future directions may include designing a large-scale elution column or a simulated moving bed system based on these determined isotherms. Also, isotherms can be used to design a control system at all scales. This would allow for an automated system. Additionally, these isotherm results can provide minimum purge requirements for a saturated stationary phase adsorbent. Adding a temperature swing and or a pressure swing to the chromatograph to resolve enantiomers is a possible future direction. This addition may eliminate the need for ethanol as a co solvent. The fractionation and collection of resolved enantiomers can be achieved by amending the chromatograph with a series of high-pressure cyclones. These would allow for controlled depressurization of the supercritical fluid and crystallization of the pure enantiomer.

REFERENCES

Agranat, I., Caner, H., & Caldwell, J. (2002). Putting Chirality to Work. *Nature Reviews Drug Discovery*, 1, 753-768.

Ahrends, R., & Schluter, H. (2010). Application of Displacement Chromatography for the Proteome Analysis of a Human Plasma Protein Fraction. *Journal of Chromatography A*, 1217 (19), 3321-3329.

Ali, I., Saleem, K., Hussain, I., Gaitonde, V., & Aboul‐Enein, H. (2009). Polysaccharides Chiral Stationary Phases in Liquid Chromatography. *Separation & Purification Reviews*, 38 (2), 97-147.

Allenmark, C. (1991). Chromatographic Enantioseparation Methods and Application (2nd ed.). New York: Ellis Horwood.

Arai, Y., Sako, T., & Takebayashi, Y. (Eds.). (2002). Supercritical Fluids Molecular Interactions, Physical Properties, and New Applications. Heidelberg: Springer-Verlag.

Ashraf-Khorassani, M., Nazem, N., Taylor, L. T., & Coleman, W. M. (2008). Isolation, Fractionation, and Identification of Sucrose Esters from Various Oriental Tobaccos Employing Supercritical Fluids. *Beitraege zur Tabakforschung International*, 23 (1), 32-45.

Asnin, L. & Guiochon, G. (2005). Calibration of a Detector for Nonlinear Responses. *Journal of Chromatography A,* 1089, 105–110.

Asnin, L. & Guiochon, G. (2005). Calibration of Detector Responses using the Shape and Size of Band Profiles Case of a Nonlinear Response Curve. *Journal of Chromatography A*, 1089, 101–104.

Atkins, P. W. (1999). Physical Chemistry (6th ed.). New York: W.H. Freeman and Co.

Bamba, T. (2008). Application of Supercritical Fluid Chromatography to the Analysis of Hydrophobic Metabolites. *Journal of Separation Science*, 31 (8), 1274-1278.

Berche, B., Henkel, M., & Kenna, R. (2009). Critical Phenomena: 150 Years Since Cagniard de la Tour. *Journal of Physical Studies*, 13, 3201.

Berezkin, V. G. (1990). Chromatographic Adsorption Analysis: Selected Works of M.S. Tswett. New York: Ellis Horwood.

Bidlingmeyer, B. A., & Warren, F. V. (1884). Column Efficiency Measurements. *Analytical Chemistry*, 56, 950-957.

Bohart, G. S., & Adams, E. Q. (1920). Modeling of Breakthrough Curve of Toxic Gases. *Journal of the American Chemical Society*, 42 (523), 158-170.

Brooks, W., Guida, C., & Daniel, K. (2011). The Significance of Chirality in Drug Design and Development. *Current Topics in Medicinal Chemistry*, 11 (7), 760-770.

Brunelli, C., Dunkle, M., Morris, S., & Sandra, P. (2009). Development of a Generic Method for Supercritical Fluid Chromatography using Thiourea. *Chromatography Today*, 5-8.

Brunellia, C., Zhao, Y., Brown, M.-H., & Sandra, P. (2008). Development of a Supercritical Fluid Chromatography High-resolution Separation Method Suitable for Pharmaceuticals Using Cyanopropyl Silica. *Journal of Chromatography A*, 1185 (2), 263-272.

Brunner, G. & Johannsen, M. (2006). New Aspects on Adsorption from Supercritical Fluid Phases. *Journal of Supercritical Fluids*, 38, 181-200.

Brunner, G. (2005). Supercritical Fluids: Technology and Application to Food Processing. *Journal of Food Engineering*, 67, 21-33.

Bui, H., Masquelina, T., Peruna, T., Castlea, T., Dagea, J., & Kuoa, M.-S. (2008). Investigation of Retention Behavior of Drug Molecules in Supercritical Fluid Chromatography Using Linear Solvation Energy Relationships. *Journal of Chromatography A*, 1206 (2), 186-195.

Byrne, N., Hayes-Larson, E., Liao, W., & Kraml, C. (2008). Analysis and Purification of Alcohol-sensitive Chiral Compounds Using 2,2,2-trifluoroethanol as a Modifier in Supercritical Fluid Chromatography. *Journal of Chromatography B*, 875 (1), 237-242.

Caldwell, J. (1999). Through the Looking Glass in Chiral Drug Development. *Modern Drug Discovery*, 2, 51-60.

Cavazzini, A., Kaczmarski, K., Szabelski, P., Zhou, D., Liu, X., & Guiochon, G. (2001). Modeling of the Separation of the Enantiomers of 1-phenyl-1-propanol on Cellulous Tribenzoate. *Analytical Chemistry*, 73, 5704-5715.

Charton, F., & Nicoud, R.-M. (1995). Complete Design of a Simulated Moving Bed. *Journal of Chromatography A*, 702 (1), 97-112.

Collins, J. J. (1967). The LUB/equilibrium Section Concept for Fixed-bed Adsorption. *Chemical Engineering Progress Symposium Series*, 74 (63), 31-40.

Dal Nogare, S., & Harden, J. C. (1959). Programmed Temperature Gas Chromatography Apparatus. *Analytical Chemistry*, 31 (11), 1829-1832.

Depta, A., Giese, T., Johannsen, M., & Brunner, G. (1999). Separation of Stereoisomers in a Simulated Moving Bed-supercritical Fluid Chromatography Plant. *Journal of Chromatography A*, 865, 175–186.

Desmortreuxa, C., Rothaupt, M., West, C., & Lesellier, E. (2009). Improved Separation of Furocoumarins of Essential Oils by Supercritical Fluid Chromatography. *Journal of Chromatography A*, 1216 (42), 7088-7095.

Dewar, R. A. (1960). The Flame Ionization Detector a Theoretical Approach. *Journal of Chromatography*, 6, 312-323.

Diack, M., & Guiochon, G. (1991). Adsorption Isotherm and Overloaded Elution Profiles of Phenyldodecane on Porous Carbon in Liquid Chromatography. *Analytical Chemistry*, 63, 2608-2613.

Do, D. D. (1998). Adsorption Analysis: Equilibria and Kinetics. London: Imperial College Press.

Dose, E., Jacobson, S., & Guiochon, G. (1991). Determination of Isotherms from Chromatographic Peak Shapes. *Analytical Chemistry*, 63, 833-839.

Esmaeilzadeh, F., & Goodarznia, I. (2005). Separation of Phenanthrene from Anthracene Oil using Supercritical Carbon Dioxide. *Chemical Engineering Technology*, 28, 106-109.

Ettre, L. S. (1990). Fifty Years of GC Instrumentation. LC GC, 8, 716-724.

Ettre, L. S. (2000). Chromatography: the Separation Technique of the 20th Century. *Chromatographia*, 51 (1/2), 7-17.

Ettre, L. S., & Hinshaw, J. V. (1993). Basic Relationships of Gas Chromatography. Cleveland: ADVANSTAR Communications.

Ettre, L. S., & Sakodynskii, K. I. (1993). Gas Chromatography. *Chromatographia*, 35, 223-231.

Ettre, L. S., & Zlatkis, A. (Eds.). (1979). 75 Years of Chromatography - A Historical Dialogue. Amsterdam: Elsevier.

Feal, R. G., & Nicholls, D. G. (Eds.). (2009). MLA Handbook for Writers of Research Papers (7 ed.). New York: The Modern Language Association of America.

Felinger, A., Cavazzini, A., & Guiochon, G. (2003). Numerical Determination of the Competitive Isotherm of Enantiomers. *Journal of Chromatography A*, 986, 207–225.

Felix, G., Berthod, A., Piras, P., & Roussel, C. (2008). Supercritical Fluid Chromatographic Separations. *Separation and Purification Reviews*, 37 (3), 229-301.

Filippova, N. (1998). Adsorption and Heat of Adsorption onto Polymer Particular Surface by Inverse Gas Chromatography. *Journal of Colloid and Interface Science*, 197, 170-176.

Freund, E., Abel, S., Huthmann, E., & Lill, J. (2009). Chiral Chromatography in the Early Phases of Pharmaceutical Development. *Chimica Oggi*, 62-64.

Frey, G. & Grushka, E. (1996). Numerical Solution of the Complete Mass Balance Equation in Chromatography. *Analytical Chemistry*, 68, 2147-2154.

Ganetsos, G., & Barker, P. E. (Eds.). (1993). Preparative and Production Scale Chromatography. New York: Marcel Dekker.

Gao, X., Chen, H., Schwarzschild, M. A., & Ascherio, A. (2011). Use of Ibuprofen and Risk of Parkinson's Disease. *Neurology*, 76 (10), 863-869.

Gere, D. R., Board, R., & McManigill, D. (1982). Supercritical Fluid Chromatography with Small Particle Diameter Packed Columns. *Analytical Chemistry*, 54 (4), 736-740.

Giddings, J. C. (1963). Liquid Chromatography with Operating Conditions Analogous to Those of Gas Chromatography. *Analytical Chemistry*, 35 (13), 2215-2216.

Giddings, J. C. (1965). Dynamics of Chromatography, Part I, Principles and Theory. New York: Marcel Dekker.

Giovanni, O., Mazzotti, M., Morbidelli, M., Denet, F., Hauck, W., & Nicoud, R. (2001). Supercritical Fluid Simulated Moving Bed Chromatography II. Langmuir Isotherm. *Journal of Chromatography A*, 919, 1–12.

Golshan-Shirazi, S., Huang, J., & Guiochon, G. (1991). Comparison of an Experimental Competitive Isotherm and the Levan-Vermeulen Model and Prediction of Band Profiles in a Case of Selectivity Reversal. *Analytical Chemistry*, 91, 1147-1154.

Goshan-Shirazi, S., & Guiochon, G. (1989). Experimental Characterization of the Elution Profiles of High Concentration Chromatographic Bands using the Analytical Solution of the Ideal Model. *Analytical Chemistry*, 61, 462-467.

Griffith, J., James, D., & Phillips, C. S. (1952). Gas Chromatography. *Analyst*, 77 (921), 897-903.

Gritti, F. & Guiochon, G. (2003). Effect of the Mobile Phase Composition on the Isotherm Parameters and the High Concentration Band Profiles in Reversed-phase Liquid Chromatography. *Journal of Chromatography A*, 995, 37–54.

Gritti, F. & Guiochon, G. (2003). Band Splitting in Overloaded Isocratic Elution Chromatography II. New Competitive Adsorption Isotherms. *Journal of Chromatography A*, 1008, 23–41.

Gritti, F. & Guiochon, G. (2003). New Thermodynamically Consistent Competitive Adsorption Isotherm in RPLC. *Journal of Colloid and Interface Science*, 264, 43–59.

Gritti, F. & Guiochon, G. (2003). Repeatability and Reproducibility of High Concentration Data in Reversed-phase Liquid Chromatography I. Overloaded Band Profiles on Kromasil-C18. *Journal of Chromatography A*, 1003, 43–72.

Gritti, F., & Guiochon, G. (2003). Influence of a Buffered Solution on the Adsorption Isotherm and Overload Band Profiles of an Ionizable Compound. *Journal of Chromatography A*, 905, 197-210.

Gritti, F., Gotmar, G., Stanley, B., & Guiochon, G. (2003). Determination of Single Component Isotherms and Affinity Energy Distribution by Chromatography. *Journal of Chromatography A*, 988, 185–203.

Gritti, F., Piatkowski, W., & Guiochon, G. (2002). Comparison of the Adsorption Equilibrium of a Few Low-molecular Mass Compounds on a Monolithic and a Packed Column in Reversed-phase Liquid Chromatography. *Journal of Chromatography A*, 978, 81–107.

Guiochon, G., & Lin, B. (2003). Modeling for Preparative Chromatography. San Diego, California: Academic Press.

Guiochon, G., Felinger, A., Shirazi, D. G., & Katti, A. M. (2006). Fundamentals of Preparative and Nonlinear Chromatography (2nd ed.). San Diego, California: ELSEVIER Inc.

Guiochon, G., & Gritti, F. (2005). Systematic Errors in the Measurement of Adsorption Isotherms by Frontal Analysis: Impact of the Choice of Column Hold-up Volume, Range and Density of the Data Points. *Journal of Chromatography A*, 1097, 98-115.

Guiochon, G., Cavazzini, A., & Felinger, A. (2003). Numerical Determination of the Competitive Isotherms of Enantiomers. *Journal of Chromatography A*, 986, 207-225.

Guiochon, G., Andrzejewska, A., & Kaczmarski, K. (2009). Theoretical Study of the Accuracy of the Pulse Method, Frontal Analysis, and Frontal Analysis by Characteristic Points for the Determination of Single Component Adsorption Isotherms. *Journal of Chromatography A*, 1216, 1067-1083.

Guvenc, A., Mehmetoglu, U., & Calimli, A. (1998). Supercritical CO2 Extraction of Ethanol from Fermentation Broth Using in a Semi-Continuous System. *Journal of Supercritical Fluids*, 13, 325-329.

Hagglund, I. & Stahlberg, J. (1997). Ideal Model of Chromatography Applied to Charged Solutes in Reversed-phase Liquid Chromatography. *Journal of Chromatography A*, 761, 3-11.

Heremans, K., & Smeller, L. (1998). Protein Structure and Dynamics at High Pressure. *Biochimica et Biophysica Acta*, 1386, 353-370.

Heuer, C., Kniep, H., & Falk, T. S.-M. (1999). Comparison of Various Process Engineering Concepts of Preparative Chromatography. *Chemical & Engineering Technology*, 21 (6), 469-477.

Heuer, C., Kusters, E., Plattner, T., & Seidel-Morgenstern, A. (1998). Design of the Simulated Moving Bed Process Based on Adsorption Isotherm Measurements using a Perturbation Method. *Journal of Chromatography A*, 827, 175–191.

Hines, A. L., & Maddox, R. N. (1985). Mass Transfer Fundamentals and Applications. Upper Saddle River, New Jersey: Prentice Hall Inc.

Horvath, C. G., & Lipsky, S. R. (1966). Use of Liquid Ion Exchange Chromatogaphy for the Separation of Organic Compounds. *Nature*, 211 (5050), 748-749.

Huber, J. F., & Gerritse, R. G. (1971). Evaluation of Dynamic Gas Chromatographic Methods for the Determination of Adsorption and Solution Isotherms. *Journal of Chromatography A*, 58 (C), 137-158.

Huhnerfussa, H., & Shah, M. R. (2009). Enantioselective Chromatography-A Powerful Tool for the Discrimination of Biotic and Abiotic Transformation Processes of Chiral Environmental Pollutants. *Journal of Chromatography A*, 1216 (3), 481-502.

Hur, J. & Wankat, P. (2006). Separation from Quaternary Mixtures: Linear Isotherm Systems. *Industrial Engineering Chemical Res*, 45, 8713-8722.

Jacobson, J. M., Frenz, J. H., & Horvath, C. (1987). Measurement of Competitive Adsorption Isotherms by Frontal Chromatography. *Industrial & Engineering Chemistry Research*, 26 (1), 43-50.

Jacobson, J. M., Frenz, J. H., & Horvath, C. (1987). Measurement of Competitive Adsorption Isotherms by Frontal Chromatography. *Industrial & Engineering Chemistry Research*, 26 (1), 43-50.

James, A. T. (1952). Gas-liquid Partition Chromatography: The Separation of Volatile Aliphatic Amines and of the Homologues of Pyridine. *Biochemical Journal*, 52 (2), 242-247.

James, A. T., & Martin, A. J. (1952). Gas-liquid Partition Chromatography: The Separation and Micro-estimation of Volatile Fatty Acids from Formic Acid to Dodecanoic Acid. *Biochemical Journal*, 50, 679-690.

James, A. T., Martin, A. J., & Smith, G. H. (1952). Gas-liquid Partition Chromatography: The Separation and Micro-estimation of Ammonia and the Methylamines. *Biochemical Journal*, 52, 238-242.

Jandera, P., & Komers, D. (1997). Fitting Competitive Adsorption Isotherms to the Experimental Distribution Data in Reversed-phase Systems. *Journal of Chromatography A*, 762, 3-13.

Jha, S. & Madras, G. (2004). Modeling of Adsorption Equilibria in Supercritical Fluids. *Journal of Supercritical Fluids*, 32, 161–166.

Johannsen, M. (2001). Separation of Enantiomers of Ibuprofen on Chiral Stationary Phases by Packed Column Supercritical Fluid Chromatography. *Journal of Chromatography A*, 937, 135–138.

Johannsen, M. (2007). Chromatographic Separation Processes. [Online]. http://www.tu-harburg.de/ibb/Education.html

Jorgenson, J. W., & Lukacs, K. D. (1981). Zone Electrophoresis in Open-tubular Glass Capillaries. *Analytical Chemistry*, 53 (8), 1298-1302.

Jozwik, M., Kaczmarski, K., & Freitag, R. (2005). Investigation of the Steric Mass Action Formalism in the Simulation of Breakthrough Curves on a Monolithic and a Packed Bed Column. *Journal of Chromatography A*, 1073, 111–121.

Jusforgues, P. (1995). Process Scale Liquid Chromatography. (G. Subramanian, Ed.) New York: VCH Publishers.

Kalogirou, E., Bassiotis, I., Artemiadi, T., Margariti, S., Siokos, V., & Roubani-Kalantzopoulou, F. (2002). Experimental Adsorption Isotherms Based on Inverse Gas Chromatography. *Journal of Chromatography A*, 969, 81–86.

Keulemans, A. I. (1957). Gas Chromatography. New York: Reinhold.

King, J., Johnson, J., & Friedrich, J. (1989). Extraction of Fat Tissue from Meat Products with Supercritical Carbon Dioxide. *Agricultural and Food Chemistry*, 951-954.

Kiran, E., & Brennecke, J. F. (Eds.). (1993). Supercritical Fluid Engineering Science Fundamentals and Applications. Washington: American Chemical Society.

Kirkland, J. J. (1971). High Speed Liquid-partition Chromatography with Chemically Bonded Organic Stationary Phases. *Journal of Chromatographic Science*, 206-214.

Klesper, E., & Corwin, A. H. (1962). High Pressure Gas Chromatography above Critical Temperatures. *Journal of Organic Chemistry*, 27, 700-701.

Kraml, C. M., Zhou, D., Byrne, N., & McConnel, O. (2005). Enhanced Chromatographic Resolution of Amine Enantiomers as Carbobenzyloxy Derivatives in High-Performance Liquid Chromatography and Supercritical Fluid Chromatography. *Journal of Chromatography A*, (1100), 108-115.

L'Italien, Y., Thibault, J., & LeDuy, A. (1989). Improvement of Ethanol Fermentation Under hyperbaric Conditions. *Biotechnology and Bioengineering*, 33, 471–476.

Laub, R. J., & Pecsok, R. L. (1978). Physiochemical Applications of Gas Chromatography. New York: John Wiley & Sons Inc.

Lee, M. L., & Markides, K. E. (Eds.). (1990). Analytical Supercritical Fluid Chromatography and Extraction. Provo: Chromatography Conference Inc.

Levenspiel, O. (1999). Chemical Reaction Engineering (3rd ed.). New York: John Wiley & Sons.

Lim, B., Chin, C., & Tan, R. (1995). Determination of Competitive Adsorption Isotherms of Enantiomers on a Dual-site Adsorbent. *Separations Technology* 5, 213-228.

Lovelock, J. E. (1958). A Sensitive Detector for Gas Chromatography. *Journal of Chromatography*, 35-46.

Lubbert, M., Brunner, G., & Johannsen, M. (2007). Adsorption Equilibria of α- and β-tocopherol from Supercritical Mixtures of Carbon Dioxide and 2-propanol onto Silica by Means of Perturbation Chromatography. *Journal of Supercritical Fluids,* 42, 180–188.

Mack, W., Sunol, S., & Sunol, A. (2005). Separation of Flurbiprofen Enantiomers on a Chiral Stationary Phase by Supercritical Fluid Chromatography. *AIChE Annual Meeting Proceedings*, Cincinnati, Ohio: American Institute of Chemical Engineers Inc.

Mangelings, D., & Vander Hayden, Y. (2008). Chiral Applications of Supercritical Fluid Chromatography. *Journal of Separation Sciences*, 1252-1273.

Martin, A. J. & Synge, R. L. (1941). A New Form of Chromatogram Employing Two Liquid Phases. *Biochemical Journal* (35), 1358-1367.

Martinez, J. L. (Ed.). (2008). Supercritical Fluid Extraction of Nutraceuticals and Bioactive Compounds. Boca Raton: CRC Press.

McHugh, M. A., & Krukonis, V. J. (1986). Supercritical Fluid Extraction. Boston: Butterworth Publishers.

Milbachler, K., Kaczmarske, K., Seidel-Morgenstern, A., & Guiochon, G. (2002). Measurement and Modeling of the Equilibrium Behavior of the Troger's Base Enantiomers on an Amylase-based Chiral Stationary Phase. *Journal of Chromatography A*, 955, 35-52.

Molina, B. & Johannsen, M. (2009). Adsorption Equilibria of Benzoic Acid on Silica Gel from Supercritical Carbon Dioxide. *Journal of Supercritical Fluids,* 42, 168-175.

Moss, G. P. (Ed.). (1996). Basic Terminology of Stereochemistry (IUPAC Recommendations 1996). *Pure & Applied Chemistry*, 68 (12), 2193-2222.

Mukhopadhyay, M. (2000). Natural Extracts Using Supercritical Carbon Dioxide. Boca Raton: CRC Press.

Myers, M. N., & Giddings, J. C. (1966). Ultra High Pressure Gas Chromatography in Micro Columns to 2000 Atmospheres. *Separation Science*, 1 (6), 761-776.

Nagle, R. K., & Saff, E. B. (1996). Fundamentals of Differential Equations (4th ed.). New York: Addison-Wesley Publishing Co.

Ottiger, S., Kluge, J., Rajendran, A., Mazzotti, M. (2007). Enantioseparation of 1-phenyl-1-propanol on Cellulose-derived Chiral Stationary Phase by Supercritical Fluid Chromatography II. Non-linear Isotherm. *Journal of Chromatography A*, 1162, 74–82.

Pasteur, L. (1848). On the Relations That Can Exist Between Crystalline Form and Chemical Composition and the Sense of Rotary Polarization. *Annales de Chimie et de Physique*, 24 (6), 442-449.

Patel, K. Automatic Generation of Global Phase Equilibrium Diagram from Equation of State. Dissertation, University of South Florida, 2007.

Paulaitis, M. E., Penninger, J. M., Gray Jr., R. D., & Davidson, P. (Eds.). (1983). Chemical Engineering at Supercritical Fluid Conditions. Kent, England: Butterworths Ltd.

Peng, D. Y., & Robinson, D. B. (1076). A New Two-constant Equation of State. *Industrial and Engineering Chemistry: Fundamentals*, 15, 59-64.

Peper, S., Lubbert, M., Johannsen, M., & Brunner, G. (2002). Separation of Ibuprofen Enantiomers by Supercritical Fluid Simulated Moving Bed Chromatography. *Separation Science and Technology*, 37, 2545-2566.

Prausnitz, J. M., Lichtenthaler, R. N., & Azevedo, E. G. (1999). Molecular Thermodynamics of Fluid-Phase Equilibria (3rd ed.). Upper Saddle River, New Jersey: Prentice Hall Inc.

Quinones, I. & Guiochon, G. (1996). Application of Different Isotherm Models to the Description of Single-component and Competitive Adsorption Data. *Journal of Chromatography A*, 734, 83-96.

Rajendran A., Mazzotti, M., & Morbidelli, M. (2005). Enantioseparation of 1-phenyl-1-propanol on Chiralcel OD by Supercritical Fluid Chromatography I. Linear Isotherm. *Journal of Chromatography A*, 1076 183-188.

Reid, R. C., Prausnitz, J. M., & Poling, B. E. (1987). The Properties of Gases and Liquids. New York: McGraw Hill.

Roles, J. & Guiochon, G. (1991). Determination of the Surface Energy Distribution Using Adsorption Isotherm Data Obtained by Gas-solid Chromatography. *Journal of Physical Chemistry,* 95, 4098-4109.

Roubani-Kalantzopoulou, F. (2004). Review: Determination of Isotherms by Gas–solid Chromatography Applications. *Journal of Chromatography A*, 1037, 191–221.

Ruthven, D. M. (1984). Principles of Adsorption and Adsorption Processes. New York: Wiley and Sons.

Sanal, I., Bayraktar, E., Mehmetoglu, & Ucalimli, A. (2005). Determination of Optimum Conditions for sc-(CO_2+Ethanol) Extraction of Beta Carotene from Apricot Pomace using Response Surface Methodology. *Journal of Supercritical Fluids*, 34, 331–338.

Schmidt-Traub, H. (Ed.). (2005). Preparative Chromatography of Fine Chemicals and Pharmaceutical Agents. Weinheim: WILEY-VCH Verlag GmbH & Co.

Schoenmakers, P. J., & Uunk, L. G. (1987). Effects of the Column Pressure Drop in Packed-column Supercritical-fluid Chromatography. *Chromatographia*, 24 (1), 51-57.

Sellergren, B. & Shea, K. (1995). Origin of Peak Asymmetry and the Effect of Temperature on Solute Retention in Enantiomer Separations on Imprinted Chiral Stationary Phases. *Journal of Chromatography A*, 690, 29-39.

Senorans, F. J., & Ibanez, E. (2002). Analysis of Fatty Acids in Fluids by Supercritical Fluid Chromatography. *Analytica Chimica Acta*, 465 (1), 131-144.

Shah, R. R. (2003). Stereochemical Aspects of Drug Action and Disposition. (M. Eichelbaum, & B. Testa, Eds.) New York: Springer.

Sheldon, R. A. (1993). Chirotechnology Industrial Synthesis of Optically Active Compounds. New York: Marcel Dekker.

Sie, S. T., & Rijnders, G. W. (1967). Chromatography with Supercritical Fluids. *Analytica Chimica Acta*, 38, 31-44.

Sie, S. T., Van Beersum, W., & Rijnders, G. W. (1966). High-pressure Gas Chromatography and Chromatography with Supercritical Fluids. I. The Effect of Pressure on Partition Coefficients in Gas-liquid Chromatography. *Separation Science*, 1, 459-490.

Skerget, M., Novak, Z., Knez, Z., & Kravanja, Z. (2002). Estimation of Solid Solubilities in Supercritical Carbon Dioxide: Peng–Robinson Adjustable Binary Parameters in the Near Critical Region. *Fluid Phase Equilibria*, 203, 111–132.

Snyder, L. R. (1967). An Experimental Study of Column Efficiency in Liquid-solid Adsorption Chromatography. *Analytical Chemistry*, 33, 698-704.

Soave, G. (1972). Equilibrium Constants from a Modified Redlich-Kwong Equation of State. *Chemical Engineering Science*, 27, 1197-1203.

Sofer, G., & Hagel, L. (1997). Handbook of Process Chromatography A Guide to Optimization, Scale-up and Validation. San Diego: Academic Press.

Staerk, D., Shitangkoon, A., Winchester, E., Vigh, G., Felinger, A., & Guiochon, G. (1996). Determination of the Gas-liquid Partition Isotherms of the Enantiomers of Methyl

2-chloropropionate on Trichloroacetyl Pentyl β-cyclodextrin using the Elution by Characteristic Points Method. *Journal of Chromatography A*, 734, 155-162.

Subramanian, G. (Ed.). (1995). Process Scale Liquid Chromatography. Weinheim: VCH Verlagsgesellschaft.

Sunol, A., Sunol S. Substitution of Solvents by Safer Products and Process. Handbook of Solvents. Ed. Wypych,G., Wypych, J. Toronto:ChemTec, 2001. 1419-1484.

Terfloth, G. (2001). Review: Enantioseparations in Super- and Subcritical Fluid Chromatography. *Journal of Chromatography A*, 906, 301–307.

Terfloth, G., Pirkle, W., Lynam, K., & Nicolas, E. (1995). Broadly Applicable Polysiloxane-based Chiral for High-performance Liquid Chromatography Stationary Phase and Supercritical Fluid Chromatography. *Journal of Chromatography A*, 705, 185-194.

Tester, J. W., & Modell, M. (1997). Thermodynamics and Its Applications (3rd ed.). Upper Saddle River, New Jersey: Prentice Hall.

Thielmann, F. (2004). Review: Introduction into the Characterization of Porous Materials by Inverse Gas Chromatography. *Journal of Chromatography A*, 1037, 115–123.

Tien, C. (1994). Adsorption Calculations and Modeling. Newton, Massachusetts: Butterworth-Heinemann.

Tiselius, A. (1937). A New Apparatus for Electrophoretic Analysis of Colloidal Mixtures. *Transactions of the Faraday Society*, 33, 524.

Topallar, H. & Bayrak, Y. (1999). Investigation of Adsorption Isotherms of Myristic, Palmitic and Stearic Acids on Rice Hull Ash. *Turkish Journal of Chemistry*, 23, 193-198.

Tswett, M. (1906). Physikalisch-chemische Studien Euber das Chlorophyll Die Adsorption. *Berichte der Deutschen Chemischen Gesellschaft*, 24, 384-393.

U.S. Food and Drug Administration. (2003). Pharmaceutical cGMPS for the 21st Century. Washington: U.S. Department of Health and Human Services.

Valenzuela, D. P., & Myers, A. L. (1989). Adsorption Equilibrium Data Handbook. Englewood Cliffs: Prentice Hall Inc.

Van Arnum, P. (2006). Single-Enantiomer Drugs Drive Advances in Asymmetric Synthesis. *Pharmaceutical Technology*, 45-57.

van Deemter, J. J., Zuiderweg, F. J., & Klinkenberg, A. (1956). Longitudinal Diffusion and Resistance to Mass Transfer as Causes of Nonideality in Chromatography. *Chemical Engineering Science*, 271-289.

Varma, A., & Morbidelli, M. (1997). Mathematical Methods in Chemical Engineering. New York: Oxford University Press Inc.

Vente, J. A., Bosch, H., de Haan, A. B., & Bussmann, P. J. (2005). Evaluation of Sugar Sorption Isotherm Measurement by Frontal Analysis under Industrial Processing Conditions. *Journal of Chromatography A*, 1066, 71-79.

Wankat, P. C. (1986). Large-Scale Adsorption and Chromatography. Boca Raton, Florida: CRC Press Inc.

Welch, C. J. (1994). The Whelk O1 Chiral Stationary Phase. *Journal of Chromatography A*, 666, 3-26.

Wenda, C., & Rajendran, A. (2009). Enantioseparation of Flurbiprofen on Amylose-Derived Chiral Stationary Phase by Supercritical Fluid Chromatography. *Journal of Chromatography A*, 1216 (50), 8750-8758.

Wilson, W. (1994). Direct Enantiomeric Resolution of Ibuprofen and Flurbiprofen by Packed Column SFC. *Chirality*, 6216-6219.

Xie, J., & Yanik, G. W. (2011). Resolution of Racemic Gamma Lactone Flavors on Chiralpak AD by Packed Column Supercritical Fluid Chromatography. *Food Chemistry*, 124 (3), 1107-1112.

Yang, X. & Matthews, M. (2003). Equilibrium and Kinetics Properties of *p*-dichlorobenzene and Toluene on Silica Gel in Dense CO_2 by Chromatography Analysis. *Chemical Engineering Journal*, 93, 163–172.

APPENDICES

Appendix A Operation of Supercritical Fluid Chromatograph

Turn on the Lauda chiller that circulates in the syringe pump used for CO_2 delivery and set the temperature to –2°C. Turn on the HP 1050 UV detector. Wait until HP1050 displays on the screen. Press lamp on, then press enter. Fifty minutes are needed for the lamp to warm up. Set the pressure to the desired back pressure on the automated back pressure regulator. Turn on the column oven that surrounds the column and set the temperature to the desired temperature. The temperature of the water bath is measured with a thermometer. The temperature of the water bath can be set by adjusting the knob on the heater. Temperatures below 31.1°C are below the supercritical temperature of CO_2. Check that there is sufficient liquid in the flask connected to the flush of the auto sampler. Turn on the auto sampler. Make sure the level of liquid in the collector flask is above the tubing that runs from the back pressure regulator. Prepare the mobile phase by filling the syringe pump with 100mL of CO_2. The temperature of the water bath must be below 0°C before adding CO_2 or else gas phase CO_2 will fill the syringe pump instead of liquid CO_2. Connect the HP1050 UV detector to the computer. The cable runs from the analog out of the UV detector to the National Instruments connector block that is connected to the computer. Open Labview then open the appropriate Labview data collection program. Begin pumping CO_2 at 2.85 mL/min and pumping ethanol at 0.05 mL/min. This provides a total flow rate of 1 ml/min through the column. When the pressure of the system builds to the set pressure of the back pressure regulator, bubbles will be produced in the collector flask. Wait for the system to reach steady state and make injections.

Appendix A (Cont.)

By setting the UV detector wavelength below the carbon dioxide cut-off wavelength (300 nm), fluctuations in carbon dioxide concentration can be detected. When the system reaches steady state samples can be injected into the system.

Separation Procedure

Prepare sample vial. Sample vial has 1 mL volume. Weigh sample on analytical balance and dissolve in organic modifier in sample vial. Place a sample vial in the auto sampler position 1. Set the auto sampler to obtain a sample from the proper location. If the auto sampler becomes clogged, press the flush key. Press balance on the HP 1050 UV/Vis detector. Inject the first sample with the auto sampler. When the auto sampler makes a puff sound, press run on the Labview screen. If there is baseline drift on the first run, press balance before starting a new run. Separations can be accomplished as long as system at steady state.

Shut Down Procedure

Turn off the HPLC pump and the syringe pump. Return the system to atmospheric pressure slowly. Reducing pressure too quickly could damage the system. Run 20 mL of ethanol through the column at 1ml/min. Watch the pressure of the system carefully. If the pressure goes too high, reduce the flow rate or press stop until the pressure is low enough. If the pressure exceeds 350 atm the auto sampler will be damaged. Turn off the auto sampler. Turn off the water bath heater that surrounds the column.

Appendix A (Cont.)

Turn off the cooler that runs through the syringe pump jacket. Turn off the UV detector. Disconnect the cable from the computer. The following procedures are recommended for incorporation into your particular system tests. In the event that a problem is suspected in the operation or performance of an ISCO syringe pump, following these steps can often help to isolate and correct a problem in the field, eliminating the time and expense of returning the unit to the factory for servicing. Syringe pump users who regularly pump caustic or viscous substances should perform these procedures periodically to ensure uninterrupted operation.

To pressure check connect a fill line to the pump inlet with an on/off valve and calibrated external pressure gauge. With the valve open, fill the cylinder to at least 50mL with at least 95% distilled and degassed water, and 5% isopropanol.

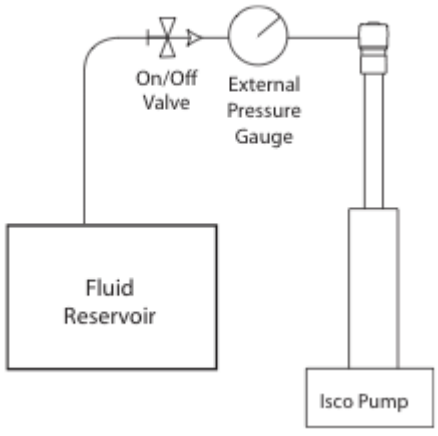

Figure A1. Syringe Pump Setup for Pressure Check

Appendix A (Cont.)

Perform the following steps to verify proper operation of the pressure transducer:

1. Press CONST PRESS button on the pump controller.
2. Enter a pressure set-point of 1,000 psi.
3. Purge air from the system by opening the fill line and running the pump.
4. Press STOP button on pump controller.
5. Zero the transducer by pressing the ZERO PRESS button then the A button
6. Close the valve and press the RUN button.
7. Relive the pressure by pressing the REFILL button until the pressure is at 0 psi.

Leak Check

Perform the following steps to verify that the cylinder is in satisfactory condition.

1. Close the refill valve and pressurize the pump to the maximum pressure by pressing the CONST PRESS, PRESSURE (A), MAX (C), RUN buttons.
2. Allow the pump to stabilize for 15 minutes. Then record an initial reading of the remaining volume.
3. After a minimum run time of 30 minutes, record a second reading of the volume.
4. Calculate the flow rate.
5. Relieve the pressure by pressing the REFILL button until the pressure is at 0 psi.

Appendix A (Cont.)

Flow Rate Check

Perform the following steps to verify proper operation of the cylinder drive mechanism. Place a metric beaker or burette under the refill tube, and program the controller to fill the beaker at a flow rate of 25mL/min for 1 minute.

1. Press PGM GRAD.
2. Press 3 for single pump programming.
3. Press CONTINUE.
4. Press PROGRAM
5. The screen will display: ENTER FILE# [X].
    a. Select any number from 1 to 99 to name the program file, then press ENTER.
6. Press FLOWRATE ( ), 27.76, and ENTER.
7. Press STEP FWD ( ) to enter program step 1.
    a. Press 1 > 0 > ENTER.
    b. Press 2 > 100 > ENTER.
    c. Press 4 > .1 > ENTER.
8. Press INSERT to enter program step 2.
    a. Press 2 > 100 > ENTER.
    b. Press 4 > .8 > ENTER.
9. Press INSERT to enter program step 3.
    a. Press2>0>ENTER.
    b. Press 4 > .1 > ENTER.

Appendix A (Cont.)

10. Press STORE.
11. Press OPTION.
12. Press NEXT ACTION repeatedly until the screen displays: RETURN TO INITIAL AND HOLD
13. Press PREVIOUS to return to the main menu.
14. Press RUN ( ) two times.
15. Take metric beaker and carefully measure volume collected. The volume of liquid in the beaker after one run should be 25 mL +/- 0.25 mL.

Appendix B FACP Sample Calculation Procedure

Export Labview chromatogram file to Microsoft Excel as a text delimited file. The Microsoft Excel file will consist of two columns: the raw time [min] and the detector signal [volts]. The number of data points for each file is dependent on the experiment run time. A typical sampling rate is 1 point per second.

The raw time is then converted to units of volume by multiplying the raw time with the solvent flow rate. The solvent flow rate through the column is determined experimentally with the hold-up time determination. The hold-up time is determined by injecting a 10 µL sample of co-solvent (e.g. ethanol, methanol, acetone, etc.) into the column and recording the amount of time from injection to detector signal. The volumetric flow rate of solvent is then calculated from experimental conditions and the column volume. For example, the hold-up time, t_M for a 10 µL injection of ethanol in 95:5 CO_2:EtOH at 130 Bar and 40^oC was 1.4 min.

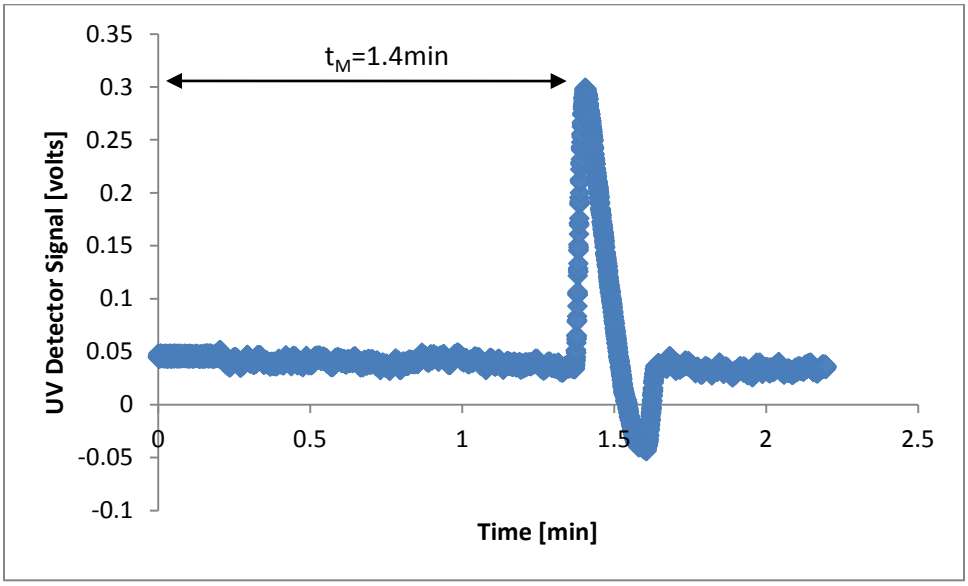

Figure B1. Hold-up Time Experimental Determination

Appendix B (Cont.)

The volumetric flow set at the syringe pump delivering CO_2 is 2.85 mL/min and 0.15 mL/min for the EtOH HPLC pump. The actual volumetric flow rate through the column is shown in Equation B1.

$$\frac{V_{column}}{\dot{V}} = t_M \qquad \frac{4.15\text{mL}}{\dot{V}} = 1.4\,\text{min} \qquad \dot{V} = 2.96\ \text{mL/min} \tag{B1}$$

The 2.96 mL/min flow rate is used to convert the raw time to volume as shown in Equations B2, B3, B4, and B5.

$$\text{Raw Time} * \text{Volumetric Flow Rate Actual} = \text{Volume} \tag{B2}$$

$$0.5\,\text{min} * \frac{2.96\text{mL}}{\text{min}} = 1.48\text{mL} \tag{B3}$$

$$20\text{min} * \frac{2.96\text{mL}}{\text{min}} = 59.2\text{mL} \tag{B4}$$

$$50\text{min} * \frac{2.96\text{mL}}{\text{min}} = 148.0\text{mL} \tag{B5}$$

The detector signal must be converted from volts to concentration units. The detector voltage ranges from 0-1.2 volts. First the detector signal is multiplied by a scaling factor. The scaling factor is a parameter for the UV detector that allows for the

entire detector signal to be seen on a chromatograph. Without the scaling factor, the detector signal may get truncated and analysis is extremely difficult unless the concentration of analyte is low. The scaling used for the experiment was 4. After multiplying the detector signal by the scaling factor the baseline noise must be subtracted out to obtain the unobstructed detector signal. A stable baseline for each experiment is established by passing solvent through the column and detection at the experimental conditions for at least an hour to ensure steady state before determining the hold-up time and the subsequent experiment. The baseline at system steady state is typically around 0.05 volts.

The calibration factor for each experiment is determined from a mass balance on the solute injected into the system. The mobile phase concentration of the solute is calculated by determining the dosage amount of an injection and then dividing by the experimental volumetric flow rate. A sample calculation for the mobile phase concentration is shown in Equations B6 and B7.

$$\frac{30\text{mgIbu}}{\text{mLEtOH}} * 0.15\text{mL EtOH} = 4.5\text{mgIbu} \qquad \text{(B6)}$$

$$\frac{4.5\text{mgIbu}}{2.96\text{ mL EtOH}} = \frac{1.5203\text{mg}}{\text{mL Solvent}} = \text{Mobile Phase Concentration} \qquad \text{(B7)}$$

The mobile phase concentration is set equal to the maximum voltage recorded by the detector. Figure B2 shows a maximum voltage of 0.25 volts.

Appendix B (Cont.)

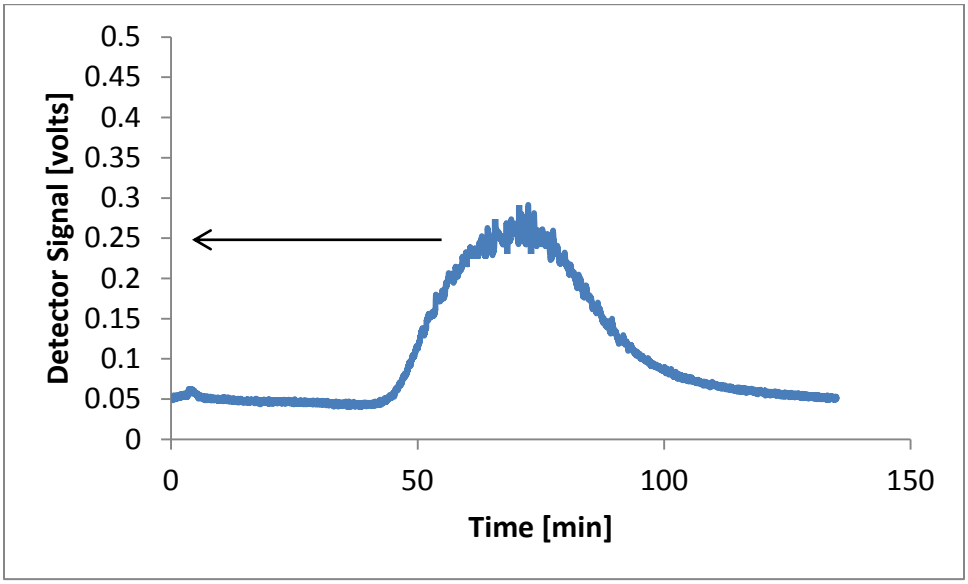

Figure B2. Chromatogram S-ibuprofen 40°C 130 Bar Showing Max Concentration-Voltage Relationship

The maximum voltage is multiplied by the scaling factor and the background noise is subtracted from it. The resultant voltage is then set equal to the diluted mobile phase concentration of the solute in the solvent. Sample calculations showing how the calibration factor is determined are shown in Equations B8 and B9.

$$(0.25\text{volts}*4)-0.18\text{volts} = 0.82\text{volts} \rightarrow \text{Unobstructed Detector Signal} \qquad \text{(B8)}$$

$$\text{Calibration Factor}\left[\frac{\text{volts}}{\text{mg/mL}}\right] = \frac{0.82\text{volts}}{1.5\text{mg/mL}} = 0.55\left[\frac{\text{volts}}{\text{mg/mL}}\right] \qquad \text{(B9)}$$

Appendix B (Cont.)

The unobstructed detector signal is then divided by a calibration factor to convert volts to concentration with units of [mg/mL]. A sample calculation for converting the detector signal [volts] to concentration [mg/mL] is shown in Equations B10 and B11.

$$\frac{\text{Raw Signal*Scaling Factor - Baseline}}{\text{Calibration Factor}} = \text{Concentration} \qquad \text{(B10)}$$

$$\frac{(0.07\text{volts}*4)-0.18\text{volts}}{0.55\,\frac{\text{volts}}{\text{mg/mL}}} = 0.1818\,\text{mg/mL} \qquad \text{(B11)}$$

At this point we now have the chromatogram as a function of solute concentration and solvent volume. Graphically, the chromatogram is shown in Figure B3.

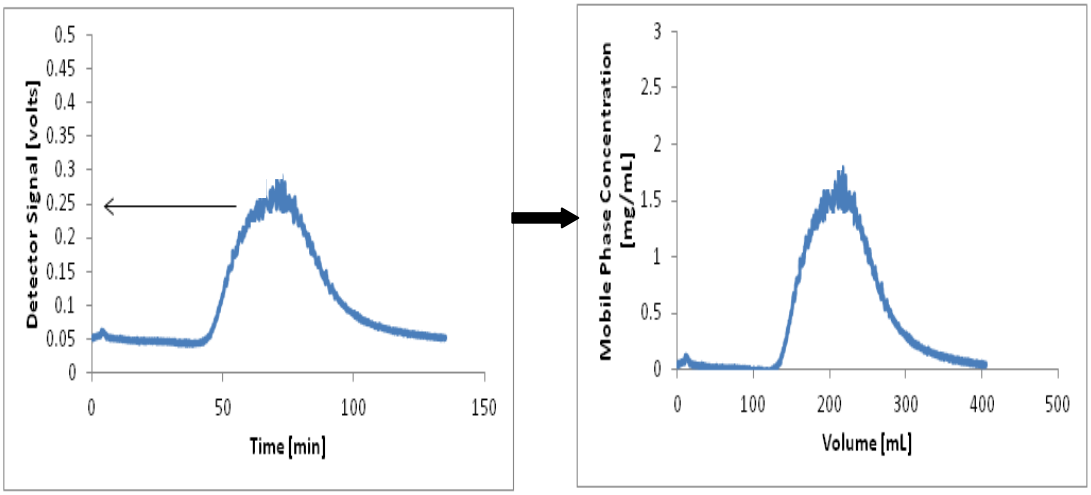

Figure B3. Chromatogram Transformation

Appendix B (Cont.)

Next, the point at which solute desorption begins must be determined. This is done by data inspection to find the last point where the solute concentration is at a maximum and recording the associated volume. Graphically, it may be shown that this point is located at 215 mL of effluent volume as seen in Figure B4.

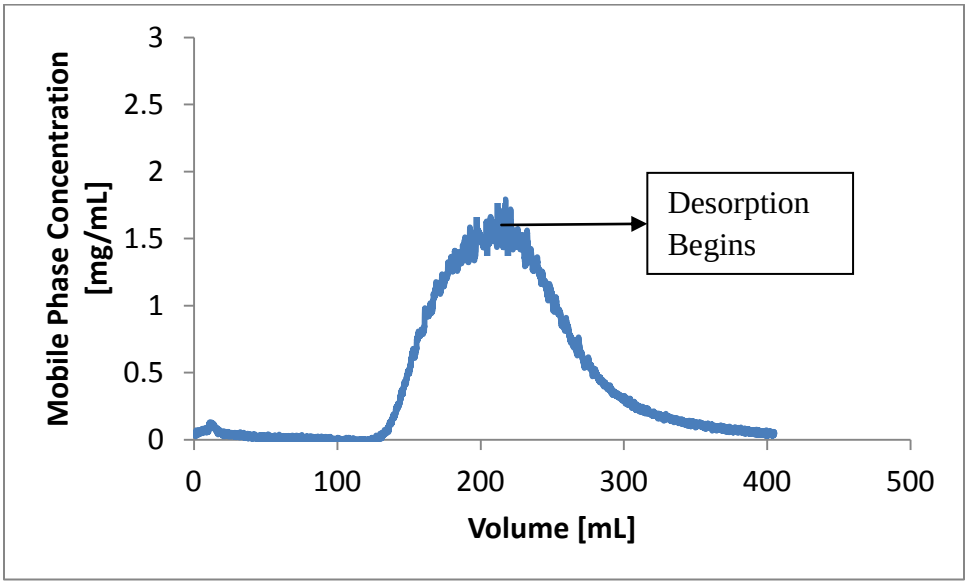

Figure B4. Chromatogram Showing Mobile Phase Concentration vs. Volume

This volume of 215 mL is used as a baseline to calculate the threshold volume of the desorption curve. The threshold volume is the solvent volume less the volume where desorption begins. Essentially this action shifts the entire curve to the left hand side of the plot removing everything prior to desorption. This is shown in Figure B5.

Appendix B (Cont.)

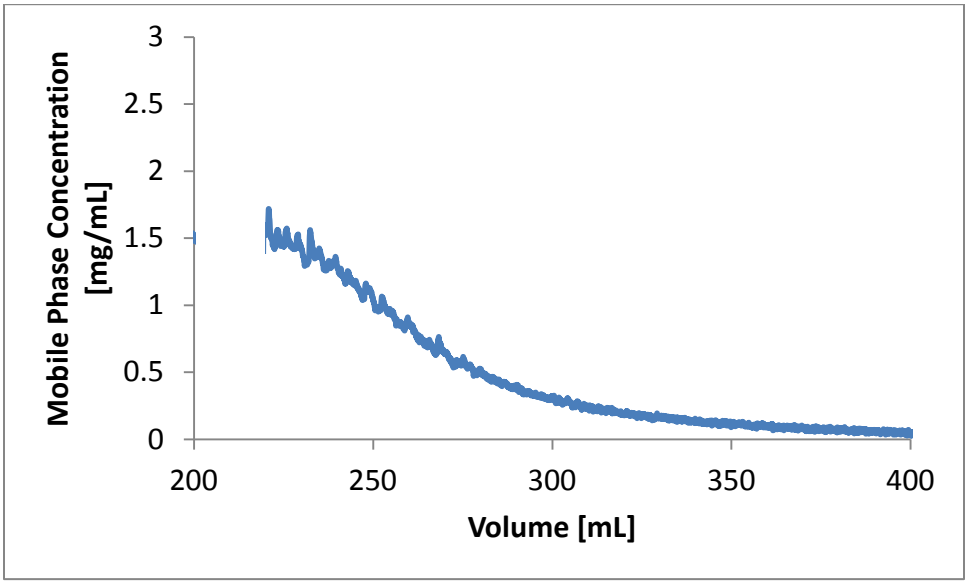

Figure B5. Graph of Desorption Portion of Chromatogram

A sample calculation for the threshold volume of the desorbed solute profile is shown in Equations B12, B13, and B14.

$$225\text{mL} - 215\text{mL} = 10\text{mL} \quad \text{(B12)}$$

$$250\text{mL} - 215\text{mL} = 35\text{mL} \quad \text{(B13)}$$

$$300\text{mL} - 215\text{mL} = 85\text{mL} \quad \text{(B14)}$$

The desorption portion of the chromatogram is then plotted against the threshold volume as shown in Figure B6.

Appendix B (Cont.)

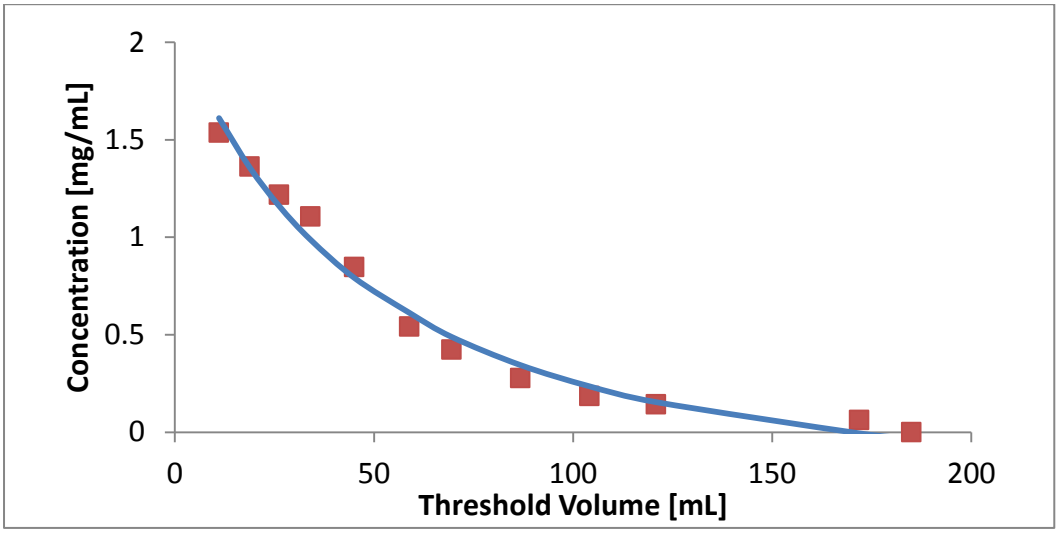

Figure B6. Plot of Concentration vs. Threshold Volume

The average mass of solute desorbing must be calculated next. This is done by taking the difference between the two threshold volumes. The calculation is a trapezoid rule integration of the desorption portion of the chromatogram. Sample calculations for the average mass of solute are shown in Table B1.

Table B1. Average Mass Calculations

Threshold Volume [mL]	**Concentration [mg/mL]**	**Average Mass [mg]**
13.340	1.536	(21.128-13.340)*(1.362+1.536)/2=11.284
21.128	1.362	(28.585-21.128)*(1.218+1.362)/2=9.6191
28.585	1.218	(36.538-28.585)*(1.107+1.218)/2=9.246

Appendix B (Cont.)

As a check, the average mass desorbing from the column should be decreasing as the threshold volume increases, eventually reaching zero.

The total mass desorbing from the column is the next calculation to perform. The total mass desorbing from the column is calculated by summing up the average mass calculated from the average mass calculation in the opposite direction. Table B2 shows these calculations.

Table B2. Total Desorbed Mass Calculations

Threshold Volume [mL]	**Concentration [mg/mL]**	**Average Mass [mg]**	**Total Desorbed Mass [mg]**
13.340	1.536	11.284	11.284+18.857=30.141
21.128	1.362	9.619	9.246+9.619=18.857
28.585	1.218	9.246	9.246

Next, the mass on the column must be calculated. This calculation takes into account solute concentration, the threshold volume, and the specific volume adsorption for the column packing material per unit mass. The specific volume adsorption per unit mass is typically determined by BET porosity measurements. For these experiments, a value of 0.16 mL/g is taken as the specific volume adsorption per unit mass. This value of 0.16 mL/g represents the volume of packing material that is not available for solute sorption. The mass of stationary phase adsorbent packing is taken as 3g. Sample calculations for the solute mass still on the column are shown in Table B3.

Appendix B (Cont.)

Table B3. Solute Mass on Stationary Phase Calculations

Threshold Volume [mL]	**Concentration [mg/mL]**	**Average Mass [mg]**	**Total Desorbed Mass [mg]**	**(v-ax)c [mg]**
13.340	1.536	11.284	30.141	(13.34-(0.16*3))*1.531=19.753
21.128	1.362	9.619	18.857	(21.128-(0.16*3))*1.362=28.123
28.585	1.218	9.246	9.246	(28.585-(0.16*3))*1.218=34.232

Now the values for the solute mass still on the column are added to the mass of solute desorbed from the column. These results are shown in Table B4.

Table B4. Total Column Solute Mass Calculations

Threshold Volume [mL]	**Concentration [mg/mL]**	**Average Mass [mg]**	**Total Desorbed Mass [mg]**	**(v-ax)c [mg]**	**Total Column Solute Mass [mg]**
13.340	1.536	11.284	30.141	19.753	30.141+19.753=49.894
21.128	1.362	9.619	18.857	28.123	18.857+28.123=46.980
28.585	1.219	9.246	9.246	34.232	9.246+34.232=43.418

Appendix B (Cont.)

After the total column solute mass is calculated, the mass of packing must be removed from the calculation. This is done by dividing the total column mass by the packing mass as shown in Table B5. Note the column loading is mass of solute per mass of packing or [mg/g].

Table B5. Column Load Calculation

Threshold Volume [mL]	**Concentration [mg/mL]**	**Average Mass [mg]**	**Total Desorbed Mass [mg]**	**(v-ax)c [mg]**	**Total Column Solute Mass [mg]**	**Column Load [mg/g]**
13.340	1.536	11.284	30.141	19.753	49.894	49.894/3=16.63
21.128	1.362	9.619	18.857	28.123	46.980	46.980/3=15.66
28.585	1.219	9.246	9.246	34.232	43.418	43.418/3=14.47

As a check, the lowest threshold volume should have the highest column loading. The values for the column loading are then taken and regressed as a function of concentration. Figure B7 shows the plot of column loading vs. concentration.

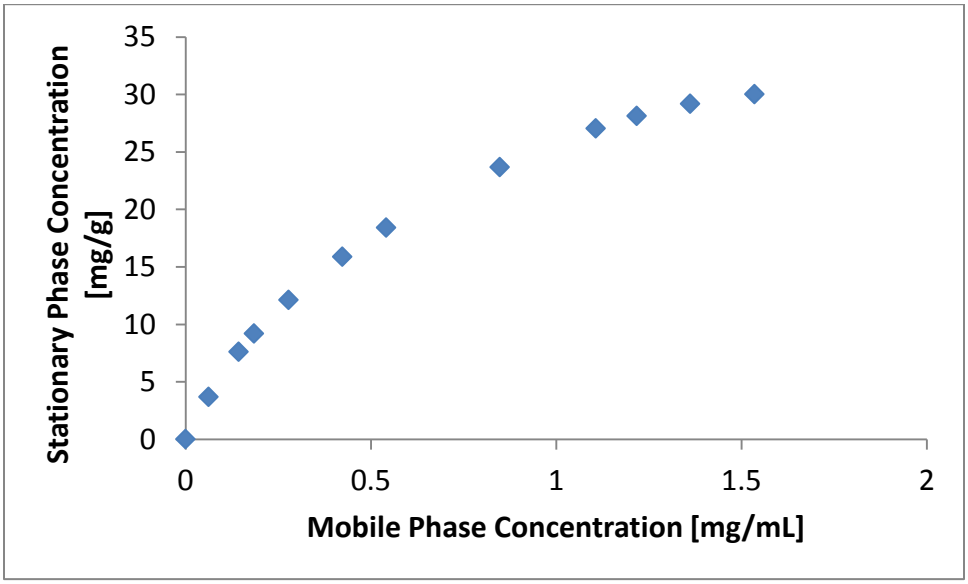

Figure B7. S-ibuprofen Isotherm Loading vs. Concentration 40°C and 130 Bar

The number of parameters regressed is dependent on the type of model chosen. The two-parameter Langmuir isotherm model was chosen for this work. The Langmuir isotherm model is given by Equation B15.

$$q = \frac{q_s bC}{(1 + bC)} \tag{B15}$$

where q_s and b are the regressed parameters. The regression can be done in software packages like Microsoft Excel, Matlab, or LoggerPro.

Appendix B (Cont.)

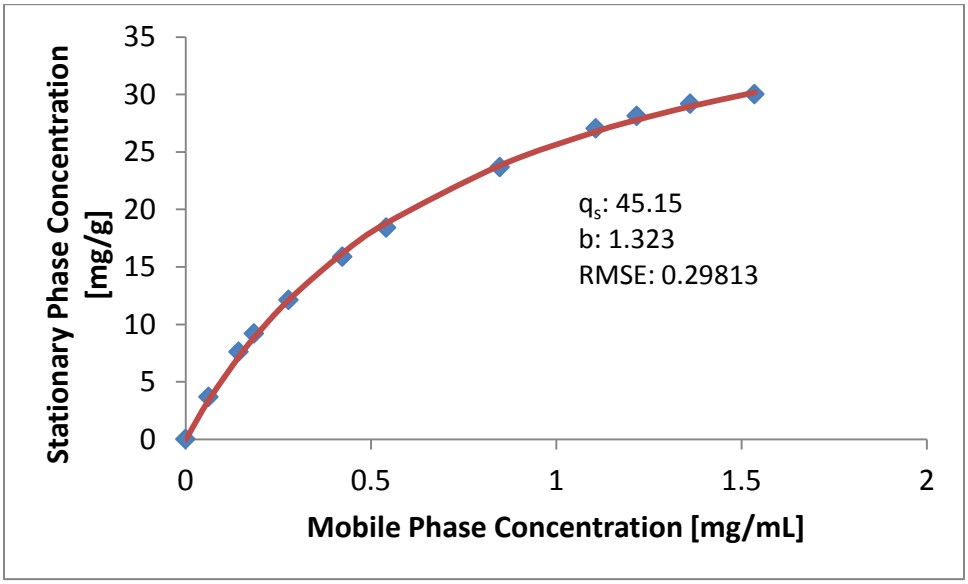

Figure B8. Experimental Isotherm and Langmuir Model Regression

Appendix C Matlab M-File for Automated Isotherm Determination

```
function f = datareader(file, F, MW, CA, num_peaks)
if nargin == 0
   file = input('File name to import (default.input): ');
   if isempty(file) file = 'default.input'; end


   F = input('Flow Rate (mL/min)? (3)');
   if isempty(F) F = 3; end  %mL/min

   MW = input('Molecular Weight of compound being injected? (206)');
   if isempty(MW) MW = 206; end %gm/mol

   CA = input('Amount of compound being injected into column (mg/mL)? (15)');
   if isempty(CA) CA = 15; end %mg/mL

   N = CA/(MW*100*100); % number of moles
   w = 3; %gm

   data = importdata(file);

   x_axis = data(:,1);
   y_axis = data(:,2); % scaling factor
   area = trapz(x_axis,y_axis);
   Vg = F*x_axis; %mL/gm
   C = (N/(F*area))*y_axis; %
   polyfitcoef_1 = polyfit(Vg,C,5);
   newC = polyval(polyfitcoef_1,Vg);
   polyfitcoef_2 = polyfit(newC,Vg,3);
   polysym = poly2sym(polyfitcoef_2);
   intpolysym = int(polysym);
   intpolycoef = sym2poly(intpolysym);
   q = polyval(intpolycoef,C); %
   plot(C,q)
   title_name = input('Title of graph?','s');
   title(title_name)
   xlabel('Concentration (mmol/mL)');
   ylabel('Q (mmol/mL)');
   savedata = [C q];
   save(title_name,'savedata','data')
else
   warning off all
   fig1 = gca(figure);
   color = ['r' 'g' 'b'];
```

```
if isempty(file) file = 'default.input'; end
if isempty(F) F = 3; end  %mL/min
if isempty(MW) MW = 206; end %gm/mol
if isempty(CA) CA = 15; end %mg/mL

N = CA/(MW*100*100); % number of moles


w = 3; %gm

data = importdata(file,'\t');

hold(fig1,'on');
plot(data(:,1),data(:,2),':r');
xlabel('Time')
ylabel('Absorbance')
legend('Original Data')

%%%%%%%%%%%%%%%%%%%%%%%%%%%%%%%%%%%%%%%%%%%%%%%
%Smoothing data

smooth_data = smooth(data(:,2));
for i = 1:3
    smooth_data = smooth(smooth_data);
end

%%%%%%%%%%%%%%%%%%%%%%%%%%%%%%%%%%%%%%%%%%%%%%%
%Histogram of distribution of y values
[n,xout] = hist(smooth_data,70);
[peaks,locs] = findpeaks(n,'minpeakheight',50);
[c,index] = min(peaks);

tail_end = xout(locs(index));
```

Appendix C (Cont.)

```
plot(data(:,1),smooth_data);
legend('Original Data','Smoothed Data');
box('on');
hold(fig1,'off');

data_mean = mean(smooth_data);
data_std = std(smooth_data);
cutoff = data_mean + data_std;

[peaks,locs] = findpeaks(smooth_data,'minpeakheight',cutoff,'minpeakdistance',5);
```

Appendix C (Cont.)

```
   while length(peaks) > num_peaks
      smooth_data = smooth(smooth_data);
      [peaks,locs] = findpeaks(smooth_data,'minpeakheight',cutoff,'minpeakdistance',5);
   end

   % Plot markers for the points where our isotherms are integrated
   hold(fig1,'on');
   peak_times = [];
   for i = 1:length(locs)
      peak_times = [peak_times data(locs(i),1)];
   end
   plot(peak_times,peaks,'gs');
   hold(fig1,'off');

   if length(locs) > 1
      for i = 1:length(locs)
         if i ~= length(locs)
            end_point(i) = min(smooth_data(locs(i):locs(i+1)));
            end_point_index(i) = locs(i) +
find(smooth_data(locs(i):locs(i+1))==end_point(i));
         else
            end_point(i) =
smooth_data(locs(i)+min(find((smooth_data(locs(i):length(smooth_data))-
tail_end)<0.001)));
            end_point_index(i) = locs(i) +
find(smooth_data(locs(i):length(smooth_data))==end_point(i));
         end
      end
   else
      end_point_index = locs(1)+min(find((smooth_data(locs(1):length(smooth_data))-
tail_end)<0.001));
      end_point(1) =
smooth_data(locs(1)+min(find((smooth_data(locs(1):length(smooth_data))-
tail_end)<0.001)));
   end

   disp(' ');
   disp(' ');
   disp('Information on analyzed data:')
   disp('----------------------------')
   disp(' ');
   disp(['Number of peaks: ',num2str(length(end_point_index))]);
   disp(' ');
   for i = 1:length(end_point_index)
```

Appendix C (Cont.)

```
        disp(['Peak #',num2str(i),':     Time: ',num2str(data(locs(i),1)),'     Absorbance: 
',num2str(data(locs(i),2))]);
    end
    %%%%%%%%%%%%%%%%%%%%%%%%%%%%%%%%%%%
    fig2 = gca(figure);
    for i = 1:length(locs)
        x_axis = data(locs(i):end_point_index(i),1);
        y_axis = (smooth_data(locs(i):end_point_index(i)))-data(end_point_index(i),2);
        if isempty(find(y_axis<0)) ~= 1
            y_axis = (smooth_data(locs(i):end_point_index(i)))-
data(end_point_index(length(i)),2);
        end
        area = trapz(x_axis,y_axis);
        Vg = (F/w)*x_axis; %mL/gm
        C = (N/(F*area))*y_axis; %
        polyfitcoef_1 = polyfit(Vg,C,5);
        newC = polyval(polyfitcoef_1,Vg);
        polyfitcoef_2 = polyfit(newC,Vg,3);
        polysym = poly2sym(polyfitcoef_2);
        intpolysym = int(polysym);
        intpolycoef = sym2poly(intpolysym);
        q = polyval(intpolycoef,C); %

        hold(fig2,'on');
 %plot(fig2,C,q,color(i))
        plot(C,q)

        box('on');

        %title(file)
        xlabel('Concentration (mmol/mL)');
        ylabel('Q (mmol/mL)');
        savedata{i} = [C q];
        e = [C,q];
        save (sprintf('%s_isotherm_%d.csv', file, i), 'e', '-ascii', '-tabs');
    end
    hold(fig2,'off');
    %save(file,'savedata','data')
end
 saveas(fig1,sprintf('%s_BandProfiles.fig', file))
saveas(fig2,sprintf('%s_Isotherms.fig', file))
saveas(fig1,sprintf('%s_BandProfiles.jpg', file))
saveas(fig2,sprintf('%s_Isotherms.jpg', file))
disp('Done!')
```

Appendix C (Cont.)

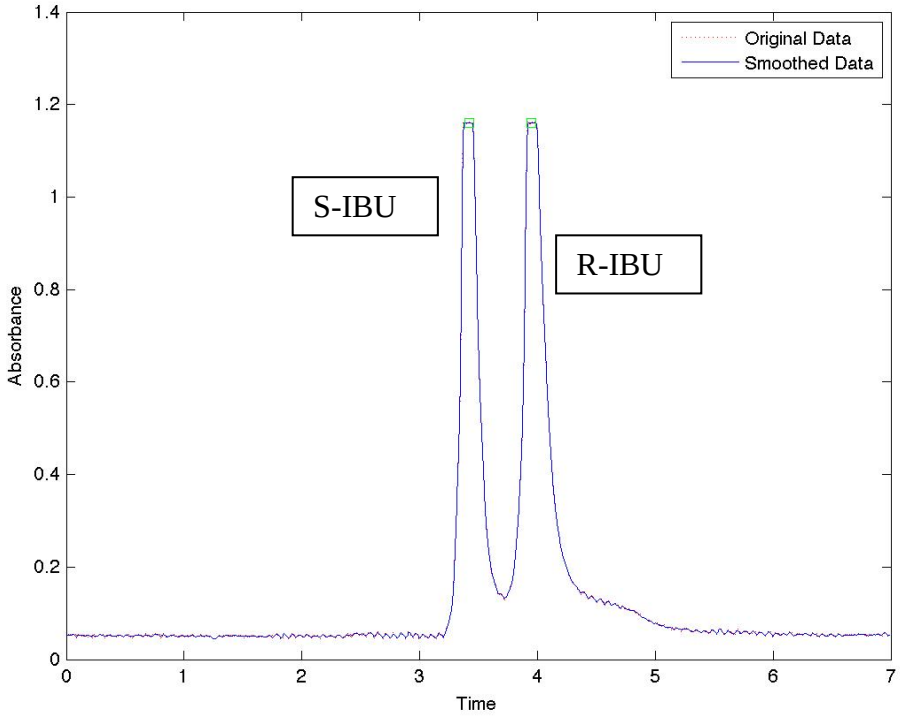

Figure C1. Automated Generation of Raw Data Finding Peaks

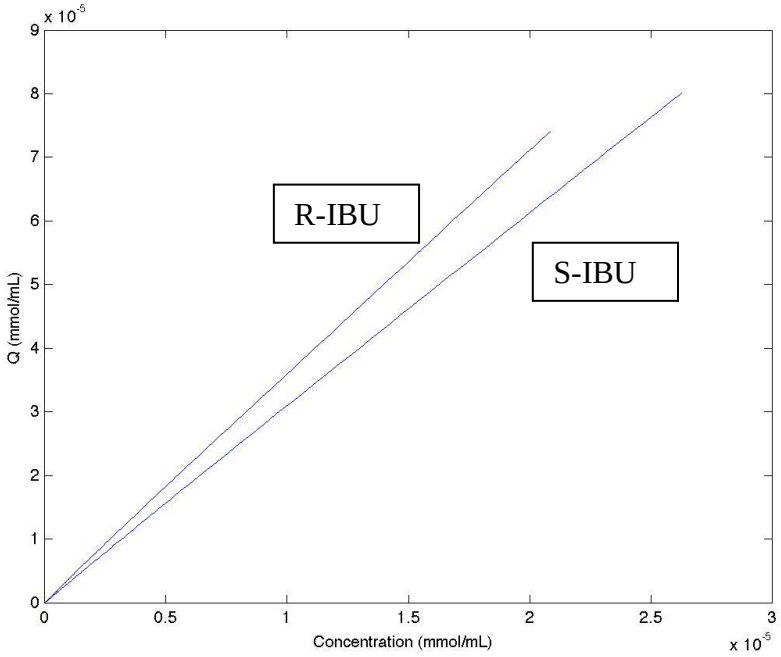

Figure C2. Isotherms Generated Automatically Using Data Reader

Appendix D Matlab M-File Solution of Chromatographic Bed

```
function f = Equilibrium_Dispersive()

 disp('Problem Definition')
disp(' ')
disp(' ')
choice1 = input('1) Load Variables or 2) Input Variables?');
if choice1 == 1
   filename = input('Mat file name? ');
   load filename
elseif choice1 == 2
   D_L = input('Coefficient of Axial Diffusion, D_L (7.6e-5): ');
   if isempty(D_L) D_L = 7.6e-5; end
   e = input('Total porosity of the column packing, e (.86): ');
   if isempty(e) e = .86; end
   F = (1-e)/e;
   u = input('Mobile Phase Velocity, u (.00016667): ');
   if isempty(u) u = .00016667; end
   a = input('Linear relationship, a (1): ');
   if isempty(a) a = 1; end
    b = input('Langmuir coefficient, b: ');

   L = input('Dimension L (.1): ');
   if isempty(L) L = .1; end
   t_max = input('Maximum Calculation Time (100): ');
   if isempty(t_max) t_max = 100; end
   t_p = input('Dirac Pulse Time, t_p (30): ');
   if isempty(t_p) t_p = 30; end

   disp(' ')
   disp('Initial Conditions');
   disp(' ')

   C_t_0 = input('C at t = 0 for 0 <= z <= L (0): ');
   if isempty(C_t_0) C_t_0 = 0; end

   disp(' ')
   disp('Boundary Conditions');
   disp(' ')

   C_z_0_1 = input('C at z = 0 for 0 <= t <= t_p (10): ');
   if isempty(C_z_0_1) C_z_0_1 = 10; end
   % C_z_0_2 = input('C at z = 0 for t >= t_p: ');
   % C_z_L_1 = input('C at z = L for 0 <= t <= t_p: ');
```

Appendix D (Cont.)

```
   % C_z_L_2 = input('C at z = L for t_p <= t: ');

    % C(1:n/2,m) = C_z_0_1;
   % C(n/2:n,m) = C_z_0_2;


   stability_check = 1;
   while stability_check == 1
      m = input('Number of divisions in z(14): ');
      if isempty(m) m = 14; end
      h = L/m; %dz
      z_vector = 0:h:L;
       n = input('Number of timesteps(200): ');
      if isempty(n) n = 200; end
      tau = t_max/n; %dt
      t_p_t = t_p/tau;
      time_vector = 0:tau:t_max;

%        stability = (u*tau)/((1+(F*a))*h);

%        if stability >= .01
%           disp('A different number of divisions or timesteps have to be provided. Current
values generate unstable difference scheme!');
%        elseif stability < .01
%           break
%        end

      C = zeros(n+1,m+1);

      C(1,:) = C_t_0;
      C(1:t_p_t+1,1) = C_z_0_1;
      C(t_p_t+1:n+1,1) = 0;

      filename = 'pdevariables';
      save filename D_L F e u a L m h t_max t_p n tau t_p_t C_t_0 C_z_0_1
      coef_1 = (u*tau)/((2*h)*(1+(F*a)));
      coef_2 = (u^2*tau^2)/(2*((1+(F*a))^2)*(h^2));
      coef_3 = (D_L*tau)/((h^2)*(1+(F*a)));
      i = 2;
      time_check = 1;
      while time_check == 1 %i = time
         z_check = 1;
         j = 1;
```

Appendix D (Cont.)

```
        while z_check == 1 %j = space
            j = j + 1;
            if j == m + 1
                z_check = 0;
            else
                C(i,j) = C(i-1,j) - (coef_1*((C(i-1,j+1)-C(i-1,j-1)))) + (coef_2*(C(i-1,j+1)-
(2*C(i-1,j))+C(i-1,j-1))) + (coef_3*(C(i-1,j+1)-(2*C(i-1,j))+C(i-1,j-1)));
                if C(i,j) > C_z_0_1
                    disp('An error has occurred. Please look at "dz" and "dt" again.');
                    time_check = 0;
                    break
                elseif C(i,j) < C_z_0_1
                    continue
                end
            end
        end
        i = i + 1;
        if i == n + 2
            time_check = 0;
            stability_check = 0;
        end
    end
  end
end
gca1 = gca(figure(1));
surf(gca1,z_vector,time_vector,C);
xlabel(gca1,'z')
ylabel(gca1,'Time (s)')
zlabel(gca1,'Concentration')
gca2 = gca(figure(2));
plot(time_vector,C(:,14));
xlabel(gca2,'Time (s)')
ylabel(gca2,'Concentration')
past_peak_vector = C(find(C(:,14)==max(C(:,14))):length(C(:,14)),14);
past_time_vector = find(C(:,14)==max(C(:,14))):length(C(:,14))
Appendix D (Cont.)
plot(past_time_vector,past_peak_vector)
global p
p = polyfit(past_time_vector,past_peak_vector',3)
C_computed = C_function(past_time_vector);
plot(past_time_vector,C_computed)
int_C =
quad(@C_function,past_time_vector(1),past_time_vector(length(past_time_vector(1))))
function C = C_function(past_time_vector)
```

Appendix D (Cont.)

```
global p
C = (p(1)*past_time_vector.^3) + (p(2)*past_time_vector.^2) + (p(3)*past_time_vector)
+ p(4);
```

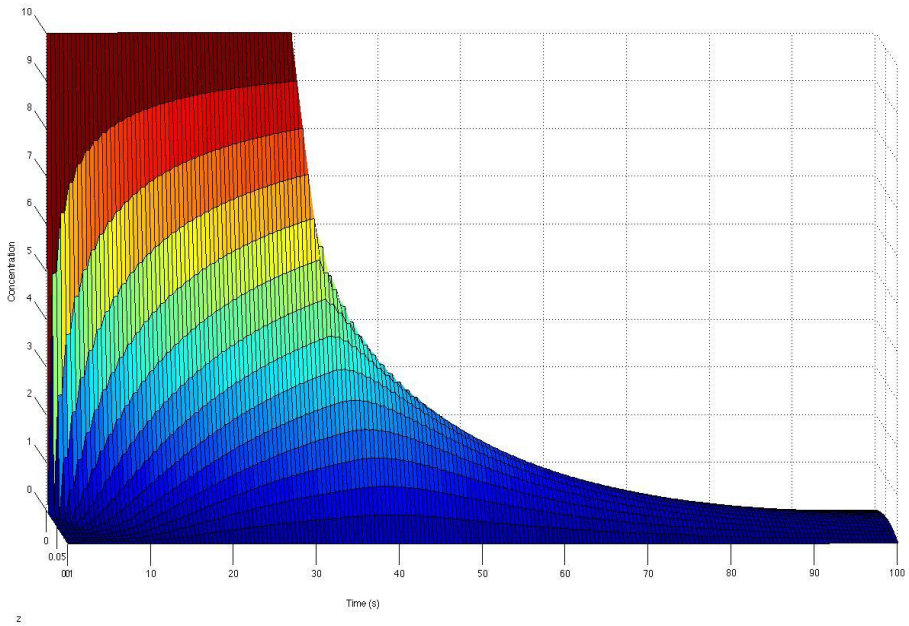

Figure D1. Solution of Equilibrium Dispersive Model

Appendix E Matlab M-File Chromatography Axial Dispersion

```
function [z,t,u] = chromaxdisp(nz,nt,dz,dt,phi,u0,bc)
%Initialization
if nargin < 7
   error('Invalid number of inputs.')
end
%Position vector
nz = fix(nz);
z = [0:nz]*dz;
%Time vector
nt = fix(nt);
t = [0:nt]*dt;
r = phi*dt/dz^2;
%Coefficients of finite difference eqn
alph = r-dt/(2*dz);
bet = 1-2*r;
g = r+dt/(2*dz);
u0 = (u0(:).')'; %Make sure it's a column vector
if length(u0) ~= nz+1
   error('Length of the vector of initial condition is not correct.')
end
[a,b] = size(bc);
if a ~= 2
   error('Invalid number of boundary conditions.')
end
if b < 2 | b > 3
   error('Invalid boundary condition.')
end
if b == 2 & max(bc(:,1)) <= 2
   bc = [bc zeros(2,1)];
end
%Set initial conditions
u(:,1) = u0;
c = zeros(nz+1,1);
%Iteration on t
for n = 2:nt+1
```

Appendix E (Cont.)

```
    %Lower x boundary condition
    switch bc(1,1)
        case 1
            A(1,1) = 1;
            c(1) = bc(1,2);
        case {2, 3}
            A(1,1) = -3/(2*dz) - bc(1,3);
            A(1,2) = 2/dz;
            A(1,3) = -1/(2*dz);
            c(1) = bc(1,2);
    end

    %Internal points
    for i = 2:nz
        A(i,i-1) = -alph;
        A(i,i) = 1+2*r;
        A(i,i+1) = -g;
        c(i) = alph*u(i-1,n-1) + bet*u(i,n-1) + g*u(i+1,n-1);
    end

    %Upper z boundary condition
    switch bc(2,1)
        case 1
            A(nz+1,nz+1) = 1;
            c(nz+1) = bc(2,2);
        case {2, 3}
            A(nz+1,nz+1) = 3/(2*dz) - bc(2,3);
            A(nz+1,nz) = -2/dz;
            A(nz+1,nz-1) = 1/(2*dz);
            c(nz+1) = bc(2,2);
    end
    u(:,n) = inv(A)*c; %Solving the set of equations
end
```

Appendix F CO_2:EtOH PRSV Code

```
function co2ethanoldensity
Tc=[304.19 516.25]';
Pc=[73.82 63.84];
R=8.314e-2;   % bar-liter/mol-K
T=40+273.15;
P=130;   % in bar
k12=0.084
xg=[0.95 0.05];
omega=[.228 .637]';
nc=length(Tc);
z=fsolve(@myfun1,0.2)
density=P/(z*R*T)  % in mol/liter

function F=myfun1(x)
global xg Tc Pc omega R T P nc k12  c12
ac=0.45724*R^2*Tc.^2./Pc;
alpha=(1+(0.37464+1.54226*omega-0.26992*omega.^2).*(1-
(T*ones(nc,1)./Tc).^0.5)).^2;

a=ac.*alpha;
b=0.0778*R*Tc./Pc;
a12=(1-k12)*(a(1)*a(2))^0.5;
am=xg(1)^2*a(1)+2*xg(1)*xg(2)*a12+xg(2)^2*a(2);
bm=xg(1)*b(1)+xg(2)*b(2);

Am=am*P/(R^2*T^2);
Bm=bm*P/(R*T);

F=x(1)^3-(1-Bm)*x(1)^2+(Am-3*Bm^2-2*Bm)*x(1)-(Am*Bm-Bm^2-Bm^3);
```

Appendix F (Cont.)

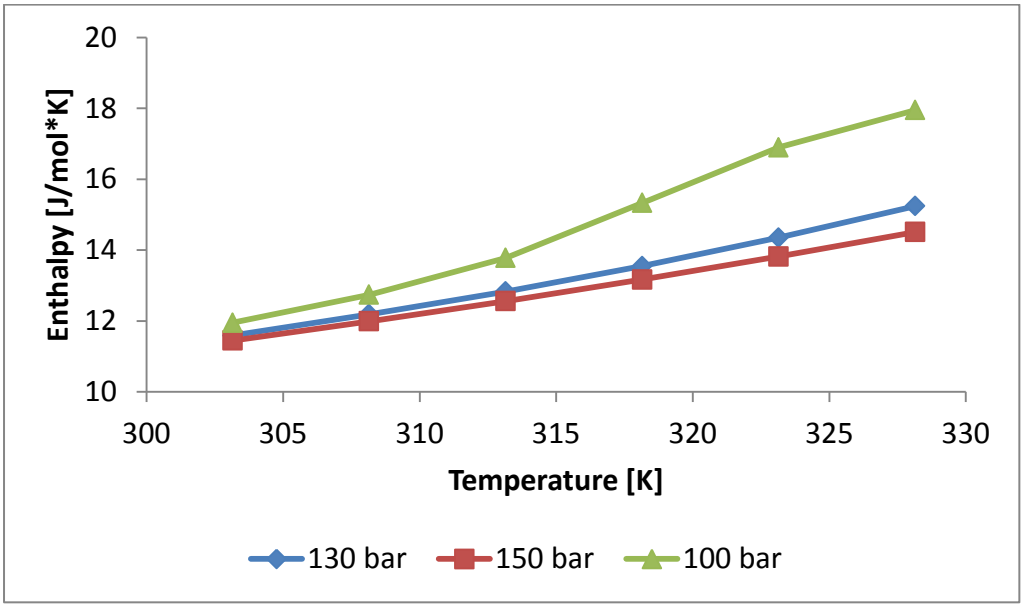

Figure F1. Enthalpy of Supercritical CO_2

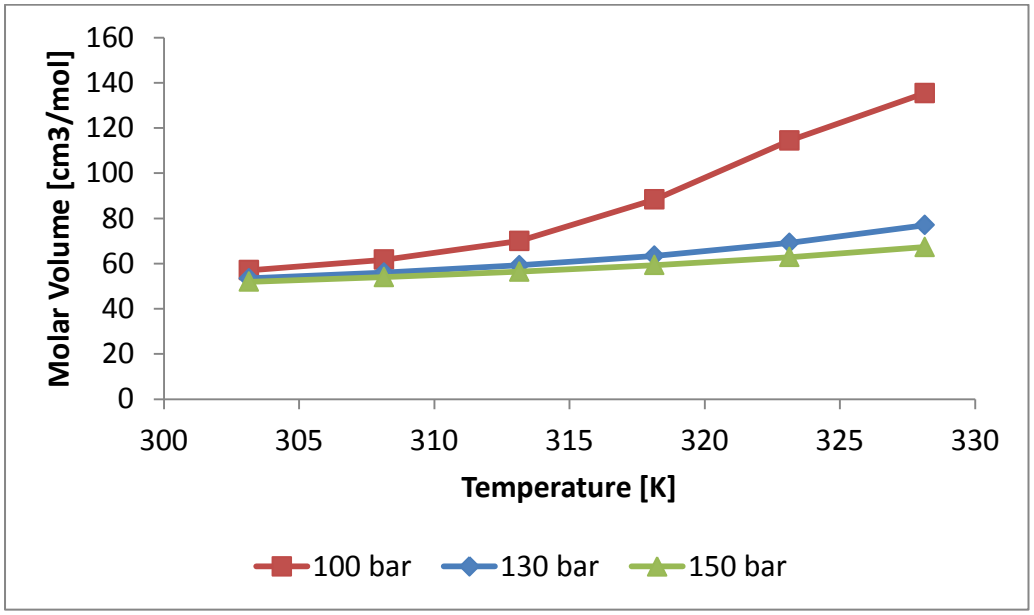

Figure F2. Molar Volume of Supercritical CO_2

Appendix F (Cont.)

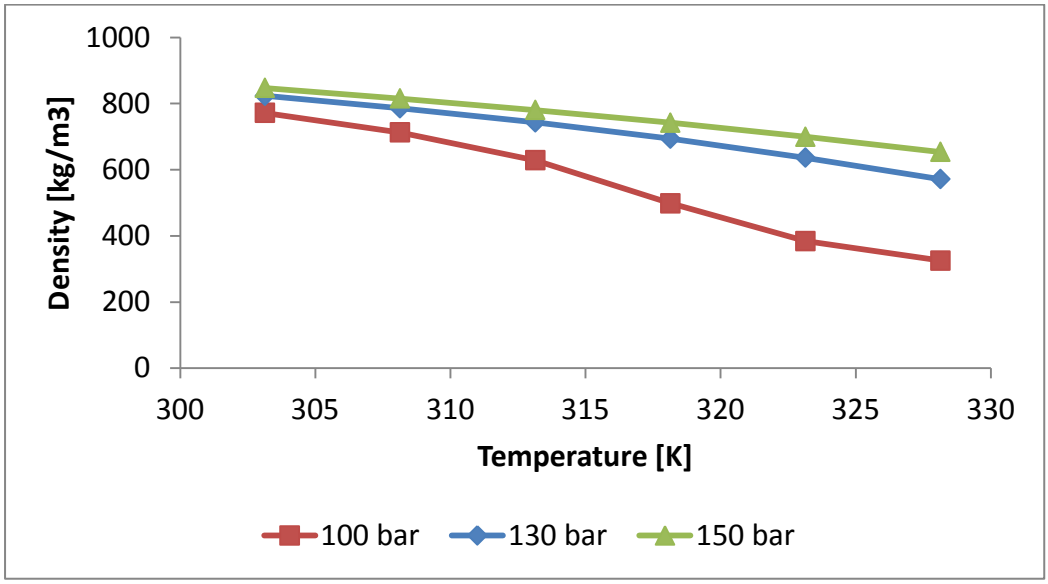

Figure F3. Enthalpy of Supercritical CO_2

Appendix G Chromatograms and Isotherms Pulse Method

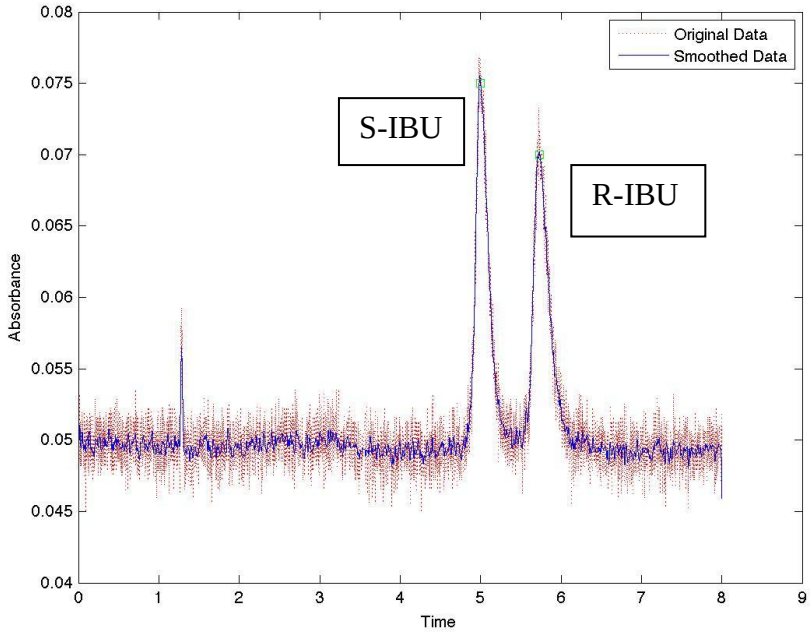

Figure G1. Ibuprofen Racemate Chromatogram 15mg 40^{o}C 100 Bar

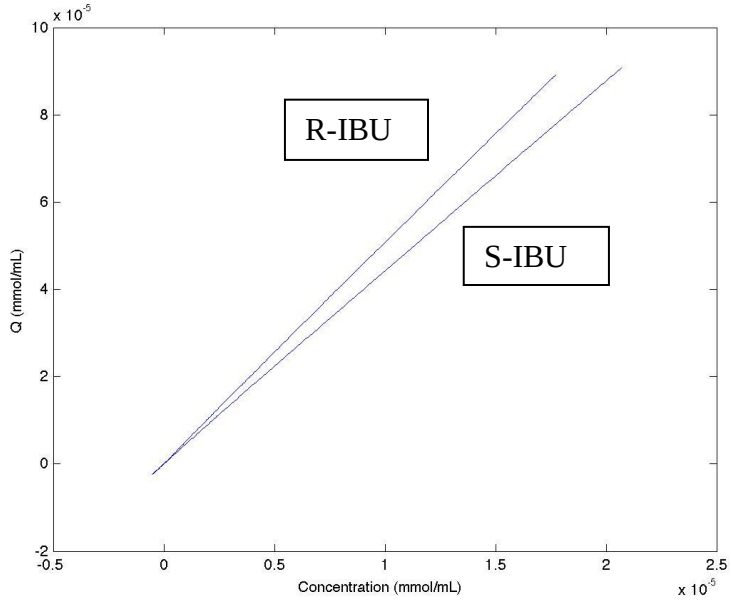

Figure G2. Ibuprofen Racemate Isotherms 15mg 40^{o}C 100 Bar

Appendix G (Cont.)

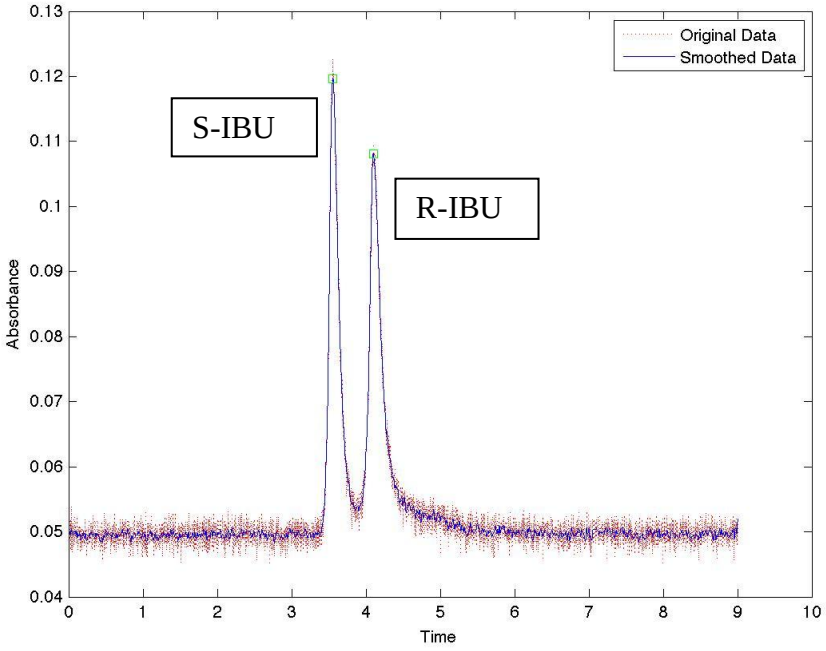

Figure G3. Ibuprofen Racemate Chromatogram 30mg 40^{o}C 150 Bar

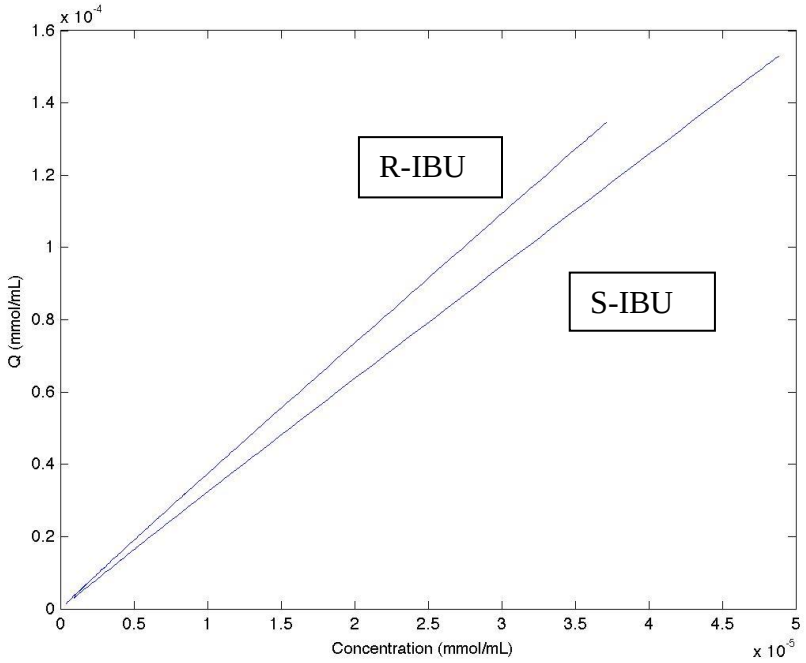

Figure G4. Ibuprofen Racemate Isotherms 30mg 40^{o}C 150 Bar

Appendix G (Cont.)

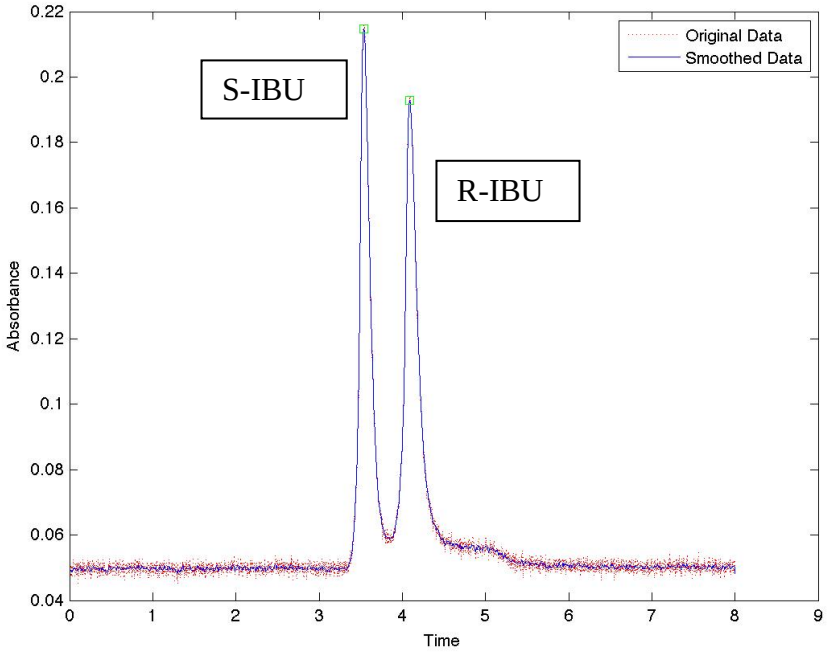

Figure G5. Ibuprofen Racemate Chromatogram 50mg 30^{o}C 150 Bar

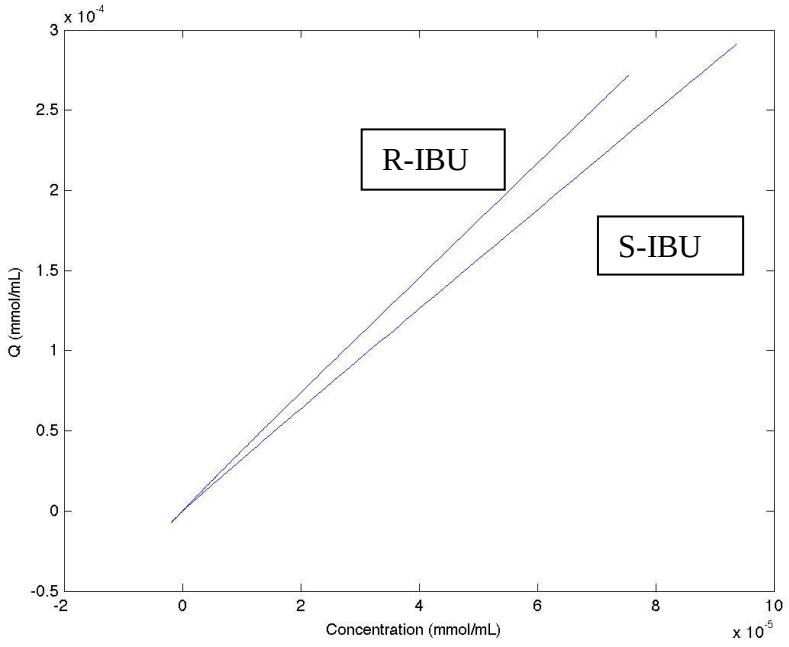

Figure G6. Ibuprofen Racemate Isotherms 50mg 30^{o}C 150 Bar

Appendix G (Cont.)

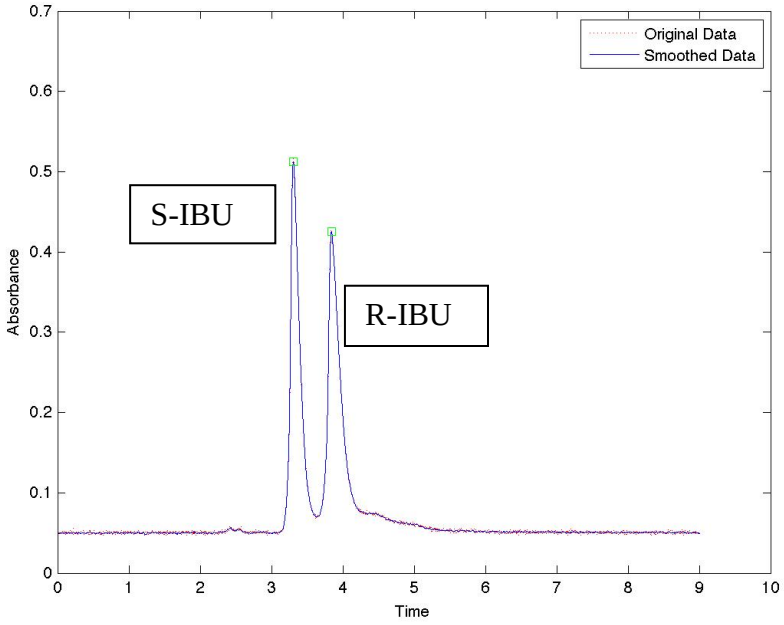

Figure G7. Ibuprofen Racemate Chromatogram 100mg 30^{o}C 150 Bar

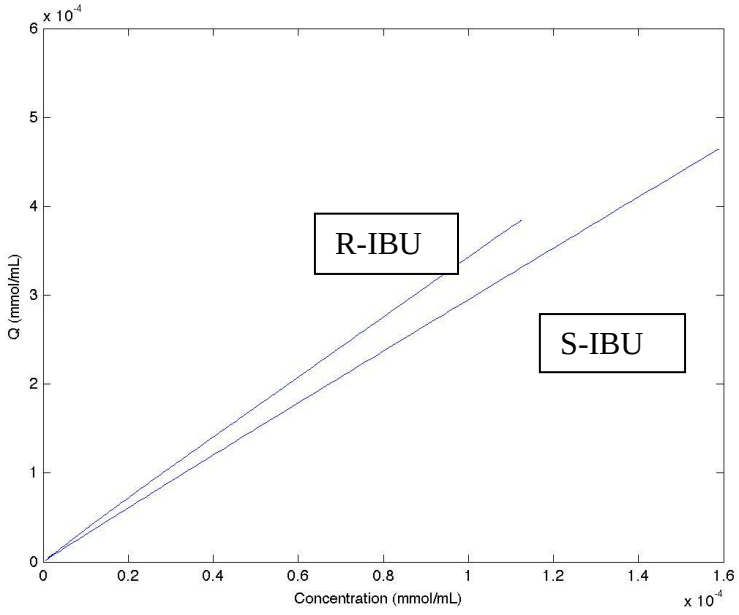

Figure G8. Ibuprofen Racemate Isotherms 100mg 30^{o}C 150 Bar

Appendix H System Hold-up Time and Column Volumetric Flow Rate

Table H1. Flow Rate Calculation from Experimental Hold-up Time

Temperature [^{o}C]	**Pressure [Bar]**	**Hold-up Time [min]**	**Flow Rate [mL/min]**
40	100	1.10	4.1547/1.10=3.777
45	100	1.22	4.1547/1.22=3.405
50	100	1.58	4.1547/1.58=2.629
40	130	1.40	4.1547/1.40=2.967
45	130	1.32	4.1547/1.32=3.147
50	130	1.67	4.1547/1.67=2.487
40	150	1.28	4.1547/1.28=3.245
45	150	1.19	4.1547/1.19=3.491
50	150	1.42	4.1547/1.42=2.925

ABOUT THE AUTHOR

Wade Mack received his Bachelor of Science in Chemical Engineering at the University of South Florida. He continued on at USF and received his master's degree in Chemical Engineering in 2003. During that time he worked for the Department of Chemistry as an organic chemistry laboratory instructor. At the same time he worked as a research assistant for the USF Peptide Synthesis Laboratory. Wade worked in the Drug Discovery Department of the H. Lee Moffitt Cancer Center and Research Institute as a research assistant.

Wade also was an instructor of the Unit Operations Laboratory for the Department of Chemical and Biomedical Engineering. Wade was a teaching assistant for the senior design course, Chemical Engineering Process and Plant Design. As a research assistant in the Laboratory of Environmentally Friendly Engineered Systems, he helped develop the supercritical fluid chromatography pilot processing plant. Additionally, he assisted in the facilitation and maintenance of the other high-pressure operation units in the laboratory.

Wade enjoys biking, running and playing soccer. He also enjoys reading the history of science, and playing drums. Wade plans on working in industry and teaching after graduation.